PROGRESS IN PHYSICS

"All scientists shall have the right to present their scientific research results, in whole or in part, at relevant scientific conferences, and to publish the same in printed scientific journals, electronic archives, and any other media." — Declaration of Academic Freedom, Article 8

PROGRESS IN PHYSICS

A Scientific Journal on Advanced Studies in Theoretical and Experimental Physics, including Related Themes from Mathematics. This journal is registered with the Library of Congress (DC, USA).

This journal is powered by LaTeX

A variety of books can be downloaded free from the Digital Library of Science:
http://fs.gallup.unm.edu/ScienceLibrary.htm

December 2023   Vol. 19, Issue 2

CONTENTS

Information for Authors

Progress in Physics has been created for rapid publications on advanced studies in theoretical and experimental physics, including related themes from mathematics and astronomy. All submitted papers should be professional, in good English, containing a brief review of a problem and obtained results.

All submissions should be designed in LaTeX format using *Progress in Physics* template. This template can be downloaded from *Progress in Physics* home page http://www.ptep-online.com

Preliminary, authors may submit papers in PDF format. If the paper is accepted, authors can manage LaTeXtyping. Do not send MS Word documents, please: we do not use this software, so unable to read this file format. Incorrectly formatted papers (i.e. not LaTeXwith the template) will not be accepted for publication. Those authors who are unable to prepare their submissions in LaTeXformat can apply to a third-party payable service for LaTeX typing. Our personnel work voluntarily. Authors must assist by conforming to this policy, to make the publication process as easy and fast as possible.

Abstract and the necessary information about author(s) should be included into the papers. To submit a paper, mail the file(s) to the Editor-in-Chief.

All submitted papers should be as brief as possible. Short articles are preferable. Large papers can also be considered. Letters related to the publications in the journal or to the events among the science community can be applied to the section *Letters to Progress in Physics*.

All that has been accepted for the online issue of *Progress in Physics* is printed in the paper version of the journal. To order printed issues, contact the Editors.

Authors retain their rights to use their papers published in *Progress in Physics* as a whole or any part of it in any other publications and in any way they see fit. This copyright agreement shall remain valid even if the authors transfer copyright of their published papers to another party.

Electronic copies of all papers published in *Progress in Physics* are available for free download, copying, and re-distribution, according to the copyright agreement printed on the titlepage of each issue of the journal. This copyright agreement follows the *Budapest Open Initiative* and the *Creative Commons Attribution-Noncommercial-No Derivative Works 2.5 License* declaring that electronic copies of such books and journals should always be accessed for reading, download, and copying for any person, and free of charge.

Consideration and review process does not require any payment from the side of the submitters. Nevertheless the authors of accepted papers are requested to pay the page charges. *Progress in Physics* is a non-profit/academic journal: money collected from the authors cover the cost of printing and distribution of the annual volumes of the journal along the major academic/university libraries of the world. (Look for the current author fee in the online version of *Progress in Physics*.)

————————————

Interpretation of Quantum Mechanics in Terms of Discrete Time I

Young Joo Noh

E-mail: yjnoh777@gmail.com, Seongnam, Korea.

From the discretization of time, the nonlocality of matter and electromagnetic waves can be inferred. These nonlocal waves provide a new perspective on the nonlocality of quantum phenomena, such as wave collapse and entanglement, and the wave-particle duality. Interactions can be divided into bound states and scattering, which are all described by the modified Dirac equation. From the modified Dirac equation, the quantum condition of the bound state can be obtained. Regarding scattering, elastic scattering is related to wave nature, and inelastic scattering is related to particle nature. The wave nature is expressed in all bound states and elastic scattering, and the particle nature corresponds to the case of inelastic scattering. And, in the case of inelastic scattering, a model for wave collapse is presented.

1 Introduction

The significance of this paper is to newly understand quantum mechanics from the point of view of discrete time. Quantum mechanics is a system established by experiment, but its interpretation is diverse. However, it is rare to have a perspective that integrates and coherently interprets the various phenomena of quantum mechanics. The perspective of discrete time is very different from existing interpretations, but it provides an interesting perspective. Since the new perspective is very unfamiliar, I will briefly summarize the contents presented in the previous papers [1–3].

The analysis of the dynamical system from the perspective of discrete time has opened a new way to see things that have not been understood in the existing quantum mechanics or existing results from a completely different perspective. In the first paper [1], from the point of view of discrete time, matter is divided into two types with completely different dynamic principles. Type 1 is an ordinary matter that satisfies the Dirac equation, and type 2 is completely new. Type 2 does not interact with the gauge fields and is only affected by gravity. And considering its energy density, it can be interpreted as dark matter.

Since existing relativistic quantum mechanics cannot explain anomalies during interactions, it has no choice but to lead to quantum field theory that assumes second quantization and vacuum energy. This theory is based on the ontological basis of the statistical mechanical analogy that a field is a collection of independent infinite harmonic oscillators. On the other hand, the type 1 field does not make such an ontological assumption. If type 1 is a free particle, it can be interpreted as an ordinary matter that satisfies the Dirac equation, but the concept of the field is quite different from the existing one. In the type 1 field, the current harmonic oscillation is determined by contributions from the past and future of discrete time Δt. From this point of view, it was shown that the mass and charge of elementary particles during interactions must be corrected by causal delay, and this correction

showed that it can explain anomalies such as anomalous magnetic moment and Lamb shift [2,3].

2 The meaning of discrete time

Discrete time means that there is a minimum value of time change, which is a unit of time that cannot be further divided. In other words, it can be said that "time does not pass" from one click of time to the next, and if we consider the hypothetical events on this unit of time, we can infer that they all occurred at the same time. Thus, a discrete unit of time is a collection of simultaneous events.

By the way, this collection of simultaneous events has a special character. Before discussing that, consider the following thought experiment. Observer A is in a car moving at speed v. There is a light source in the middle of the car and light detectors on the front and rear walls of the car. The events in which light reaches both detectors are simultaneous for observer A. However, for B, a stationary observer outside the car, the two events are not simultaneous. Because the car is moving, the light reaching the rear becomes an event that occurs earlier than the light reaching the front. This relativity of simultaneity is a natural result of the special theory of relativity based on the concept of continuous space-time.

However, in discrete time, the relativity of simultaneity is limited. Under the same circumstances, if a car moves by Δl in discrete time Δt, what happens to observer B during which simultaneous events to observer A occur? For observer B, Δt is a situation in which time does not pass from one click to the next click, so the events until the movement by Δl are simultaneous. Thus, within the range of time Δt, simultaneous events for observer A are also simultaneous events for observer B. In other words, in discrete time, local absolute simultaneity is established. Such a discussion holds within Δt. Of course, the relativity of simultaneity is established as time passes beyond the click of Δt. Hypothetical events in Δt do not hold the Lorentz transformation and cannot be expressed in Minkowski space-time, which is based on the concept of continuous space-time. However, since the theory of relativ-

ity is established beyond the Δt click, for example, the time Δt for observer B is $\Delta t' = \Delta t/\gamma$ for observer A. In summary, discrete time can be said to be a collection of events in which local absolute simultaneity is established.

In the previous paper [2], Δt was defined as the time for light to pass through the Compton wavelength of a matter, $\Delta t \overset{\text{def}}{=} \frac{\hbar}{mc^2}$. If the Compton wavelength is regarded as the "spatial domain" of a matter, Δt can be regarded as the "temporal domain" of the matter. Therefore, what the above discussion means is that the relativity of simultaneity is established outside matter, and the absoluteness of simultaneity dominates inside matter. Discrete time is not a concept of objective reality that clicks regardless of matter, like Newton's concept of absolute time, but a unique click inherent in matter.

Let's find out the characteristics of the field defined in discrete time. Since the field defined in continuous space-time holds the local principle, the local parts of the field can change independently. However, if the field defined in discrete time can change locally and independently, the basic premise of discrete time is violated because time must also change as a variable in response to the change of field. Therefore, a field defined in discrete time cannot be changed locally, and all parts of the field must act simultaneously. That is, a field defined in discrete time cannot be divided.

3 Formation of nonlocal waves

In discrete time, the spinor $\Psi(x^\mu)$ at any point x^μ of type 1 is given by the sum of Δt future and past contributions to x^μ, so that $\Psi(x^\mu)$ evolves into $e^{-i\Delta x^\alpha p_\alpha}\Psi(x^\mu)$ [1]. Eq. (1) and Fig. 1 show this as a formula and figure, respectively.

$$(x^\mu + \Delta x^\mu)\,\Psi(x^\mu) - x^\mu\Psi(x^\mu + \Delta x^\mu)$$
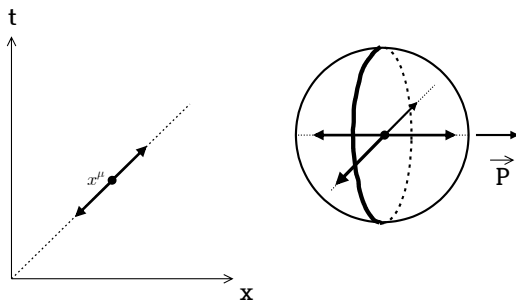$$= \Delta x^\mu e^{-i\Delta x^\alpha P_\alpha}\Psi(x^\mu)\,. \tag{1}$$

Fig. 1: Contributions of spinors at x^μ.

The left side of Fig. 1 shows spinors contributing from Δt future and past at x^μ, in the 1+1 dimension, and the right side shows them in 3-dimensional real space. All points on the right hemisphere are Δt future and all points on the left hemisphere are past. At the center point, all spinors contributing

from the future appear to the left, and all spinors contributing from the past appear to the right. As discussed in the previous section, all events in the right hemisphere are simultaneous events, and all events in the left hemisphere are also simultaneous events.

Furthermore, spinors at every point on the right hemisphere can also be represented as contributions from future and past spinors. Then, the same sphere can be drawn at every point on the right hemisphere, and this process can be repeated over and over again. As a result, a wavefront with the same phase can be represented as the left side of Fig. 2.
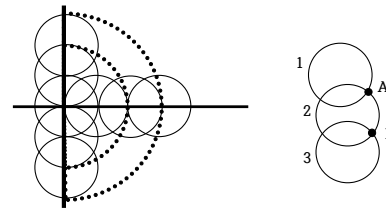
Fig. 2: Formation of simultaneous wavefronts.

By the way, the wavefront formed in this way has special properties. On the right side of Fig. 2, A is the common point of 1 and 2. Point A is simultaneous with all points on hemisphere 1 and also with all points on hemisphere 2. Therefore, all points on hemispheres 1 and 2 are simultaneous with each other. This is established only when hemispheres 1 and 2 overlap. Since this process can continue to expand, all the points on the wavefront shown on the left in Fig. 2 are simultaneous.

This simultaneous wavefront is not local. If we consider the field defined on this wavefront, as discussed in the previous section, it cannot change locally. Interactions occurring at one point on the wavefront occur simultaneously at all points on the wavefront. A wavefront is nonlocal, but the local principle still applies between one wavefront and another. This non-locality of type 1 waves is fundamentally different from the wave concept explained only by the existing local principle.

So far, we have discussed the nonlocality of a type 1 wave, that is, a matter field wave. We will now discuss the nonlocality of electromagnetic waves. The electric and magnetic fields individually obviously apply the local principle. But what about electromagnetic waves? In judging the nonlocality of electromagnetic waves, I will refer again to the proposition discussed earlier. In discrete time, the collection of simultaneous events establishes local absolute simultaneity. Therefore, if a wavefront composed of certain simultaneous events has local absolute simultaneity, it can be judged that the wavefront is a nonlocal wave.

Electromagnetic waves are produced by accelerating electric charge. Around the accelerating charge, there are kinks of the field, and these kinks are what form the wave. The kinks depend on the motion of the charge, and the motion of the charge is performed in units of discrete time Δt . Then, the kinks formed between Δt can also be said to be simultaneous events to the observer fixed on the charge, which, according to the above discussion, can also be said to be simultaneous events to the stationary observer. Therefore, electromagnetic waves can be said to have local absolute simultaneity, so they can be said to be nonlocal waves like matter field waves.

Until now, we have had a somewhat unfamiliar discussion that matter field waves and electromagnetic waves are nonlocal waves. However, in my opinion, the fact that these are nonlocal waves is already included in the existing quantum mechanics. In quantum mechanics, the energy of light is $E = h\nu$. What does this equation mean? If we try to understand it as a wave, there is no local nature of a wave at all. So, it should be understood as a particle, but what does the frequency of a particle mean? The fact that the energy of light does not depend on the local properties of the wave means that the wave is nonlocal. Light is created by kinks, the magnitude of which determines the frequency, and the total kinks form a nonlocal wavefront. An interaction at one point of the wavefront acts simultaneously on all parts of the wavefront. Therefore, the energy of light does not depend on the local properties of the wave, but is proportional only to its frequency.

4 Wave collapse and wave-particle duality

Quantum mechanics has various interpretations depending on the meaning of the wave function and measurement. In this paper, these meanings are as follows. The wavefunction is not a probability concept, but an objective real field, and the measurement is merely the interaction between elementary particles.

Based on the discussion in the previous section, let's infer the wave collapse, which is an intrinsic property of nonlocal waves, and the particle nature of matter and light.

When an electron interacts with an electromagnetic wave, the wavefront of the electron and the wavefront of the electromagnetic wave meet. If one part of the wavefront of an electron is affected by an electromagnetic wave, all parts of the wavefront of an electron are simultaneously affected because of the intrinsic property of nonlocal waves. It is as if all the information of the electron wavefront is concentrated at the point of contact and interacts with the electromagnetic wave. This can be seen as a kind of wave collapse, and it can be said to be the definition of the particle nature of electrons. This discussion can be equally applied to electromagnetic waves interacting with electrons. Electromagnetic waves are also nonlocal waves, and when interacting with electrons, the entire wave is concentrated in a local area, which is the particle

nature of light, that is, the definition of a photon. The electrons and photons concentrated in this local area exchange energy and momentum as particles. In other words, the interaction—which we will discuss in the next section, corresponds to inelastic scattering—occurs on a "quantum" unit. After the interaction, they move as new free waves, each with new energy and momentum. In the next section I will present a mathematical model for the collapse of matter waves.

The wave-particle duality is one of the most important phenomena that reveals the essence of quantum mechanics, and contains a deep mystery about the existence of matter. However, current understanding of this remains superficial. It is difficult to understand that matter or photons choose one state among particle or wave depending on the situation*. If there is a correct theory, there must be a clear reason for having a particular state in a particular situation. The reality of quantum mechanical existence presented in this paper is as follows. A nonlocal wave causes a wave collapse at a specific interaction to acquire particle properties, and when the interaction disappears, the wave properties are restored. This process is repeated.

Speaking of electromagnetism, fields with local properties are real, and their waves (as nonlocal waves) are real, and photons formed by the collapse of waves are real. We discussed earlier that the quantum of a photon energy should depend only on its frequency, but there is one more thing to consider here. When an electromagnetic wave is generated by kinks caused by the acceleration of an electric charge, the amount of the charge becomes a variable of the photon energy. The quantum concept of photon energy is established only when the charge amount of all free elementary particles is the same. In reality it is. That is, quantization of photon energy is established by quantization of charge.

5 Bound state and scattering

In terms of discrete time, interacting particles satisfy the modified Dirac equation [2].

$$D_m \Psi = \left(i\gamma^\mu \partial_\mu - f_{1r}\gamma^\mu p_\mu - f_{2r}\gamma^\mu \Delta p_\mu \right) \Psi = 0 \,. \qquad (2)$$

where

$$f_{1r} = \mathrm{Re}(f_1) = \frac{1}{3}\,\mathrm{Re}\left(\frac{e^{-ix^\alpha p_\alpha}}{e^{-ix^\alpha p_\alpha} + 2\left(e^{-ix^\alpha \Delta p_\alpha} - 1\right)} \right)$$
$$f_{2r} = \mathrm{Re}(f_2) = \frac{1}{3}\,\mathrm{Re}\left(\frac{2e^{-ix^\alpha \Delta p_\alpha}}{e^{-ix^\alpha p_\alpha} + 2\left(e^{-ix^\alpha \Delta p_\alpha} - 1\right)} \right) . \qquad (3)$$

Eq. (2) is a first-order linear differential equation, and the way it is applied differs depending on the type of interaction

---

*Wheeler's delayed choice experiment clearly shows the contradiction of the existing quantum mechanical view of duality. And the Elitzur–Vaidman bomb tester claims that interaction-free measurements are possible based on the existing viewpoint. In my next paper, I will present a new interpretation of these experiments from the new perspective presented above.

– scattering and bound state. In the case of the scattering process, for example, the scattering of electron and photon interacts in an extremely limited space-time region, so the modified Dirac equation is also applied only in such a limited space-time region. On the other hand, in the case of ceaseless interaction, such as in the bound state, the modified Dirac equation holds without limitation because the interaction occurs in a relatively wide space-time region.

5.1 Bound state

5.1.1 $\Delta \mathbf{p}_\mu \ll \mathbf{p}_\mu$

In this case, that is, when the interaction is very small, f_{1r}, f_{2r}, and the modified Dirac equation is as follows

$$f_{1r} \cong \frac{1}{3}, \quad f_{2r} \cong \frac{2}{3}\cos\left(x^\alpha p_\alpha\right)$$

$$\left(i\gamma^\mu \partial_\mu - \frac{1}{3}\gamma^\mu p_\mu - \frac{2}{3}\cos\left(x^\alpha p_\alpha\right)\gamma^\mu \Delta p_\mu\right)\Psi = 0. \tag{4}$$

The solution of (4) satisfies the following equation

$$\partial_\mu \Psi = -\frac{i}{3}\left(p_\mu + 2\cos\left(x^\alpha p_\alpha\right)\Delta p_\mu\right)\Psi. \tag{5}$$

And the solution of (5) is as follows

$$\Psi = c\exp\left[-\frac{i}{3}\int^{x^\mu}\left(p_\mu + 2\cos\left(x'^\alpha p_\alpha\right)\Delta p_\mu\right)dx'^\mu\right]$$

$$= c\exp\left[-\frac{i}{3}p_\mu x^\mu - \frac{2i}{3}\int^{x^\mu}\cos\left(x'^\alpha p_\alpha\right)\Delta p_\mu dx'^\mu\right]. \tag{6}$$

Δp_μ means interaction, so it is determined according to the specific situation. If it is an electrostatic potential like the potential in a hydrogen atom, Δp_μ is independent of the integral variable in (6) because there is only a scalar potential energy component that is independent of time. Thus

$$\Psi = c\exp\left[-\frac{i}{3}\left(p_\mu x^\mu + 2\epsilon\left(\Delta p_\mu\right)\sin\left(x^\mu p_\mu\right)\right)\right]. \tag{7}$$

$\epsilon\left(\Delta p_\mu\right)$ is a small quantity linear to Δp_μ. In (7), for Ψ to be a free wave, i.e. harmonic oscillation, $\sin\left(x^\mu p_\mu\right) = 0$, so the following quantum condition is derived

$$x^\mu p_\mu = n\pi \ (n = 0, \pm 1, \pm 2, \cdots). \tag{8}$$

For any given p_μ, x^μ that satisfies (8) has as its solution a certain region in space-time. Harmonic oscillations that exist in this region can be referred to as standing waves. As a simple example, consider the case where the electron in a hydrogen atom is in uniform circular motion. In this case, the phase value is as follows

$$\oint\left(Edt - \vec{P}\cdot d\vec{x}\right) = E\oint dt - \vec{P}\cdot\oint d\vec{x}$$

$$= -mvr\pi = n\pi \tag{9}$$

$$\therefore L = mvr = n.$$

Eq. (9) agrees with the well-known Bohr's quantum condition for the hydrogen atom.

In (7), when $\epsilon \to 0$, the 4-momentum appearing in the phase part is not p_μ but $p_\mu/3$. This result is questionable because the system we are dealing with is a system in which a free particle with 4-momentum p_μ becomes $p_\mu + \Delta p_\mu$ by interaction. However, as we will see later, this does not violate the law of conservation of energy at all.

In the case of $\Delta p_\mu \to 0$, if $\gamma^\mu p_\mu = m$ is used, (4) can be expressed as follows

$$i\frac{\partial \Psi}{\partial t} = \left(\vec{\alpha}\cdot\hat{P} + \frac{1}{3}\beta m\right)\Psi. \tag{10}$$

In (7), the free wave solution is as follows for $\epsilon \to 0$

$$\Psi = \begin{pmatrix}\varphi \\ \chi\end{pmatrix}\exp\left(-\frac{i}{3}x^\mu p_\mu\right). \tag{11}$$

In (11), φ and χ are two-component spinors. Using (12), (10) becomes (13)

$$\frac{\partial \Psi}{\partial t} = \frac{1}{3}E\Psi, \quad \hat{P}\Psi = \frac{1}{3}\vec{P}\Psi. \tag{12}$$

$$E\Psi = \left(\vec{\alpha}\cdot\vec{P} + \beta m\right)\Psi. \tag{13}$$

In (13), the energy of Ψ is $\pm\sqrt{\vec{P}^2 + m^2}$, which is equal to the energy of the free particle before interaction. So, as expected, energy is conserved.

5.1.2 $\Delta \mathbf{p}_\mu = \mathbf{p}_\mu$

In this case, the modified Dirac equation is:

$$\left\{i\gamma^\mu \partial_\mu - \left(f_{1r} + f_{2r}\right)m\right\}\Psi = 0. \tag{14}$$

$$G\left(x^\mu\right) \stackrel{\text{def}}{=} f_{1r} + f_{2r} = \text{Re}\left(\frac{1}{3 - 2e^{ix^\mu p_\mu}}\right)$$

$$= \frac{3\cos\left(x^\mu p_\mu\right) - 2}{13 - 12\cos\left(x^\mu p_\mu\right)}. \tag{15}$$

In (14), the condition for Ψ to become a plane wave in a specific space-time region is that G must be constant, which means that G has an extreme value in that region. Therefore, the following condition must be satisfied

$$\partial_\lambda G\left(x^\mu\right) = -\frac{15\,p_\lambda\sin\left(x^\mu p_\mu\right)}{\left(13 - 12\cos\left(x^\mu p_\mu\right)\right)^2} = 0. \tag{16}$$

Eq. (16) is the same quantum condition as in $\Delta p_\mu \ll p_\mu$.

Eq. (14) is related to pair production. If Δp_μ is the 4-momentum of the incident photon and $p_\mu = p_\mu^{elctron} + p_\mu^{positron}$, that is, the sum of the 4-momentum of the electron and the positron, Ψ in (14) becomes the wave function for the entire

electron and positron. This plane wave will persist until a new interaction occurs. If an interaction occurs on one side (electron) of this free wave, the whole system will be affected at the same time due to the characteristics of nonlocal waves, so the other side (positron) will also "experience the same interaction at the same time". This can be said to be the mechanism of entanglement.

5.2 Scattering

In the case of elastic scattering, there is no change in the energy of the incident particle. That is, since $\Delta p_0 = 0$ and $|\vec{P'}| = |\vec{P}|$ hold, the incident wave and the reflected wave have the same wavelength, so it is predicted that wave collapse will not occur when they interact. Assuming that the interaction occurs within the range of Δt during elastic scattering, $\Delta p_\mu = 0$ and $f_{1r} = 1/3$ just before and after the interaction, so the following free wave equation is established

$$\left(i\gamma^\mu \partial_\mu - \frac{1}{3}m\right)\Psi = 0. \tag{17}$$

On the other hand, in inelastic scattering, there is a change in the energy of the incident particle and the target particle. This means that the properties of the wave before and after the interaction are different. The mechanism that enables this process is the concept of wave collapse discussed in section 4. During inelastic scattering, a nonlocal wave instantly collapses and becomes a particle state. In this particle state, energy and momentum are exchanged, and as a result, a new wave corresponding to new energy and momentum is formed. We will now present a model for this wave collapse.

When an interaction occurs in a local region in spacetime, the modified Dirac equation is also applied only in a local region. In this case, f_{1r} and f_{2r} must, of course, be quantities defined in a local region. Therefore, f_{1r} and f_{2r} must be corrected to converge to 0 at large x^μ. In this case, the collapse of the wave inevitably occurs.

In order to model the wave collapse during inelastic scattering, we introduce a damping factor ϵ_μ that satisfies the following condition

$$x^\mu = \left(t, |\vec{x}|\,\hat{n}_{\vec{x}}\right), \quad \epsilon_\mu = \left(\epsilon_0, |\vec{\epsilon}|\,\hat{n}_{\vec{\epsilon}}\right)$$

$$\mathrm{e}^{-\epsilon_\mu x^\mu} \to 0, \quad \text{as } x^\mu \to \infty, \quad \text{for } \hat{n}_{\vec{x}} \cdot \hat{n}_{\vec{\epsilon}} = -1. \tag{18}$$

And if the new 4-momentum p'_μ is defined as follows, the modified Dirac equation and f'_{1r}, f'_{2r} are as follows. For simplicity, we will discuss wave collapse for the special case $\Delta p_\mu = a p_\mu$ (a is a real number)

$$p'_\mu = p_\mu - i\epsilon_\mu$$

$$\left\{i\gamma^\mu \partial_\mu - \left(f'_{1r} + a f'_{2r}\right)\gamma^\mu p'_\mu\right\}\Psi = 0. \tag{19}$$

where

$$\begin{aligned}
f'_{1r} &= \frac{1}{3}\,\mathrm{Re}\left(\frac{\mathrm{e}^{-ix\cdot p'}}{\mathrm{e}^{-ix\cdot p'} + 2\left(\mathrm{e}^{-iax\cdot p'} - 1\right)}\right) \\
&= \frac{1}{3}\,\mathrm{Re}\left(\frac{\mathrm{e}^{-\epsilon\cdot x}\mathrm{e}^{-ix\cdot p}}{\mathrm{e}^{-\epsilon\cdot x}\mathrm{e}^{-ix\cdot p} + 2\left(\mathrm{e}^{-\epsilon\cdot x}\mathrm{e}^{-iax\cdot p} - 1\right)}\right) \\
f'_{2r} &= \frac{2}{3}\,\mathrm{Re}\left(\frac{\mathrm{e}^{-iax\cdot p'}}{\mathrm{e}^{-ix\cdot p'}\mathrm{e}^{-ix\cdot p} + 2\left(\mathrm{e}^{-iax\cdot p'} - 1\right)}\right) \\
&= \frac{2}{3}\,\mathrm{Re}\left(\frac{\mathrm{e}^{-\epsilon\cdot x}\mathrm{e}^{-iax\cdot p}}{\mathrm{e}^{-\epsilon\cdot x}\mathrm{e}^{-ix\cdot p} + 2\left(\mathrm{e}^{-\epsilon\cdot x}\mathrm{e}^{-iax\cdot p} - 1\right)}\right).
\end{aligned} \tag{20}$$

In (20), both f'_{1r} and f'_{2r} converge to 0 at large x^μ by $\mathrm{e}^{-\epsilon_\mu x^\mu}$ factor. Now let's find the solution of (19)

$$\partial_\mu \Psi = -\frac{i}{3}p'_\mu\left(1 + S'\right)\Psi$$

$$\text{where } S'(x) = \mathrm{Re}\left(\frac{2(a-1)\mathrm{e}^{-\epsilon\cdot x}\mathrm{e}^{-iax\cdot p} + 2}{\mathrm{e}^{-\epsilon\cdot x}\mathrm{e}^{-ix\cdot p} + 2\left(\mathrm{e}^{-\epsilon\cdot x}\mathrm{e}^{-iax\cdot p} - 1\right)}\right). \tag{21}$$

$$\begin{aligned}
\Psi &= c\,\exp\left\{-\frac{i}{3}p'_\mu \int^{x^\mu}\left(1 + S'\right)dx'^\mu\right\} \\
&= c\,\exp\left\{-\frac{i}{3}\left(x^\mu p_\mu + p_\mu \int^{x^\mu} S'dx'^\mu\right)\right\} \times \\
&\quad \times \exp\left(-\frac{1}{3}\epsilon_\mu x^\mu - \frac{1}{3}\epsilon_\mu \int^{x^\mu} S'dx'^\mu\right).
\end{aligned} \tag{22}$$

As expected, since the factor $\mathrm{e}^{-\frac{1}{3}\epsilon_\mu x^\mu}$ exists in Ψ, it converges to 0 at large t. This means the collapse of the wave.

Of course, these results are different from the concept of simultaneous wave collapse of nonlocal waves discussed above. The reason is the fundamental limitation of the modified Dirac equation. Since the modified Dirac equation does not accurately represent the behavior of non-local waves, but approximates it to the behavior of local waves in continuous space-time, it cannot describe concepts such as simultaneous collapse of waves. But, it can be said that it has value as a model of wave collapse. On the other hand, in the interaction such as the bound state, there is no phenomenon such as wave collapse, but a standing wave is formed, so the modified Dirac equation representing the behavior of a local wave represents the exact behavior of the wave.

6 Conclusions

One of the most important concepts inferred from the discretization of time is the nonlocality of matter and electromagnetic waves. The nonlocality of waves can naturally cause wave collapse when interacting. This state of wave collapse means particle nature and also corresponds to the quantum state. What this paper concludes about the wave-particle duality is that particle and wave properties are not selected by matter according to circumstances, but are determined only

by the way of interaction. It is done by analysis of the modified Dirac equation.

Interactions can be divided into bound states and scattering, which are all described by the modified Dirac equation. Quantum conditions can be obtained in a bound state, which is expected to be the same as in conventional quantum mechanics. Scattering can be divided into elastic scattering and inelastic scattering, both of which are forms of interaction. Elastic scattering is related to wave nature and inelastic scattering is related to particle nature. According to the analysis of the modified Dirac equation, the wave nature is expressed in all bound states and elastic scattering. An example is the Davisson–Germer experiment which demonstrates the wave nature of electrons. The particle nature correspond to the case of inelastic scattering. Examples include the photoelectric effect and Compton scattering.

The particle nature resulting from the collapse of nonlocal waves encompasses the quantum concept of the existing quantum mechanics, and the nonlocal wave concept encompasses the existing classical field. For matter (nonlocal waves, and particle nature due to wave collapse), and for electromagnetics (classical fields, nonlocal waves, and particle nature due to wave collapse), each stage of existence participates in interaction as a physical reality.

References

1. Noh Y. J. Propagation of a Particle in Discrete Time. *Progress in Physics*, 2020, v. 16, 116–122.

2. Noh Y. J. Anomalous Magnetic Moment in Discrete Time. *Progress in Physics*, 2021, v. 17, 207–209.

3. Noh Y. J. Lamb Shift in Discrete Time. *Progress in Physics*, 2022, v. 18, 126–130.

4. Elitzur A. and Vaidman L. Quantum Mechanical Interaction-Free Measurements. *Foundations of Physics*, 1993, v. 23, 987–997.

5. Wheeler J. A. The "Past" and the "Delayed-Choice" Double-Slit Experiment. In: Marlow A. R. Mathematical Foundations of Quantum Theory. Academic Press, New York, 1978, pp. 9–48.

6. Penrose R. The Road to Reality. Jonathan Cape, 2004.

7. Cohen-Tannoudji C., Diu B., Laloe F. Quantum Mechanics. Hermann, Paris, France, 1977.

The Arrow of Time and Its Irreversibility

Gerald F. Thomas

MINOS Technologies Inc., 176-6A The Donway West, Toronto, ON, M3C 2E8, Canada.
E-mail: gfthomas@minostechinc.com

Quantum thermodynamics strives to extend classical thermodynamics and nonequilibrium statistical physics to ensembles of sizes below the thermodynamic limit with the full inclusion of quantum effects. This paper uses the nonrelativistic quantum mechanics of a lone system in a thermal bath to relate its wave function's local phase to Lorentz-Faraday forces acting thereon. In the intake of heat from its surroundings, such a system's entropy increases with the gain connected to the gradient field of its local phase whose subharmonicity within the boundary of its volume is a necessary and sufficient condition for it to comply with the second law of thermodynamics (SLT). The thermodynamic arrow of time necessitates irreversible over reversible processes as determined by the gradient field of the phase. Conservative Lorentz-Faraday forces identified herein impress on the system to engender irreversible (reversible) change and entropy gain (stasis) in its exchange of heat with its environment under the discernment of the thermodynamic arrow of time and regardless of the time-reversal symmetry of such venerable frameworks as electrodynamics and quantum mechanics. Entropy production is greatest when the local phase is subharmonic within the system's nominal volume. A means of time-averaging entropy and free energy changes under nonstandard-state conditions with the accommodation of phenomenological relaxation is provided. Both the SLT and Faraday's law of induction are of similar vintage and status. Surprisingly, they share a hitherto unrecognized connection at the microscopic level. Faraday's law of induction is shown to hold for a lone system provided the gradient of its local phase is finite, a necessary and sufficient condition for it not to present with its alleged paradoxes and contradictions despite its technological successes rivalling those of the SLT. There is no evidence to deny the successes of both the SLT and Faraday's law for science and technology. In compliance with Earnshaw's theorem, the potential of the Lorentz-Faraday force is shown to stabilize a lone system just like the Coulomb (or Newtonian) potential while continuing to fulfill the virial theorem. A consequence of the time asymmetry of entropy is the impossibility of travel to the past as to cause entropy changes to decrease contrary to the SLT. Further consequences of entropy's time asymmetry include at least the nonexistence of magnetic monopoles, the observed matter-antimatter asymmetry in leptonic and baryonic matter, and the role of axion-like particles in accounting for the absence of charge-parity violations in strong interactions without necessarily answering for dark matter. Within the range of validity of gravito(electro)magnetism, dark energy is identified as the work done by the Heaviside analog of the Lorentz-Faraday force in causing the accelerated expansion of the Universe without reference to either a finite cosmological constant or an unstable vacuum state transition. In the practice of reductionism, macroscopic physics supervenes upon the microscopic, the SLT being the most conspicuous exception to that superfluous tenet. The supersedence of classical thermodynamics over quantum mechanics and electrodynamics across spatio-temporal scales ranging from an individual quantized system to its known Universe has been shown herein. Additionally, in showing that reversible (irreversible) processes are affiliated with the particle (wave) behavior of matter, attention has been drawn to a heretofore overlooked connection between the different roles of classical thermodynamics and quantum mechanics and electrodynamics in respect to arrow-of-time asymmetry and wave-particle duality.

1 Introduction

1.1 Background and purpose

Charge conjugation (C), parity (P), and time (T) are the three most important discrete symmetries and hold for all physical phenomena in Nature: C symmetry conjugates all charges, P symmetry flips spatial orientations, and T-symmetry reverses the direction of time. The CPT theorem [1] asserts that any local field theory that is invariant under Lorentz transformations must also be invariant under the combined operation of the three discrete transformations for all fundamental interactions with causality and energy positivity as obligatory, if stealth, constraints [2,3, for e.g.]. The CPT triad is an exact symmetry

with any combination short of the three being a violation of the remainder so that, for example, a violation of CP symmetry is equivalent to a violation of T-symmetry [4]. Essentially, the CPT theorem links the charges C (matter and antimatter) of states with their spacetime PT symmetries. These symmetries are broken in the known Universe as first acknowledged in the early 1950's with the revelation of P asymmetry in weak interactions by Lee and Yang [5] and quickly confirmed by Chien-Shiung Wu and her team [6].

T-asymmetry is what gives rise to our experience of the passage of time. Its basis is the second law of thermodynamics (SLT), the only T-asymmetric law in physics, one which stipulates that the entropy of a system can never decrease. Time symmetry ensures that physical laws follow their time-reversed paths when we imagine reversing time. The SLT says differently. Max Planck, thermodynamicist and one of the founders of quantum physics, remarks [7, loc. cit., pp. 103–104] in respect to the SLT that:

> The limitations to the law, if any, must lie in the same province as its essential idea, in the observed Nature, and not in the Observer. That man's experience is called upon in the deduction of the law is of no consequence; for that is, in fact, our only way of arriving at a knowledge of natural law. But the law once discovered must receive recognition of its independence at least in so far as Natural Law can be said to exist independent of Mind. Should any one deny this, he would have to deny the possibility of natural science.

Planck foresaw that a myriad versions of the SLT would be proposed [8–10, for e.g.], not by Nature but by Mind.

T-symmetry is the symmetry of most physical laws under a time-reversal transformation. Physical processes – whether classical or quantum mechanical – are time-symmetric and following Newton's lead, Maxwell, Einstein, and Schrödinger expressed their respective theories in terms of deterministic equations necessitating initial and occasionally boundary conditions on the collegial assumption that there was a beginning and an ambient space from where such evolutions would occur.

It has been known [11] for some time that electroweak interactions in neutral K mesons exhibit a small violation of CP symmetry. Direct CP violation was observed in the KTeV Collaboration [12] so that, by the CPT theorem, T violation must occur. Independently of the CPT theorem (i.e. no assumptions about CP or CPT violation or invariance were made), direct detection of T reversal violation was achieved by the BaBar Collaboration [13] proving that the laws of physics are not identical whether time runs forwards or backwards. So far, CP violations have not been observed [14, 15, et passim] in strong interactions and since there is no known reason for this absence it is referred to as the strong CP problem.

An extensive body of work exists on attempts to measure permanent electric dipole moments (EDMs) of subatomic particles which, with their spin angular momenta, would directly violate both CP and T symmetries [16, et passim]. Current searches for T reversal violations through precision laboratory measurements of the EDMs of atoms and molecules [17–23] are now sufficiently sensitive to detect signatures of some particles with masses of more than 10 TeV. There are many experiments [24, for e.g.] attesting to the inviolability of CPT in Nature. Among the phenomena that the Standard Model of Particle Physics (SM) – and extensions beyond the SM – do not explain include the absence of magnetic monopoles, matter-antimatter asymmetry, neutrino masses, supersymmetry, and gravity. While the possibility of CP violations in the baryon sector was anticipated in 1958 by Okubo [25], it is only lately that such effects beyond the SM have been observed [26, 27].

Nor does the SM provide the connection between microscopic T violations and irreversibility in thermodynamics. Discrete symmetries have just recently been investigated with entangled neutral kaons [28] and in ortho-positronium decays [29]: neither investigation drew any connection between their null results with the T-asymmetry of the SLT as established herein. That T-symmetry is counterintuitive is generally excused by the claim that the SM handles only local properties, not global ones like entropy. One outcome of this paper is to provide that connection in which the two rub shoulders to the advantage of entropy and its governing SLT.

The Standard Model of Cosmology (SMC) is based on the SM and the General Theory of Relativity (GTR) [30, for e.g]. It also depends on several additional assumptions: that the Universe was created in the Big Bang from pure energy; that the known mass-energy content of the Universe is given by luminous matter whose gravitational interaction is described by the GTR; and the cosmological principle by which the idea that the Universe is homogeneous and isotropic on cosmic scales was popularized. The Λ Cold Dark Matter (ΛCDM) variant of the SMC, with six free parameters and several ansatzes, posits that only $\sim 5\%$ of the content of the Universe is in the form of baryonic matter with the balance comprised of cold, slow-moving dark matter – invisible matter that interacts with baryons via gravity alone and thought to make up $\sim 25\%$ of the total mass content in addition to dark energy – a repulsive force inferred from observational data of type Ia supernovae and thought to promote the accelerating expansion [31, 32] of the Universe against gravity and accounting for $\sim 70\%$ of its matter-energy inventory. Cold dark matter is thought to have clumped into large masses which gravitationally attracted baryonic matter, forming the large-scale structures of the Universe. Remnants of dark matter clumps are observed as halos surrounding galaxies. Currently the primary candidates for dark matter are primordial black holes [33], axions [34], sterile neutrinos [35], weakly interacting massive particles (WIMP) [36, et passim], and the lat-

est, erebons [37]. Despite a wealth of evidence favoring their existence [38, 39, for e.g.], neither dark matter [40] nor dark energy [41] have been conclusively detected to date.

With improvements in the accuracy of cosmological observations, so too do challenges [42] to ΛCDM appear. Alternatives [43, 44, et passim] to ΛCDM that dispense with dark matter, dark energy, or both do so [45] by altering the known long-range nature of gravity, an approach not without its own perils and pitfalls [46, 47]. As with the SM and its shortcomings, the ΛCDM, for all its successes, cannot explain such key concepts in our understanding of the known Universe as dark matter, cosmic inflation [48], dark energy, and with the advent of the JWST data, the surprising appearance of massive candidate galaxies [49–51] within ∼ 600 Myr of the Big Bang.

First introduced by Sadi Carnot [52] and Rudolf Clausius [53], the concept of entropy in classical thermodynamics related to systems away from equilibrium. What is meant here by entropy is that which the early adopter of Bayesian probability [54], the physical chemist Linhart [55–57] considered in deriving an expression for the heat capacity as a function of temperature from classical thermodynamic principles that he then successfully applied to the experimental standard entropy data of many substances over a broad range in temperature. As Bekenstein remarked (*Scientific American*, April 1, 2007), "This law is central to physical chemistry and engineering; it is arguably the physical law with the greatest impact outside physics." Without regard to the microscopic details of a system, thermodynamics is tasked with identifying which operations are technically feasible and which resources can be exploited to effect economically sustainable state transformations. Generally, macroscopic phenomena are not time-reversal invariant, prompting Eddington [58] to term this dichotomy in the nature of time as the thermodynamic "arrow of time".

Statistical mechanics was developed later and applied to many-bodied systems at or near equilibrium by such luminaries as Gibbs, Boltzmann, Planck [7] et *inter alia*. Discounting any perceived disrespect, that framework and its principles, in the absence of evidence to the contrary, does not regulate a single molecule or its known Universe. Just so, a horde of molecules in their Universe(s) are subject to the SLT without exception. This is the primary premise of this paper.

Many papers and books [59–70, for e.g.] intended to provide an explanation of the arrow of time focus on the initial (and to a lesser extent, boundary conditions) of the Universe whose initial conditions unknown [71, 72, et passim]. Feynman [73, loc. cit., p. 116]'s "past hypothesis" posits that the early Universe had low entropy in compliance with the SLT. Subsequently, Roger Penrose argued [74, 75, et passim] that the curvature of the Weyl tensor vanishes at any initial singularity (including the Big Bang) so that the evolution of the Universe be close to a Friedman-Robertson-Walker model of matter in near perfect thermal equilibrium at ∼ 10^{15} K ≃

1 GeV whose gravitational degrees of freedom remain unexcited until triggered at the ∼ 375,000 yr cosmic microwave background (CMB) milestone in the aftermath of a low-entropy constraint as had been hypothesized by Feynman.

Penrose [76] proposed a conformal cyclic cosmology (CCC). This is an eternal recurrence process, whereby universes are spawned, grow, and die in a sequence of aeons, with post-evaporating black holes and the arguable loss of information [77] at their singularity leaving traces of Hawking points (large temperature gradients between ring-like anomalies) of their primordial existences in the CMB of progeny universes based on evidence [78, for e.g.] that has so far failed to hold up to scrutiny [79–81]. By hypothesis, aeons have neither a beginning nor an end and contain only massless particles, photons and gravitons. Penrose's theory includes the existence of erebons, hypothetical heavy particles with masses of about the Planck mass that are candidate particles for dark matter but which are ultimately unstable since at the end of an aeon there must be an absence of mass to get to the conformal invariance pivotal to CCC.

It is a popular claim that because entropy is an extensive property, the reason violations of the SLT are not seen is due to molar statistics: as systems reduce in size, fluctuations (sic uncertainties) increase so that violations ought to become more probable. Challenges to the SLT and proposals for its replacement abound [8–10,82–84, for e.g]. However, without their independent verification including computer simulations that openly demonstrate the positivity* of dynamics [85, 86], the SLT is indomitable regardless of premature reports of its putative demise.

Pioneering work by Hill [87] in the early 1960s showed how thermodynamics could be applied to many small systems – aerosols, colloids, dust, and nanosystems. The thermodynamics of small systems has taken on a new importance due to the development of nanoscience, with thermodynamics as applied to nanoscale particles being now known as nanothermodynamics [88, 89]. The nanothermodynamics community has for some time broadened its enquiries into the single-molecule domain beyond the thermodynamic limit [90–93] without invoking quantum phenomena. Quantum thermodynamics [94, 95] tries to go even further by striving to extend classical thermodynamics and nonequilibrium statistical physics to ensembles of sizes below the thermodynamic limit with the full inclusion of quantum effects, even for nanoscale objects [96] and single trapped quantum systems [97]. It differs from statistical mechanics in its attention to dynamical processes out of equilibrium [98]. Kosloff [99] has provided a perspective on a dynamical view of quantum thermodynamics in which the laws of thermodynamics are true in any quantum circumstance [100, et passim].

Extending thermodynamics beyond its bulk matter limits

---

*Adjusting what should be a positive solution to zero on first detecting it going negative is an all too-common programming practice.

is increasingly prevalent in the push towards the fabrication of miniaturized systems offering technological advantages. The main benefit of single-molecule investigation is the deconstruction of ensemble averages to provide information about complex systems since in natural systems the average outcome of the group is rarely the same as the outcome of the individual which may be all that is important. Ensemble averages depend on probability distribution functions and a medley of principles and assumptions that are not applicable to a lone system. Even though the time average of an observable of a system is directly related to experiment, empiricism has lost favor lately to computer simulation that replaces averages over time by instantaneous averages over an ensemble. Quantum mechanics governs the dynamics of individual subatomic, atomic, and molecular systems with well-predicted outcomes. Whether a system is small (a molecule) or not (the known Universe) is relative to its context and how that affects it and our attention to it.

Interest in single molecule behavior received a significant boost following Neher and Sakmann's 1991 award of the Nobel Prize in Physiology or Medicine for discoveries revealing the function of single ion channels via their development of the patch clamp technique (*Scientific American*, March 1992) through which biological scientists could inexpensively isolate ion channels of cell membranes that engage in cellular signaling processes. This resulted in a momentous revolution in cell biology – unseen in physics notwithstanding Schrödinger's *What is Life* manifesto proclaiming physics' dominance over biology – leading to greater understanding of disease mechanisms and the discovery of new therapeutic drugs. As recently as the early 1980s, the notion of cell membranes and their information networks of single ion channels were being challenged by the now debunked [101] and obdurate belief [102] that the cell and even life itself is explicable in terms of the "nano-protoplasm" whose function and properties are inextricably tethered to the framework of statistical mechanics. The rapid progress in quantitative single-molecule measurements are well documented [103, 104, et passim] and contrast with the obsolete "new view" [105, et passim] energy landscape ensemble approach to the protein folding problem which relies almost exclusively on computer simulation of the chemical physics modeling [106, 107] of such.

X-ray crystallography and cryo-electron microscopy have traditionally allowed the imaging of biomolecules at the atomic level using samples that have been crystalized at ultracold temperatures. Atomic force microscopy (AFM) of molecules allows them to be probed under more physiologically appropriate conditions. A localization image reconstruction algorithm [108] can process data from multiple scans of single molecules and can even be used retroactively to reveal new details hidden in old AFM data. Instead of observations on hundreds of molecules, the same molecule is observed hundreds of times in calculating a high-resolution map. Such

a map, from the same molecule as it transits from one conformation to the next and not from thousands of molecules in one or the other conformation, mitigates the potentially misleading results that can occur when averaging data from many molecules when only one matters. Advances in single-molecule microscopy have evolved to permit the study of systems ranging from small molecules to living cells with the prospect of revolutionizing the modern biosciences [109–111, for e.g.].

In principle, reliable structural information in conjunction with the use of computational methods should guide structure-based screening to drug discovery and design. Long after Dirac [112, loc. cit., p. 714] advised that it "…becomes desirable that approximate practical methods of applying quantum mechanics should be developed, which can lead to an explanation of the main features of complex atomic systems without too much computation," such pursuit led to the realization [113, loc. cit., p. 109] of the "central embarrassment of molecular mechanics, namely that energy minimization or molecular dynamics generally leads to a model that is less like the experimental structure," whether through such excuses as deficiencies in force fields (potentials), limitations in computational power allegedly to be solved with supercomputers of the past but now demanding quantum computers of tomorrow, artifacts in structures [114] that result from collecting crystallographic data under cryogenic conditions to minimize radiation damage, etc.

With its roots in phenomenology, Clausius' inequality defines the change in entropy for a cyclic process (including full-body immersion in its surroundings) and its role as a measure of the dispersal of energy or heat at a specified temperature. If the amount of energy added by heating and the temperature can be measured during the process, Clausius' inequality can be used to determine whether the process is reversible or irreversible by carrying out the integration in the inequality. The following provides an alternative way of distinguishing between the two extremes for systems whose notion of work is no different than that in all of physics even if their dynamics is governed by time-reversible quantum mechanics without resort to any particular entropy functional.

Introduction of the concept of entropy and its permissible changes through Clausius' expression of the SLT predates both Gibbs' notion of the statistical ensemble and Boltzmann's specific entropy functional connecting the macroscopic system with the probabilistic populations of microscopic states amenable to that ensemble. Unlike thermodynamics, Boltzmann-Gibbs statistical mechanics, whatever its successes, has limited domains of applicability as known to its practitioners, including so-called anomalous systems that have strong long-range effects, nonlocal correlations between different subsystems of a system, nonMarkovian behavior, violations of reductionism for such thermodynamic properties as entropy and internal energy, etc. Having found no systematic way to uniquely determine how to describe the en-

tropy of dynamical systems who survey their configuration spaces in ways more complex than prescribed by ergodicity, Tsallis [115] proposed a nonextensive (nonadditive) measure [116] which generalizes Boltzmann-Gibbs extensive (additive) metric to deal with such anomalous systems. The Boltzmann-Gibbs and Tsallis entropies are each time invariant and applicable at best to systems at or near thermal equilibrium. Neither of these entropies are *a priori* applicable to nonequilibrium systems which is why here, in consideration of a single molecule, no appeal to either extensive or nonextensive statistical mechanics is made but rather to classical thermodynamics, electrodynamics, and quantum mechanics as appropriate descriptors in their respective macroscopic and microscopic milieus. Time-dependent entropy changes are given by Clausius' inequality as follows from his formulation of the SLT on the basis of a cyclical thermodynamic process to distinguish an irreversible from a reversible change of a lone system in a thermal field.

Thermodynamic systems under sentient observation are embedded in the known Universe and are never "isolated" [117] or "notional": they are either closed or open, closed if they exchange only heat with their environment and open if they exchange mass with or without the exchange of heat with their surroundings. For all their intrigue, such quasi "isolated" systems as Bose-Einstein [118, 119] and Fermi-Dirac [120] condensates do neither and are of no interest here. According to the SLT, systems of interest generate entropy in a time-asymmetric way in accord with the macroscopic concept of entropy and common experience. That classical and quantum dynamics and electrodynamics suggest otherwise has led to a deluge of researches in recent years that offer explanations for this so-called time-reversal symmetry breaking or claims that the SLT is subject to regular violations. Here, the primary intent is to show that, at the microscopic level, entropy is T-asymmetric and requires neither the intercession of time-reversal symmetry breaking mechanisms nor assent to the belief that the SLT can be controllably broken.

The purpose of this paper is to provide the physical basis for the SLT's T-asymmetry from T-symmetric quantum mechanics and electrodynamics without obliging either of them to relinquish their mutual time-reversal invariance. The route to this is simple if somewhat circuitous relative to that of Stenger [121, loc. cit., 3972]'s, say:

> It is hard to see how the breakdown of T-symmetry at the microscale implies time irreversibility at the macroscale, although I am not prepared to rule it out,

an opinion easily brought up to speed as will be shown by beginning in the first instance at the molecular scale before moving on to reveal that the same considerations apply in larger-scale self-gravitating systems.

Materials and structures are the products of the evolution of the Universe. How they appeared and their subsequent transformations are pivotal to our understanding of the Universe and our place within it. All dissipative structures in the Universe including all forms of life, owe their existence to the fact that the Universe started in a low entropy state and has not yet reached equilibrium [122, et passim]. Deep considerations of such phenomena are beyond the scope of this paper and its specific purpose: to explain why the arrow of time is asymmetric regardless of the time-reversal invariance of quantum mechanics and electrodynamics.

The paper uses the nonrelativistic quantum mechanics of a single molecule to relate its wave function's local phase to forces acting on its nuclei and electrons in the presence of a thermal environment. In the intake of sensible heat from its surroundings, such a molecule's entropy increases with the gain in entropy determined by its molecular structure as connected to the gradient field of its wave function's local phase whose subharmonicity is shown to be a necessary and sufficient condition for it to comply with the SLT. The thermodynamic arrow of time necessitates irreversible over reversible processes as determined by the gradient field of the local phase. Conservative Lorentz-Faraday forces impressing on the nuclei and electrons of the molecule engender irreversible (reversible) change and entropy gain (stasis) in its exchange of heat with its environment under the discernment of the thermodynamic arrow of time and regardless of the time-reversal symmetry [123], [124, cf. Ch. 26] of quantum mechanics or electrodynamics. The implications of the gradient of the local phase on entropy production and Faraday's law of induction are also explored. Additionally, it is shown that in a heat bath a molecule in molar amounts is stable provided its internal electrodynamic potential is subharmonic within its nominal volume V, a fact first anticipated long ago by Earnshaw [125]. This leads into the question of molecular stability as gauged by the virial theorem and by extension to the stability of self-gravitating objects.

A molecule – with its myriad of allowed relative motions determined by its stabilizing potential in analogy with the vibrations of an oscillating string – serves here as a spoiler to its Universe and its equally important if less familiar subsystems. The paper draws a comparison between a single molecule described quantum mechanically in the nonrelativistic limit and its Universe treated in the weak field limit of general relativity, each interrogated under similar thermal circumstances, prior to their respective destinies in anticipation that across such disparate spacetime scales what one learns might surprise in their similarity and simplicity.

1.2 Notation

Rationalized Planck units are used throughout unless otherwise indicated (wayward 4π's excepted). The gradient ∇ formally operates on vector and scalar fields drawn from a Euclidean space whose fiber bundle is a trivial Cartesian product mapping $R^n = \boldsymbol{R}^M \times \boldsymbol{r}^N$ of the molecular structure of an elec-

trically neutral molecule of M nuclei (base, R with gradient $\partial/\partial R = \nabla_R$) of known elemental composition (atomic number Z_i, $i = 1, M$) and the coordinate space (fiber, r with gradient $\partial/\partial r = \nabla_r$) of its N electrons so that each of the $n = M+N$ elements of $\mathbf{x}$ lies in R^3. If $m_{k_j} > 0$, $j = 1, 2, 3; k = 1, \ldots, n$ are the masses of the particles and [] denotes the integer part, $k_j = 1 + [(j-1)/3]$ in order that all three coordinates of a particle relative to a body-fixed origin in the observer's frame at the center of mass are scaled by the same mass. The kinetic energy, its virial, and related quantities of any system of interest (be it an atom, molecule, ion, the known Universe, etc.) free from the clutter of the masses of nuclei and electrons are expressed here as Lebesgue integrals whose operative measures (for volumes V, positions $\mathbf{x}$, etc.) use mass-weighted coordinates. The only limit on n is that imposed by Nature [126, et passim] so that neutral (i.e. $\sum_{i=1}^{M} Z_i = N$) polyatomic molecules (governed by the Coulomb potential) or the known Universe (governed by the Newtonian potential), while their sizes cannot estimate *a priori*, both are $n \geq 4$-body systems whose dynamics are unknown and perhaps even unknowable. The inner product $\langle \mathbf{x}, \mathbf{y} \rangle$ of $\mathbf{x}, \mathbf{y} \in R^n$ is a scalar as is the Euclidean norm $\|\mathbf{x}\| = \sqrt{\langle \mathbf{x}, \mathbf{x} \rangle}$. An orientable surface ∂V has a unit normal $\hat{\mathbf{n}} = \nabla V/|\nabla V|$ at a regular point where[*] $\nabla = \nabla_R \times \nabla_r$ and is undefined at a critical point where ∇V vanishes. The normal $\hat{\mathbf{n}}$ to V twists and turns from regular point to regular point as the boundary ∂V bends in different directions, behavior captured by the local self-adjoint shape operator $\mathbf{S} = -\nabla \cdot \hat{\mathbf{n}}$ [130, cf. Ch. 5], [131, cf. Ch. 6, Ex. 11, pp. 141–142]. The directional derivative of V at a regular point is $D_{\hat{\mathbf{n}}} V = \nabla V \cdot \hat{\mathbf{n}} = \partial V/\partial \hat{\mathbf{n}}$ which is a maximum of $|\nabla V|$ (minimum of $-|\nabla V|$) when $\hat{\mathbf{n}}$ is in the same (opposite) direction as (to) $\hat{\mathbf{n}}$, respectively. The eigenvectors and eigenvalues of $\mathbf{S}$ provide the principal directions and principal curvatures of V, respectively. The principal directions specify the directions a curve embedded in V must travel to have maximum and minimum curvature, these being given by the principal curvatures. Quantum expectation values are denoted by angular parentheses $\langle \blacksquare \rangle$ and their time averages by an over bar $\overline{\langle \blacksquare \rangle}$. Without loss of generality, generic functions are smooth with compact support $C^\infty(R^n)$.

1.3 Outline

The article is organized as follows: In the next section, the thermodynamics of a single molecule in contact with a heat bath is considered. This is followed by consideration of the Faradaic induction of a single molecule. In the succeeding section the relation of the two featured topics are discussed in detail. The central finding of the T-asymmetry of entropy is

---

[*]Finite binary cross products $\times$ exist only in R^3 and R^7 [127]. Their extension to R^n is through the Hodge dual of the exterior product $\wedge$ of $n-1$ vectors in R^n and their Gramian determinant [128, cf. Ch. 7], [129, cf. Ch. 8]. The use here of vector calculus instead of the exterior calculus of differential forms is that it more clearly serves as the universal lingua franca of general physics for the disparate topics under discussion.

shown to rest on the hypothesis that the thermodynamic arrow of time is set by the local phase of the wave function of the system of interest whose falsifiability is illustrated through a number of demonstrations for self-gravitating systems. The requirement that the phase be subharmonic in a volume under curvature flow is emphasized whatever the size and shape of the system.

It is not the intent here to calculate the entropy in any system, be it a single molecule or any other particle or structure in its known Universe, but rather to point out that, whatever their fate in a thermal field, the T-asymmetry of entropy changes will feature in their evolution until it hardly matters. Both experimental demonstration and computer simulation are outside the scope of this paper. Equally, deliberations of generalized thermodynamics specific to black holes are not part of this paper.

2 Thermodynamics in a thermal field

Recall that quantum theory distinguishes between two types of system states, viz. pure and mixed [132]. A system in a pure state possesses both a well-defined probability amplitude and phase. In contrast, the mixed state describes a system whose phase information is incomplete. Since the density matrix ϱ for a system to be in a statistical ensemble of different pure states is a positive semi-definite, self–adjoint operator, it has a spectral decomposition $\varrho = \sum_i \lambda_i |\varphi_i\rangle\langle\varphi_i|$ where $|\varphi_i\rangle$ are orthonormal state vectors with $\lambda_i > 0$ and $\sum_i \lambda_i = 1$. ϱ evolves via the von Neumann equation $\dot{\varrho} = [H, \varrho]$ where H is the Hamiltonian operator of the system. The von Neumann entropy of the ensemble of pure states is [133] $S(\varrho) = -\sum_i \lambda_i \ln \lambda_i = -\mathrm{Tr}(\varrho \ln \varrho)$, with the number of states needed to describe the system being the number of eigenvalues λ_i of ϱ, each of which provides the weight of its respective state. Thus, $S(\varrho) > 0$ for a mixed state and $S(\varrho) = 0$ for a pure state (with $\lambda_1 = 1$). As $\varrho = |\psi\rangle\langle\psi|$ casually goes from a pure ($\mathrm{Tr}(\varrho^2) = 1$; $S(\varrho) = 0$) to a mixed ($\mathrm{Tr}(\varrho^2) < 1$; $S(\varrho) > 0$) state, the entropy gain ΔS increases. For mixed states the entropy measures how far the state is from being pure. Apart from a factor of $k_B \ln(2)$ involving the Boltzmann constant, Gibbs thermodynamic entropy is identical to the von Neuman entropy and is most relevant for systems with a large number of degrees of freedom.

Consider a single molecule in a pure state $\psi(\mathbf{x}, t)$ of charge density $\rho(\mathbf{x}, t) = |\psi(\mathbf{x}, t)|^2$ that is $(-1)^{2s}$-symmetrized for boson (s, integer spin) and fermion (s, half-integer spin) coordinates [134, et passim]. The molecule is free of spatial confinement other than that provided by the Coulomb potential. Nuclei with integer spins are bosons and those with half-integer spins are fermions as are electrons which are spin $1/2$ elementary particles. Both $\psi(\mathbf{x}, t)$ and the operator $O(\mathbf{x}, t)$ are time dependent in the interaction picture of quantum dynamics. A state is pure if the density matrix $\varrho = |\psi\rangle\langle\psi|$ for some unit state vector ψ so that $\varrho^2 = \varrho$ and the expectation value

of a self-adjoint operator O is $\langle O \rangle = \mathrm{Tr}(\varrho O) = \langle \psi, O\psi \rangle$. Pure states are relevant if they come from the ground state in which the first excited state has a large energy gap that exceeds $\sim k_{\mathrm{B}} T$ at the absolute temperature T. If O has a complete set of eigenvectors ϕ_j with real eigenvalues o_j, then $\langle \psi, O\psi \rangle = \sum_j o_j |\langle \psi | \phi_j \rangle|^2$ where the o_j's are the possible outcomes of the measurement of O and $|\langle \psi | \phi_j \rangle|^2$ is the transition probability that this outcome occurs. This choice of state is consistent with Bridgman [135]'s operationalism with the inclusion of quantum mechanical considerations by Giles [136, 137] in a rigorous formulation [138] of thermodynamics. By and large the paper adopts the Ithaca [139] interpretation of quantum mechanics.

It is always the case that $\psi(\mathbf{x}, t)$ complies with the Pauli exclusion principle (PEP). Any pair of point particles whose exchange is constrained by the PEP are distinguishable if their separation is large compared to their de Broglie wavelength ($\lambda_{\mathrm{th}} \sim 1/k_{\mathrm{B}} T$ for massless particles [140] such as the photon or the graviton). Thus, while symmetrization is of undoubted importance, it is increasingly less crucial the further away from equilibrium a system is driven to where the very identification of $\psi(\mathbf{x}, t)$ is in doubt. Entropy quantifies the extent to which the exact state of a system of interest is in doubt and reflects deficits in whatever information is at hand to correctly make that specification. For arbitrary t, $\psi(\mathbf{x}, t)$ is given. When the system is perturbed, the state evolves with increasing loss of information or gain in entropy about its current condition. The system of minimum entropy evolves via the time-dependent Schrödinger equation and its probabilistic underpinnings. Subsequent entropy production will be related in what follows to the spontaneous work done on such a system in a heat bath by electrodynamic forces internal to the system and not to a statistical prescription of entropy more appropriate to an ensemble of such systems at or near thermal equilibrium.

In electromagnetic theory charge density is idealized as a smooth scalar function of position to be regarded as a continuous distribution, somewhat like a fluid or field. If the wave vector in its coordinate $\mathbf{x}$ representation is accompanied by an arbitrary local phase factor, nonrelativistic quantum mechanics is invariant under a local gauge transformation whether in an external [141, cf. Sec. 22 and 27] or internal [142, 143] electromagnetic field. In the latter case the evolution of the probability density $\rho = |\psi|^2$ fulfills the continuity equation, a quasilinear first-order conservation law partial differential equation (PDE),

$$\frac{\partial \rho}{\partial t} + \nabla \cdot \mathbf{j} = 0 \,, \tag{1a}$$

within a deformable volume element dV centered at $\mathbf{x}$ in terms of the divergence of the probability current

$$\mathbf{j}(\mathbf{x}, t) = -\frac{i}{2} \left(\psi^*(\mathbf{x}, t) \nabla \psi(\mathbf{x}, t) - \psi(\mathbf{x}, t) \nabla \psi^*(\mathbf{x}, t) \right) \tag{1b}$$

to ensure unitarity at all $(\mathbf{x}, t)$ in analogy with the mainte-

nance of mass, charge, and heat balance in continuum mechanics, electrodynamics, and thermodynamics, respectively. When $\nabla \cdot \mathbf{j} > 0$ so that the number density is decreasing in dV then $\partial \rho / \partial t < 0$ and conversely. If V is large enough to be essentially unbounded, ψ is square integrable and vanishes at infinity where Sommerfeld [144, cf. §28]'s radiation condition ensures that infinity is an absorber (sink) but not an emitter (source) and that once probability current exits the scene it does not reenter (a rigorous requirement for the existence and uniqueness of ψ). For future reference, notice that the current density $\mathbf{j}(\mathbf{x}, t)$ is an even function of time [145], i.e. $\mathbf{j}(\mathbf{x}, t) = \mathbf{j}(\mathbf{x}, -t)$, under Wigner [123], [124, cf. Ch. 26]'s prescription for time reversal in quantum mechanics. Recall [145] also that the probability density ρ is even in t.

For ψ expressed in polar form as $\psi(\mathbf{x}, t) = e^{i\theta(\mathbf{x}, t)} \sqrt{\rho(\mathbf{x}, t)}$, the continuity equation reduces to

$$\frac{\partial \rho}{\partial t} + \nabla \cdot (\rho \nabla \theta) = 0 \tag{2}$$

in terms of the probability density ρ and a finite local phase factor θ which has units of action, i.e. [energy][time] or [momentum][length]. With ψ being single valued so too is ρ. Wherever ψ vanishes so too do ρ and $\mathbf{j} = \rho \nabla \theta$.

If $\nabla \theta$ vanishes so does $\mathbf{j}$ and the system is in a stationary state with normalizable ρ. Here the focus is on the situation where $\nabla \theta$ is finite almost everywhere, a circumstance governed by the Morse-Sard theorem [146, 147] to the effect that critical points at which $\nabla \theta = 0$ are few to none compared to regular points where $\nabla \theta \neq 0$. That said, there are several reasons to support the view that θ is subharmonic ($\nabla^2 \theta > 0$) in V [148, 149], viz.

1. At nodes in ψ, $\theta = \tan^{-1}(\mathrm{Im}\,\psi / \mathrm{Re}\,\psi)$ is indeterminate. If the potential energy part of H has no explicit time dependence, Hamilton's principal function $\theta(\mathbf{x}, t)$ (classically, W) is additively separable in $\mathbf{x}$ and t, i.e. $\theta(\mathbf{x}, t) = \phi(\mathbf{x}) - Et$, where $E = \langle \psi | H | \psi \rangle$ is the energy expectation value for normalized ψ, $\phi(\mathbf{x})$ (classically, S) is Hamilton's characteristic function, and $\nabla \theta(\mathbf{x}, t) = \nabla \phi(\mathbf{x})$ is the time-invariant gradient or relative phase*. In the hydrodynamic interpretation [152], [153, et passim] of quantum mechanics, where substituting $\psi = e^{i\theta}|\psi|$ into the Schrödinger equation gives a system of two coupled PDEs, viz. a continuity equation for ρ treated as a classical fluid and a surreal quantum potential modification of the classical Hamilton-Jacobi equation for θ which is of $O(\hbar^2)$ in the rationalized Planck constant $\hbar$, $\nabla \theta = \nabla \phi$ is taken to represent the momenta of all particles (nuclei and electrons), an interpretation adopted by Schrödinger in formulating wave mechanics following both Hamilton's analogy between geometric optics

---

* Schrödinger [150] explained how he had come upon the wave equation and identified ϕ as what he termed the "phase angle of the wave function" [150, loc. cit., p. 499; p. 505] it regulates, as inspired by de Broglie [151].

and classical mechanics and de Broglie's wave-particle hypothesis [151, 154], [155, cf. Ch. VIII], [156], [157, cf. Ch. 2.2.4] in which a wave train is associated with the motion of a material particle, the frequency and wavelength being related to the energy and momentum by the Planck-Einstein relation for radiation quanta.

The optico-mechanical analogy invoked by Schrödinger [158] in arriving at his eponymous wave equation for $\psi(\mathbf{x}, t)$ is well documented [159–162] and does not need to be rehashed here. Suffices to say that in his interpretation and adaption of de Broglie's "phase wave" ideas, Schrödinger denied any real meaning to ϕ since to do so would imply that one could speak meaningfully of electric charge being in a particular place or following a single path (sic trajectory) in an atom and capitalized *inter alia* on two interrelated observations [163], viz. (i) recognition that the gradients $\nabla\theta(\mathbf{x}, t) = \nabla\phi(\mathbf{x})$ are normal to the wave fronts or level sets of $\theta(\mathbf{x}, t)$, the surfaces of constant action; and, (ii) that since the light rays of optics are normal to those wave fronts, so too are particles whose uncertain loci follow the undulations in $\nabla\phi(\mathbf{x})$ so that the direction of $\mathbf{j} = \rho\nabla\phi$ is locally normal to the level sets of de Broglie waves[*] of local phase ϕ. Note that $\nabla\phi$ is distinct from the group velocity of its localized wave packet[†].

In retracing this optico-mechanical analogy one sees that to $O(\hbar^0)$ the Hamilton-Jacobi equation for the relative phase $\nabla\phi$ is

$$\frac{1}{2}(\nabla\phi)^2 = E - \mathcal{V}, \qquad (3a)$$

where $\mathcal{V}$ is the potential energy. Schrödinger recognized that (3a) has the solution $e^{i\nabla\psi}$ whereupon

$$\frac{1}{2}(\nabla\psi)^2 - (E - \mathcal{V})\psi^2 = 0, \qquad (3b)$$

and a variational problem [168] on ψ leads to the time-independent wave equation which he applied to the H

---

[*]In showing the equivalence of his formulation of wave mechanics to the matrix mechanics approach of Heisenberg et al [164–166], Schrödinger acknowledged [167, loc. cit., p. 735, fn. 2] his indebtedness to de Broglie's extension of wave-particle duality for photons to matter and Einstein's advocacy of that extension to him.

[†]The amplitude $\sqrt{\rho}$ has no unique position or velocity but is smeared over space as a wave packet of phase ϕ. In a double-slit interferometer it is particles that are detected, not delocalized waves as $\sqrt{\rho}$ implies: photons and particles travel as waves but hit the detector as particles. This raises the problem of how $\sqrt{\rho}$ from its source changes from wave to particle. Bohr and Heisenberg (in their Copenhagen interpretation of quantum mechanics) claimed that it was the observer who decides the outcome. ρ is a wave of probability (via Born's conjecture, according to which one must expect to find the particle where ρ is high) provided $\sqrt{\rho}$ collapses at the screen regardless that it arrived there as a wave travelling through all slits without prejudice while interfering as a wave enroute to the detector. Just how $\sqrt{\rho}$ collapses is an open question whose resolution endures as the so-called "measurement problem" whose most popular if arguable rationalization is the many worlds interpretation of quantum mechanics.

---

atom and post haste produced its time-dependent equivalent wherewith wave mechanics was born [163, et passim]. At this point ϕ and $\nabla\phi$ appear to have fallen through the cracks to be replaced by all things ψ until de Broglie [151, 154]'s and Madelung [152]'s earlier work was resuscitated by David Bohm in the early 1950s, through his retention of the connection $\nabla\phi = \mathbf{j}/\rho$ as a guidance law governing particle motions pursuant to their deterministic trajectories in what is an active alternative [169–171, et passim] to the Copenhagen interpretation of quantum mechanics with its focus on probabilistic energy and angular momentum eigenvalues, and dubbed de Broglie-Bohm mechanics, pilot-wave theory, causal interpretation, etc. by its practitioners [172, for e.g.]. Hereon while $\mathbf{j} = \rho\nabla\phi$ in terms of the wave-particle velocity $\nabla\phi$ and the charge density $\rho = |\psi|^2$ is acknowledged, Bohmism is otherwise ignored in proceeding.

Invoking de Broglie [151, 154]'s interpretation of Sommerfeld [173]'s (and Wilson [174]'s) quantization rule, a condition which ensures that matter waves make standing waves only at discrete energies, suggests that

$$\oint_{\partial V} da\, \hat{\mathbf{n}} \cdot \nabla\phi = \int_V d\mathbf{x}\, \nabla^2\phi = 2\pi k, \qquad (4)$$

where $\hat{\mathbf{n}}$ is a unit normal to ∂V on a patch of area da, ϕ is both multivalued and subharmonic in V, and $k \in \mathbb{Z}^+$. At nodes in ρ, $\mathbf{j}$ vanishes but not necessarily $\nabla\phi$ which may jump in discrete amounts and, since by Stoke's theorem $\int_V d\mathbf{x} \cdot \nabla \times \nabla\phi$ vanishes, there are no accompanying vortices should any such jumps occur. A measurement on a system subject to (4) would result in a jump in its state, a collapse of its wave function ψ following which its phase ϕ and its gradient $\nabla\phi$ would vanish whereupon it would find itself in a reversible state.

2. The flux of the probability current $\mathbf{j}$ has two contributions, viz.

$$\nabla \cdot \mathbf{j} = \rho\,\nabla^2\phi + \nabla\rho \cdot \nabla\phi, \qquad (5)$$

the first of which is positive if ϕ is subharmonic while the second governs whether the amount of charge within a differential volume dV is decreasing (increasing) according as it is of positive (negative) sign.

This allows (1a) to be rewritten as

$$\frac{D\rho}{Dt} + \rho\,\nabla^2\phi = 0 \qquad (6)$$

in terms of the substantial derivative $D/Dt = \partial/\partial t + \nabla\phi \cdot \nabla$. In an Eulerian specification of the flow field of ρ, the total derivative consists of two terms, the first $\partial/\partial t$ of which provides the changes at a fixed position due to unsteadiness in the flow while the second $\nabla\phi \cdot \nabla$

gives the rate at which ρ is convected to that location. Neither contribution vanishes in an unsteady flow. The substantive flow of ρ will be accelerating if ϕ is subharmonic ($\nabla^2\phi > 0$). Physically, pursuit of ρ whether it relates to a single molecule or any other particle or structure in its known Universe from a Lagrangian or an Eulerian perspective is a matter of convenience. For the present purposes the latter is chosen.

3. If $\mathbf{j}$ is decomposed via the Helmholtz-Hodge theorem [175–178] to the sum of longitudinal and transverse parts whereby $\mathbf{j} = \mathbf{j}_\| + \mathbf{j}_\perp$ with $\mathbf{j}_\|$ and $\mathbf{j}_\perp$ being parallel and orthogonal to $\nabla\phi$ and $\nabla \times \mathbf{j}_\| = 0$ and $\nabla \cdot \mathbf{j}_\perp = 0$, respectively, then $\rho\nabla^2\phi = \nabla\cdot\mathbf{j}_\perp = 0$ and $\nabla\rho\cdot\nabla\phi = \nabla\cdot\mathbf{j}_\|$, where for $\mathbf{x}, \mathbf{x}' \in V \subseteq R^n$

$$\mathbf{j}_\|(\mathbf{x},t) = -\int_V d\mathbf{x}' \frac{\nabla' \cdot \mathbf{j}(\mathbf{x}',t)}{4\pi|\mathbf{x}-\mathbf{x}'|} + \oint_{\partial V} da' \frac{\hat{\mathbf{n}}' \cdot \mathbf{j}(\mathbf{x}',t)}{4\pi|\mathbf{x}-\mathbf{x}'|} \tag{7a}$$

and

$$\mathbf{j}_\perp(\mathbf{x},t) = \int_V d\mathbf{x}' \frac{\nabla' \times \mathbf{j}(\mathbf{x}',t)}{4\pi|\mathbf{x}-\mathbf{x}'|} - \oint_{\partial V} da' \frac{\hat{\mathbf{n}}' \times \mathbf{j}(\mathbf{x}',t)}{4\pi|\mathbf{x}-\mathbf{x}'|}, \tag{7b}$$

so that $\nabla \cdot \mathbf{j} = \nabla \cdot \mathbf{j}_\|$. If V recedes to infinity and $\mathbf{j}$ is regular there, the above surface integrals vanish. This decomposition of $\mathbf{j}$ results in ϕ being harmonic which is not pursued for the aforesaid reasons in addition to the following.

4. By the maximum principle [149, 179], if ϕ is subharmonic in V it attains its maximum on ∂V and not in the interior of V.

5. In the finale of this paper, an arguably propitious ending to a moribund and timeless Universe [180, 181, for e.g.] is suggested.

A molecule is a sufficiently stable, electrically neutral group of at least two atoms in all manner of configurations and shapes held together by covalent bonds in the long-range Coulomb field acting between its constituent electrons and nuclei. It may consist of atoms of a single or different elements or of isotopes of the same element. Molecules are of many types and shapes but for each the problem in describing their nuclear motions differ. The arrangement of their atoms allows them to rotate coupling to the vibrations of their nuclei as well as to the orbital and spin angular momenta of their electrons. Condensed phases exhibiting metallic bonding, noncovalent bonds (ionic and hydrogen bonds), glasses (solids in a vitreous state), and materials of several classes (dielectrics, conductors, semiconductors, insulators, etc.) do not strictly present as single molecules, that object whose response to minimal interrogation is consistent with reductionist inquiry. As a single molecule contacts a heat bath of low-to-moderate temperature on ∂V it becomes excited: its nuclei move with the absorption of photons (vibrational energy) or rotons (angular momentum energy) and under the aegis of its Hamiltonian operator the configuration of its electrons and nuclei changes while endeavoring to maintain stability as it restores equilibrium through the redistribution of energy among its low-frequency degrees of freedom. If equilibrium is unattainable or the heat reservoir is at a high enough temperature the molecule will rip apart, dissociating into other smaller molecules or sundry reactive fragments (free radicals, atoms, ions, bare nuclei, free electrons, etc.) which eventually relax to stable entities through collisional deactivation with each other or the spontaneous emission of light. In macromolecules the transduction of the energy available falls within physiologically sustainable thermal limits of biological processes when mediated by specific enzymes with the involvement of ancillary molecular devices (membranes, filaments, channels, templates, etc.) [182].

Thermodynamics [183, for e.g.] is independent of quantum mechanics and its concepts which equate the internal energy U to the sum of the kinetic and potential energies of all elementary particles that comprise the system. Molecular stability does not rest solely with the Hamiltonian operator of the "isolated" molecule. Neither the system's state ψ nor its expected energy $\langle H \rangle$ is a stationary state or an energy level of the molecule, respectively, whose environment contains both matter and radiation [184], the molecule being amenable to the receipt of sensible heat only from its environment. In addition to the conservative Coulomb interactions included in the potential part of the Hamiltonian operator are Lorentz-Faraday interactions between the electrons and nuclei of the molecule that are affected by the surroundings in which a molecule resides. The internal force $\boldsymbol{F}_{\text{int}}(\mathbf{x},t)$ acting within a molecule viewed as a closed conservative system (*vide infra*) is

$$\boldsymbol{F}_{\text{int}} = \frac{\partial\mathbf{j}}{\partial t}\, u(T)\,, \tag{8a}$$

where $u(T)$ is the Heaviside step function, it being 1 if $T > 0$ and 0 otherwise (when the system is "isolated"). Hereon $u(T)$ is dropped in $\boldsymbol{F}_{\text{int}}$, its requisite presence being understood. At finite T, $\boldsymbol{F}_{\text{int}}$ is a conservative Lorentz-Faraday force acting on the nuclei and electrons of the molecule and gives rise to an energy contribution $\nabla\cdot\boldsymbol{F}_{\text{int}}(\mathbf{x},t)$ to their kinematic motions; otherwise $\boldsymbol{F}_{\text{int}}$ is zero and inoperative. Like $\mathbf{j}(\mathbf{x},t)$, $\boldsymbol{F}_{\text{int}}(\mathbf{x},t)$ is a self-adjoint operator.

Since $\mathbf{j}(\mathbf{x},t) = \rho(\mathbf{x},t)\,\nabla\phi(\mathbf{x})$ and with the use of (1a), (8a) may be rewritten as

$$\frac{\partial\mathbf{j}}{\partial t} + \nabla\phi\,\nabla\cdot\mathbf{j} = 0\,, \tag{8b}$$

a quasilinear first-order PDE for $\mathbf{j}(\mathbf{x},t)$. In contrast to (1a), (8b) is not a continuity but rather an advection equation. Un-

der time reversal (8b) is

$$\frac{\partial \mathbf{j}}{\partial t} - \nabla \phi \, \nabla \cdot \mathbf{j} = 0. \tag{8c}$$

If the initial/boundary-value problem PDE in (8b) has the solution $\mathbf{j}(\mathbf{x}, t) = \rho(\mathbf{x}, t) \, \nabla \phi(\mathbf{x})$, the backward initial/boundary-value problem PDE in (8c) is physically equivalent to the forward time (8b) with the sign of $\nabla \cdot \mathbf{j}$ flipped. If ϕ is subharmonic, $\nabla^2 \phi > 0$ independently of the sign of t.

A thermodynamic process changes the state of a system under the action of a driving force, external or internal. The larger the force, the more the process proceeds, perhaps, subject to kinetic constraints. A reversible process is an idealization that can be reversed at any time by an infinitesimal change in the driving force that reverses its sign; it must occur infinitely slowly so that the system and its surroundings have time to relax through staged equilibria ultimately leading each to reach stasis. There are no truly reversible processes in Nature, only calculations for them that are applied to real processes which are irreversible and whose original state cannot be restored without concomitant changes to the surroundings.

Thermodynamics is concerned only with the effects of heat and work in the interaction between a system and its environment. Its laws not only exert their influence in every field of the natural sciences, but also play a part in all industrial processes in which energy is transferred. It does not inquire into the mechanism of phenomena and so it is unconcerned with what happens on an atomic or subatomic scale even though that perspective can help to give deeper meaning to its laws and concepts. The branch of science concerned with this is statistical mechanics, the mechanics of such a large number of atoms or molecules that specifying the state of each is impossible and one is forced to use statistical methods. Entropy is calculated via Boltzmann-Gibbs statistics applicable to ensemble representations of the system under study which, however, are unavailable here. Single molecule techniques [185, 186] reveal behavior masked in ensemble averages of complex systems.

There are many physical statements of the SLT any one of which can be used to show its equivalence to another and to prove the mathematical statement of the SLT: there exists a state function (entropy, S) whose change ΔS for any spontaneous process satisfies the Clausius inequality [53, 187]

$$\Delta S(t) \geq \oint_{\partial V} \frac{dQ}{T} \geq 0 \tag{9}$$

which encapsulates the increase in entropy principle. The distinction between the system and its surroundings must be unambiguous through the presence of a *bona fide* boundary across which the flux of matter, charge, heat, etc. can freely pass. A constant-temperature (T) heat bath with which the system is in contact through its boundary ∂V serves as the

surroundings. The integral is over the surface ∂V that constitutes the boundary between the molecule of volume V and its environment. The Clausius integral $\oint_{\partial V} dQ/T$ is positive for irreversible processes, is zero for reversible processes, and can never be negative. The inequality implies that the entropy given to the environment is greater than the entropy transferred as heat from the hot reservoir. The operative Carnot cycle here is a fiduciary audit of the net exodus of efflux over the coverage of ∂V contacting the heat bath. It is this audit that undermines all supposed objections to the SLT, just as Planck [7, loc. cit., pp. 103–104] anticipated. If $\oint_{\partial V} dQ/T$ vanishes, $1/T$ is an integrating factor [188, 189] for dQ, an inexact differential.

The two best-known statements of the SLT are: (1) If a system undergoes a Carnot cyclic process it cannot turn heat entering the system into work done on the surroundings with unit fractional efficiency (Kelvin-Planck statement); (2) Heat cannot flow spontaneously from a cooler to a hotter object (Clausius' statement). Historically, the mathematical formulation of the SLT was reached through the empirical study of the limitations of steam-driven heat engines designed to convert one form of energy (sensible heat) into mechanical energy (work) at the start of the industrial revolution. Nowadays engines or motors run the gamut from electrical, pneumatic, hydraulic, molecular, etc. using sundry working media. The exchange of work and the working element between a system and its surroundings is always an irreversible process. An alternative mathematical approach to the foundations of thermodynamics emerged from the study of nonlinear deformations of continuous media [190, for e.g.].

The Clausius inequality provides a means of delimiting the entropy change of any process that begins at equilibrium to which state it returns as if nothing happened with no overall change in the entropy of the system and its surroundings, or begins in an arbitrary state to end with a net production of entropy; it means that no process can decrease the entropy of the Universe and, together with the zeroth law of thermodynamics, implies that a temperature of absolute zero is unreachable. Equipped with a false antecedent, the claim that the concept of entropy is inapplicable to single systems (a molecule and its Universe, for e.g.) but only to ensembles of them is as counterfactual [191] as it is casuistic [192]. The Clausius inequality is based on his statement of the SLT and provides a means of distinguishing reversible from irreversible processes based on the earlier findings of Carnot (without his view that heat is a fluid) and independently of volume number density (sic thermodynamic limit).

The first law of thermodynamics relates the internal energy or enthalpy U to heat Q and work W as

$$dU = dQ + dW, \tag{10a}$$

or

$$-dW \leq -dF, \tag{10b}$$

an expression of the fact that the same change dU in U can be produced either by the sole addition of sensible heat $đQ$ or work $đW$ or by contributions from both. The signs used correspond to the IUPAC[*] and not the Clausius convention whereby all net energy transfers from the surroundings (system) to the system (surroundings) are positive (negative), respectively. Here, $đQ = TdS$ and relates U to T, S, and the Helmholtz free energy $F = U - TS$, this being the amount of energy free to do work in response to entropy losses. Gradients in F are the driving forces of all biochemical processes and their reliable calculation [193, et passim] is intensively pursued. The internal energy U is the sum of the sensible heat Q accumulated by the system and the work W done by it although physically each differs from the other. Like $đQ$, $đW$ is an inexact differential and is called the configuration work; it is the amount of work done changing the configuration of a system from one to another and depends on how the work is done, i.e. on the path taken between the initial and final configurations. Energy (kinetic, potential) is an attribute that matter and radiation have or can acquire or lose. Unlike entropy, energy is a conserved quantity but this is difficult to audit especially when it dissipates or thermalizes. Both kinetic and potential energies are interconvertible and their scales are arbitrary. Heat (thermal, radiation) is a process in which a system acquires or loses energy as a consequence of it having a different temperature than its surroundings. Work is a transfer of energy to or from a system by any means other than heat; it can be fully converted into heat as in friction but heat can only be partially converted to work. There is no entropy associated with energy transfer as work. Although the first law places no restriction on the direction of a process, it does not guarantee that the process will occur, that being decided by the SLT in conjunction with physical and chemical kinetics considerations.

The SLT asserts that [133, 194, for e.g.] natural processes are irreversible, i.e. the entropy $S(t)$ always increases as the system strays from equilibrium at an absolute temperature $T(\mathbf{x}, t)$ via an exchange of heat (and its transformation to mechanical work) $đQ = d\mathbf{x} \cdot \boldsymbol{F}_{\text{int}}(\mathbf{x}, t)$ with its surroundings. The zeroth law of thermodynamics leads to a definition of temperature via the relation $1/T = (\partial S/\partial U)_V$ that forms the empirical basis for the calorific measurement of entropy, with $TdS = đQ$ describing how entropy changes in the amount dS when an inexact differential amount of energy $đQ$ is introduced as heat into the system at a finite temperature $T > 0$ delineated by the zeroth law of thermodynamics.

The Clausius inequality in (9) stipulates that ΔS equals or exceeds the quantity $\oint_{\partial V} đQ/T$. Here $đQ$ is heat or energy or work. There is nothing in science or beyond to prevent the integrand in $\oint_{\partial V} đQ/T$ from being taken to be and applied to an arbitrary system without reference to Boltzmann-Gibbs or Tsallis statistical mechanics. This is precisely what is done

here in accepting $đQ$ for what it is, i.e. the heat (energy) or work (mechanical energy) conversion that occurs between the system of interest and a heat bath (its minimal environment) which it ineluctably contacts.

Regardless of the notion of temperature fluctuations [195–197, et passim] or indeterminacy providing justification for the complementarity relation $\Delta U \Delta(1/T) \geq k_{\text{B}}$ [198–200] in analogy with Heisenberg's uncertainty principle for position and momentum in quantum mechanics, here T is taken to be a parameter that is characteristic of the heat reservoir and is known *a priori* with thermal noise viewed as [201, loc. cit., p. 191] "the least disturbing for the physicist" unconcerned with emerging technologies. If T is the known temperature of the heat bath, $T(\mathbf{x}, t)$ is the temperature at $\mathbf{x} \in \partial V$. To de Broglie [202, loc. cit., p. 29] in discussing no less than the Boltzmann-Gibbs canonical distribution "...the notion of temperature is meaningful for just one molecule when that molecule is found to be in energetic contact with a thermostat of temperature T that *imposes* its temperature upon the molecule." For present purposes the thermostat is not hidden as is de Broglie [202]'s based on Bohm and Vigier [203]'s subquantum hypothesis, but rather $T = T(\mathbf{x}, t) \forall \mathbf{x} \in \partial V$ at any time t [188] as tacitly assumed by Clausius. Consequently

$$\Delta S(t) \geq \oint_{\partial V} \frac{đQ}{T} = \oint_{\partial V} \frac{da}{T} \, \hat{\mathbf{n}} \cdot \boldsymbol{F}_{\text{int}}$$
$$= \oint_{\partial V} \frac{da}{T} \, \hat{\mathbf{n}} \cdot \frac{\partial \mathbf{j}}{\partial t}. \tag{11a}$$

Quantum mechanically $\hat{\mathrm{T}}\mathbf{j}(\mathbf{x}, t)\hat{\mathrm{T}}^{-1} = \mathbf{j}(\mathbf{x}, -t)$ so that $\mathbf{j}$ is even in t since the Wigner time reversal operator $\hat{\mathrm{T}}$ is antiunitary and $\hat{\mathrm{T}}i\hat{\mathrm{T}}^{-1} = -i$ as was noted earlier. Consequently, $\boldsymbol{F}_{\text{int}}(\mathbf{x}, t) = \partial \mathbf{j}(\mathbf{x}, t)/\partial t$ is odd in t. Since $\boldsymbol{F}_{\text{int}}(\mathbf{x}, t)$ is odd because $\mathbf{j}(\mathbf{x}, t)$ is even under time reversal, it follows with reference to (8b) and (8c) that the gain in entropy $\Delta S(t)$ as given in (11a) is asymmetric in time[†], i.e. $\Delta S(t) = \Delta S(-t)$. Traveling backwards in time as is permitted by both quantum mechanics and electrodynamics would cause $\Delta S(t)$ to decrease contrary to the SLT and is consequently forbidden. Whether the process is reversible or irreversible, ΔS treats time $t \geq 0$ as a positive semi-definite parameter. Using (1a), (5), and (11a) it is clear that

$$\langle \Delta S(t) \rangle \geq \oint_{\partial V} \frac{da}{T} \rho \left(\rho \nabla^2 \phi + \nabla \rho \cdot \nabla \phi \right) \hat{\mathbf{n}} \cdot \nabla \phi \tag{11b}$$

which is the quantum Clausius inequality for the expectation value of the asymmetric $\langle \Delta S(t) \rangle = \langle \Delta S(-t) \rangle$ entropy change of a molecule in contact with a thermostat at time t. $\langle \Delta S(t) \rangle$ is monotone increasing [122, cf. Fig. 9] provided ϕ is subharmonic.

[†]A real function $f(x)$ of a real variable x is odd (asymmetric via a π reflection through the origin) iff $f(x) = -f(-x)$ or even (symmetric about the $f(x)$ axis) iff $f(x) = f(-x)$ in the domain of f.

If the single molecule under investigation here were one of an ensemble of noninteracting replicas, each similarly prepared in the same state ψ and to which considerations of Bose-Einstein, Fermi-Dirac, or Maxwell-Boltzmann statistics are not required [204, cf. §2.01], one has the same problem treated by von Neumann [205, cf. §5.2] in his appeal to Szilard [206]'s one-molecule heat engine, a scenario criticized by some [207, for e.g.], validated by many [208, cf. Ch. VI], [97, 209–213], and the first to point out the connection between entropy and information. In the absence of demons and pistons*, the thermodynamic limit [214–217], [218, cf. Ch. 14] issue is irrelevant since it does not apply to a lone molecule in a thermal bath whose sole task is to supply heat to maintain that molecule's fluctuating charge density $\rho(\mathbf{x}, t)$, current density $\mathbf{j}(\mathbf{x}, t)$, and deformable volume V. Nor does a thermodynamic limit apply to the known Universe. Previously, using only the elementary notion of work, $dQ = d\mathbf{x} \cdot \boldsymbol{F}_{\text{int}}(\mathbf{x}, t)$ was identified as the action over a differential displacement $d\mathbf{x}$ in V of the quantum mechanical Lorentz-Faraday force $\boldsymbol{F}_{\text{int}}(\mathbf{x}, t)$ given in (8a) in terms of the thermally-driven current density $\mathbf{j}$ of a single molecule.

The integrand of the integral in (11b) is also the integrand in the Claussius inequality given in (9). If it is to be estimated, it is best done using statistical methods where the integrand's dependencies $(\rho, \phi, T, \mathbf{x})$ at time t are treated as independent and identically distributed random fluctuating variables drawn repeatedly from appropriate probability distributions under the auspices of the law of large numbers. That part of the integrand in parenthesis is the outward flux of $\mathbf{j}$ across ∂V. The two inner products $\nabla \rho \cdot \nabla \phi$ and $\hat{\mathbf{n}} \cdot \nabla \phi$ in the integrand each involve outbound gradients and are positive [219–224] since these gradients make more probable glancing and head-on egress across ∂V than the biased presumption that they be tangent to the boundary ∂V, exclusively or otherwise. The only term that can cause the integral to change from positive to negative in violation of Clausius' inequality is that involving $\nabla^2 \phi$ thus making it necessary and sufficient that ϕ be subharmonic [148, 149] in V so that no such transgression occurs. Whether the Hamiltonian operator of the system of interest is autonomous or not has no bearing†

on the T-asymmetry of $\langle \Delta S(t) \rangle$ and likewise does not negate the T-symmetry of either quantum mechanics or electrodynamics.

Besides distinguishing between two possible types of processes on the basis of changes in entropy as determined by finite $\nabla \phi$, there are several other features of Clausius' inequality worth recalling: (a) it is a consequence of the SLT; (b) it is not an evolutionary relationship; (c) it does not rely on knowledge of a system's microstates, just the current state; (d) entropy is the outcome of a process; (e) it is T-asymmetric without obliging the same of any allied dynamical framework including quantum mechanics‡.

The lone molecule ensconced in a heat bath is free to visit the entirety of its configuration space demarcated by V. Since it has been shown that $\langle \Delta S(t) \rangle = \langle \Delta S(-t) \rangle$ and as an alternative to ensemble averaging, its Laplace long-time average $\overline{\langle \Delta S_\tau \rangle}$ may be taken [235, cf. p. 68] as

$$\overline{\langle \Delta S_\tau \rangle} = \frac{1}{\tau} \int_0^\infty dt \, e^{-t/\tau} \langle \Delta S(t) \rangle$$
$$= \int_0^1 dt \, e^{-t} \langle \Delta S(\tau t) \rangle, \tag{11c}$$

where $\tau > 0$ is a phenomenological relaxation time for ubiquitous exponential decay [236] that has both system and environment dependencies. Independently of τ, $\langle \Delta S(t) \rangle$ fluctuates en route to $\overline{\langle \Delta S_\tau \rangle}$ with a variance $\sigma_\tau^2 = \overline{\langle \Delta S_\tau^2 \rangle} - \overline{\langle \Delta S_\tau \rangle}^2$. Since (11c) provides a means of time averaging under nonstandard state conditions and with the accommodation of relaxation, it obviates subjective biases related to the unmeasured properties of an ensemble of replica systems. Unlike electromechanical systems where molar statistics is apropos, Avogadro quantities of macromolecules are not always available in biological and nanoscale systems where finite-time measurements come to the fore, ergodic behavior is arguably applicable, and ensembles are moot. The same applies to the known Universe. The provision of $\Delta S(t)$ data is through calorimetry or via Monte Carlo-Markov chain techniques [237, 238]. This Laplace time-averaging is equally applicable to Helmholtz $\Delta F(t)$ and Gibbs $\Delta G(t)$ free energies whose time averages $\overline{\langle \Delta F_\tau \rangle}$ and $\overline{\langle \Delta G_\tau \rangle}$ are roughly equal for entropy-driven pro-

---

*Zurek [210, loc. cit., p. 152]'s rebuttal of Jauch and Báron [211]'s primary argument reads "One may argue that the one-molecule engine cannot be analyzed by means of thermodynamics (sic statistical mechanics), because it is nowhere near the thermodynamic limit. This objection is overruled by noting that arbitrarily many "Szilard's engines" can be linked together to get a "many-cylinder" version of the original design. This will cut down fluctuations and allow one to apply thermodynamic (sic statistical mechanics) concepts without difficulty". Indeed, the entropy increase in time of an ensemble of entities is determined by their current states as affected by internal conservative potentials (Coulomb, Newtonian, thermal Lorentz-Faraday, etc.), prevailing pair-wise force fields (Lennard-Jones and more-exotic empirical variants), and external nonconservative potentials (catalysts, lasers, particle beams, etc.) that aspire to control them.

†This is consistent with Landau and Lifshift [225, loc. cit., p. 51]'s observation that "The form of the Hamiltonian for a system of particles which interact with one another cannot be derived from the general principles of

quantum mechanics alone."

‡Bohm, Gadella and coworkers [226, et passim] postulate a time asymmetric quantum theory (TAQT) by associating states and observables to two different Hardy subspaces dense in the same Hilbert space that does not distinguish between the in-states and out-states of scattering theory but which in TAQT would cause the dynamical equations (in the Schrödinger and Heisenberg pictures) to integrate to a semigroup evolution. TAQT is not without its critics [227–230]. Within a cellular automaton interpretation of quantum theory, 't Hooft [231] makes similar claims. Oliver Penrose (esteemed thermodynamicist and older brother of Roger)'s critical review [232] of Mackey [233]'s book are equally apropos to any proposal that requires quantum mechanics to waive its time reversal invariance, an imposition obviated by the SLT as will be revealed in this paper. Kuzemsky [234, et passim] has surveyed foundational issues of the problem of time and its asymmetry, a consideration outside the scope of this paper.

cesses and identical for an uncompressed single molecule [183].

Entropy generation S_{gen} (what Clausius [239, cf. Eq. 71] called production rate) is the entropy produced during a process as given by

$$S_{\text{gen}}(t) = \Delta S(t) - \oint_{\partial V} \frac{dQ}{T} \,. \tag{11d}$$

It is zero or positive for a reversible or irreversible process [240, 241], respectively. Irreversibilities degrade the performance of systems and S_{gen} is a measure of their magnitude during a process. It is impossible for $S_{\text{gen}} < 0$ so that it cannot influence the thermodynamic arrow of time any more than can F_{int}. However, whereas F_{int} is inherent to the system and its dynamics, S_{gen} is part of the process. The entropy generation S_{gen} would vanish if the requirement that ϕ be subharmonic were relaxed to it being simply harmonic in V which was previously dismissed: (11b) and (11d) imply that

$$S_{\text{gen}}^{\nabla^2 \phi > 0}(t) \geq S_{\text{gen}}^{\nabla^2 \phi = 0}(t) \geq 0 \,, \tag{11e}$$

so that subharmonic ϕ favors entropy generation more than harmonic ϕ.

In thermodynamics, work performed by a system is energy it transfers to its surroundings and the surroundings transfers energy to the system and both transfers incur a price. Even though $\oint_{\partial V} dQ/T$ is finite for natural processes, reflecting the fact that entropy is not conserved, use of the divergence theorem on $\oint_{\partial V} dQ$ gives

$$\oint_{\partial V} dQ = \oint_{\partial V} da\, \hat{\mathbf{n}} \cdot F_{\text{int}} = \int_V d\mathbf{x}\, \nabla \cdot F_{\text{int}} \tag{12a}$$

as the work done by F_{int}. The orientable manifold V of configuration space encloses the flux $\nabla \cdot F_{\text{int}}$ of F_{int} and the generalized Stokes theorem [242, 243, for e.g.] further provides

$$\oint_{\partial V} dQ = \int_V d\mathbf{x}\, \nabla \cdot F_{\text{int}} = \int_V d\mathbf{x} \cdot \nabla \times F_{\text{int}} \,. \tag{12b}$$

The divergence and curl of F_{int} are

$$\nabla \cdot F_{\text{int}}(\mathbf{x}, t) = \psi^*(\mathbf{x}, t)\nabla^2\psi(\mathbf{x}, t) - \psi(\mathbf{x}, t)\nabla^2\psi^*(\mathbf{x}, t), \tag{12c}$$

and

$$\nabla \times F_{\text{int}}(\mathbf{x}, t) = \nabla\psi^*(\mathbf{x}, t) \times \nabla\psi(\mathbf{x}, t) - \nabla\psi(\mathbf{x}, t) \times \nabla\psi^*(\mathbf{x}, t) \tag{12d}$$

respectively. The curl of F_{int} vanishes for all $\mathbf{x} \in R^n$. However, the divergence of F_{int} vanishes locally only when ψ or $\nabla\psi$ does so. Since there is no creation or destruction of charge within V and the Laplacian operator is self-adjoint, $\oint_{\partial V} dQ$ vanishes so that F_{int} does no work, i.e.

$$\begin{aligned} Q = \int_{\partial V} d\mathbf{x}\, dQ &= \int_V d\mathbf{x}\, \nabla \cdot F_{\text{int}} \\ &= -\int_V d\mathbf{x} \nabla^2 \mathcal{V}_{\text{int}} = 0 \,, \end{aligned} \tag{12e}$$

where $F_{\text{int}}(\mathbf{x}, t) = -\nabla\mathcal{V}_{\text{int}}(\mathbf{x}, t)$ with $\mathcal{V}_{\text{int}}(\mathbf{x}, t)$ being the potential energy function of $F_{\text{int}}(\mathbf{x}, t)$. Thus, despite its spatial and time dependence, $F_{\text{int}}(\mathbf{x}, t)$ is a conservative and not a dissipative force like friction or viscous drag that does negative work in the direction opposite to the displacement of its target which consequently loses energy as heat in the amount removed by such a force. The subharmonicity of ϕ is what makes F_{int} a conservative force, one that conserves mechanical energy.

3 Faradaic induction in a thermal field

Gauge theories [244] enable a reduction in the number of variables necessary to define a physical state quantum mechanically (configuration space, $\mathbf{x}$) over that required classically (phase space, $\mathbf{x}$ and $\mathbf{p}$). Electrodynamics was the first field theory to exploit gauge symmetry by recognizing that any function that can be written as a gradient could be added to the vector potential without affecting the magnetic field. Acting on a suggestion by London [245], Weyl [246, pp. 100-101] replaced the gauge scale factor with a complex quantity and turned the scale transformation into a change of phase. The gauge field of electrodynamics associates an element of the group $U(1)$ of unit complex numbers under multiplication to each path: the phase that a charged particle gets when going through a loop is the magnetic flux through the loop. The physical states of quantized systems are described [141, for e.g.] by vectors ψ of unit norm belonging to a complex Hilbert space $\mathcal{H}$. Physical observables are associated with self-adjoint operators O acting on $\mathcal{H}$ whose expectation values are scalar inner products $\langle\psi| O\psi\rangle$ in $\mathcal{H}$ that are unaffected by unitary transformations which act on both state vectors $\psi \mapsto U\psi$ and operators $O \mapsto OUO^\dagger$, where U is unitary. Thus, the multiplication of state vectors by a phase (a $U(1)$ global group transformation) $\psi \mapsto e^{i\phi}\psi$ leaves operators and physical predictions unchanged provided O does not differentiate ψ either spatially or temporally. Neither $\mathbf{j}(\mathbf{x}, t)$ nor $\partial\mathbf{j}(\mathbf{x}, t)/\partial t$ are such-like operators so that their inclusion of $U(1) = e^{i\phi}$ cannot be disregarded since the $U(1)$ phase $\phi(\mathbf{x})$ is local. This is reminiscent of earlier speculations by Schrödinger [247] based on Weyl [246]'s spacetime theory in connection with the Wilson-Sommerfeld [173, 174] quantization condition for Bohr's old quantum theory of the H atom. For this reason, ϕ is referred herein as the unadorned "phase", rather than Schrödinger [150]'s "phase angle", de Broglie's "phase wave", or Weyl's "gauge transformation", all three being essentially one and the same. Failure to notice that the Schrödinger equation is not gauge invariant under a local gauge transformation is due in large to two commonly-held notions, viz. that it takes an external electromagnetic field to do so when in fact it does not [142, 143], and that, in confounding local with global, the phase of the wave function is arbitrary when in fact it is not [248] unless it is global.

The thermal field induces an internal electromagnetic con-

servative force field $\boldsymbol{F}_{\mathrm{int}}(\mathbf{x}, t)$ of scalar potential Φ and vector potential $\mathbf{A}$ in the system whose Helmholtz-Hodge decomposition [176–178] reads as

$$\boldsymbol{F}_{\mathrm{int}} = -\nabla\Phi + \nabla \times \mathbf{A} \tag{13a}$$

into the scalar longitudinal (irrotational, curl-free) potential $\Phi(\mathbf{x}, t)$ and the vector transverse (solenoidal, div-free) potential $\mathbf{A}(\mathbf{x}, t)$ which provide, via Maxwell's equations, for the *internal* microscopic electric

$$\boldsymbol{E}_{\mathrm{int}} = -\nabla\Phi - \partial\mathbf{A}/\partial t \tag{13b}$$

and the *internal* microscopic magnetic induction

$$\boldsymbol{B}_{\mathrm{int}} = \nabla \times \mathbf{A} \tag{13c}$$

fields which at every point in space and time obey the microscopic Maxwell equations. There is only one kind of charge and the amount of it anywhere can be positive, negative, or zero subject solely to its conservation regardless of whether it is believed to be associated with a nucleus or an electron. The prominence of electromagnetic potentials in quantum theory is due in large to the work of Aharonov and Bohm [249, 250].

Rhetorically, $\mathbf{A}(\mathbf{x}, t)$ generates $\boldsymbol{B}_{\mathrm{int}}(\mathbf{x}, t)$ through its circulation and $\boldsymbol{E}_{\mathrm{int}}(\mathbf{x}, t)$ through its time dependence with $\rho(\mathbf{x}, t)$ and $\mathbf{j}(\mathbf{x}, t)$ playing supporting roles encapsulated in the Lorentz microscopic force density

$$F_{\mathrm{int}} = \rho\boldsymbol{E}_{\mathrm{int}} + \mathbf{j} \times \boldsymbol{B}_{\mathrm{int}}, \tag{13d}$$

where

$$\begin{aligned}
F_{\mathrm{tot}}(t) &= \int_V d\mathbf{x} \cdot F_{\mathrm{int}}(\mathbf{x}, t) \\
&= \oint_{\partial V} da\, \hat{\mathbf{n}} \cdot \boldsymbol{\sigma}_{\mathrm{int}}(\mathbf{x}, t) - \frac{d}{dt} \int_V d\mathbf{x} \cdot \boldsymbol{S}_{\mathrm{int}}(\mathbf{x}, t),
\end{aligned} \tag{13e}$$

is the total electromagnetic field on the charges in V, $\boldsymbol{\sigma}_{\mathrm{int}}$ is the Maxwell stress tensor, and the Poynting vector $\boldsymbol{S}_{\mathrm{int}}$ is given by

$$\boldsymbol{S}_{\mathrm{int}} = \boldsymbol{E}_{\mathrm{int}} \times \boldsymbol{B}_{\mathrm{int}}, \tag{13f}$$

and

$$\boldsymbol{F}_{\mathrm{int}} = \nabla \cdot \boldsymbol{\sigma}_{\mathrm{int}} - \dot{\boldsymbol{S}}_{\mathrm{int}} \tag{13g}$$

pursuant to the conservation of linear momentum. In (13g) the last term on the right is the time derivative of the field's photon momentum density while the first is the divergence of the stress tensor bearing on the charges in V.

Both $\Phi(\mathbf{x}, t)$ and $\mathbf{A}(\mathbf{x}, t)$ retain their spatial and nonretarded time dependencies without the $\boldsymbol{E}_{\mathrm{int}}$ and $\boldsymbol{B}_{\mathrm{int}}$ fields descending to electrostatics since the Lorenz condition [251–255] has not been invoked. Mathematically, the potentials $\Phi(\mathbf{x}, t)$ and $\mathbf{A}(\mathbf{x}, t)$ are volume integrals of the divergence and curl of $\boldsymbol{F}_{\mathrm{int}}(\mathbf{x}, t)$ scaled by the Green's function for the Laplacian

analogously to (7a) and (7b), respectively. It is clear from (1a), (5), and (13a) that the irrotational part of F_{int} is

$$\nabla\Phi = \rho\nabla^2\phi\nabla\phi \tag{14a}$$

while the solenoidal part is

$$\nabla \times \mathbf{A} = -\nabla\phi \cdot \nabla\rho\nabla\phi, \tag{14b}$$

with both parts being in the same direction as $\nabla\phi$. Neither potential is directly measurable and may be replaced by gauge-equivalent potentials θ and $\mathbf{A} + \nabla\phi$, respectively, to yield the same $\boldsymbol{E}_{\mathrm{int}}(\mathbf{x}, t)$ and $\boldsymbol{B}_{\mathrm{int}}(\mathbf{x}, t)$.

Maxwell's equations are linear dynamical PDEs that have a unique solution for given initial and boundary conditions. From these equations it is straightforward to show that the scaler $\Phi(\mathbf{x}, t)$ and vector $\mathbf{A}(\mathbf{x}, t)$ potentials satisfy

$$\Box\, \Phi = -\frac{\partial}{\partial t}\left(\nabla \cdot \mathbf{A} + \frac{\partial\Phi}{\partial t}\right) - \rho \tag{15a}$$

and

$$\Box\, \mathbf{A} = \nabla\left(\nabla \cdot \mathbf{A} + \frac{\partial\Phi}{\partial t}\right) - \mathbf{j}, \tag{15b}$$

respectively, where $\Box = \nabla^2 - \partial^2/\partial t^2$ is the d'Alembertian operator. These promote use of the Lorentz condition in which the term in parenthesis common to both is set to zero, a gauge strategy of historic [244] importance to physics.

Alternatively, use of the curl of the curl identity, Gauss's law of electricity in the curl of Faraday's law, and Gauss's law of magnetism in the curl of Maxwell-Ampère's law, allows one to arrive at the coupled inhomogeneous wave equations [256] for the $\boldsymbol{E}_{\mathrm{int}}(\mathbf{x}, t)$ and $\boldsymbol{B}_{\mathrm{int}}(\mathbf{x}, t)$ fields as

$$\Box\, \boldsymbol{E}_{\mathrm{int}} = 4\pi\left(\nabla\rho + \frac{\partial\mathbf{j}}{\partial t}\right) \tag{16a}$$

and

$$\Box\, \boldsymbol{B}_{\mathrm{int}} = -4\pi\nabla \times \mathbf{j}, \tag{16b}$$

respectively. In (16a) and (16b), $\Box$ acting on $\boldsymbol{E}_{\mathrm{int}}(\mathbf{x}, t)$ and $\boldsymbol{B}_{\mathrm{int}}(\mathbf{x}, t)$ generates inextricably coupled electromagnetic waves given sources in gradients of ρ, time-varying changes in $\mathbf{j}$, and circulations of $\mathbf{j}$. The Lorentz-Faraday force $\boldsymbol{F}_{\mathrm{int}}(\mathbf{x}, t)$ first introduced here in (8a) is none other than one of two source terms for the wave equation of $\boldsymbol{E}_{\mathrm{int}}(\mathbf{x}, t)$ and leads to the possibility of the oscillation or acceleration of charge which radiates more or less transverse to the direction of propagation. At idealized $T = 0$ where $F_{\mathrm{int}}(\mathbf{x}, t)$ is absent, the charges in an "isolated" (sic stationary state) molecule oscillate in place without accelerating and their Coulomb radiation field decays as $1/|R'|^2$ where R' is the line of sight distance to a charge [256]. More realistically, $T > 0$ causes charges in the molecule to oscillate and accelerate. This produces self-sustaining electric and magnetic fields propagating as electromagnetic waves at the speed of light which transport energy

and momentum to charged particles at large distances from the source at the expense of the accelerated charge. The electric and magnetic fields are orthogonal to each other. When $T > 0$ such that $F_{\text{int}}(\mathbf{x}, t)$ is operative, the charges oscillate and accelerate and their radiation field decays as $1/|R'|$ to surpass their shorter-ranged Coulomb radiation field [256]. Since $\nabla\rho$ ultimately vanishes* and $\nabla\times\mathbf{j} = \nabla\rho\times\nabla\phi$, the internal $\boldsymbol{E}_{\text{int}}(\mathbf{x}, t)$ and $\boldsymbol{B}_{\text{int}}(\mathbf{x}, t)$ fields are pervasive and are the source of photons to be absorbed and emitted within V in the manner first treated by Einstein [257, 258] and later by Dirac [259, 260] in analogy with gravitoelectromagnetic phenomena [261, 262], e.g. Lense-Thirring frame-dragging effects [263, 264], whose internal $\boldsymbol{E}_{\text{int,g}}$ and $\boldsymbol{B}_{\text{int,g}}$ fields (or equivalently, $\Phi_{\text{int,g}}$ and $\mathbf{A}_{\text{int,g}}$) are caused by the gravitational interaction of massive celestial objects with neighboring ones.

The $U(1)$ gauge symmetry of electromagnetism represents the group of rotations around a fixed axis. Since the end of the quark era, $U(1)$ has broken the $SU(2)$ x $U(1)$ gauge symmetry of the electroweak force whose three massive bosons $W^\pm$ and Z^0 are accompanied by a fourth massless one, the photon. Helmholtz-Hodge photons induce electrically neutral currents in a molecule, in analogy with the decay of Z^0 to neutrinos which scatter off electrons in electroweak interactions [265], and mediate scattering between nuclei and electrons that entail the transfer of momentum, spin, and energy via photon exchange but to the exclusion of charge. $U(1)$ symmetry comes from the fact that the absolute phase ϕ of ρ cannot be measured unlike its finite relative change $\nabla\phi$ as first pointed out by Weyl [248] and adopted by Dirac [266]. The importance of $U(1)$ symmetry comes from Emmy Noether's theorem which states that such gauge symmetries lead to the conservation of a related quantity. Two types of $U(1)$ gauge symmetry are salient, viz. global gauge symmetry where the phase change $\nabla\phi$ vanishes at critical points in space and leads to the conservation of charge; and local gauge symmetry where the phase is not the same at all locations and requires the introduction of an additional gauge field to keep it invariant under such finite relative changes. One may view the local gauge field as signaling phase changes from one point to another by radiatively communicating such changes and in doing so leading a molecule to engage in its own intramolecular entanglement frontier†. Molecules have many degrees of freedom but only two types of material constituents whose positions are not only correlated with each other – a type of correlation known as entanglement [267, cf. Ch. 16], [268, cf. Ch. 5], [269, cf. Ch. 17] and a key property of quantized systems exploited to effect quantum compu-

---

*$\nabla\rho$ is the source of charge that is accelerated by $F_{\text{int}} = \partial\mathbf{j}/\partial t$. Its inclusion in Clausius' inequality is unnecessary since $\langle\overline{\nabla^2\rho}\rangle$ vanishes.

†With two entangled particles one knows something about their combined properties but their individual properties are indeterminate until one makes a measurement of the state of one particle at which point one has some, but not all, information about the other. Entanglement is a nonlocal correlation between nonseparable states.

tation [270] in concert with the superposition principle – but also with its internal Helmholtz-Hodge photons whose "wave functions" [271] are inherently part of ψ.

At their prevailing low energies, Helmholtz-Hodge photons serve as the carriers of the nonconservative electromotive force (emf) [272, Sec. 6.1], [273, cf. Ch. 7]

$$\mathcal{E}(t) = \oint_{\partial V} da\,\hat{\mathbf{n}} \cdot (\boldsymbol{E}_{\text{int}} + \nabla\phi \times \boldsymbol{B}_{\text{int}}) = -\frac{d}{dt}\Phi_{\boldsymbol{B}_{\text{int}}}(t) \quad (17a)$$

of molecules through their in situ photon absorption and emission regardless of Faradaic fixtures (wires, circuits, electrodes, batteries, etc.). Emf produces a charge imbalance that causes the lighter electrons to move from nucleophilic to electrophilic regions, this movement being what is recognized as electric current. Electrons can gain or lose energy due to their interaction with $\boldsymbol{B}_{\text{int}}$ and $\boldsymbol{E}_{\text{int}}$ whereby $\boldsymbol{B}_{\text{int}}$ guides their motion, $\boldsymbol{E}_{\text{int}}$ accelerates them, and Lenz's law prescribes their direction. Of course, being internal fields rooted in the molecule's structure, $\boldsymbol{B}_{\text{int}}$ and $\boldsymbol{E}_{\text{int}}$ are not amenable to manipulation or so-called control. The deformation of V due to the magnetic Lorentz force acting on charges is the motional emf while the remaining part of $\mathcal{E}$ is the transformer emf generated by an electric field induced by a changing magnetic field. Eddy currents induced in the cores of transformers and generators dissipate energy as heat loss giving rise to temperature increases.

The quantity on the far right in (17a) is formally

$$\frac{d}{dt}\Phi_{\boldsymbol{B}_{\text{int}}}(t) = \oint_{\partial V} da\,\hat{\mathbf{n}} \cdot \left[\frac{\partial \boldsymbol{B}_{\text{int}}}{\partial t} - \nabla \times (\nabla\phi \times \boldsymbol{B}_{\text{int}})\right], \quad (17b)$$

where $\Phi_{\boldsymbol{B}_{\text{int}}}(t)$ represents the internal magnetic flux of the molecule and the Maxwell relation $\nabla \cdot \boldsymbol{B}_{\text{int}} = 0$ holds due to the absence of magnetic charges in Nature. The induced $\mathcal{E}(t)$ and the rate of change in $\Phi_{\boldsymbol{B}_{\text{int}}}(t)$ have opposite signs so that the cause (induced field) opposes the effect (changing current) in analogy with Newton's third law.

Recall that the binding of electrons to nuclei is modified somewhat by parity-violating Z^0 exchanges that manifest as parity nonconservation in both atoms [274, 275] and molecules [276, 277].

4 Discussion

4.1 Going forward

Obviously

$$\nabla\phi(\mathbf{x}) = \frac{\partial\mathbf{j}(\mathbf{x}, t)}{\partial\rho(\mathbf{x}, t)} \quad (18)$$

thus exposing the elusiveness of the relative phase which clearly changes sign under P because $\mathbf{j}$ does and ρ does not. Neither C nor T changes $\nabla\phi$. The popular assertion that the phase of ψ is arbitrary and has no physical significance is true only if that phase is global. The phase is local, however, and provides an unequivocal link to the Lorentz-Faraday force

$F_{\text{int}}(\mathbf{x}, t)$ whose effects are manifest in the unremitting operation of the SLT in blockading quantum mechanics from providing a portal to the past and without curtailing even massive objects from ultimately reaching stasis in going forward. The Lorentz-Faraday force $F_{\text{int}}(\mathbf{x}, t)$ is intrinsically T-asymmetric regardless of the initial and boundary conditions of this or other universes and without electrodynamics or quantum mechanics having to forfeit their innate time-reversal symmetries.

Weak measurement techniques [278–280] have now been extended beyond the massless photon. As long anticipated by Aharonov et al. [281], Bednorz et al. [282] have shown that weak measurements are time-reversal symmetric classically but not so quantum mechanically. More recently, Jayaseelan et al. [283], in weak measurements of the spin of ultra-cold atoms, provided evidence for absolute irreversibility and a strictly positive average arrow-of-time captured by a fluctuation theorem; they further demonstrated absolute irreversibility for measurements performed on a many-body entangled wave function. These demonstrations are consistent with Borel [284, loc. cit., pp. 2–3]'s quip that "Events with a sufficiently small probability never occur," following which he goes on to quantify "sufficiently small" for probabilities that are negligible on the human, terrestrial, and cosmic scale as descending in the order $10^{-6}, 10^{-15}$, and 10^{-80}, respectively. Recall that in particle physics, the gold standard for a discovery is 5σ, in which there is a one in 3.5 million chance of the result being a fluke. The BaBar Collaboration found [13] a 1 in 10^{43} (14σ) level of certainty for their T-asymmetry measurements and CP violation was also observed at the 16σ level, far more than needed to declare a discovery. These observations of T reversal violations in electroweak interactions are consistent with the SLT being T reversal forbidden, the primary revelation of this paper. It remains to be seen (*vide infra*) if T reversal violations are also observed in strong-force interactions.

Manifestly, $\Delta S(t)$ increases and the process is reversible or irreversible according as the gradient in ϕ vanishes or not on ∂V, respectively. The entropy gain ΔS will be proportional to the area of the boundary ∂V enclosing the nominal volume V of the system interfacing its surroundings, just as with black holes. Unlike black holes, however, molecules lack horizons and their gain of entropy is settled by the gradient field of their local phase ϕ in guaranteeing their participation in natural processes without losses from the universe of itself and its heat reservoir. Since the vorticity $\nabla \times \nabla\phi$ vanishes except [285] at nodes in ρ (and $\nabla\phi$ is singular), the entropy gain by the molecule in contacting a heat bath is sheltered from meteorological losses consistent with the absence of swirl in F_{int} when the heat is withdrawn.

Equations (17a) and (17b) reveal that Faraday's law of induction holds for a single molecule provided the gradient of its local phase is finite, a condition necessary and sufficient for it not to present with its well-known paradoxes [286–288].

Measurements of the emf $\mathcal{E}(t)$, the Helmholtz-Hodge fields E_{int} and B_{int}, and their ancillary lines of force first envisioned by Faraday [289], for a single molecule using a test charge would be as difficult as it is in quantum electrodynamics [290] but perhaps for different reasons. The long-standing validity of Faraday's law $\mathcal{E}(t) \sim \pm d\Phi_{B_{\text{int}}}(t)/dt$ in engineering applications now has a quantum basis. Of course Faraday's law induces potential, not current which is simply the induced voltage divided by the resistance of the loop. With multiple identical loops Faradays law is additive (sic extensive), i.e. $N\mathcal{E}(t)$ where $N \gg 1$ is the number of loops (windings).

4.2 The stability of a molecule

Clausius' classical virial theorem [291] relating the time averages of the kinetic energy ("vis viva") of a system of discrete particles and the virial ("ergal" or mechanical work) of the system, that being the work done by the gravitational forces (or equivalently, by $-\nabla\mathcal{V}_C$ for a molecule of Coulomb potential $\mathcal{V}_C$) has long served [292] cosmology in accounting for the stability of the most virialized objects in the Universe, clusters of stars and galaxies. The latter are filled with the intrastellar (cluster) medium (IS(C)M), an X-ray-emitting hot plasma with a typical temperature $\sim 10^7$ K. The interstellar medium (ISM), consisting of the matter (atomic, ionic, molecular, dust, cosmic rays) and radiation that occupies the space between the star systems in a galaxy, interacts magnetohydrodynamically with the ICM. Clusters are characterized by the virial radius within which the cluster's mass can be determined under the assumption of the ICM being in hydrostatic equilibrium. Clusters are thought to grow into larger systems through mass accretion flows which are merged into the ICM at a radius of several times the virial radius. Properties such as the temperature or density around the virial radius are not well known because of observational difficulties. The virial theorem holds even for systems that are not in thermal equilibrium. Dark matter's existence was first hypothesized by Zwicky [293] to account for the mass deficit found when the total sum of the masses of individual members in a galactic cluster falls far short of the virial mass whose use assumes that the cluster is stable, an assumption questioned by Ambastumian [294] who maintained that not only are the clusters unstable but they are also exploding, a controversial hypothesis whose history and impact on cosmology is reviewed by Bland-Hawthorn and Freeman [295, cf. 1.10]. A pivotal discovery in this history was Vera Rubin and Kent Ford's confirmation [296] that dark matter is required to account for the rotation of stars and spiral galaxies. Other indicators of the presence of dark matter comes from gravitational lensing [297] and from fluctuations in the power spectrum of the CMB [298].

As the Universe expanded and cooled following the Big Bang, energy was converted to subatomic particles which merged to form protons – the nuclei of H atoms, some of

those nuclei fused to form He so that the early Universe consisted almost entirely of hydrogen, helium, and in lesser amounts, lithium, beryllium, and boron. In time, these dense molecular clouds collapsed under gravity to form stars. Nuclear fusion reactions in these stars spawned more elements and stellar explosions forged even more in the process of nucleosynthesis. The most abundant (greater than 90%) element in the Universe is H followed by He all of whose isotopes are stable except for minuscule amounts of tritium (^{3}H). Molecules account for most of the observable matter in the Universe and are remarkably stable against change. That matter at equilibrium is stable is so self evident that were it otherwise its existential proof would be as redundant as it would be specious. Ordinary matter [299, for e.g.], as comprised of atoms and molecules, has both mass and volume with the former concentrated in its positively charged nuclei and the latter occupied mainly by negatively charged electrons that are of much smaller size than a typical nucleus and are ~ 2000 times lighter than a proton. The mass number A is the sum of the total number of protons (atomic number, Z) and neutrons with differing number of neutrons for the same Z giving different A's for the isotopes of that element. Bulk matter does not implode or eventually explode and is self-evidently stable across low-energy scales from fluids [300, for e.g], to solids [301, for e.g], to engineered structures designed and safety-certified without reference to atomistic considerations [302, for e.g.]. Whereas nuclei have the *Chart of the Nuclides* (~ 3000 in number) and atoms have the *Periodic Table of the Elements* (~ 120 in number), molecules (countless in number) have no such iconic organizational motif. The stability of matter resides in its nuclei, the majority of which are radioactive and undergo decay while the rest are located in the valley of stability between the proton and neutron drip lines as determined by their constitutive proton/neutron ratio and with an island of stability indicative of far longer-lived (but yet to be observed) isotopes of super-heavy elements than the known isotopes of these elements. The nucleons in the nucleus are fermions which obey the PEP and in the case of identical nucleons this results in the small but finite size of nuclei. Nuclides that do not undergo spontaneous decay are stable isotopes. There are about 252 stable isotopes among 80 elements with ^{56}Fe being the most abundant and ^{62}Ni the most stable. The nuclear (or residual strong) force binds nucleons into nuclei through the energy equivalence of their mass defects. This force is relatively short ranged compared to the Coulomb repulsion between protons, being attractive between spin-aligned nucleons until it falls off with distance and repulsive when their separations are small. Additionally, interactions between the spins and angular momenta of nucleons lead to the deformation of nuclei from purely spherical shapes. The nuclear force is known semi-empirically only but is more complicated than the Coulomb force operative between nuclei and electrons in atoms and molecules and its extension beyond the shell model is an active area of research [303, 304, for e.g].

Supersymmetry (SUSY) is the principle that there is an unknown symmetry between fermions and bosons. SUSY was developed to explain the hierarchial disparity between the strength of the electroweak force and gravity by proffering the existence of superpartners of known particles, each having the same properties as the originals except for spin, so as to curtail the magnitude of the Higgs mass from undermining the very stability of the SM construction. SUSY is the source of hypothetical WIMPs in galactic halos. There is currently no evidence for SUSY at high energies.

When Feynman remarked [305, loc. cit., pp. 3–4]:

> It appears to be one of the few places in physics where there is a rule which can be stated very simply, but for which no one has found a simple and easy explanation . . . This probably means that we do not have a complete understanding of the fundamental principle involved,

he was referring to the spin-statistics theorem (SST). Succinctly put, the SST [306] is more easily invoked than its basis and applicability are understood. The SST links the spin (half-integer or integer) property of a physical system comprised of fermions and bosons with the statistics (Fermi-Dirac or Bose-Einstein) it obeys and provides a foundation for the PEP which has long been part of even high school physics and chemistry curricula.

Proof of the SST lies outside the scope of nonrelativistic quantum mechanics: it requires the full arsenal of relativistic quantum field theory, specifically that the fields are invariant under the Poincare group, that there is a vacuum state that is invariant under this group, that all states can be built up from the vacuum by applying field operators, that the Hamiltonian is bounded below, and locality in that the fields either commute or anticommute at spacelike separations. The theorem then says that at spacelike separations boson fields of integer spin commute while fermion fields of half-integer spin anticommute whereupon the PEP emerges. As Feynman was later to recount [307], the CPT theorem illustrates why every subatomic particle must have an antiparticle partner and links to the SST with fermion wave functions changing by a sign under two CPT reflections while bosons do not. Some proofs use CPT invariance to prove the SST while other proofs do the opposite. Nonrelativistic quantum mechanics lacks analogs of both the CPT and SST. After almost a century of use, the PEP continues to lack a theoretical basis [308–311] even though experimental evidence indicates [312] that its violation has yet to be found although the search [313, 314] goes on. The PEP is a scientific principle whose philosophical status continues to be worthy of further scrutiny [315, 316, for e.g.] ever since Margenau [317] first identified it as such. Inspired as it was primarily by the work of Stoner [318] on atomic transitions and Pauli [319]'s own recognition of a binary ambiguity in the response of an electron to a Zeeman field with its intimation of a necessary "spin

quantum number" to be added to those already well known (principal, angular momentum) [154, 173, 174, 320, 321, for e.g.], few possess the deep insight into the PEP [322], particularly in respect to the conditions of its violation and their consequences for quantum gravity, say, regardless of its high-level rationale for the layout of the *Periodic Table* and its provision of degeneracy pressure accounting for the stability of white dwarfs and neutron stars.

The nuclei of many isotopes have a characteristic spin (I). Some nuclei have integral, some have fractional spins, and a few have no spin. Nuclear spin is related to the nucleon composition of a nucleus: odd A-nuclei (i.e. those having an odd number of nucleons) have fractional spins, e.g. $I = 1/2$ (^{1}H, ^{13}C, ^{19}F), $I = 3/2$ (^{11}B), and $I = 5/2$ (^{17}O); even A-nuclei composed of odd numbers of protons and neutrons have integral spins, e.g. $I = 1$ (^{2}H, ^{14}N); and even A-nuclei composed of even numbers of protons and neutrons have zero spin, e.g. $I = 0$ (^{12}C, ^{16}O, ^{32}S). Spin-1/2 nuclei have a spherical charge distribution, others have nonspherical (prolate or oblate) charge distributions and are often isomeric (long-lived excited states). Nuclei with finite spins have magnetic moments but the nonspherical nuclei also have an electric quadrupole moment. In an arbitrary molecule, some of its nuclei may be fermions (e.g. ^{1}H, ^{23}Na, ^{31}P, etc.). The PEP results in the "exclusion" of any state whose wave function does not change sign on exchanging a pair of indistinguishable fermions, whether they be spin 1/2 electrons or half-integer spin nuclei. Just so, with respect to pair interchanges, wave functions are asymmetric on the exchange of identical fermions and are symmetric on the exchange of bosons. The bosons in a molecule are nuclei whose effective charges [323–325] are reduced or shielded by the innermost electrons thus lessening their Coulombic repulsion. For the wave function $\psi(\mathbf{x}, t) = e^{i\theta(\mathbf{x}, t)}|\psi(\mathbf{x}, t)|$ the relative phase $\nabla\phi(\mathbf{x}) = \tan^{-1}\nabla(\mathrm{Im}\,\psi(\mathbf{x}, t)/\mathrm{Re}\,\psi(\mathbf{x}, t))$ is constrained by the PEP through its permutation symmetry action on $\psi(\mathbf{x}, t)$ by hypothesis. This is the essence of the PEP as it applies to an orbital-free single molecule.

Atoms and molecules have innumerable states the lowest of which is the ground state. This state persists indefinitely at the global minimum of the potential in joint compliance with the classical theorem of Earnshaw [125] and the nonrelativistic energy-time uncertainty relation [326] of Mandelshtam and Tamm for a quantum system in a nonstationary state ψ [327–331]. In the ground state, the system in dynamical equilibrium with its environment resists irreversible change in its structure unless driven beyond its thermodynamic stability, primarily through temperature and pressure changes. Excited states have finite lifetimes but not definite energies: each time they decay, the energy released is slightly different with the average energy of the emitted photon peaking at the nominal energy of the state but distributed with finite width, termed the natural linewidth. The faster they decay the broader their linewidths, and conversely [332, for e.g.]. In a thermal field, a molecule is not passively inert (sic dead) but is ready to go wherever the SLT takes it.

In engineering parlance, a molecule is a mechanical system whose input, if small, effects temporary changes through internal processes that disappear when the input is withdrawn and the system reverses to its original state with no apparent output, or whose input, if large, effects permanent changes to the system which is indelibly altered. This is like a rubber band or a balloon which when stretched or blown up too far breaks or bursts. If the stretching or blowing are not too great both objects revert reversibly back to their original states. If you repeat the stretching or blowing often enough elasticity diminishes until what a gentle tug or blow used to do no longer holds and ultimately an irreversible change occurs. The ability of a molecule to resist distortion by an outside agent and to return to its original size and shape in accord with Hooke's law when the perturbing force (optical tweezers, electromagnetic fields, interface surfaces, heat sources, etc.) is removed, qualifies it as elastic in that it undergoes reversible changes that make no distinction between the past and the future in agreement with both time-invariant classical and quantum mechanics. Most molecules are elastic only to small perturbations, beyond which permanent modification occurs with the disintegration of the molecule into sundry fragments. The limits of elasticity does not usually apply to electronic transitions, which, unlike distortions within an harmonic approximation where the energies and intensities of the disturbances are low, involve internal processes of higher excitation energies and larger oscillator strengths resulting in irreversible changes that distinguish the past from the future just as do time-asymmetric entropy increases. Stability, even in elastic systems, demands dynamical analysis [333–335, for e.g.] since static stability alone does not generally imply stability under more inelastic conditions so that just like engineered structures, molecular structures engender their own future depending on their imposed input. On opening, the Millennial Bridge across the Thames in London, forced its pedestrians to walk transversely in stride to keep their balance, unwittingly accentuating its sideways wobble until it could be cleared of people without injuries. The designers went back to the drawing board to correct what, for them, was an unanticipated synchronicity previously exhibited almost two centuries before at the Broughton Suspension Bridge near Manchester, UK, one of the earliest of such span bridge designs, where mechanical resonance induced by a platoon of troops marching in step across the bridge caused it to collapse, resulting in command to direct that in future, troops break stride on crossing bridges. The futuristic Millennial span opened some two years later to worldwide applause after remedial corrections and so far it has not duplicated Tacoma. The moral of this mechanical linear-nonlinear abyss is that caution and due diligence be exercised when dealing with bridges, aircraft, and even the macroscopic effects of molecules: Nature does not provide warranties, just

surprises. A modest Murano piece or an extravagant Koon bubble structure that shatters cannot be restored to its original state by the most skillful of artisans anymore than a denatured protein can regain its primary tertiary structure in the hands of a chemist, a biologist, or a physicist.

There is an important distinction to be made between the stability of bulk matter and the stability of a single molecule. Bulk matter stability requires [214, 215] that for a bounded potential* $E_0 > -\infty$ (stability of the first kind) or $E_0 > -a(M + N)$ (stability of the second kind), where $a > 0$ is constant and E_0 is the ground-state energy, in order that the grand canonical partition function exist in finite volume and that a thermodynamic limit exist. These prerequisites for the stability of bulk matter do not pertain to the stability of a single molecule.

The PEP was found by Dyson and Lenard [337] to be a sufficient requirement in their *pace* treatment of the stability of matter in its state of stationarity, an issue considered earlier by Onsager [338] and later by Fisher and Ruelle [339] among others where the notion of stability is not, as one would reasonably expect, related to the inclination to change because of electromechanical disturbances but rather to ensuring that the classical configuration energy or quantum mechanical ground state of a system be bounded extensively from below because energy is so and in warranting that the thermodynamic limit be shown to exist. A thermodynamic limit does not always exist and for single-molecule and some nanoscale systems in particular it does not, even though stable single molecules do exist [340, for e.g.] and their reaction dynamics are observable [341–345, for e.g.]. Dyson [346] further claimed that the PEP is necessary for the stability of a system whose electrons and nuclei are of equal or of greater mass and charge, neither of which is true in Nature any more than matter fails to implode before exploding because the PEP is operative as necessary to a bewildering explication via a cascade of inequalities [218, et passim].

Echoing Wigner [347], Astumian [348] ascribes the unreasonable effectiveness of equilibrium theory for interpreting single-molecule systems that are far from thermodynamic equilibrium to their closeness to mechanical equilibrium. The primary determinant of structures available to a molecule lies in its Coulomb potential, not in peripheral diversions such as the PEP, whether Pauli repulsions are in the mind of the beholder, etc. How the Coulomb potential responds to deformations is transparently gauged by Earnshaw [125]'s theorem which, as will be shown in the following, indicates that the Coulomb potential is robust against elastic distortions so that the molecule is consequently stable until it transitions to a mixed state under environmental influences whereupon to no great surprise it may destabilize.

Earnshaw's theorem [125], as recounted by Maxwell

[349, cf. 116] and Jeans [350, cf. 192], basically states that harmonic matter is not stable since it has no interior minima in V the least of which could correspond to a configuration where the molecule has an equilibrium point, as first defined by Lagrange [351, cf. Part 1, §3, No. 16, p. 38] for mechanical systems, which computational scientists routinely detect in electronic structure calculations as positive definite second variations [352, for e.g.] of the energy functional $E = \langle \psi, H\psi \rangle / \langle \psi, \psi \rangle \geq E_0$, where E_0 is the true ground-state energy of the self-adjoint Coulomb Hamiltonian operator [336] from which molecular thermodynamic stabilities are assessed.

The Coulomb potential energy function $\mathcal{V}_C(\mathbf{x})$ of a molecule is the sum of its attractive electron-nucleus, repulsive electron-electron, and repulsive nuclei-nuclei potentials of interaction, viz.

$$4\pi \mathcal{V}_C(\mathbf{x}) = -\sum_{i=1}^{N} \sum_{j=1}^{M} Z_j/|\mathbf{r}_i - \mathbf{R}_j| + \sum_{1 \leq i < j}^{N} 1/|\mathbf{r}_i - \mathbf{r}_j| \\ + \sum_{1 \leq i < j}^{M} Z_i Z_j/|\mathbf{R}_i - \mathbf{R}_j|, \tag{19a}$$

where $\mathbf{x} \in \mathbf{R}^M \times \mathbf{r}^N$. There are no self-repulsion terms (of nuclei or electrons) in $\mathcal{V}_C$. Of course, the Coulomb force $\mathbf{F}_C(\mathbf{x}) = -\nabla \mathcal{V}_C(\mathbf{x})$ is conservative. Equally, $\nabla \times \mathbf{F}_C = 0$ as is also required of a conservative force. Formally, the Laplacian of $\mathcal{V}_C(\mathbf{x})$ is

$$4\pi \nabla^2 \mathcal{V}_C(\mathbf{x}) = -\sum_{i=1}^{M} Z_i \delta(\mathbf{x} - \mathbf{R}_i) + \sum_{i=1}^{N} \delta(\mathbf{x} - \mathbf{r}_i) \\ + \sum_{i=1}^{M} Z_i^2 \delta(\mathbf{x} - \mathbf{R}_i), \tag{19b}$$

where the first two terms on the right are the net nuclear and electronic charge density, respectively. Thus

$$4\pi \int_V d\mathbf{x} \, \nabla^2 \mathcal{V}_C(\mathbf{x}) = \sum_{i=1}^{M} Z_i^2 - z, \tag{19c}$$

where

$$z = \sum_{i=1}^{M} Z_i - N \tag{19d}$$

is the net charge of a polyatomic ion. Earnshaw's theorem applies: $\mathcal{V}_C(\mathbf{x})$ is subharmonic ($\nabla^2 \mathcal{V}_C > 0$) and sustains interior minima in V corresponding to stable mechanical configurations. Consequently, the Coulomb potential $\mathcal{V}_C(\mathbf{x})$ is stabilizing. The stability of a polyatomic ion is due entirely to the bilateral repulsion between its nuclei. Any reduction in this repulsion through, say, nuclear screening [323] – a phenomenon unavailable to self-gravitating systems[†] – destabi-

---

*This is a condition deemed necessary [336] for the Coulomb Hamiltonian operator to be self-adjoint.

[†]Even though the gravitational and Coulomb forces are both inverse square relations, the former is always attractive because of the positive mass theorem [353, 354] while the latter may be attractive or repulsive according as the charges are different or alike.

lizes a neutral molecule or polyatomic ion. The PEP promotes stabilization by boosting nuclear screening through the dispersal of fermions and the assembly of bosons that characterizes its vague role.

The work done on an arbitrary particle (electron or nucleus) of charge q in V is

$$\int_V d\mathbf{x}\, \nabla \cdot \boldsymbol{F}_{\mathrm{C},q}(\mathbf{x}) = -q \sum_{i=1}^n q_i \int_V d\mathbf{x}\, \nabla_{\mathbf{x}_i}^2 \left(\frac{1}{|\mathbf{x} - \mathbf{x}_i|} \right) \quad (20a)$$
$$= -4\pi q z \,,$$

where

$$\boldsymbol{F}_{\mathrm{C},q}(\mathbf{x}) = -q \sum_{i=1}^n q_i \nabla_{\mathbf{x}_i} \left(\frac{1}{|\mathbf{x} - \mathbf{x}_i|} \right), \quad (20b)$$

with q_i and $\mathbf{x}_i \in \mathbf{R}^M \times \mathbf{r}^N$ as the charge and location, respectively, of any of the molecule's $n = M + N$ particles (including the one under consideration), which vanishes if $z = 0$, is exothermic if $z < 0$ as in anion formation, and endothermic if $z > 0$ as in cation formation and consistent with our previous finding that nuclear screening increases with stabilizing anion formation, and conversely. The propensity of an atomic or polyatomic species to form ions is a measure of its stability and consequent reactivity in context [355, 356, for e.g.]. The findings of Lieb and Loss [357] (whose assumptions on the separability or disentanglement of all nuclei – regardless if they in bulk supply have fractional integer spins as to follow Fermi-Dirac statistics – from the fermionic pool, we avoid) are in accord with our revelation of the preference for anion formation as observed empirically.

The Lorentz-Faraday conservative force $\boldsymbol{F}_{\mathrm{int}} = -\nabla \mathcal{V}_{\mathrm{int}}$ in (13a) is the sum of the negative gradient of the scalar potential Φ as given in (14a) and the curl of the vector potential $\mathbf{A}$ as given in (14b). Since the div curl vanishes, it is clear that $\nabla^2 \mathcal{V}_{\mathrm{int}}(\mathbf{x}, t) = \nabla^2 \Phi(\mathbf{x}, t)$ so that the Lorentz-Faraday force $\boldsymbol{F}_{\mathrm{int}}$ is stabilising just like the Coulomb force $\boldsymbol{F}_{\mathrm{C}}$ provided ϕ is subharmonic at $\mathbf{x} \in V$.

Earnshaw's theorem reveals the propensities of a fixed aggregation of nuclei and electrons acting collectively under the Coulomb potential to form mechanically stable species (molecules or polyatomic ions), isomers with identical chemical formulas but different arrangements of nuclei giving rise to structural isomerism in which chemical bonds between nuclei differ, or stereoisomerism in which the bonds are the same but the relative positions of the nuclei differ. Such isomers generally have different physical and chemical properties. Thus, the paradigmatic classical molecular structures [358–360] of chemistry are evidentially a consequence of the subharmonic nature of the Coulomb potential and not a self-styled conundrum [361] whose long-crusading resolution [362, et passim] would have it devolve to a foundational defect of quantum theory.

This proof of the mechanical stability of matter based on Earnshaw's theorem is within the grasp of anyone with high school "calculus and vectors" preparation. Additionally, the proof makes no distinction between the stability of a single molecule over that of molar amounts of them within the scope of the extensivity-intensivity [363, 364] divide. Mechanical stability of molecules as gauged by Earnshaw's criterion is of paramount importance regardless of quantum mechanics. Shell and orbital models are used to describe the arrangements of protons and neutrons in atomic nuclei and electrons in atoms and molecules, respectively. The shells or orbitals are filled with fermions in order of increasing energies except when the binding energy of the next addition is less than the last and in post hoc compliance with the PEP and Hund's rule of maximum multiplicity. The motion of the electrons in a molecule constrains the nuclei to a particular geometric configuration, one that minimizes their energy functional.

The widespread belief that the PEP is necessary and sufficient for the stability of molecules would appear to have entrenched itself in the lore of chemistry and physics when Niels Bohr proclaimed it to be so in his *Faraday Lecture* to the Chemical Society [198]. This should not come as a surprise given that the forces responsible for molecule formation in the most reductionist way from their constituent nuclei and electrons are entirely classical in origin. Since the Coulomb potential was shown to be subharmonic, Earnshaw's theorem lends credence to the fact that aggregates of nuclei and electrons can be mechanically stable independently of both the PEP and the overarching assumption that even the heaviest of nuclei cannot be fermions regardless of their spin. The Lorentz-Faraday potential is purely quantum mechanical in origin, it is operative under thermal conditions, and it is subharmonic and stabilizing.

As Chandrasekhar [365, 366] demonstrated in revealing the limiting mass above which electron degeneracy pressure in a star's core is insufficient to balance the star's own gravitational self-attraction, the PEP cannot be naively invoked independently of the Heisenberg uncertainty principle, although most chemists and high school science teachers routinely do so.

Slater [367] was first to point out the relevance of the quantum mechanical counterpart of Clausius' classical virial theorem for stationary state molecular systems [368, for e.g.]. The quantum mechanical virial theorem has been proved for polyatomics [369] and reads as

$$2\overline{\langle KE \rangle} + \overline{\langle \mathcal{V}_{\mathrm{C}} \rangle} = 0 \,, \quad (21)$$

where $\overline{\langle KE \rangle}$ and $\overline{\langle \mathcal{V}_{\mathrm{C}} \rangle}$ are the time-averaged expectation values of the kinetic KE and potential $\mathcal{V}_{\mathrm{C}}$ energies, respectively, without drawing any distinction between the masses of nuclei relative to electrons, the sole difference being in relation to their spins. Since $E = \overline{\langle KE \rangle} + \overline{\langle \mathcal{V}_{\mathrm{C}} \rangle} = 1/2 \overline{\langle \mathcal{V}_{\mathrm{C}} \rangle}$, clearly the virial theorem is closely related to the conservation of energy principle.

Clausius' derivation of the classical virial theorem used Jacobi [370]'s extension of Lagrange's treatment of the 3-

body problem to many-body systems which, in conjunction with the first law of thermodynamics, permitted him to investigate the stability of self-gravitating systems. Jacobi's approach applies equally to a molecule whether in a stationary state under Coulomb control or in a dynamic state under Lorentz-Faraday control. In this regard, the equivalence of the stability criteria of Jacobi and Earnshaw is clear: they both maintain that an harmonic molecule is unstable regardless of the PEP which of course was unknown to them. Whether molar quantities of harmonic molecules are stable or not depends on how they interact and in so doing could make each other anharmonic and potentially less stable or even unstable. Thus, water condenses to liquid and further solidifies under sundry conditions but with differences in their underlying stabilities determined by their hydrogen-bonding networks without necessarily invoking the PEP.

The virial theorem states that if any system whose conservative forces come from a potential energy function which is a power law of the distance between its constituents – such as a self-gravitating body ($\mathcal{V}_g$) or a Coulomb molecule ($\mathcal{V}_C$) – settles into equilibrium then its total energy will be balanced between the kinetic energy of those constituents and the potential energy stored due to their mutual interaction. As previously remarked, the virial theorem presupposes the applicability of the first law of thermodynamics for a stationary system. In a thermal field where the SLT reigns, the first law takes an hiatus and the steady-state virial theorem given in (21) is supervened upon by its dynamical counterpart as will now be explained. Before doing so, however, it is appropriate to note that Pollard [371] gave a derivation of the classical virial theorem which eliminates its unnecessary assumption that the system is bounded in the sense that distances between particles and the velocities of the particles remain bounded as was Ambartsumian [294]'s objection to Zwicky [293]'s use of the virial theorem, and replaced it by the condition that for the theorem to hold it is both necessary and sufficient that for $\mathbf{x}_i \in \mathbf{x}$, $\max\limits_{i<j\leq n} |\mathbf{x}_i - \mathbf{x}_j| = O(t)$ as $t \to \infty$.

In an "isolated" molecule $\mathbf{F}_{\text{int}}(\mathbf{x}, t)$ is dormant but the Coulomb molecule is stable and undergoes reversible ($\Delta S = 0$) processes without the involvement of the phase. The Coulomb potential is classical with a basis in field theory [3, for e.g.] that sees it as involving the exchange of "virtual" photons created only for the duration of the exchange process. Such an exchange force may be either attractive or repulsive and whose range is set by the energy-time uncertainty principle so that a particle of mass m and rest energy $E = mc^2$ has a range of no more than $1/2mc$ which is infinite for a massless photon whose finite momentum can exert a force known as radiation pressure. However, if it were to be driven out of equilibrium by the stabilizing $\mathbf{F}_{\text{int}}(\mathbf{x}, t)$ at $T > 0$ the local phase would regulate irreversible ($\Delta S(t) > 0$) changes in the molecule. Unlike the Coulomb force, the Lorentz-Faraday force is quantum mechanical which, when operative at fi-

nite T, produces real Helmholtz-Hodge photons of unlimited range but of finite lifetime. Since photons are bosons of unit spin, transitions involving their absorption and emission must result in unit change in the angular momentum of the system for a net-zero change consistent with the absence of internal vortices in a heated molecule as was previously noted[*].

The probability density $\rho(\mathbf{x}, t) = |\psi(\mathbf{x}, t)|^2$, written identically as

$$\rho(\mathbf{x}, t) = \int_V d\mathbf{x}' \, \psi^*(\mathbf{x}', t)\delta(\mathbf{x} - \mathbf{x}')\psi(\mathbf{x}', t), \qquad (22a)$$

where the configurational kernel is formally

$$\delta(\mathbf{x} - \mathbf{x}') = \sum_{i=1}^{M} \delta(\mathbf{x} - \mathbf{R}_i) + \sum_{j=1}^{N} \delta(\mathbf{x} - \mathbf{r}_j) \qquad (22b)$$

with $\mathbf{x}, \mathbf{x}' \in V \subseteq R^n = \mathbf{R}^M \times \mathbf{r}^N$ and $n = M + N$ is a normalization constant so that

$$\int_V d\mathbf{x} \, \rho(\mathbf{x}, t) = n, \qquad (22c)$$

to give the expectation value of the kinetic energy of motion of the molecule's constituents as

$$\begin{aligned}\langle KE(t) \rangle &= \frac{1}{2} \int_V d\mathbf{x} \, \rho(\mathbf{x}, t)|\nabla\phi(\mathbf{x})|^2 \\ &= \frac{1}{2} \int_V d\mathbf{x} \left(\sum_{i=1}^{M} |\nabla_{\mathbf{R}_i}\phi(\mathbf{x})|^2 + \sum_{j=1}^{N} |\nabla_{\mathbf{r}_j}\phi(\mathbf{x})|^2 \right). \end{aligned} \qquad (22d)$$

The virial of $\mathbf{F}_{\text{int}}(\mathbf{x}, t)$ being $\oint_{\partial V} da \, \hat{\mathbf{n}} \cdot \mathbf{F}_{\text{int}}$, within V its expectation value is

$$\begin{aligned}\langle \nabla \cdot \mathbf{F}_{\text{int}}(t) \rangle &= \int_V d\mathbf{x} \, \rho(\mathbf{x}, t)\nabla \cdot \mathbf{F}_{\text{int}}(\mathbf{x}, t) \\ &= \int_V d\mathbf{x} \left(\sum_{i=1}^{M} \phi(\mathbf{x})\nabla_{\mathbf{R}_i}^2\phi(\mathbf{x}) + \sum_{j=1}^{N} \phi(\mathbf{x})\nabla_{\mathbf{r}_j}^2\phi(\mathbf{x}) \right) \end{aligned} \qquad (22e)$$

which is the work done $Q(t)$ by $\mathbf{F}_{\text{int}}$ that the change in entropy exceeds at $T > 0$ as given by the quantized Clausius inequality in (11a) or (11b).

The sum of $2\langle KE(t) \rangle$ and $\langle \nabla \cdot \mathbf{F}_{\text{int}}(t) \rangle$ vanishes[†]

$$2\langle KE(t) \rangle + \langle \nabla \cdot \mathbf{F}_{\text{int}}(t) \rangle = 0. \qquad (22f)$$

---

[*]The Coulomb force acting between two charges is generally not parallel to the vector separating them and so exerts a torque on each which means that the angular momentum of any charge changes all the time with the two charges merely "exchanging angular momentum" whose total is conserved. A similar but more complex exchange process [372, for e.g.] undoubtedly takes place between the charged constituents of a molecule and its internal Helmholtz-Hodge electromagnetic field.

[†]Wigner has pointed out [373, loc. cit., p. viii] that "It is a well known fact . . . " (pausing until resuming his unswerving accuracy) "It is well known to some people that every operator can be made self-adjoint." For $f \in L^2$, $\langle f, \nabla^2 f \rangle + \langle \nabla f, \nabla f \rangle = 0$, a fact acknowledged by Slater [367].

This extension of the virial theorem to nonstationary dynamics involving internal Lorentz-Faraday forces is consistent with Milne [374]'s demonstration that the virial theorem continues to hold true if the particles are acted on by external frictional forces proportional to their velocities and Collins' [375, loc. cit., p. 97] remark:

> To date the virial theorem has been applied to systems in or near equilibrium. It is worth remembering that perhaps the most important aspect of the theorem is that it is a global theorem. Thus systems in a state of rapid dynamic change are still subject to its time dependent form.

The relation of KE to Q often presents as an unwitting pitfall. Recall that heat and temperature are not the same: heat is the total kinetic energy while temperature is the average kinetic energy with the difference depending on the number of degrees of freedom of the system and the dispersal or spread of energy at that temperature as quantified by entropy [376, et passim]. Nor are work and heat synonymous. As remarked before, work is the transfer of energy by any means other than heat except if associated with a nonconservative force like friction, but heat can only be partly converted to work.

The Morse-Sard theorem [146, 147] precludes the sum $2KE + \nabla \cdot \boldsymbol{F}_{\text{int}}$ from vanishing locally except at the critical points of ϕ, a set of measure zero. This means that $2KE + \nabla \cdot \boldsymbol{F}_{\text{int}}$ does not vanish over subregions or fragments of the molecule (or a self-gravitating body) as to provide virialized building blocks transferable in noumena to other molecules (or self-gravitating bodies) in violation of the no-cloning theorem [377–379] of quantum mechanics.

Just as with entropy changes $\overline{\langle \Delta S_\tau \rangle}$ given by (11c) for arbitrary relaxation times (1/rates) under nonstandard state conditions, the Laplace long-time averages

$$\overline{\langle KE_\tau \rangle} = \int_0^1 ds \, e^{-s} \langle KE(\tau s) \rangle \qquad (22\text{g})$$

and

$$\overline{\langle \nabla \cdot \boldsymbol{F}_{\text{int}\tau} \rangle} = \int_0^1 ds \, e^{-s} \langle \nabla \cdot \boldsymbol{F}_{\text{int}}(\tau s) \rangle \qquad (22\text{h})$$

and their fluctuations are to be ascertained empirically. The time average of (22f) is $2\overline{\langle KE_\tau \rangle} + \overline{\langle \nabla \cdot \boldsymbol{F}_{\text{int}\tau} \rangle}$ and vanishes.

All objects at finite T emit thermal radiation as quantified by their emissivity [380], a dimensionless number $0 < \epsilon < 1$ covering the range from perfect reflector to perfect emitter and defined as the ratio of the energy radiated to that radiated by a blackbody at the same temperature and wavelength and under the same viewing conditions. An exception to this are black holes: classically, they are black body absorbers that do not emit anything but with the inclusion of quantum processes they can emit radiation and particles. Molecules emit energy that departs from a Planck distribution so the infrared light emitted by vibrating molecules can be used to identify their presence.

The energy density carried by an electromagnetic wave whose source lies in the internal fields of the molecule is given by their Poynting vector [381, 382, for e.g.] and the resultant radiation pressure is

$$\boldsymbol{p}_{\text{rad}}(\mathbf{x}, t) = \boldsymbol{E}_{\text{int}}(\mathbf{x}, t) \times \boldsymbol{B}_{\text{int}}(\mathbf{x}, t). \qquad (23\text{a})$$

Ideally, the photons constitute a black-body photon gas of low but finite intensity due to their relativistic speed. Consequently,

$$W = \oint_{\partial V} dW = \oint_{\partial V} da \, \hat{\mathbf{n}} \cdot \boldsymbol{p}_{\text{rad}}(\mathbf{x}, t) = \epsilon \, \sigma_{\text{SB}} \, T^4 V, \qquad (23\text{b})$$

where $\sigma_{\text{SB}} = \pi^2/60$ is the Stefan-Boltzmann constant. This, together with (12e), ensures that U is in compliance with the first law of thermodynamics and with d'Alembert's principle from which the conservation of energy follows as a consequence [155, cf. Ch. IV]. In the absence of a thermal context, the molecule is a stationary system with the conservative internal force $\boldsymbol{F}_{\text{int}}$ inoperative and with the Coulomb force $\boldsymbol{F}_C$ providing for its stability. The wave function's local phase has no bearing on the first law and features only when the system is open to exchanges of heat with its surroundings at finite $T > 0$. Even in the absence of a cyclotron, a heated atomic-ionic-molecular system would be expected to exhibit cyclotron-like radiation emissions [383] contributing to W as its electrons and ions accelerate in the magnetic part of its internal Helmholtz-Hodge radiation field. If an atom at rest in the vicinity of a black hole can undergo spontaneous emission [384] there is nothing to prevent a molecule in a heat bath from doing likewise.

The Higgs potential determines whether the Universe is in a true (stable) or a false (metastable) vacuum state. The SM indicates [385] that the known Universe is in a metastable state that could spontaneously collapse through tunneling decay although not anytime soon since the lifetime of a metastable universe is predicted to be much longer than the current age (~ 13.8 Gyr) of the known Universe [386].

4.3 The absence of magnetic monopoles

Dirac [266] introduced magnetic monopoles to explain the quantization of electric charge [387] and to promote reciprocity between electricity and magnetism. He showed that the magnetic charge g_D and the electric charge e are related by $2g_D e = k$, where $k \in \mathbb{Z}$ thus uncovering the quantization of electric charge, so that when $k = 1$, say $g_D = e/2\alpha \simeq 68.5e$, where α ($\simeq 1/137$) is the Sommerfeld fine-structure constant. Assuming that the classical radius of an electron and the "radius" of a Dirac monopole are equal, one finds that their masses m_e and m_m are related by $m_m \simeq 4700 m_e$, making the magnetic (and gravitational forces) between two monopoles many times stronger than those between two electrons, on which basis searches have been conducted at every new accelerator.

If magnetic charges ρ_m and magnetic currents $\mathbf{j}_m$ were to exist, Faraday's law resulting from taking the curl of $\boldsymbol{E}_{\text{int}}$ as given in (13b) while recalling that curl grad vanishes and then replacing the curl in $\mathbf{A}$ by $\boldsymbol{B}_{\text{int}}$ as given in (13c), would read as

$$-\nabla \times \boldsymbol{E}_{\text{int}} = \alpha \left(4\pi \mathbf{j}_m + \frac{\partial \boldsymbol{B}_{\text{int}}}{\partial t}\right) \qquad (24a)$$

and the Ampère-Maxwell law would read as

$$\nabla \times \boldsymbol{B}_{\text{int}} = \alpha \left(4\pi \mathbf{j} + \frac{\partial \boldsymbol{E}_{\text{int}}}{\partial t}\right), \qquad (24b)$$

and the two would look more alike. The curl of $\boldsymbol{E}_{\text{int}}$ suggests that its solenoidal part would be generated by the time-varying $\boldsymbol{B}_{\text{int}}$ and moving magnetic charges $\mathbf{j}_m$ while the curl of $\boldsymbol{B}_{\text{int}}$ would imply that its solenoidal part would be generated by the time-varying $\boldsymbol{E}_{\text{int}}$ and moving electric charges $\mathbf{j}$. In both cases it is the movement of charge, whether magnetic or electric, that causes current flow while the time-varying fields are mutually generative. Additionally, the analogs of (1a) and (13d) are

$$\frac{\partial \rho_m}{\partial t} + \nabla \cdot \mathbf{j}_m = 0, \qquad (25a)$$

and

$$F_m = \rho_m \boldsymbol{B}_{\text{int}} - \mathbf{j}_m \times \boldsymbol{E}_{\text{int}}, \qquad (25b)$$

respectively, while the coupled wave equations in (16a) and (16b) have the electric and magnetic fields and their sources interchanged to give

$$\Box \boldsymbol{B}_{\text{int}} = -4\pi \left(\nabla \rho_m + \frac{\partial \mathbf{j}_m}{\partial t}\right) \qquad (25c)$$

and

$$\Box \boldsymbol{E}_{\text{int}} = -4\pi \nabla \times \mathbf{j}_m, \qquad (25d)$$

respectively.

Dirac [266]'s seminal paper makes specific reference to Weyl [388]'s gauge phase $U(1)$ and thereafter [266, 387] alludes to the vector potential of an external electromagnetic field without recourse to the adiabatic theorem [389]. The addition of the action $4\pi g_D k$ to the local phase ϕ makes no difference to its relative phase $\nabla \phi$ so that as a gauge fix this inclusion of the Dirac magnetic monopole does not ensure its detection.

However, in contrast to the polar vector $\mathbf{j}$ which is T even, the axial vector $\mathbf{j}_m$ is T odd so that the magnetic monopole's analog $\partial \mathbf{j}_m/\partial t$ of the Lorentz-Faraday force given in (8a) is even in time, a circumstance that would not only cause it to decelerate magnetic charge via (25c) but more importantly cause $\Delta S(t)$ to be symmetric in time at finite T in violation of the SLT as was argued earlier. This violation, perhaps, is why Nature has found no recent use for the elusive magnetic monopole [390–394], there being only a couple of reports [395, 396] of its detection neither of which were ever

replicated. Were one to exist, a magnetic monopole would rank as a new elementary particle for which $\nabla \cdot \boldsymbol{B}_{\text{int}} = 4\pi \rho_m$ is finite and would exhibit a PT violation so as to change sign under C [397, cf. Sec. 8]. Driven by $T > 0$, the integrability of $\theta = \phi - Et$ conveyed in (4) does not require the presence of a nodal line emanating from a magnetic monopole to cause ϕ to jump in value upon each complete cycle it makes around ∂V. Currently there is no explanation for the quantization of electric charge and it is taken to be an empirical fact.

Dirac's synthesis [266] implies that magnetic monopoles may exist. Their dismissal here applies equally to alternative proposals for their production. Grand unification theories [398–400, for e.g.] (GUTs) predict that shortly after the Big Bang magnetic monopoles were created whose conservation of magnetic charge stabilized them against decay as relics of the past. Indeed, the original impetus for inflationary theories [401, 402, for e.g.] of the Universe [403–407] was the so-called "monopole problem". If the early Universe underwent a phase transition because the symmetry of GUT accruing from the supposed coupling of electromagnetic interactions with the electroweak and strong forces into a single force was broken then, in principle, magnetic monopoles should have been produced in abundance. As yet, there is no empirical evidence for any such primordial monopoles. Inflation supposedly diluted their density in the Universe so that it is unlikely in Borel's sense that one will ever be detected. An alternative to the dilution explanation is simply that there are none. Forty years after his provocative paper, Dirac is quoted [408, loc. cit., p. vii] in a letter written to Abdus Salam at Trieste that "I am inclined now to believe that monopoles do not exist. Too many years have gone without any encouragement from the experimental side." Thermodynamics requires that electric charge be a scalar and magnetic charge be a pseudoscalar under T reversal. Since both charges are alike and cannot independently flip signs only one of them exists and it is not the magnetic monopole. This has not led to any curb in the enthusiastic pursuit of monopoles wherever they hide. However, the MoEDAL Collaboration at the LHC* failed [409, et passim] to detect magnetic monopoles with $g_D = 1, 2, 3$ and masses up to 75 GeV/c^2 at the 95 % confidence level via the magnetic dual of the Sauter-Schwinger [410, 411] proposal[†].

4.4 The scarcity of antimatter

The known Universe is primarily filled with matter, not antimatter [30, cf. Ch. 7]. There are no natural forms of antiparticles on Earth. Yet, antiprotons and positrons, the antiparticles of protons and electrons, respectively, can be produced in particle accelerators to serve vital roles in medical

---

*Large Hadron Collider

[†]This proposal of a mechanism for pair production is not a demonstrable "effect" in the ranks of the photoelectron, Zeeman, Stark, etc., each of which has been experimentally confirmed while to date the Sauter-Schwinger proposal has not.

physics [412]. The production of light antinuclei ($\overline{\mathrm{d}}$, $^3\overline{\mathrm{He}}$, and $^4\overline{\mathrm{He}}$, for e.g.) composed of antiprotons and antineutrons in high-energy cosmic-ray collisions with the ISM or from their annihilation of unknown dark-matter particles are under scrutiny within the AMS Collaboration on the ISS [413] and the ALICE Collaboration at CERN [414]. It has been intimated [415,416] that the observation of antihelium is the existence of antimatter-dominated regions containing anticlouds or antistars, it being estimated that there are ~ 2.5 ppb antistars within several hundred light years from our Sun.

If the C symmetry of the Lorentz-Faraday force $F_{\text{int}} = \partial\mathbf{j}/\partial t$ were possible it would amount to its T reversal (equivalently, a CP-violation) which is prohibited by the SLT. The baryon number is conserved in all interactions of the SM with the exception of chiral anomalies involving sphalerons – saddle points of the electroweak potential – for which there is no experimental evidence. Both GUT and SUSY allow violations of the conservation of baryon and lepton numbers through proton decay, but this too has never been observed.

The oppositely-charged proton and electron are the primary representatives of the baryonic and leptonic particles and their antiproton and positron particles are of opposite sign. In their electromagnetic interactions, C symmetry on the proton would result in a T reversal since the Lorentz-Faraday force will go from being odd to even in t. For the electron, however, no such T reversal occurs since the Lorentz-Faraday force remains odd in t for the positron. In short, the SLT rules out the copious presence of antiprotons in the Universe for the same reason as the nonobservance there of magnetic monopoles: they are both in violation of the SLT. In contrast, the production of positrons in the Universe is in compliance with the SLT.

Neutrinos have many sources: supernovae, the Sun, the Earth and its atmosphere, nuclear reactors, particle accelerators, etc.; they have no charge; they interact via the electroweak force and, perhaps, gravity; they are observed indirectly via the particles that emerge when a neutrino hits a detector; they have left-handed helicities (spin antiparallel to momentum). Nobody knows if neutrinos (ν_e, ν_μ, ν_τ) are their own antiparticles ($\overline{\nu}_e$, $\overline{\nu}_\mu$, $\overline{\nu}_\tau$) but all six leptons are regarded as distinct elementary particles in the SM. Neutrinos are the most abundant matter particles in the Universe and are candidates for dark matter. Hypothetical sterile neutrinos (which are believed to be right-handed and to interact only by gravity) have not been found in either the MicroBooNE [417] or the STEREO [418] experiments. The primary international experiments for neutrino science are NOvA, T2K, and DUNE. Due in large to their small but finite masses [419], neutrinos change flavor (e, μ, τ) in flight, a transformation known as neutrino oscillation [420, 421], behavior that lies beyond the purview of the SM. If the oscillations of neutrinos are different from that of their antineutrinos – a result which is currently not known within the 5σ standard of the SM – CP is broken with which neutrinos violate T-symmetry. This

would relegate neutrinos to the same league of CP violators as quarks [422, cf. Sec. 13]. Cosmic leptogenesis [423, 424, for e.g.] and baryogenesis [425, 426, for e.g] are related if for no other arguable reason than that they both occur under the same conditions of thermal disequilibrium to which statistical mechanics is inapplicable.

If B and L are the baryon and lepton numbers, at thermal equilibrium both $\langle B \rangle_T$ and $\langle L \rangle_T$ vanish so there is no net generation of either number. This justifies our prior application of Clausius' inequality for the time-dependent change in the entropy to show that baryons are in violation of the T-asymmetry of the SLT. This equally applies to leptons (neutrino oscillations, regardless) and is consistent with Sakharov [427, 428]'s departure from thermal equilibrium criterion for particle asymmetry, be it a baryon or a lepton.

Leptons and baryons are in violation of the SLT through their disregard for the T-asymmetry of entropy that accrues from the subharmonicity of the local phase ϕ whose gradient $\nabla\phi$ is the velocity of the wave packet of the lepton or baryon resulting in their mutual observed asymmetry. In short, the SLT is the reason why the cosmos is free of antimatter whether it be leptonic or baryonic.

4.5 The strong CP problem

Probe images [429] of the light outside the Milky Way (the cosmic optical background, COB) have implicated axions, hypothetical finite mass, neutral, spin zero, long-lived bosons, as candidate sources [430, 431] of dark matter to explain why through their decay into photons the light seen in the COB is brighter than expected. The original reason [432, 433] for proposing the existence of axions was to explain why CP violations present in weak interactions are absent in strong interactions [14, 15, et passim] as evidenced by the nonobservance [434] of an EDM of a neutron. Prompted by Peccei-Quinn axion theory [432, 433] for the strong CP problem, Wilczek and coworkers [435, 436] were among the first to identify axions as possible progenitors of wave-like dark matter. Because low-mass axions are thought to emanate from the interiors of hot stars as possible cold Bose-Einstein condensates [437] and to couple to two photons in a magnetic field, the CAST Collaboration at CERN [438] directs a strong magnetic field at our Sun to detect the X-ray photons from axions but has yet to report any findings. The search continues [439–441] but has so far failed to report their presence. Regardless, elusive axions could serve a purpose different from being suggestive of an equally elusive dark matter.

Wilczek [442] showed that the electrodynamics of axions can be described if one adds a term of the form $a\boldsymbol{B}_{\text{int}} \cdot \boldsymbol{E}_{\text{int}}$ to the Maxwell Lagrangian for an electromagnetic field ($\boldsymbol{E}_{\text{int}}$, $\boldsymbol{B}_{\text{int}}$), where a describes the strength of the axion field. This adds further charge density $-\nabla a \cdot \boldsymbol{B}_{\text{int}}$ to Gauss' law and current density $\nabla a \times \boldsymbol{E}_{\text{int}} + \dot{a}\boldsymbol{B}_{\text{int}}$ to Maxwell-Ampre's law, reflecting the fact that $a(\mathbf{x}, t)$ is both P and T odd. Recall-

ing [145] that under T reversal, E_{int} is even while B_{int} is odd, the inclusion of axions as sources of $(E_{\text{int}}, B_{\text{int}})$ in (16a,16b) does not reverse the arrow of time in violation of the SLT so that CPT invariance holds for axion-mediated strong interactions. This contrasts to both magnetic monopoles and antimatter discussed previously where the opposite is true and neither are observed in accord with the reality of the SLT.

A recent study [443] of a single gravitationally-lensed quasar found its Einstein rings [444] to exhibit anomalies suggesting the presence of wave-like behavior consistent with ultralight axions as a more viable dark matter candidate than WIMPs.

SM predicted EDMs are many orders of magnitude below current experimental limits. The aforesaid SLT restoration of CPT invariance for strong CP interactions via axions does not bode well for measurement of the EDMs of subatomic particles which have never been found [445–447, for e.g.] below what is effectively naught for a bona fide dipole moment regardless of significant instrumental and Bayesian data processing advances. Neither the SM nor the SMC provides an explanation for leptonic or baryonic asymmetry.

4.6 Heaviside dark energy and the expansion of the Universe

Imagine replacing the nuclei and electrons of a molecule with uncharged point particles of arbitrary masses such that their Coulomb potential is replaced by the gravitational potential and ρ, ϕ, $\mathbf{j}$, and F_{int} go over into ρ_{g}, ϕ_{g}, $\mathbf{j}_{\text{g}}$, and $F_{\text{int,g}}$, respectively, as the electromagnetic molecule analogizes to a self-gravitating body, which will proxy here as the Universe. Unlike the molecule in a heat bath catered to by the zeroth law of thermodynamics at finite temperature T, the Universe is alone in a CMB mean temperature [448] of ~ 2.725 K.

Gravitoelectromagnetism (GEM) connects the mass density ρ_{g} and the mass current density $\mathbf{j}_{\text{g}} = \rho_{\text{g}} \nabla \phi_{\text{g}}$ in a gravitational field as Maxwell-like equations, an analogy (with $\epsilon_0 \rightarrow -1/4\pi G$) first pointed out by the late-nineteenth century physicist and electrical engineer Oliver Heaviside [449, 450]. As a linear approximation to GTR [451, 452] in the weak-field limit without being Lorentz invariant, GEM is the field theory for the hypothesized graviton, a neutral and massless boson thought to propagate transversely on the null geodesics of the metric tensor at the speed of light, just as photons do in geometric optics.

On 11 February 2016 the Laser Interferometer Gravitational Wave Observatory (LIGO) announced [453] it had detected gravitational waves produced by the merger of two black holes more than a billion light years from Earth. The Universe is filled with massive objects which undergo rapid accelerations that generate detectable gravitational waves of four LIGO-defined categories, viz. Continuous, Compact Binary Inspiral, Stochastic, and Burst. Through their specific interactions these massive objects cause $\partial \mathbf{j}_{\text{g}}/\partial t$ to accelerate

a test particle of velocity $\nabla \phi_{\text{g}}$ with attendant gravitational waves: just like F_{int}, this source $F_{\text{int,g}}$ is odd in time and is fueled by the gradient in ρ_{g}. Gravitational waves do not travel backwards despite the indifference of electrodynamics and quantum mechanics to the direction of time. Consequently, within the range of validity of GEM, the Universe is T-asymmetric in compliance with the SLT and harbors neither gravitomagnetic monopoles nor antimatter contrary to the earlier findings of Sakharov [427, 428] who restored CPT invariance by invoking an anti-Universe that proceeded in reverse time since the Big Bang and where antimatter dominates. Paradoxically, Sakharov's anti-Universe was rediscovered recently by Turok and coworkers [454, 455] in a new cosmological model that *inter alia* includes a sterile neutrino-based dark matter hypothesis. Like Sakharov's, it too violates the T-asymmetry of the SLT as does their mutual anti-Universe.

Recall that the Maxwell stress tensor $\sigma_{\text{int,g}}$ has units of negative pressure*, with the diagonal elements providing the tension and the off-diagonal elements the shear, and represents the contribution of electromagnetism to the source of the gravitational field (curvature of spacetime) in GTR. The Poynting vector $S_{\text{int,g}} = E_{\text{int,g}} \times B_{\text{int,g}}$ provides the energy density of the gravitational waves emanating from the self-gravitating object as it expands at a rate that is accelerating just like the known Universe [457, et passim] due to the repulsive effect of $F_{\text{int,g}}$ on the gravitational field. Dark energy is the work done by the Heaviside analog $F_{\text{int,g}} = \nabla \cdot \sigma_{\text{int,g}} - \dot{S}_{\text{int,g}}$ of the Lorentz-Faraday force in causing this accelerating expansion, such energy being dark because gravitons are likely undetectable [458, 459].

The recently launched European Euclid telescope plans to investigate dark energy and dark matter in a Universe wherein $\sim 95\%$ of its inventory is unknown. Dark energy is quantified by an equation of state parameter [460, for e.g.] w, the ratio of pressure to density. All indications are that w is close to -1 suggesting that the pressure is both outward (sic negative) and constant.

Alternatively,

$$w(t) \propto F_{\text{int,g}}/\rho_{\text{g}} = \nabla \phi_{\text{g}} \ln \dot{\rho}_{\text{g}} . \tag{26}$$

For the known Universe, $w(t)$ affects both its geometry, via $\nabla \phi_{\text{g}}$, and the growth rate of its structures, via $\ln \dot{\rho}_{\text{g}}$, so that $w(t) \leq 0$. The dark energy induced expansion is irreversible provided $\nabla \phi_{\text{g}}$ is finite in conjunction with $\ln \dot{\rho}_{\text{g}}$ serving as a time-varying sensitivity measure for $w(t)$; otherwise the Universe is in steady-state or is imploding, neither of which is believed to be true.

No one knows how the world will end but Katie Mack provides a guide [181] to some of the possibilities. Since

---

*Botanists [456, for e.g.] use the negative pressure $\rho h g$ of sap to explain how in the absence of an internal pump, ρ-density water ascends a height h through the xylem and phloem tissue against the acceleration due to gravity g for the tallest of trees.

the guide first appeared, several other speculative hypotheses have come along. For example, new early dark energy [461] with the potential to resolve the tension between recent local measurements of the expansion rate of the Universe using supernovae data and the expansion rate inferred from the early Universe via the CMB; dark matter particles with an extra force [462] proportional to the velocity squared mimics the temporal evolution of the effect of a cosmological constant; a mechanism [463] by which a dynamical form (quintessence) of dark energy could cause the acceleration of the Universe to cease and then transition from expansion to a phase of slow contraction of yet-another cyclic universe.

In contrast to such prevailing dogma, the preceding identification via (26) herein of dark energy as the work done by the Heaviside analog of the Lorentz-Faraday force in causing this accelerating expansion makes no reference to a cosmological constant Λ [464, 465] and its relation to the accelerating expansion of the cosmos [466]. There is no known experiment that can distinguish between Λ and a vacuum energy density. This ambiguity results in dark energy [467] and vacuum energy [468] being pursued as the leading candidates of finite Λ. Unruh and coworkers [469] tackled this beguiling problem in favor of the gravitational property of the quantum vacuum (assuming it gravitates in compliance with the equivalence principle of GTR) to suggest that there is no necessity for a finite Λ to explain the observed slowly accelerating expansion of the Universe as opposed to its catastrophic explosion*. Were T to approach zero, the self-gravitating object would no longer expand but could conceivably fragment or implode before dying as it ceases to emit further gravitons in assuring that its enthalpy U vanishes in compliance with the first law of thermodynamics†. If the Universe is stable, dark energy can maintain its current value, the laws of physics prevail into the future, and its fate will be an eventual heat death. However, if as is popularly believed, it is unstable or metastable because the mass of the Higgs boson is appreciably less than that of the top quark [471], the quantum vacuum may spontaneously decay to a lower-energy state whereupon black holes consume galaxies and each other before eventually evaporating via Hawking radiation [472] emissions. At that point, all that remains in the Universe are photons and gravitons and wayward masses so remote from each other that they do not interact with anything, gravitationally or otherwise. Frautschi [473, loc. cit. p. 599] failed to identify a scheme for the immortality of life: his hope that radiant energy production would continue without limit so that life capable of using it forever can be created is not likely to transpire.

As the only survivors of that *fin de cosmos*, photon and graviton fields resort interminably to Gertsenshtein [474] exchange in which one field produces the other under the aegis of their respective $B_{\text{int,g}}$. The process is irreversible in accord with the quantum Clausius inequality given in (11b) provided the respective ϕ_g for the photon and graviton field is subharmonic. At this juncture time stops and is superfluous since in the absence of mass it lacks measure.

With possibly one provocative exception [475–477], all indications [478] are that the known Universe is flat or, if it has any curvature, it is small. Since the boundary ∂V is embedded in $V(t)$, the Willmore functional [479] of $V(t)$ given by

$$\mathcal{W}(V(t)) = \oint_{\partial V} da \, \hat{\mathbf{n}} \cdot (H(\mathbf{x})^2 - K(\mathbf{x})) \geq 0 \,, \qquad (27)$$

serves as a measure of how much $V(t)$ deviates from a hypersphere on which $H^2 = K$ everywhere, where H is the local mean curvature (average trace of $\mathbf{S}$, the shape operator) and K is the local Gaussian curvature (determinant of $\mathbf{S}$) of $V(t)$. Finite $\mathcal{W}(V(t))$ provides a route to monitor local changes under Willmore flow [480] and provides an alternative to the pursuit of a cosmological constant based on the Weyl curvature of the Maxwell stress tensor $\sigma_{\text{int,g}}$ [74, 481].

Once the Willmore flow of $V(t)$ is established, the phase $\phi_{\text{int,g}}$ is provided via the Perron-Wiener-Brelot solutions to a Dirichlet problem [482, cf. Ch. 4] on the boundary ∂V whereon it is maximized and within which it is subharmonic. The phase is furthermore relatable to its hyperspherical harmonic expansions [483, 484] available in principle for many-body systems beyond banal one- and two-particle approaches. With $\mathcal{W}(V(t))$ and $\phi_{\text{int,g}}$ so determined, the de Broglie-Sommerfeld condition in (4) comes into its own in providing the distribution of mass $\rho_{\text{int,g}}$ in the system as a function of energy and its sidekick, entropy.

4.7 Recirculation

Under extreme mechanical loading or shearing conditions, materials are driven so far from equilibrium that they and their molecules change shape irreversibly. Cell membranes tend to position themselves so as to minimize their Willmore energy [485], a finding consistent with the long-standing importance for both biologic [486, cf. Ch. 9], [487], [488] and nonbiologic [489] specificity disregarded in the fog of one upmanship [490].

A neutral atom of atomic number Z has a boundary $\partial V \subseteq R^N$ with $N = Z$. A lone atom in V at $T > 0$ is orientationally spherical and its V is of finite mean curvature $1/r_Z$ and Gaussian curvature $1/r_Z^2$, where r_Z is the atomic radius. For a molecule at $T > 0$ within $\partial V \subseteq R^n$ with $n = M + N$, the stabilizing Lorentz-Faraday $\mathcal{V}_{\text{int}}(\mathbf{x})$ and Coulomb $\mathcal{V}_C(\mathbf{x})$ potentials are noncentral and V is unlikely to be spherical. There is

---

*After a brief ($\ll 1$ s) period of inflationary expansion (sic stretching), the Universe ostensibly contracted for ~ 9 billion years before it started to expand again at an accelerating rate fueled by dark energy or, equivalently, an energy density homogeneously distributed in the vacuum that is many orders of magnitude larger than the value Einstein thought it ought to have.

†If ever $0 < T \ll 1$, Q and W vanish via (12e) and (23b), respectively, so that $U = 0$ and $F = 0$ whereat nothing further happens since no more work can be done at which time ΔS vanishes, a view first proposed by Thomson (sic Kelvin) [470] and commonly known as the Heat Death (aka Big Freeze) of the Universe.

       Gerald F. Thomas. The Arrow of Time and Its Irreversibility

no *a priori* reason why any but the simplest of molecules cannot take on knotted configurations in their chemical graphs. The volume of a molecule is not necessarily a simply connected surface whose boundary is free of holes. Pursuit of the protean development of *V* for a molecule under Willmore flow might provide an algorithmic basis for those notions of molecular volume and shape in use since pioneered by Einstein and Perrin but found wanting by some [362, et passim].

5 Conclusion

By simplifying the system of interest to that of a single entity – a molecule or any other particle or structure in its known Universe – whose only descriptor is its wave function from which the Lorentz-Faraday force emerges without appeal to the equipartition theorem [491, for e.g.] but rather from the gradient of its phase when the system connects to a thermal field, whence it relays both the direction of time and entropy increases to the observable macroscopic world of thermodynamics from the microscopic worlds of quantum mechanics and electrodynamics.

Both the SLT and Faraday's law of electrodynamics are of similar vintage and status. Surprisingly, they share a hitherto unrecognized connection at the microscopic level. Whereas the former receives unrelenting challenges and suggested modifications, the latter presents just a few conceptual difficulties and paradoxes for some but without offers to replace it for any technological benefit over that which it has long wielded. Here it was shown that both laws are easily understood by standard quantum mechanics that does not dismiss the local phase of a system's state as being as physically unimportant as is widely promulgated.

The relationship between the thermodynamic arrow of time and time-reversal symmetry in nonrelativistic quantum mechanics was shown to lie in the continuity equation for the probability density and its connection to the probability current through the local phase of the charge amplitude. The change in the entropy of an autonomous molecule in contact with a heat bath was shown to be asymmetric in time and increases (irreversible process) or remains unchanged (reversible process) according as the relative change in its wave function's local phase is finite or vanishes, respectively. Thermal equilibrium is attained though weak neutral currents caused by internal electric and magnetic fields originating with the conservative Lorentz-Faraday forces acting on the nuclei and electrons of a molecule as affected by its hotter environment.

The evolution of **j** as identified in (8b) is driven by the feedback $\nabla \cdot \mathbf{j}$ as modulated by the finite time-independent gradient of ϕ, the phase of the wave function ψ. This feedback is integral to a system in a thermal field and however it determines the dynamics of the system, in no way does it control that dynamics. If the feedback is negative it tends to produce stability as evidenced by the fulfillment of the virial theorem.

The SLT determines that the feedback loop evolution is negative, consistent with Sommerfeld [144, cf. §28]'s radiation condition on ψ as was previously noted (*vide supra*). If, however, the feedback is positive as identified in (8c), it gives rise to instabilities as manifested by violations of the virial theorem, exemplified by dark energy acceleration of the Universe in the weak field limit, for instance.

Processes between the system and its surroundings driven by nonthermal gradients are similarly accompanied by an increase in the total entropy whose T-asymmetry prevails through its ongoing relation to the rate of change in the probability current, an operator that is even in time. While the wave function's local phase was shown not to influence the system's necessary fulfillment of the first law of thermodynamics, its subharmonicity was shown to be a necessary and sufficient condition for it to comply with the SLT as first formulated by Clausius. The time asymmetry of $\Delta S(t)$ additionally implies that the detection of permanent EDMs of subatomic particles (electron, proton, neutron, muon) – a consequence of CP violations and T-asymmetry in particle physics, with or without the assumptions of CPT symmetry [28, 29] – may never succeed. Indeed, the latest high-precision measurement [492] of the EDM of an electron drew a blank. The spectroscopic technique used by Roussy et al. [492] has an estimated mass reach of 40 TeV, an order of magnitude higher than at the LHC.

It is worth noting that the Hamiltonian operator of the system has played no explicit role in this exposition other than through the ubiquitous self-adjointness of the Laplacian, confined or free. Entropy production is greater when the local phase is subharmonic on the boundary rather than within the molecular volume. Faraday's law of induction was shown to hold for a single molecule provided the gradient of its local phase is finite, a necessary and sufficient condition for it not to present with its well-known paradoxes.

The primary contribution of this paper is the identification of internal conservative Lorentz-Faraday forces acting on the nuclei and electrons of a molecule in a thermal field and their decomposition into coupled internal electric and magnetic fields. This highlights the role of the dynamic probability current in causing entropy changes to be T-asymmetric contrary to the received word [98, 493–495, for e.g] that the direction of the arrow of time in macroscopic systems ought to originate from dominant (sic fundamental) time-reversal symmetric classical and microscopic dynamics or quantum fluctuation relations when in reality the opposite applies due to fact that the world is observed macroscopically even if perceived microscopically. Additionally, it brings out the role of the local phase of the state in distinguishing reversible from irreversible thermodynamic processes in accord with Clausius' formulation of the SLT and in providing a microscopic basis for Faraday's law of induction through the presence of electrically neutral currents mediated by photon exchange in all intramolecular interactions involving the nuclei and elec-

trons of the molecule and so revealing the greater importance of electrodynamics over electrostatics as long ago asserted by Earnshaw in accounting for the stability of molecules.

Due to its failure to fully live up to its marquee standing, the SMC has spurred many explorations beyond its domain for "new physics" but without first addressing what is its most fundamental oversight: its failure to comply with the SLT and its corollary, that entropy increases in irreversible processes to punctuate the evolution of the known Universe.

By going back to Clausius' inequality and interpreting it quantum mechanically, what has been done here is to refute the claim that time is reversible in showing that the entropy gain is T-asymmetric for a molecule – or any other particle or structure in its Universe – from their initial appearance in a thermal field to their final destiny. This paper makes only one prediction: travel to the past is impossible either quantum mechanically or electromagnetically, not because it is as highly improbable as it is found to be, but because it would cause entropy changes to decrease contrary to the SLT. The GTR has played no role in this finding*.

The asymmetry in entropy invalidates several falsifiable predictions of the SMC attributable to its disregard for the SLT – including, the cosmic facts that magnetic monopoles do not exist, that antimatter is scarce to none, that hypothetical axions explain the strong CP paradox without necessarily accounting for dark matter, and that dark energy is the basis for the accelerated expansion of the known Universe.

In the practice of reductionism, macroscopic physics supervenes upon the microscopic, the SLT being the most conspicuous exception to that superfluous tenet. The supersedence of classical thermodynamics over quantum mechanics and electrodynamics across spatio-temporal scales ranging from an individual quantized system to its known Universe has been shown herein. Additionally, in showing that reversible (irreversibility) processes are affiliated with the particle $\nabla\phi = 0$ (wave $\nabla\phi > 0$) behavior of matter, attention has been drawn to a heretofore overlooked connection between the different roles of classical thermodynamics and time-invariant quantum mechanics and electrodynamics in respect to arrow-of-time asymmetry and wave-particle duality.

Acknowledgements

---

*Solutions to the GTR field equations exist that purport to provide for time travel via closed time-like curves [496, et passim]. These speculative universes accommodate an Orwellian endless present where history pauses, just as in the case of reversible processes where $\Delta S(t) = 0$ and distinguishing later from earlier (and vice versa) events does not matter. With irreversible processes, however, $\Delta S(t) > 0$ and discerning current from past events counts as it does in the known Universe in harmony with the SLT; attempting to know past from present events implies that $\Delta S(t) < 0$ whereby evolution reverses, a physical impossibility that historians and allied scholars adroitly avoid.

References

1. G. Lüders. Proof of the TCP Theorem. *Ann. Phys.*, 1957, v. 2, 1–15.

2. C. P. Burgess and G. D. Moore. The Standard Model: A Primer. Cambridge University Press, New York, 2007.

3. M. D. Schwartz. Quantum Field Theory and the Standard Model. Cambridge University Press, New York, 2014.

4. R. G. Sachs. The Physics of Time Reversal. University of Chicago Press, Chicago and London, 1987.

5. T. D. Lee and C. N. Yang. Question of Parity Conservation in Weak Interactions. *Phys. Rev.*, 1956, v. 104, 254–258.

6. Chien-Shiung Wu, E. Ambler, R. W. Hayward *et al.* Experimental Test of Parity Conservation in Beta Decay. *Phys. Rev.*, 1957, v. 105, 1413–1415.

7. M. Planck. Treatise on Thermodynamics. Longmans, Green & Co., London, New York, & Bombay, 1903.

8. V. Čápek and D. P. Sheehan. Challenges to the Second Law of Thermodynamics. Springer, Dordrecht, Netherlands, 2005.

9. F. Brandao, M. Horodecki, N. Ng *et al.* The second laws of quantum thermodynamics. *Proc. Natl. Acad. Sci. USA*, 2015, v. 112, 3275–3279.

10. G. E. Crooks and S. Still. Marginal and conditional second laws of thermodynamics. *EPL*, 2019, v. 125, 40005.

11. J. H. Christenson, J. W. Cronin, V. L. Fitch *et al.* Evidence for the 2π Decay of the K_m^0 Meson. *Phys. Rev. Lett.*, 1964, v. 13, 138–140.

12. A. Alavi-Harati *et al.* [The KTeV Collaboration]. Observation of Direct CP Violation in $K_{S,L} \to \pi\pi$ Decays. *Phys. Rev. Lett.*, 1999, v. 83, 23–27.

13. J. P. Lees *et al.* [The BABAR Collaboration]. Observation of Time-Reversal Violation in the B^0 Meson System. *Phys. Rev. Lett.*, 2012, v. 109, 211801.

14. K. R. Schubert. T violation and CPT tests in neutral-meson systems. *Prog. Part. Nucl. Phys.*, 2015, v. 81, 1–38.

15. J. Bernabéu and F. Martínez-Vidal. Time-Reversal Violation. *Annu. Rev. Nucl. Part. Sci.*, 2015, v. 65, 403–427.

16. T. E. Chupp, P. Fierlinger, M. J. Ramsey-Musolf *et al.* Electric dipole moments of atoms, molecules, nuclei, and particles. *Rev. Mod. Phys.*, 2019, v. 91, 015001.

17. I. B. Khriplovich and S. K. Lamoreaux. CP Violation Without Strangeness. Springer-Verlag, Berlin and Heidelberg, 1997.

18. E. A. Hinds. Testing Time Reversal Symmetry Using Molecules. *Phys. Scr.*, 1997, v. T70, 34–41.

19. E. D. Commins. Electric Dipole Moments of Leptons. *Adv. At. Mol. Opt. Phys*, 1999, v. 40, 1–55.

20. J. Engel, M. J. Ramsey-Musolf, and U. van Kolck. Electric dipole moments of nucleons, nuclei, and atoms: The Standard Model and beyond. *Prog. Part. Nucl. Phys.*, 2013, v. 71, 21–74.

21. T. Chupp and M. Ramsey-Musolf. Electric dipole moments: a global analysis. *Phys. Rev. C*, 2014, v. 91, 035502.

22. W. B. Cairncross and J. Ye. Atoms and molecules in the search for time-reversal symmetry violation. *Nat. Rev. Phys.*, 2019, v. 1, 510–521.

23. P. Mohanmurthy and J. A. Winger. Estimation of CP violating EDMs from known mechanisms in the SM. *PoS*, 2021, v. ICHEP2020, 265–276.

24. C. Patrignani *et al.* (Particle Data Group). Review of Particle Physics. *Chin. Phys. C*, 2016, v. 40, 100001.

25. S. Okubo. Decay of the Σ^+ Hyperon and its Antiparticle. *Phys. Rev.*, 1958, v. 109, 984–985.

26. R. Aaij *et al.* [The LHCb Collaboration]. Measurement of matter-antimatter differences in beauty baryon decays. *Nat. Phys.*, 2017, v. 13, 391–396.

27. M. Ablikim *et al*. [The BESIII Collaboration]. Probing CP symmetry and weak phases with entangled double-strange baryons. *Nature*, 2022, v. 606, 64–69.

28. D. Babusci *et al*. [The KLOE-2 Collaboration]. Precision tests of quantum mechanics and $\mathcal{CPT}$ symmetry with entangled neutral kaons at KLOE. *J. High Energ. Phys.*, 2022, v. 59.

29. P. Moskal, A. Gajos, M. Mohammed *et al*. Testing CPT symmetry in ortho-positronium decays with positronium annihilation tomography. *Nat. Commun.*, 2021, v. 12, 5658.

30. C. Bambi and A. D. Dolgov. Introduction to Particle Cosmology. Springer-Verlag, Berlin and Heidelberg, 2016.

31. A. G. Riess *et al*. [High-Z Supernova Search Team]. Observational evidence from supernovae for an accelerating universe and a cosmological constant. *Astron. J.*, 1998, v. 116, 1009–1038.

32. S. Perlmutter *et al*. [Supernova Cosmology Project]. Measurements of Ω and Λ from 42 high-redshift supernovae. *Ap. J.*, 1999, v. 517, 565–586.

33. B. Carr, F. Kühnel, and M. Sandstad. Primordial black holes as dark matter. *Phys. Rev. D*, 2016, v. 94, 083504.

34. P. W. Graham, I. G. Irastorza, S. K. Lamoreaux *et al*. Experimental Searches for the Axion and Axion-Like Particles. *Ann. Rev. Nucl. Part. Sci.*, 2015, v. 65, 485–514.

35. A. Boyarsky, M. Drewes, T. Lasserre *et al*. Sterile Neutrino Dark Matter. *Prog. Part. Nucl. Phys.*, 2019, v. 104, 1–45.

36. D. Buttazzo, P. Panci, N. Rossi *et al*. Annual modulations from secular variations: relaxing DAMA? *J. High Energ. Phys.*, 2020, v. 137.

37. R. Penrose. The Big Bang and its Dark-Matter Content: Whence, Whither, and Wherefore. *Found. Phys.*, 2018, v. 48, 1177–1190.

38. S. van den Bergh. A Short History of the Missing Mass and Dark Energy Paradigms. In: V. J. Martínez, V. Trimble, and M. J. Pons-Bordería, eds. Historical Development of Modern Cosmology, Volume 252. ASP Conference Proceedings, San Francisco, 2001, pp. 75–83.

39. E. Oks. Brief review of recent advances in understanding dark matter and dark energy. *New Astron. Rev.*, 2021, v. 93, 101632.

40. J. Liu, X. Chen, and X. Ji. Current status of direct dark matter detection experiments. *Nat. Phys.*, 2017, v. 13, 212–216.

41. S. Vagnozzi, L. Visinelli, P. Brax *et al*. Direct detection of dark energy: The XENON1T excess and future prospects. *Phys. Rev. D*, 2021, v. 104, 063023.

42. L. Perivolaropoulos and F. Skara. Challenges for ΛCDM: An update. *New Astron. Rev.*, 2022, v. 95, 101659.

43. M. A. Green, J. W. Moffat, and V. T. Toth. Modified gravity (MOG), the speed of gravitational radiation and the event GW170817/GRB170817A. *Phys. Lett. B*, 2018, v. 780, 300–302.

44. C. Skordis and T. Złośnik. New Relativistic Theory for Modified Newtonian Dynamics. *Phys. Rev. Lett.*, 2021, v. 127, 161302.

45. P. D. Mannheim. Alternatives to dark matter and dark energy. *Prog. Part. Nuc. Phys.*, 2006, v. 56, 340–445.

46. S. Dodelson. The Real Problem with MOND. *Int. J. Mod. Phys. D*, 2011, v. 20, 2749–2753.

47. G. D. Starkman. Modifying gravity: you cannot always get what you want. *Phil. Trans. R. Soc. A*, 2011, v. 369, 5018–5041.

48. E. Abdalla, G. F. Abellán, A. Aboubrahim *et al*. Cosmology intertwined: A review of the particle physics, astrophysics, and cosmology associated with the cosmological tensions and anomalies. *J. High Energ. Ap*, 2022, v. 34, 49–211.

49. N. Menci, M. Castellano, P. Santini *et al*. High-redshift Galaxies from Early JWST Observations: Constraints on Dark Energy Models. *Astrophys. J.*, 2022, v. 938, L5.

50. M. Boylan-Kolchin. Stress testing ΛCDM with high-redshift galaxy candidates. *Nat. Astron*, 2023.

51. I. Labbé, P. van Dokkum , E. Nelson *et al*. A population of red candidate massive galaxies ~ 600 Myr after the Big Bang. *Nature*, 2023, v. 616, 266–269.

52. R. H. Thurston, ed. Reflections on the Motive Power of Heat. John Wiley & Sons, New York, 1897.

53. R. Clausius and W. R. Browne, transl. The Mechanical Theory of Heat. McMillan, London, 1879.

54. E. B. Starikov. Many Faces of Entropy or Bayesian Statistical Mechanics. *ChemPhysChem*, 2010, v. 11, 3387–3394.

55. G. A. Linhart. The Relation Between Entrophy and Probability. The Integration of the Entropy Equation. *J. Am. Chem. Soc.*, 1922, v. 44, 140–142.

56. G. A. Linhart. Correlation of Entropy and Probability. *J. Am. Chem. Soc.*, 1922, v. 44, 1881–1886.

57. G. A. Linhart. Correlation of Heat Capacity, Absolute Temperature and Entropy. *J. Chem. Phys.*, 1933, v. 1, 795–797.

58. A. S. Eddington. The Nature of the Physical World. McMillan, London, 1928.

59. A. Vilenkin. Boundary conditions in quantum cosmology. *Phys. Rev. D*, 1986, v. 33, 3560–3569.

60. D. S. Goldwirth and T. Piran. Entropy, Inflation and the Arrow of Time. *Class. Quant. Grav.*, 1991, v. 8, L155–L160.

61. S. W. Hawking, R. Laflamme, and G. W. Lyons. Origin of time asymmetry. *Phys. Rev. D*, 1997, v. 47, 5342–5356.

62. S. M. Carroll and J. Chen. Spontaneous Inflation and the Origin of the Arrow of Time. Technical Report EFI-2004-33, Enrico Fermi Institute, Department of Physics, and Kavli Institute for Cosmological Physics, University of Chicago, Chicago, 2004.

63. C. Kiefer. Quantum Cosmology and the Arrow of Time. *Braz. J. Phys.*, 2005, v. 35, 296–299.

64. R. M. Wald. The Arrow of Time and the Initial Conditions of the Universe. *Stud. Hist. Phil. Mod. Phys.*, 2006, v. 37, 394–398.

65. L. M. Krauss and R. J. Scherrer. The return of a static universe and the end of cosmology. *Gen. Rel. Gray.*, 2007, v. 39, 1545–1550.

66. J. J. Halliwell, J. Perez-Mercader, and W. H. Zurek, eds. Physical Origins of Time Asymmetry. Cambridge University Press, New York, 1993.

67. H. Price. Time's Arrow & Archimedes' Point. Oxford University Press, New York, 1996.

68. H. D. Zeh. The Physical Basis of the Direction of Time. Springer, Berlin, Heidelberg, and New York, 5 edition, 2007.

69. S. Carroll. From Eternity to Here: The Quest for the Ultimate Theory of Time. Dutton, New York, 2010.

70. L. Mersini-Houghton and R. Vaas, eds. The Arrows of Time: A Debate in Cosmology. Springer-Verlag, Berlin and Heidelberg, 2012.

71. V. K. Narayanan and R. A. Croft. Recovering the primordial density fluctuations: a comparison of methods. *Astrophys. J.*, 1999, v. 515, 471–486.

72. U. Frisch, S. Matarrese, R. Mohayaee *et al*. A reconstruction of the initial conditions of the Universe by optimal mass transportation. *Nature*, 2002, v. 417, 260–262.

73. R. Feynman. The Character of Physical Law. MIT Press, Cambridge, MA, 1967.

74. R. Penrose. Singularities and time-asymmetry. In: S. W. Hawking and W. Israel, eds. General Relativity: An Einstein Centenary Survey. Cambridge University Press, Cambridge, UK, 1979, pp. 581–638.

75. R. Penrose. Causality, quantum theory and cosmology. In: S. Majid, ed. On Space and Time. Cambridge University Press, New York, 2008, pp 150–200.

76. R. Penrose. Cycles of Time: An Extraordinary New View of the Universe. The Bodley Head, London, 2010.

77. M. López, P. Bonizzi, K. Driessens *et al*. Searching for ring-like structures in the cosmic microwave background. *Mon. Not. R. Astron. Soc.*, 2023, v. 519, 922–930.

78. D. An, K. A. Meissner, P. Nurowski *et al*. Apparent evidence for Hawking points in the CMB Sky. *Mon. Not. R. Astron. Soc.*, 2020, v. 495, 3403–3408.

79. D. L. Jow and D. Scott. Re-evaluating evidence for Hawking points in the CMB. *J. Cosmol. Astropart. Phys.*, 2020, v. 2020, 021–031.

80. R. Fernández-Cobos, A. Marcos-Caballero, and E. Martínez-González. Radial derivatives as a test of pre-Big-Bang events on the Planck data. *Mon. Not. R. Astron. Soc.*, 2020, v. 499, 1300–1311.

81. E. Bodnia, V. Isenbaev, K. Colburn *et al*. Conformal Cyclic Cosmology Signatures and Anomalies of the CMB Sky. *J. Cosmol. Astropart. Phys.*, 2023, v. 2023, 0xx21–0xx31.

82. G. M. Wang, E. M. Sevick, R. Mittag *et al*. Experimental Demonstration of Violations of the Second Law of Thermodynamics for Small Systems and Short Time Scales. *Phys. Rev. Lett.*, 2002, v. 89, 050601.

83. D. M. Carberry, J. C. Reid, G. M. Wang *et al*. Fluctuations and Irreversibility: An Experimental Demonstration of a Second-Law-Like Theorem Using a Colloidal Particle Held in an Optical Trap. *Phys. Rev. Lett.*, 2004, v. 101, 140601.

84. S. Deffner and E. Lutz. Generalized Clausius Inequality for Nonequilibrium Quantum Processes. *Phys. Rev. Lett.*, 2010, v. 105, 170402.

85. G. Argentieri, F. Benatti, R. Floreanini *et al*. Violations of the second law of thermodynamics by a non-completely positive dynamics. *EPL*, 2014, v. 107, 5007.

86. G. Argentieri, F. Benatti, R. Floreanini *et al*. Complete Positivity and Thermodynamics in a Driven Open Quantum System. *J. Stat. Phys.*, 2015, v. 159, 1127–1153.

87. T. L. Hill. Thermodynamics of Small Systems. *J. Chem. Phys.*, 1962, v. 36, 3182–3197.

88. T. L. Hill. A Different Approach to Nanothermodynamics. *Nano Lett.*, 2001, v. 1, 273–275.

89. D. Bedeaux, S. Kjelstrup, and S. K. Schnell. Nanothermodynamics: General Theory. PoreLab, Trondheim, Norway, 2020.

90. D. Keller, D. Swigon, and C. Bustamante. Relating Single-Molecule Measurements to Thermodynamics. *Biophys. J.*, 2003, v. 84, 733–738.

91. C. Bustamante, J. Liphardt, and F. Ritort. The Nonequilibrium Thermodynamics of Small Systems. *Physics Today*, 2005, v. 87, 43–48.

92. J. M. Rubi, D. Bedeaux, and S. Kjelstrup. Thermodynamics for Single-Molecule Stretching Experiments. *J. Phys. Chem. B*, 2006, v. 110, 12733–12737.

93. E. Bering, S. Kjelstrup, D. Bedeaux *et al*. Entropy Production beyond the Thermodynamic Limit from Single-Molecule Stretching Simulations. *J. Phys. Chem. B*, 2020, v. 124, 8909–8917.

94. J. Gemmer, M. Michel, and G. Mahler. Quantum Thermodynamics: Emergence of Thermodynamic Behavior Within Composite Quantum Systems. Springer, Berlin and Heidelberg, 2 edition, 2009.

95. F. Binder, L. A. Correa, C. Gogolin, J. Anders, and G. Adesso, eds. Thermodynamics in the Quantum Regime. Springer Nature, Switzerland, 2018.

96. R. S. Whitney, R. Sánchez, and J. Splettstoesser. Quantum Thermodynamics of Nanoscale Thermoelectrics and Electronic Devices. In: F. Binder, L. A. Correa, C. Gogolin, J. Anders, and G. Adesso, eds. Thermodynamics in the Quantum Regime. Springer Nature, Switzerland, 2018, pp. 175–206.

97. S. T. Dawkins, O. Abah, K. Singer *et al*. Single Atom Heat Engine in a Tapered Ion Trap. In: F. Binder, L. A. Correa, C. Gogolin, J. Anders, and G. Adesso, eds. Thermodynamics in the Quantum Regime. Springer Nature, Switzerland, 2018, pp. 887–896.

98. K. Funo, M. Ueda, and T. Sagawa. Quantum Fluctuation Theorems. In: F. Binder, L. A. Correa, C. Gogolin, J. Anders, and G. Adesso, eds. Thermodynamics in the Quantum Regime. Springer Nature, Switzerland, 2018, pp. 249–274.

99. R. Kosloff. Quantum Thermodynamics: A Dynamical Viewpoint. *Entropy*, 2013, v. 15, 2100–2128.

100. R. Alicki and R. Kosloff. Introduction to Quantum Thermodynamics: History and Prospects. In: F. Binder, L. A. Correa, C. Gogolin, J. Anders, and G. Adesso, eds. Thermodynamics in the Quantum Regime. Springer Nature, Switzerland, 2018, pp. 1–36.

101. L. G. Palmer and J. Gulati. Potassium Accumulation in Muscle: A Test of the Binding Hypothesis. *Science*, 1976, v. 194, 521–523.

102. G. Ling. Nano-protoplasm: the Ultimate Unit of Life. *Physiol. Chem. Phys. & Med. NMR*, 2007, v. 39, 111–234.

103. A. A. Deniz, S. Mukhopadhyay, and A. Lemke. Single-molecule biophysics: at the interface of biology, physics and chemistry. *J. R. Soc. Interface*, 2008, v. 5, 15–45.

104. S. A. Claridge, J. J. Schwartz, and P. S. Weiss. Electrons, Photons, and Force: Quantitative Single-Molecule Measurements from Physics to Biology. *ACS Nano*, 2011, v. 5, 693–729.

105. R. L. Baldwin. The nature of protein folding pathways: The classical versus the new view. *J. Biomol. NMR*, 1995, v. 5, 103–109.

106. C. L. Brooks III, M. Gruebele, J. N. Onuchic *et al*. Chemical physics of protein folding. *Proc. Natl. Acad. Sci. USA*, 1998, v. 95, 11037–11038.

107. P. G. Wolynes, W. A. Eaton, and A. R. Fersht. Chemical physics of protein folding. *Proc. Natl. Acad. Sci. USA*, 2012, v. 109, 17770–17771.

108. G. R. Heath, E. Kots, J. L. Robertson *et al*. Localization atomic force microscopy. *Nature*, 2021, v. 594, 385–390.

109. N. G. Walter, C.-Y. Huang, A. J. Manzo *et al*. Do-it-yourself guide: how to use the modern single-molecule toolkit. *Nat. Meth.*, 2008, v. 5, 475–489.

110. M. C. Leake. Single-Molecule Cellular Biophysics. Cambridge University Press, Cambridge, UK, 2013.

111. M. C. Leake. The physics of life: one molecule at a time. *Phil. Trans. R. Soc. B*, 2013, v. 368, 20120248.

112. P. A. M. Dirac. Quantum Mechanics of Many-Electron Systems. *Proc. R. Soc. Lond. A*, 1929, v. 123, 714–733.

113. P. Koehl and M. Levitt. A brighter future for protein structure prediction. *Nat, Struct. Biol.*, 1999, v. 6, 108–111.

114. S. Y. C. Bradford, L. E. Khoury, Y. Ge *et al*. Temperature artifacts in protein structures bias ligand-binding predictions. *Chem. Sci.*, 2021, v. 12, 11275–11293.

115. C. Tsallis. Nonextensive Statistical Mechanics: Construction and Physical Interpretation. In: M. Gell-Mann and C. Tsallis, eds. Nonextensive Entropy: Interdisciplinary Applications. Oxford University Press, New York, 2004, pp. 1–53.

116. C. Tsallis. Introduction to Nonextensive Statistical Mechanics. Springer, New York, 2009.

117. C. Caratheodory. Untersuchungen über die Grundlagen der Thermodynamik. *Math. Ann.*, 1909, v. 67, 355–386.

118. M. H. Anderson, J. R. Ensher, M. R. Matthews *et al*. Observation of Bose-Einstein Condensation in a Dilute Atomic Vapor. *Science*, 1995, v. 269, 192–201.

119. K. B. Davis, M. O. Mewes, M. R. Andrews *et al*. Bose-Einstein Condensation in a Gas of Sodium Atoms. *Phys. Rev. Lett.*, 1995, v. 75, 3969–3973.

120. C. A. Regal, M. Greiner, and D. S. Jin. Observation of Resonance Condensation of Fermionic Atom Pairs. *Phys. Rev. Lett.*, 2004, v. 92, 040403.

121. V. J. Stenger. Timeless Reality. Prometheus Books, Amherst, NY, kindle edition, 2000.

122. C. H. Lineweaver and C. A. Egan. Life, gravity and the second law of thermodynamics. *Phys. Life Revs.*, 2008, v. 5, 225–242.

123. E. P. Wigner. Über die Operation der Zeitumkehr in der Quantenmechanik. *Göttinger Nachrichten, Math-Phys.*, 1932, 546–559.

124. E. P. Wigner. Group Theory. Academic Press, New York, 1959.

125. S. Earnshaw. On the Nature of the Molecular Forces which regulate the Constitution of the Luminiferous Ether. *Trans. Camb. Phil. Soc.*, 1842, v. 7, 97–114.

126. B. Zhang *et al*. The Largest Synthetic Structure with Molecular Precision: Towards a Molecular Object. *Angew. Chem. Int. Ed. Engl.*, 2011, v. 50, 737–740.

127. Z. K. Silagadze. Multi-dimensional vector product. *J. Phys. A*, 2002, v. 35, 4949–4953.

128. P. Lounesto. Clifford Algebras and Spinors. Cambridge University Press, Cambridge, UK, 2 edition, 2001.

129. J. Gallier. Geometric Methods and Applications. Springer, New York, Dordrecht, Heidelberg, and London, 2 edition, 2011.

130. B. O'Neill. Elementary Differential Geometry. Academic Press, Boston, 2 edition, 2006.

131. M. P. do Carmo. Riemannian Geometry. Birkhäuser, Boston, 1992.

132. U. Fano. Description of states in quantum mechanics by density matrix and operator techniques. *Rev. Mod. Phys.*, 1957, v. 29, 74–93.

133. F. Reif. *Fundamentals of Statistical and Thermal Physics*. McGraw-Hill, New York, 1965.

134. A. Jabs. Connecting Spin and Statistics in Quantum Mechanics. *Found. Phys.*, 2010, v. 40, 776–792.

135. P. W. Bridgman. The Thermodynamics of Plastic Deformation and Generalized Entropy. *Rev. Mod. Phys.*, 1950, v. 22, 56–63.

136. R. Giles. Mathematical Foundations of Thermodynamics. Pergamon Press, New York, 1964.

137. R. Giles. An Elementary Introduction to Entropy via Irreversibility. *Pure & Appl. Chem.*, 1970, v. 22, 503–509.

138. W. K. Burton. Constructive Thermodynamics. In: L. Beklemishev, ed. Contributions to Mathematical Logic, Volume 50. North Holland, Amsterdam, 1968, pp. 75–89.

139. N. D. Mermin. The Ithaca interpretation of quantum mechanics. *Pramana – J. Phys.*, 1998, v. 51, 549–565.

140. Z. Yan. General thermal wavelength and its applications. *Eur. J. Phys.*, 2000, v. 21, 625–631.

141. P. A. M. Dirac. The Principles of Quantum Mechanics. Oxford University Press, London, 4 edition, 1967.

142. T. K. R. Dastidar and K. R. Dastidar. Gauge Invariance in Non-Relativistic Quantum Mechanics. *Nuov. Cim. B*, 1994, v. 109, 1115–1118.

143. T. K. R. Dastidar and K. R. Dastidar. Local Gauge Invariance of Relativistic Quantum Mechanics and Classical Relativistic Fields. *Mod. Phys. Lett. A*, 1995, v. 10, 1843–1846.

144. A. Sommerfeld. Partial Differential Equations of Physics. Academic Press, New York, 1949.

145. E. H. Wichmann. Symmetries and the Connection Between Spin and Statistics in Rigorous Quantum Field Theory. *AIP Conf. Proc.*, 2001, v. 596, 201–231.

146. A. P. Morse. The behaviour of a function on its critical set. *Ann. Math.*, 1939, v. 40, 62–70.

147. A. Sard. The measure of the critical values of differentiable maps. *Bull. Amer. Math. Soc.*, 1942, v. 48, 883–890.

148. W. K. Hayman and P. B. Kennedy. Subharmonic Functions, Vol. 1. Academic Press, London, New York, and San Francisco, 1976.

149. W. K. Hayman. Subharmonic Functions, Vol. 2. Academic Press, San Diego, CA, 1989.

150. E. Schrödinger. Quantisierung als Eigenwertproblem. *Ann. Phys.*, 1926, v. 384, 489–527.

151. L. de Broglie. Recherches sur la théorie des Quanta. *Ann. Phys. (Paris)*, 1925, v. 10, 22–128.

152. E. Madelung. Quantentheorie in hydrodynamischer Form. *Z. Phys.*, 1926, v. 40, 322–326.

153. W. P. Schleich, D. M. Greenberger, D. H. Kobe *et al*. Schrödinger equation revisited. *Proc. Natl. Acad. Sci. USA*, 2013, v. 110, 5374–5379.

154. L. de Broglie. A tentative theory of light quanta. *Phil. Mag.*, 1924, v. 47, 446–458.

155. C. Lanczos. The Variational Principles of Mechanics. University of Toronto Press, Toronto, 1949.

156. J. Masoliver and A. Ros. From classical to quantum mechanics through optics. *Eur. J. Phys.*, 2010, v. 31, 171–192.

157. J. J. Sakurai and J. Napolitano. Modern Quantum Mechanics. Cambridge University Press, Cambridge, UK, 3 edition, 2021.

158. E. Schrödinger. Collected Papers on Wave Mechanics. Chelsea Publishing Company, New York, 3 edition, 1982.

159. L. Wessels. Schrödinger's Route to Wave Mechanics. *Stud. Hisr. Phil. Sci.*, 1979, v. 10, 311–340.

160. H. Kragh. Erwin Schrödinger and the Wave Equation: The Crucial Phase. *Cemaunu*, 1982, v. 26, 154–197.

161. J. Mehra and H. Rechenberg. The Historical Development of Quantum Theory, Volume 5, Erwin Schrödinger and the Rise of Wave Mechanics, Part 1: Schrödinger in Vienna and Zurich 1887-1925. Springer-Verlag, New York, 1987.

162. J. Mehra and H. Rechenberg. The Historical Development of Quantum Theory, Volume 5, Erwin Schrödinger and the Rise of Wave Mechanics, Part 2: The Creation of Wave Mechanics; Early Response and Applications 1925-1926. Springer-Verlag, New York, 1987.

163. E. Schrödinger. An Undulatory Theory of the Mechanics of Atoms and Molecules. *Phys. Rev.*, 1926, v. 28, 1049–1070.

164. W. Heisenberg. Über quantentheoretische Umdeutung kinematischer und mechanischer Beziehungen. *Z. Phys.*, 1925, v. 33, 879–893.

165. M. Born and P. Jordan. Zur Quantenmechanik. *Z. Phys.*, 1925, v. 34, 858–888.

166. M. Born, W. Heisenberg, and P. Jordan. Zur Quantenmechanik II. *Z. Phys.*, 1926, v. 35, 557–615.

167. E. Schrödinger. Über das Verhältnis der Heisenberg-Born-Jordanschen Quantenmechanik zu der meinen. *Ann. Phys.*, 1926, v. 384, 734–756.

168. E. Schrödinger. Quantisierung als Eigenwertproblem. *Ann. Phys.*, 1926, v. 384, 361–376.

169. X. Oriols and J. Mompart, eds. Applied Bohmian Mechanics: From Nanoscale Systems to Cosmology. Jenny Stanford Publishing Pte. Ltd., Singapore, 2 edition, 2019.

170. Á S. Sanz and S. Miret-Artés. A Trajectory Description of Quantum Processes. I. Fundamentals. Springer-Verlag, Berlin and Heidelberg, 2012.

171. Á S. Sanz and S. Miret-Artés. A Trajectory Description of Quantum Processes. II. Applications. Springer-Verlag, Berlin and Heidelberg, 2014.

172. A. Drezet. Forewords for the Special Issue 'Pilot-wave and Beyond: Louis de Broglie and David Bohm's Quest for a Quantum Ontology'. *Found. Phys.*, 2023, v. 53, 62.

173. A. Sommerfeld. Zur Quantentheorie der Spectrallinien. *Ann. Phys.*, 1916, v. 356, 1–94.

174. W. Wilson. The Quantum-Theory of Radiation and Line Spectra. *Phil. Mag.*, 1915, v. 29, 795–802.

175. D. H. Kobe. Helmholtz's theorem revisted. *Am. J. Phys.*, 1986, v. 54, 552–554.

176. J. Cantarella, D. DeTurck, and H. Gluck. Vector calculus and the topology of domains in 3-space. *Am. Math. Monthly*, 2002, v. 109, 409–442.

177. H. Bhatia, G. Norgard, V. Pascucci *et al*. The Helmholtz-Hodge Decomposition – A Survey. *IEEE Trans. Vis. Comput. Graph.*, 2013, v. 10, 1386–1404.

178. H. Bhatia, V. Pascucci, and P-T. Bremer. The Natural Helmholtz-Hodge Decomposition for Open-Boundary Flow Analysis. *IEEE Trans. Vis. Comput. Graph.*, 2013, v. 20, 1566–1578.

179. L. E. Fraenkel. An Introduction to Maximum Principles and Symmetry in Elliptic Problems. Cambridge University Press, Cambridge, UK, 2000.

180. F. C. Adams and G. Laughlin. The Five Ages of the Universe. TOUCHSTONE, New York, 1999.

181. K. Mack. The End of Everything: Astrophysically Speaking. Scribner, New York, 2020.

182. D. E. Green and H. D. Zande. Universal energy principle of biological systems and the unity of bioenergetics. *Proc. Natl. Acad. Sci. USA*, 1981, v. 78, 5344–5347.

183. R. Haase. Survey of Fundamental Laws. In: W. Jost, ed. Physical Chemistry: An Advanced Treatise. Volume I, Thermodynamics. Academic Press, Inc., New York, 1971, pp. 1–239.

184. H. C. Longuet-Higgins. The quantum mechanical theory of environmental effects. *Proc. R. Soc. Lond. A*, 1960, v. 255, 63–68.

185. R. Rigler, M. Orrit, and T. Basché, eds. Single Molecule Spectroscopy. Springer, New York, 2001.

186. A. Gräslund, R. Rigler, and J. Widengren, eds. Single Molecule Spectroscopy in Chemistry, Physics and Biology. Springer, New York, 2010.

187. W. H. Cropper. Rudolf Clausius and the road to entropy. *Am. J. Phys.*, 1986, v. 54, 1068–1074.

188. R. C. Tolman and P. C. Fine. On the Irreversible Production of Entropy. *Rev. Mod. Phys.*, 1948, v. 20, 51–77.

189. V. C. Weiss. The uniqueness of Clausius's integrating factor. *Am. J. Phys.*, 2006, v. 74, 699–705.

190. D. R. Owen. A First Course in the Mathematical Foundations of Thermodynamics. Springer-Verlag, New York, 1984.

191. D. Lewis. Counterfactual Dependence and Time's Arrow. *Noûs*, 1979, v. 13, 455–476.

192. J. Dunn. Fried Eggs, Thermodynamics, and the Special Sciences. *Brit. J. Phil. Sci.*, 2011, v. 62, 71–98.

193. Ch. Chipot and A. Pohorille, eds. Free Energy Calculations. Springer, Berlin, Heidelberg, and New York, 2007.

194. D. Kondepudi and I. Prigogine. Modern Thermodynamics. John Wiley & Sons, Chichester, UK, 2 edition, 2015.

195. U. Seifert. Stochastic thermodynamics, fluctuation theorems and molecular machines. *Rep. Prog. Phys.*, 2012, v. 75, 126001.

196. A. Puglisi, A. Sarracino, and A. Vulpiani. Temperature in and out of equilibrium: A review of concepts, tools and attempts. *Physics Reports*, 2017, v. 709–710, 1–60.

197. D. Zhang, X. Zheng, and M. Di Ventra. Local temperatures out of equilibrium. *Physics Reports*, 2019, v. 830, 1–66.

198. N. Bohr. Chemistry and Quantum Theory of Atomic Constitution. *J. Chem. Soc.*, 1932, v. 1, 349–384.

199. H. J. D. Miller and J. Anders. Energy-temperature uncertainty relation in quantum thermodynamics. *Nat. Commun.*, 2018, v. 9, 2203.

200. Z. Roupas. Thermodynamic origin of quantum time-energy uncertainty relation. *J. Stat. Mech.*, 2021, v. 2021, 093207.

201. B. Mandelbrot. An Outline of a Purely Phenomenological Theory of Statistical Thermodynamics: I. Canonical Ensembles. *IRE Trans. Inform. Theory*, 1956, v. IT-2, 190–203.

202. L. de Broglie. The Thermodynamics of the isolated particle (or the hidden thermodynamics of particles. Gauthier-Villars Editor, Paris, 1964.

203. D. Bohm and J. P. Vigier. Model of the Causal Interpretation of Quantum Theory in Terms of a Fluid with Irregular Fluctuations. *Phys. Rev.*, 1954, v. 96, 208–216..

204. E. A. Guggenheim. Thermodynamics. Elsevier, New York, 7 edition, 1985.

205. J. von Neumann, R. T. Beyer, transl., and N. A. Wheeler, ed. Mathematical Foundations of Quantum Mechanics. Princeton University Press, Princeton, NJ, New edition, 2018.

206. L. Szilard. Über die Enfropieuerminderung in einem thermodynamischen System bei Eingrifen intelligenter Wesen. *Z. Phys.*, 1929, v. 53, 840–856.

207. J. M. Jauch and J. G. Báron. Entropy, Information, and Szilard's Paradox. *Helv. Phys. Acta*, 1972, v. 45, 220–232.

208. O. Penrose. Foundations of Statistical Mechanics. Pergamon Press, New York, 1970.

209. C. de Beauregard and M. Tribus. Information and Thermodynamics. *Helv. Phys. Acta*, 1972, v. 47, 238–247.

210. W. H. Zurek. Maxwell's Demon, Szilard's Engine and Quantum Measurements. In: G. T. Moore and M. O. Scully, eds. Frontiers of Nonequilibrium Statistical Physics. Plenum Press, New York, 1984, pp. 151–161.

211. E. Lubkin. Keeping the Entropy of Measurement: Szilard Revisited. *Int. J. Theor. Phys.*, 1987, v. 26, 523–535.

212. L. C. Biedenharn and J. C. Solem. A Quantum-Mechanical Treatment of Szilard's Engine: Implications for the Entropy of Information. *Found. Phys.*, 1995, v. 25, 1221–1229.

213. J. V. Koski, V. F. Maisi, J. P. Pekola *et al*. Experimental realization of a Szilard engine with a single electron. *Proc. Natl. Acad. Sci. USA*, 2014, v. 111, 13786–13789.

214. J. L. Lebowitz and E. H. Lieb. Existence of Thermodynamics for Real Matter with Coulomb Forces. *Phys. Rev. Lett.*, 1969, v. 22, 631–634.

215. E. H. Lieb and J. L. Lebowitz. The Constitution of Matter: Existence of Thermodynamics for Systems Composed of Electrons and Nuclei. *Adv. Math.*, 1972, v. 9, 316–398.

216. C. Hainzl, M. Lewin, and J. P. Solovej. The thermodynamic limit of quantum Coulomb systems. Part I. General theory. *Adv. Math.*, 2009, v. 221, 454–487.

217. C. Hainzl, M. Lewin, and J. P. Solovej. The thermodynamic limit of quantum Coulomb systems. Part II. Aplications. *Adv. Math.*, 2009, v. 221, 488–546.

218. E. H. Lieb and R. Seiringer. The Stability of Matter in Quantum Mechanics. Cambridge University Press, Cambridge, UK, 2009.

219. R. C. Geary. The Frequency Distribution of the Quotient of Two Normal Variables. *J. R. Stat. Soc.*, 1930, v. 93, 442–446.

220. E. V. Huntington. Frequency Distributions of Products and Quotients. *Ann. Math. Stat.*, 1939, v. 10, 195–198.

221. C. C. Craig. On the Frequency Function of XY. *Ann. Math. Stat.*, 1936, v. 7, 1–15.

222. C. C. Craig. On the Frequency Distributions of the Quotient and of the Product of Two Statistical Variables. *Am. Math. Mon.*, 1942, v. 49, 26–32.

223. L. A. Aroian. Some Methods of Evaluation of a Sum. *J. Am. Stat. Assoc.*, 1944, v. 39, 511–515.

224. L. A. Aroian. The Probability Function of the Product of Two Normally Distributed Random Variables. *Ann. Math. Stat.*, 1947, v. 18, 265–271.

225. L. B. Landau and E. M. Lifshitz. Quantum Mechanics: Non-relativistic Theory. Pergamon Press, Oxford, 2 edition.

226. A. R. Bohm, M. Gadella, and P. Kielanowski. Time Asymmetric Quantum Mechanics. *SIGMA*, 2011, v. 7, 086.

Gerald F. Thomas. The Arrow of Time and Its Irreversibility

227. R. de la Madrid. On the inconsistency of the Bohm-Gadella theory with quantum mechanics. *J. Phys. A*, 2006, v. 39, 9255–9268.

228. M. Gadella and S. Wickramasekara. Comment on 'On the inconsistency of the Bohm-Gadella theory with quantum mechanics'. *J. Phys. A*, 2007, v. 40, 4665–4669.

229. R. de la Madrid. Reply to "Comment on 'On the inconsistency of the Bohm-Gadella theory with quantum mechanics'". *J. Phys. A*, 2007, v. 40, 4671–4681.

230. H. Baumgärtel. Time asymmetry in quantum mechanics: a pure mathematical point of view. *J. Phys. A*, 2008, v. 41, 304017.

231. G. 't Hooft. The Cellular Automaton Interpretation of Quantum Mechanics. Springer, Cham, Heidelberg, New York, Dordrecht, and London, 2016.

232. O. Penrose. Time warp. *Nature*, 1993, v. 362, 510.

233. M. C. Mackey. Time's Arrow: The Origins of Thermodynamic Behavior. Springer-Verlag, New York, 1992.

234. A. L. Kuzemsky. In Search of Time Lost: Asymmetry of Time and Irreversibility in Natural Processes. *Found. Sci.*, 2020, v. 25, 597–645.

235. S. Golden. Quantum Statistical Foundation of Chemical Kinetics. Clarendon Press, Oxford, 1969.

236. L. Fonda, G. C. Ghirardi, A. Rimini *et al*. On the Quantum Foundations of the Exponential Decay Law. *Nuov. Cim. A*, 1973, v. 15, 689–704.

237. N. Metropolis, A. W. Rosenbluth, M. N. Rosenbluth *et al*. Equation of State Calculations by Fast Computing Machines. *J. Chem. Phys.*, 1953, v. 23, 1087–1092.

238. W. K. Hastings. Monte Carlo sampling methods using Markov chains and their applications. *Biometrika*, 1970, v. 57, 97–109.

239. R. Clausius. Ueber verschiedene für die Anwendung bequeme Formen der Hauptgleichungen der mechanischen Wärmetheorie. *Ann. Phys. Chem.*, 1865, v. 201, 353–400.

240. S. I. Sandler. Chemical, Biochemical, and Engineering Thermodynamics. John Wiley & Sons, Hoboken, NJ, 5 edition, 2016.

241. Y. Demirel and V. Gerbaud. Nonequilibrium Thermodynamics. Elsevier, Amsterdam and New York, 4 edition, 2019.

242. C. Nash and S. Sen. Topology and Geometry for Physicists. Academic Press, Orlando, FL, 1983.

243. H. Whitney. Geometric Integration Theory. Princeton University Press, Princeton, NJ, 1957.

244. L. O'Raifeartaigh. The Dawning of Gauge Theory. Princeton University Press, Princeton, NJ, 1997.

245. F. London. Quantenmechanische Deutung der Theorie von Weyl. *Z. Phys.*, 1927, v. 42, 375–389.

246. H. Weyl. The Theory of Groups and Quantum Mechanics. Dover Publications, Inc., New York, 1950. P. H. Robinson, transl. Gruppentheorie und Qantenmechanik, 2nd rev. ed., 1930.

247. E. Schrödinger. Über eine bemerkenswerte Eigenschaft der Quantenbahnen eines einzelnen Elektrons. *Z. Phys.*, 1923, v. 12, 13–23.

248. H. Weyl. Gravitation and the Electron. *Proc. Natl. Acad. Sci. USA*, 1929, v. 15, 323–334.

249. Y. Aharonov and D. Bohm. Significance of electromagnetic potentials in the quantum theory. *Phys. Rev.*, 1959, v. 115, 485–491.

250. Y. Aharonov and D. Bohm. Further considerations on electromagnetic potentials in the quantum theory. *Phys. Rev.*, 1961, v. 123, 1511–1524.

251. W. K. H. Panofsky and M. Phillips. Classical Electricity and Magnetism. Addison Wesley, New York, 2 edition, 1962.

252. A. O'Rahilly. Electromagnetic Theory: A Critical Examination of Fundamentals. Dover Publications, Inc., Mineola, NY, 1965.

253. J. D. Jackson. Classical Electrodynamics. John Wiley & Sons, Hoboken, NJ, 3 edition, 1999.

254. A. Zangwill. Modern Electrodynamics. Cambridge University Press, New York, 2012.

255. D. J. Griffiths. Introduction to Electrodynamics. Pearson, Upper Saddle River, NJ, 4 edition, 2013.

256. J. Schwinger, L. L. DeRaad Jr., K. A. Milton and W. y. Tsai. Classical Electrdynamics. CRC Press, Boca Raton, FL, 2018.

257. A. Einstein. Strahlungs-Emission und -Absorption nach der Quantentheorie. *Verhandl. D. Deutch. Phys. Ges.*, 1916, v. 18, 318–323.

258. A. Einstein. Zur Quantentheorie der Strahlung. *Phys. Zeit.*, 1917, v. 18, 121–128.

259. P. A. M. Dirac. The Quantum Theory of the Emission and Absorption of Radiation. *Proc. R. Soc. Lond. A*, 1927, v. 114, 243–265.

260. P. A. M. Dirac. The Quantum Theory of Dispersion. *Proc. R. Soc. Lond. A*, 1927, v. 114, 710–728.

261. B. Mashhoon. Gravitoelectromagnetism: A Brief Review. In: L. Iorio, ed. The Measurement of Gravitomagnetism: A Challenging Enterprise. NOVA Science Publishers, Inc., Hauppauge, NY, 2007, pp. 29–40.

262. C. W. F. Everitt *et al*. Gravity Probe B: Final Results of a Space Experiment to Test General Relativity. *Phys. Rev. Lett.*, 2011, v. 106, 221101.

263. W. de Sitter. On Einstein's theory of gravitation, and its astronomical consequences. *Mon. Not. R. Astron. Soc.*, 1916, v. 77, 155–184.

264. B. Mashhoon, F. W. Hehl, and D. S. Theiss. On the gravitational effects of rotating masses: The Thirring-Lense papers. *Gen. Rel. Gray.*, 1984, v. 16, 711–750.

265. P. D. B. Collins, A. D. Martin, and E. J. Squires. Particle Physics and Cosmology. Wiley-Interscience, New York, 1989.

266. P. A. M. Dirac. Quantised Singularities in the Electromagnetic Field. *Proc. R. Soc. Lond. A*, 1931, v. 133, 60–72.

267. G. Auletta, M. Fortunato, and G. Parisi. Quantum Mechanics. Cambridge University Press, New York, 2009.

268. G. Grynberg, A. Aspect, and C. Fabre. Introduction to Quantum Optics. Cambridge University Press, New York, 2010.

269. T. Engel and P. Reid. Physical Chemistry. Pearson Education, Inc., New York, 3 edition, 2012.

270. T. D. Ladd, F. Jelezko, R. Laflamme *et al*. Quantum Computers. *Nature*, 2010, v. 464, 45–53.

271. J. E. Sipe. Photon wave functions. *Phys. Rev. A*, 1995, v. 52, 1875–1893.

272. D. M. Cook. The Theory of the Electromagnetic Field. Dover Publications, Inc., New York, 2002.

273. D. K. Cheng. Field and Wave Electromagnetics. Addison Wesley, Reading, MA, 2 edition, 1989.

274. C. S. Wood, S. C. Bennett, D. Cho *et al*. Measurement of Parity Nonconservation and an Anapole Moment in Cesium. *Science*, 1997, v. 275, 1759–1763.

275. M.-A. Bouchiat. Atomic parity violation: Early days, present results, prospects. *Nuov. Cim. C*, 2012, v. 35, 78–84.

276. M. S. Safronova, D. Budker, D. DeMille *et al*. Search for new physics with atoms and molecules. *Rev. Mod. Phys.*, 2018, v. 90, 025008.

277. J. W. Blanchard, J. P. King, T. F. Sjolander *et al*. Molecular parity nonconservation in nuclear spin couplings. *Phys. Rev. Research*, 2020, v. 2, 023258.

278. Y. Aharonov, D. Z. Albert, and L. Vaidman. How the result of a measurement of a component of the spin of a spin-$\frac{1}{2}$ particle can turn out to be 100. *Phys. Rev. Lett.*, 1988, v. 60, 1351–1354.

279. J. Dressel, M. Malik, F. M. Miatto *et al*. Understanding quantum weak values: Basics and applications. *Rev. Mod. Phys.*, 2014, v. 86, 307–316.

280. L. Vaidman. Weak value controversy. *Phil. Trans. R. Soc. A*, 2017, v. 375, 20160395.

281. Y. Aharonov, P. G. Bergmann, and J. L. Lebowit. Time Symmetry in the Quantum Process of Measurement. *Phys. Rev.*, 1964, v. 134, 1410–1416.

282. A. Bednorz, K. Franke, and W. Belzi. Noninvasiveness and time symmetry of weak measurements. *New J. Phys.*, 2013, v. 15, 023043.

283. M. Jayaseelan, S. K. Manikandan, A. N. Jordan *et al*. Quantum measurement arrow of time and fluctuation relations for measuring spin of ultracold atoms. *Nature Communications*, 2021, v. 12 (1), 1847.

284. É. Borel. Probabilities and Life. Dover Publications, Inc., New York, 1962.

285. J. O. Hirschfelder. The angular momentum, creation, and significance of quantized vortices. *J. Chem. Phys.*, 1977, v. 67, 5477–5483.

286. A. Nussbaum. Faraday's law paradoxes. *Phys. Educ.*, 1972, v. 7, 231–232.

287. A. López-Ramos, J. R. Menéndez, and C. Piqué. Conditions for the validity of Faraday's law of induction and their experimental confirmation. *Eur. J. Phys.*, 2008, v. 29, 1069–1076.

288. P. Kinsler. Faraday's Law and Magnetic Induction: Cause and Effect, Experiment and Theory. *Physics*, 2020, v. 2, 150–163.

289. M. Faraday. Thoughts on Ray-vibrations. *Phil. Mag. S. 3.*, 1846, v. 28, 345–350.

290. N. Bohr and L. Rosenfeld. Field and Charge Measurements in Quantum Electrodynamics. *Phys. Rev.*, 1950, v. 78, 794–798.

291. R. Clausius. On a Mechanical Theorem Applicable to Heat. *Phil. Mag.*, 1870, v. 40, 122–127.

292. A. S. Eddington. The Kinetic Energy of a Star Cluster. *Mon. Not. R. Astron. Soc.*, 1916, v. 76, 525–548.

293. F. Zwicky. On the Masses of Nebulae and of Clusters of Nebulae. *Ap. J.*, 1937, v. 86, 217–246.

294. V. A. Ambartsumian. On the Evolution of Galaxies. In: R. Stoops, ed. La Structure et révolution de l'univers. 13th Solvay Conference, Brussels, 1958, pp. 241–279.

295. J. Bland-Hawthorn and K. Freeman. Near Field Cosmology – The Origin of the Galaxy and the Local Group. In: B. Moore, ed. The Origin of the Galaxy and Local Group. Springer, Berlin and Heidelberg, 2014, pp. 3–156.

296. V. C. Rubin and W. K. Ford Jr. Rotation of the Andromeda Nebula from a Spectroscopic Survey of Emission Regions. *Ap. J.*, 1970, v. 159.

297. D. Walsh, R. F. Carswell, and R. J. Weymann. 0957 + 561 A, B: twin quasistellar objects or gravitational lens? *Nature*, 1979, v. 279, 381–384.

298. D. N. Spergel, R. Bean, O. Doré *et al*. Three-Year Wilkinson Microwave Anisotropy Probe (WMAP) Observations: Implications for Cosmology. *Astrophys. J. Suppl.*, 2007, v. 170, 377–408.

299. J. J. Brehm and W. J. Mullin. Introduction to the Structure of Matter. John Wiley & Sons, New York, 1989.

300. J. 0. Hirschfelder, C. F. Curtiss, and R. B. Bird. Molecular Theory of Gases and Liquids. John Wiley & Sons, New York, 1954.

301. M. Born and K. Huang. Dynamical Theory of Crystal Lattices. Oxford University Press, London, 1962.

302. K. S. Surana. Advanced Mechanics of Continua. CRC Press, Boca Raton, FL, 2015.

303. D. J. Dean. Beyond the nuclear shell model. *Phys. Today*, 2007, v. 60, 48–53.

304. N. Schunck, ed. Energy Density Functional Methods for Atomic Nuclei. Institute of Physics, Bristol and Philadelphia, 2019.

305. R. P. Feynman, R. B. Leighton, and M. Sands. The Feynman Lectures on Physics, v. 3, Quantum Mechanics. Addison-Wesley, Reading, MA, 1965.

306. R. F. Streater and A. S. Wightman. PCT, Spin and Statistics, and All That. Addison Wesley, Reading, MA, 1989.

307. R. P. Feynman. The Reason for Antiparticles. In: Elementary Particles and the Laws of Physics: The 1986 Dirac Memorial Lectures. Cambridge University Press, New York, 1987, pp. 1–59.

308. M. Altunbulak and A. Klyachko. The Pauli Principle Revisited. *Commun. Math. Phys.*, 2008, v. 282, 287–322.

309. I. G. Kaplan. The Pauli Exclusion Principle. Can It Be Proved? *Found. Phys.*, 2013, v. 43, 1233–1251.

310. I. G. Kaplan. The Pauli Exclusion Principle. John Wiley & Sons, New York, 2017.

311. I. G. Kaplan. Modern State of the Pauli Exclusion Principle and the Problems of Its Theoretical Foundation. *Symmetry*, 2021, v. 13, 21–37.

312. I. G. Kaplan. The Pauli Exclusion Principle and the Problems of Its Experimental Verification. *Symmetry*, 2020, v. 12, 320–334.

313. S. R. Elliott, B. H. LaRoque, V. M. Gehman *et al*. An Improved Limit on Pauli-Exclusion-Principle Forbidden Atomic Transitions. *Fortschr. Phys.*, 2012, v. 42, 1015–1030.

314. J. Marton, C. Berucci, M. Cargnelli *et al*. Underground Test of Quantum Mechanics: The VIP2 Experiment. In: A. Khrennikov and B. Toni, eds. Quantum Foundations, Probability and Information. Springer International Publishing AG, Cham, Germany, 2018.

315. M. Massimi. Pauli's Exclusion Principle. Cambridge University Press, New York, 2006.

316. J. Bain. CPT Invariance and the Spin-Statistics Connection. Oxford University Press, Oxford, 2016.

317. H. Margenau. The Exclusion Principle and Its Philosophical Importance. *Phil. Sci.*, 1944, v. 11, 187–208.

318. E. C. Stoner. The Distribution of Electrons amongst Atomic Levels. *Phil. Mag.*, 1924, v. 48, 719–736.

319. W. Pauli. Über den Einfluß der Geschwindigkeitsabhängigkeit der Elektronenmasse auf den Zeemaneffekt. *Z. Phys.*, 1925, v. 31, 373–385.

320. L. de Broglie. Waves and Quanta. *Nature*, 1923, v. 112, 540.

321. N. Bohr and D. Coster. Röntgenspektren und periodisches System der Elemente. *Z. Phys.*, 1923, v. 12, 342–374.

322. W. Pauli. Über den Zusammenhang des Abschlusses der Elektronengruppen im Atom mit der Komplexstruktur der Spektren (On the Connexion between the Completion of Electron Groups in an Atom with the Complex Structure of Spectra). *Z. Phys.*, 1925, v. 31, 765–783.

323. J. C. Slater. Atomic Shielding Constants. *Phys. Rev.*, 1930, v. 36, 57–64.

324. E. Clementi and D. L. Raimondi. Atomic Screening Constants from SCF Functions. *J. Chem. Phys.*, 1963, v. 38, 2686–2689.

325. E. Clementi, D. L. Raimondi, and W. P. Reinhardt. Atomic Screening Constants from SCF Functions. II. Atoms with 37 to 86 Electrons. *J. Chem. Phys.*, 1967, v. 47, 1300–1307.

326. L. Mandelstam and I. Tamm. The Uncertainty Relation Between Energy and Time in Non-relativistic Quantum Mechanics. *J. Phys. USSR*, 1945, v. 9, 249–254.

327. E. P. Wigner. On the Time-Energy Uncertainty Relation. In: A. Salam and E. P. Wigner, eds. Aapects of Quantum Theory. Cambridge University Press, Cambridge, UK, 1972, pp. 237–247.

328. P. Busch. On the Energy-Time Uncertainty Relation. Part I: Dynamical Time and Time Indeterminacy. *Found. Phys.*, 1990, v. 20, 1–32.

329. P. Busch. On the Energy-Time Uncertainty Relation. Part II: Pragmatic Time Versus Energy Indeterminacy. *Found. Phys.*, 1990, v. 20, 33–43.

330. J. Hilgevoord. The uncertainty principle for energy and time. *Am. J. Phys.*, 1996, v. 64, 1451–1456.

331. J. Hilgevoord. The uncertainty principle for energy and time. II. *Am. J. Phys.*, 1998, v. 66, 396–402.

332. W. R. Hindmarsh. Atomic Spectra. Pergamon Press, Oxford and New York, 1967.

333. V. V. Bolotin. The Dynamic Stability of Elastic Systems. Holden-Day, San Francisco, CA, 1964.

334. R. W. Clough and J. Penzien. Dynamics of Structures. Computers & Structures, Inc., Berkeley, CA, 3 edition, 2003.

335. Z. P. Bazant and L. Cedolin. Stability of Structures. World Scientific Publishing, Singapore, 2010.

336. T. Kato. Fundamental properties of Hamiltonian operators of Schrödinger type. *Trans. Am. Math. Soc.*, 1951, v. 70, 195–211.

337. F. J. Dyson and A. Lenard. Stability of Matter I. *J. Math. Phys.*, 1967, v. 8, 423–434.

338. L. Onsager. Electrostatic interaction of molecules. *J. Phys. Chem.*, 1939, v. 43, 189–196.

339. M. E. Fisher and D. Ruelle. The Stability of Many-Particle Systems. *J. Math. Phys.*, 1966, v. 7, 260–270.

340. X. He, K. Wang, J. Zhuang *et al*. Coherently forming a single molecule in an optical trap. *Science*, 2020, v. 370, 331–335.

341. S. W. Hla, L. Bartels, G. Meyer *et al*. Inducing All Steps of a Chemical Reaction with the Scanning Tunneling Microscope Tip: Towards Single Molecule Engineering. *Phys. Rev. Lett.*, 2000, v. 85, 2777–2780.

342. D. G. de Oteyza, P. Gorman, Y.-C. Chen *et al*. Direct Imaging of Covalent Bond Structure in Single-Molecule Chemical Reactions. *Science*, 2013, v. 340, 1434–1437.

343. A. Riss, A. P. Paz, S. Wickenburg *et al*. Imaging single-molecule reaction intermediates stabilized by surface dissipation and entropy. *Nat. Chem.*, 2016, v. 8, 678–683.

344. T. W. Chamberlain, J. Biskupek, S. T. Skowro *et al*. Stop-Frame Filming and Discovery of Reactions at the Single-Molecule Level by Transmission Electron Microscopy. *ACS Nano*, 2017, v. 11, 2509–2520.

345. Y. Liu, M.-G. Hu, M. A. Nichols *et al*. Precision test of statistical dynamics with state-to-state ultracold chemistry. *Nature*, 2021, v. 593, 379–384.

346. F. J. Dyson. Ground-State Energy of a Finite System of Charged Particles. *J. Math. Phys.*, 1967, v. 8, 1538–1545.

347. E. P. Wigner. The Unreasonable Effectiveness of Mathematics in the Natural Sciences. *Commun. Pure App. Math.*, 1960, v. 13, 1–14.

348. R. D. Astumian. The unreasonable effectiveness of equilibrium theory for interpreting nonequilibrium experiments. *Am. J. Phys.*, 2006, v. 74, 683–688.

349. J. C. Maxwell. Treatise on Electricity and Magnetism, Vol. 1. Oxford University Press, Oxford, 1873.

350. J. H. Jeans. The Mathematical Theory of Electricity and Magnetism. Cambridge University Press, Cambridge, UK, 5 edition, 1927.

351. J. L. Lagrange. Méchanique Analytique. La Veuve Desaint, Paris, 1788.

352. J. Cizek and J. Paldus. Stability Conditions for the Solutions of the Hartree-Fock Equations for Atomic and Molecular Systems. Application to the Pi-Electron Model of Cyclic Polyenes. *J. Chem. Phys.*, 1967, v. 47, 3976–3985.

353. R. Schoen and S.-T. Yau. The Energy and the Linear Momentum of Space-Times in General Relativity. *Commun. Math. Phys*, 1981, v. 79, 47–51.

354. E. Witten. A New Proof of the Positive Energy Theorem. *Commun. Math. Phys*, 1981, v. 80, 381–402.

355. Y. Marcus. A simple empirical model describing the thermodynamics of hydration of ions of widely varying charges, sizes, and shapes. *Biophys. Chem.*, 1994, v. 51, 111–127.

356. J. D. Gillaspy. Highly charged ions. *J. Phys. B*, 2001, v. 34, 93–130.

357. E. H. Lieb and M. Loss. Existence of Atoms and Molecules in Non-Relativistic Quantum Electrodynamics. *Adv. Theor. Math . Phys.*, 2003, v. 7, 667–710.

358. L. Pauling and S. B. Hendricks. The Prediction of the Relative Stabilities of Isosteric Isomeric Ions and Molecules. *J. Am. Chem. Soc.*, 1926, v. 48, 641–651.

359. L. Pauling. The Nature of the Chemical Bond. Cornell University Press, Ithaca, NY, 3 edition, 1960.

360. L. Pauling. The Architecture of Molecules. *Proc. Natl. Acad. Sci. USA*, 1964, v. 51, 977–984.

361. S. J. Weininger. The Molecular Structure Conundrum: Can Classical Chemistry be Reduced to Quantum Chemistry? *J. Chem. Ed.*, 1984, v. 61, 939–944.

362. R. G. Woolley. The Molecular Structure Conundrum. *J. Chem. Ed.*, 1985, v. 62, 1082–1084.

363. R. C. Tolman. The Measurable Quantities of Physics. *Phys. Rev.*, 1917, v. 9, 237–253.

364. O. Redlich. Intensive and Extensive Properties. *J. Chem. Ed.*, 1970, v. 47, 154–156.

365. S. Chandrasekhar. On stars, their evolution and their stability. *Rev. Mod. Phys.*, 1984, v. 56, 137–147.

366. S. Chandrasekhar. The Highly Collapsed Configurations of a Stellar Mass. (Second Paper.). *Mon. Not. R. Astron. Soc.*, 1935, v. 95, 207–225.

367. J. C. Slater. The Virial and Molecular Structure. *J. Chem. Phys.*, 1933, v. 1, 687–691.

368. G. Marc and W. G. McMillan. The Virial Theorem. *Adv. Chem. Phys.*, 1985, v. 58, 209–361.

369. M. A. Ranade. Virial Theorem for a Molecule. Master's thesis, North Texas State University, Denton, TX, 1972.

370. A. Clebsch, ed. Jacobi's Lectures on Dynamics. Hindustan Book Agency, New Delhi, 2 edition, 2009.

371. H. Pollard. A Sharp Form of the Virial Theorem. *Bull. Amer. Math. Soc.*, 1964, v. 70, 703–705.

372. K. Y. Bliokh, J. Dressel, and F. Nori. Conservation of the spin and orbital angular momenta in electromagnetism. *New J. Phys.*, 2014, v. 16, 093037.

373. J. Lewins and M. Becker, eds. Advances in Nuclear Science and Tecitnology: Volume 19. Festschrift in Honor of Eugene P. Wigner. Plenum Press, New York, 1987.

374. A. E. Milne. An Extension of the Theorem of the Virial. *Phil. Mag.*, 1925, v. 50, 409–414.

375. G. W. Collins II. The Virial Theorem in Stellar Astrophysics. Pachart Pub. House, Tucson, AZ, 1978.

376. H. S. Leff. Entropy, Its Language, and Interpretation. *Found. Phys.*, 2007, v. 37, 1744–1766.

377. J. L. Park. The Concept of Transition in Quantum Mechanics. *Found. Phys.*, 1970, v. 1, 23–33.

378. W. K. Wootters and W. H. Zurek. A single quantum cannot be cloned. *Nature*, 1982, v. 299, 802–803.

379. V. Buzek and M. Hillery. Quantum copying: Beyond the no-cloning theorem. *Phys. Rev. A*, 1996, v. 54, 1844–1852.

380. S. Msindo, G. G. Nyambuya, and C. Nyamhere. Plausible Fundamental Origins of Emissivity (I). *Prog. Phys.*, 2021, v. 17, 10–13.

381. M. Dalarsson N. Dalarsson and L. Golubović. Introductory Statistical Thermodynamics. Academic Press, Burlington, MA, 2011.

382. F. Schwabl. Statistical Mechanics. Springer-Verlag, Berlin, Heidelberg, and New York, 2 edition, 2010.

383. O. Heaviside. The Radiation from an Electron describing a Circular Orbit. *Nature*, 1904, v. 69, 293–294.

384. H. Yu and W. Zhou. Do static atoms outside a Schwarzschild black hole spontaneously excite? *Phys. Rev. D*, 2007, v. 76, 044023.

385. G. Degrassi, S. Di Vita, J. Elias-Miró *et al*. Higgs mass and vacuum stability in the Standard Model at NNLO. *J. High Energ. Phys.*, 2012, v. 98.

386. [Planck Collaboration]. Planck 2018 results. VI. Cosmological parameters. *Astron. Astrophys.*, 2020, v. 641, A6.

387. P. A. M. Dirac. The Theory of Magnetic Poles. *Phys. Rev.*, 1948, v. 74, 817–830.

388. H. Weyl. Gravitation and electricity. *Sitzungsber. Königl. Preuss. Akad. Wiss.*, 1918, v. 26, 465–480.

389. M. Born and V. Fock. Beweis des Adiabatensatzes. *Z. Phys.*, 1928, v. 51, 165–180.

390. E. Amaldi. On the Dirac Magnetic Poles. In: G. Putti, ed. Old and New Problems in Elementary Particles. Addison Wesley, New York and London, 1968, pp. 1–61.

391. E. Amaldi and N. Cabibbo. On the Dirac Magnetic Poles. In: A. Salam and E. P. Wigner, eds. Aapects of Quantum Theory. Cambridge University Press, Cambridge, UK, 1972, pp. 185–212.

392. A. S. Goldhaber and W. P. Trower. Resource letter MM1: magnetic monopoles. *Am. J. Phys.*, 1990, v. 58, 429–439.

393. K. A. Milton. Theoretical and experimental status of magnetic monopoles. 2006, v. 69, 1637–1711.

394. L. Patrizii and M. Spurio. Status of Searches for Magnetic Monopoles. *Annu. Rev. Nucl. Part. Sci.*, 2015, v. 65, 279–302.

395. P. B. Price, E. K. Shirk, W. Z. Osborne *et al*. Evidence for Detection of a Moving Magnetic Monopole. *Phys. Rev. Lett.*, 1975, v. 35, 487–490.

396. B. Cabrera. First Results from a Superconductive Detector for Moving Magnetic Monopoles. *Phys. Rev. Lett.*, 1982, v. 48, 1378–1381.

397. P. G. H. Sandars. Magnetic Charge. *Contemp. Phys.*, 1966, v. 7, 419–429.

398. G. 't Hooft. Magnetic monopoles in unified gauge theories. *Nucl. Phys. B*, 1974, v. 79, 276–284.

399. A. M. Polyakov. Particle spectrum in the quantum field theory. *JETP Lett.*, 1974, v. 20, 194–195.

400. T. W. B. Kibble. Some Implications of a Cosmological Phase Transition. *Phys. Rev.*, 1980, v. 67, 183–199.

401. J. A. Gonzalo. Inflationary Cosmology Revisited. World Scientific Publishing, Singapore, 2005.

402. M. Lemoine, J. Martin, and P. Peter, eds. Inflationary Cosmology. Springer-Verlag, Berlin and Heidelberg, 2010.

403. A. A. Starobinsky. A New Type of Isotropic Cosmological Models Without Singularity. *Phys. Lett. B*, 1980, v. 91, 99–102.

404. A. H. Guth. Inflationary universe: A possible solution to the horizon and flatness problems. *Phys. Rev. D*, 1981, v. 23, 347–356.

405. M. B. Einhorn and K. Sato. Monopole Production in the Very Early Universe in a First-Order Phase Transition. *Nucl. Phys. B*, 1981, v. 180, 385–404.

406. A. D. Linde. A New Inflationary Universe Scenario: A Possible Solution of the Horizon, Flatness, Homogeneity, Isotropy and Primordial Monopole Problems. *Phys. Lett. B*, 1982, v. 108, 389–393.

407. A. Albrecht and P. J. Steinhardt. Cosmology for Grand Unified Theories with Radiatively Induced Symmetry Breaking. *Phys. Rev. Lett.*, 1982, v. 48, 1220–1223.

408. N. Craigie, P. Goddard, and W. Nahm, eds. Monopoles in Quantum Field Theory: Proceedings of the Monopole Meeting, Trieste, Italy, December, 1981. World Scientific Publishing, Singapore, 1982.

409. B. Achary *et al*. [The MoEDAL Collaboration]. Search for magnetic monopoles produced via the Schwinger mechanism. *Nature*, 2022, v. 602, 63–67.

410. F. Sauter Über das Verhalten eines Elektrons im homogenen elektrischen Feld nach der relativistischen Theorie Diracs. *Z. Phys.*, 1931, v. 69, 742–764.

411. J. Schwinger. On Gauge Invariance and Vacuuwn Polarization. *Phys. Rev.*, 1951, v. 82, 664–679.

412. R. A. Lewis, G. A. Smith, and S. D. Howe. Antiproton portable traps and medical applications. *Hyperfine Inter.*, 1997, v. 109, 155–164.

413. M. Aguilar *et al*. [The AMS Collaboration]. Antiproton Flux, Antiproton-to-Proton Flux Ratio, and Properties of Elementary Particle Fluxes in Primary Cosmic Rays Measured with the Alpha Magnetic Spectrometer on the International Space Station. *Phys. Rev. Lett.*, 2016, v. 117, 091103.

414. S. Acharya *et al*. [The ALICE Collaboration]. Measurement of anti-^{3}He nuclei absorption in matter and impact on their propagation in the Galaxy. *Nat. Phys.*, 2023, v. 19, 61–71.

415. V. Poulin, P. Salati, I. Cholis *et al*. Where do the AMS-02 antihelium events come from? *Phys. Rev. D*, 2019, v. 99, 023016.

416. S. Dupourqué, L. Tibaldo, and P. von Ballmoos. Constraints on the antistar fraction in the Solar System neighborhood from the 10-year Fermi Large Area Telescope gamma-ray source catalog. *Phys. Rev. D*, 2021, v. 103, 083016.

417. P. Abratenko *et al*. [The MicroBooNE Collaboration]. Search for Neutrino-Induced Neutral-Current Δ Radiative Decay in MicroBooNE and a First Test of the MiniBooNE Low Energy Excess under a Single-Photon Hypothesis. *Phys. Rev. Lett.*, 2022, v. 128, 111801–111809.

418. H. Almazán *et al*. [The STEREO Collaboration]. Interpreting Reactor Antineutrino Anomalies with STEREO data. *Nature*, 2023, v. 613, 257–261.

419. H. Murayama. The origin of neutrino mass. *Phys. World*, 2002, v. 15, 35–39.

420. Y. Fukuda *et al*. [The Super-Kamiokande Collaboration]. Evidence for Oscillation of Atmospheric Neutrinos. *Phys. Rev. Lett.*, 1998, v. 81, 1562–1567.

421. Q. R. Ahmad *et al*. [The SNO Collaboration]. Direct Evidence for Neutrino Flavor Transformation from Neutral-Current Interactions in the Sudbury Neutrino Observatory. *Phys. Rev. Lett.*, 2002, v. 89, 011301.

422. M. Tanabashi *et al*. [Particle Data Group]. Review of Particl Physics. *Phys. Rev. D*, 2018, v. 98, 030001.

423. S. Davidson, E. Nardi, and Y. Nir. Leptogenesis. *Phys. Rev.*, 2008, v. 466, 105–177.

424. C. S. Fong, E. Nardi, and A. Riotto. Leptogenesis in the Universe. *Adv. High Energy Phys.*, 2012, v. 2012, 158303.

425. A. Riotto and M. Trodden. Recent Progress in Baryogenesis. *Ann. Rev. Nucl. Part. Sci.*, 1999, v. 49, 35–75.

426. P. Fileviez Pérez, C. Murgui, and A. D. Plascencia. Baryogenesis via leptogenesis: Spontaneous B and L violation. *Phys. Rev. D*, 2021, v. 104, 055007.

427. A. D. Sakharov. Violation of CP Invariance, C Asymmetry, and Baryon Asymmetry of the Universe. *Sov. Phys. JETPL*, 1967, v. 5, 24–27.

428. A. D. Sakharov. Cosmological models of the Universe with reversal of time's arrow. *Sov. Phys. JETP*, 1980, v. 52, 349–351.

429. J. L. Bernal, G. Sato-Polito, and M. Kamionkowski. Cosmic Optical Background Excess, Dark Matter, and Line-Intensity Mapping. *Phys. Rev. Lett.*, 2022, v. 129, 231301.

430. P. Sikivie. Dark Matter Axions. *Int. J. Mod. Phys. A*, 2010, v. 25, 554–563.

431. D. J. E. Marsh. Axion cosmology. *Phys. Reports*, 2016, v. 643, 1–79.

432. R. D. Peccei and H. R. Quinn. *CP* Conservation in the Presence of Pseudoparticles. *Phys. Rev. Lett.*, 1977, v. 38, 1440–1443.

433. R. D. Peccei and H. R. Quinn. Constraints imposed by *CP* conservation in the presence of pseudoparticles. *Phys. Rev. D*, 1977, v. 16, 1791–1797.

434. C. Abel *et al*. Measurement of the Permanent Electric Dipole Moment of the Neutron. *Phys. Rev. Lett.*, 2020, v. 124, 081803.

Gerald F. Thomas. The Arrow of Time and Its Irreversibility

435. F. Wilczek. Problem of strong *P* and *T* invariance in the presence of instantons. *Phys. Rev. Lett.*, 1978, v. 40, 279–282.

436. J. Preskill, M. B. Wise, and F. Wilczek. Cosmology of the Invisible Axion. *Phys. Lett. B*, 1983, v. 120, 127–132.

437. P. Sikivie and Q. Yang. Bose-Einstein Condensation of Dark Matter Axions. *Phys. Rev. Lett.*, 2009, v. 103, 111301.

438. V. Anastassopoulos *et al*. [The CAST Collaboration]. New CAST limit on the axion-photon interaction. *Nat. Phys.*, 2017, v. 13, 584–590.

439. T. Braine *et al*. [The ADMX Collaboration]). Extended Search for the Invisible Axion with the Axion Dark Matter Experiment. *Phys. Rev. A*, 2020, v. 124, 101303.

440. F. Chadha-Day, J. Ellis, and D. J. E. Marsh. Axion dark matter: What is it and why now? *Science*, 2022, v. 8, 3618.

441. Y. K. Semertzidis and S. Youn. Axion dark matter: How to see it? *Sci. Adv.*, 2022, v. 8, 9928.

442. F. Wilczek. Two Applications of Axion Electrodynamics. *Phys. Rev. Lett.*, 1987, v. 58, 1799–1802.

443. A. Amruth, T. Broadhurst, J. Lim, *et al*. Einstein rings modulated by wavelike dark matter from anomalies in gravitationally lensed images. *Nat. Astron.*, 2023.

444. A. Einstein. Lens-Like Action of a Star by the Deviation of Light in the Gravitational Field. *Science*, 1936, v. 84, 506–507.

445. J. J. Hudson, D. M. Kara, I. J. Smallman *et al*. Improved measurement of the shape of the electron. *Nature*, 2011, v. 473, 493–497.

446. J. Baron *et al*. [The ACME Collaboration]. Order of Magnitude Smaller Limit on the Electric Dipole Moment of the Electron. *Science*, 2014, v. 343, 269–272.

447. V. Andreev *et al*. [The ACME Collaboration]. Improved limit on the electric dipole moment of the electron. *Nature*, 2018, v. 562, 355–360.

448. D. J. Fixsen. The Temperature of the Cosmic Microwave Background. *Astrophys. J.*, 2009, v. 707, 916–920.

449. O. Heaviside. A Gravitational and Electromagnetic Analogy. *The Electrician*, 1893, v. 31, 281–282.

450. O. Heaviside. A Gravitational and Electromagnetic Analogy. *The Electrician*, 1893, v. 31, 359.

451. R. M. Wald. General Relativity. The University of Chicago Press, Chicago, IL, 1984.

452. M. Maggiore. Gravitational Waves, Volume 1: Theory and Experiment. Oxford University Press, New York, 2008.

453. B. P. Abbott *et al*. [The LIGO Scientific Collaboration and Virgo Collaboration]. Observation of Gravitational Waves from a Binary Black Hole Merger. *Phys. Rev. Lett.*, 2016, v. 116, 061102.

454. L. Boyle, K. Finn, and N. Turok. *CPT*-Symmetric Universe. *Phys. Rev. Lett.*, 2018, v. 121, 251301.

455. L. Boyle, K. Finn, and N. Turok. The Big Bang, CPT, and Neutrino Dark Matter. *Ann. Phys.*, 2020, v. 438, 168767.

456. M. T. Tyree and M. H. Zimmermann. Xylem Structure and the Ascent of Sap. Springer-Verlag, Berlin, Heidelberg, and New York, 2 edition, 2002.

457. P. J. E. Peebles and B. Ratra. The cosmological constant and dark energy. *Rev. Mod. Phys.*, 2003, v. 75, 559–606.

458. T. Rothman and S. Boughn. Can Gravitons be Detected? *Found. Phys.*, 2006, v. 36, 1801–1825.

459. F. Dyson. Is a Graviton Detectable? *Int. J. Mod. Phys. A*, 2013, v. 28, 1330041.

460. M. Kunz. The phenomenological approach to modeling the dark energy. *C. R. Phys.*, 2012, v. 13, 539–565.

461. F. Niedermann and M. S. Sloth. Resolving the Hubble tension with new early dark energy. *Phys. Rev. D*, 2020, v. 102, 063527.

462. K. Loeve, K. S. Nielsen, and S. H. Hansen. Consistency Analysis of a Dark Matter Velocity-dependent Force as an Alternative to the Cosmological Constant. *Astrophys. J.*, 2021, v. 910, 98–101.

463. C. Andrei, A. Ijjas, and P. J. Steinhardt. Rapidly descending dark energy and the end of cosmic expansion. *Proc. Natl. Acad. Sci. USA*, 2022, v. 119, e2200539119.

464. S. Weinberg. The cosmological constant. *Rev. Mod. Phys.*, 1989, v. 61, 1–23.

465. J. Martin. Everything you always wanted to know about the cosmological constant problem (but were afraid to ask). *C. R. Phys.*, 2012, v. 13, 566–665.

466. P. Astier and R. Pain. Observational evidence of the accelerated expansion of the universe. *C. R. Phys.*, 2012, v. 13, 521–538.

467. R. Durrer. What do we really know about dark energy? *Phil. Trans. R. Soc. A*, 2011, v. 369, 5102–5114.

468. J. Solà. Cosmological constant and vacuum energy: old and new ideas. *J. Phys.: Conf. Ser.*, 2013, v. 453, 012015.

469. Q. Wang, Z. Zhu, and W. G. Unruh. How the huge energy of quantum vacuum gravitates to drive the slow accelerating expansion of the Universe. *Phys. Rev. D*, 2017, v. 95, 103504.

470. W. Thomson. On a Universal Tendency in Nature to the Dissipation of Mechanical Energy. *Proc. R. Soc. Edin.*, 1857, v. 3, 139–142.

471. T. Markkanen, A. Rajantie, and S. Stopyra. Cosmological Aspects of Higgs Vacuum Metastability. *Front. Astron. Space Sci.*, 2018, v. 5, 40.

472. S. W. Hawking. Particle Creation by Black Holes. *Commun. Math. Phys*, 1975, v. 43, 199–220.

473. S. Frautschi. Entropy in an Expanding Universe. *Science*, 1982, v. 217, 593–599.

474. M. E. Gertsenshtein. Wave resonance of light and gravitational waves. *Sov. Phys. JETP*, 1961, v. 41, 113–114.

475. E. Di Valentino, A. Melchiorri, and J. Silk. Planck evidence for a closed Universe and a possible crisis for cosmology. *Nat. Astron.*, 2020, v. 4, 196–203.

476. E. Di Valentino, O. Mena, S. Pan *et al*. In the realm of the Hubble tension – a review of solutions. *Class. Quantum Grav.*, 2021, v. 38, 153001.

477. E. Di Valentino. Challenges of the Standard Cosmological Model. *Universe*, 2022, v. 8, 399.

478. N. Aghanim *et al*. [The Planck Collaboration]. Planck 2018 results VI. Cosmological parameters. *A&A*, 2020, v. 641, A6.

479. T. Willmore. Riemannian Geometry. Claredon Press, Oxford, 1993.

480. M. Droske and M. Rumpf. A level set formulation for Willmore flow. *Interfaces Free Bound.*, 2004, v. 6, 361–378.

481. R. Penrose. Difficulties with Inflationary Cosmology. *Ann. NY Acad. Sci.*, 1989, v. 571, 249–264.

482. D. Medková. The Laplace Equation. Springer International Publishing AG, Cham, Germany, 2018.

483. T. K. Das. Hyperspherical Harmonics Expansion Techniques. Springer India, New Delhi, 2016.

484. J. E. Avery and J. S. Avery. Hyperspherical Harmonics and Their Physical Applications. World Scientific Publishing, Singapore, 2018.

485. S. Müller and M. Röger. Confined Structures of Least Bending Energy. *J. Diff. Geom.*, 2014, v. 97, 109–139.

486. M. V. Vol'kenshtein. Molecules and Life. Plenum Press, New York, 1970.

487. L. E. Kay. Molecular Biology and Pauling's Immunochemistry: A Neglected Dimension. *Hist. Phil. Life Sci.*, 1989, v. 11, 211–219.

488. L. Pauling. Molecular basis of biological specificity. *Nature*, 1974, v. 248, 769–771.

489. L. Pauling. Analogies between Antibodies and Simpler Chemical Substances. *Chem. & Eng. News*, 1946, v. 24, 1064–1065.

490. D. Chandler and P. G. Wolynes. Exploiting the isomorphism between quantum theory and classical statistical mechanics of polyatomic fluids. *J. Chem. Phys.*, 1981, v. 74, 4078–4095.

491. P. L. Taylor and J. Tabachnik. Entropic forces – making the connection between mechanics and thermodynamics in an exactly soluble model. *Eur. J. Phys.*, 2013, v. 34, 729–736.

492. T. S. Roussy, L. Caldwell, T. Wright *et al*. An improved bound on the electron's electric dipole moment. *Science*, 2023, v. 381, 46–50.

493. E. M. Sevick, R. Prabhakar, S. R. Williams *et al*. Fluctuation Theorems. *Annu. Rev. Phys. Chem.*, 2008, v. 59, 603–633.

494. M. Campisi and P. Hänggi. Fluctuation, Dissipation and the Arrow of Time. *Entropy*, 2011, v. 13, 2024–2035.

495. C. Jarzynski. Equalities and Inequalities: Irreversibility and the Second Law of Thermodynamics at the Nanoscale. *Annu. Rev. Condens. Matter Phys.*, 2011, v. 2, 329–351.

496. P. Marquet. The Exact Gödel Metric. *Prog. Phys.*, 2021, v. 17, 133–138.

Fractal Quantization of Speed in Physics of Numerical Relations

Hartmut Müller

Rome, Italy
E-mail: hm@interscalar.com

The paper proposes a numeric-relational approach to the stability of real systems of coupled periodical processes and shows that it leads to fractal quantization of frequencies, wavelengths, and speeds caused by fractal scalar fields of transcendental numerical attractors. Applied to the stability of planetary systems, the approach predicts fractal quantization of orbits, orbital and rotational periods, and orbital speeds. On examples, the paper shows that the mean orbital speeds of planets, planetoids and large moons of the solar system are consistent with the prediction.

Introduction

Towards the end of the 19th century, many physicists were convinced that the theoretical basics were complete and that there was nothing fundamentally new to discover. History proved them wrong. They didn't yet know quantum physics.

First it was the periodicity of the chemical properties of the elements, then there were regularities in the atomic spectra that pointed to a new physics.

Today, many physicists are convinced that the only thing that matters is to unite quantum theory with general relativity. But again, unexpected regularities appear on the empirical horizon, which are still dismissed as coincidences. This time we are dealing with regularities in the dynamics of planetary systems that cannot be derived from Kepler's laws or Einstein's theory of gravity. These are regularities in the distribution of orbital and rotational periods as well as gravitational parameters. Some of these regularities are highlighted in my papers [1, 2].

In the present article, we deal with regularities in the distribution of orbital speeds. For example, why is Jupiter's orbital speed identical to that of its moon Europa? Why is Saturn's orbital speed identical to that of its moon Dione? By the way, both moons are the fourth largest in their systems. Why is the orbital speed of Uranus identical to that of its moon Miranda? Why is the orbital speed of Jupiter's moon Io identical to that of the planetoid Ceres?

From the perspective of celestial mechanics, these regularities are not more than coincidences. From the perspective of our numeric-relational approach, these regularities are expected effects of a new relational physics.

Theoretical Approach

In a series of papers [1–6] and a book [7] I have introduced a numeric-relational approach to physics and demonstrated its application in particle physics, astrophysics, geophysics, engineering, and biophysics.

In particular, this approach leads to the conclusion that coupled periodical processes can avoid destabilizing mutual parametric resonance, if their frequency ratios approximate transcendental numbers. Among all transcendental numbers, Euler's number $e = 2.71828\ldots$ and Archimedes' number $\pi = 3.14159\ldots$ are unique. Indeed, the real power function of Euler's number is the only one that coincides with its own derivatives. In the consequence, Euler's number allows avoiding mutual parametric resonance between any coupled periodic processes including their derivatives [8]. In this way, Euler's number acts as primeval source of stability in systems of coupled periodic processes.

Archimedes' number determines the length of the circumference. The transcendence of the circumference avoids interruptions and makes impossible to define the start or endpoint of circular or elliptical motion. Hence, Archimedes' number makes possible eternal orbital motion, rotation, and oscillation. Perhaps that is why it is impossible to *completely* stop oscillations, for example, the thermal oscillations of atoms. In this way, Archimedes' number acts as primeval source of motion and kinetic energy.

Integer and rational powers of $e = 2.71828\ldots$ and $\pi = 3.14159\ldots$ form two complementary fractal scalar fields of transcendental attractors – the *Euler field* and the *Archimedes field*, as I have shown in [6]:

$$\mathcal{E} = e^{\mathcal{F}} \qquad\qquad \mathcal{A} = \pi^{\mathcal{F}}$$

Both fields are k-dimensional projections of the fundamental fractal $\mathcal{F}$ that is given by finite canonical continued fractions of integer attractors $n_0, n_1, n_2, \ldots, n_k$:

$$\mathcal{F} = \langle n_0; n_1, n_2, \ldots, n_k \rangle = n_0 + \cfrac{1}{n_1 + \cfrac{1}{n_2 + \cdots + \cfrac{1}{n_k}}}$$

In astronomical scales, the orbital periods and distances of the planets, planetoids and large moons in the solar system obey both the Euler field and the Archimedes field. Also their rotational periods obey the Euler field, as shown in [9]. In subatomic scales, the mass-ratios of elementary particles obey the Euler field [10].

Compared to the majority of known particles, electron and proton are exceptionally stable. Their life-spans top everything that is measurable, exceeding 10^{29} years [11]. This is why normal matter is formed by nucleons and electrons. According to our numeric-relational approach, electron and proton are stable, because the ratio of their eigenfrequencies approximates an integer power of Euler's number and its square root, which makes impossible proton-electron parametric resonance in their ground states.

The eigenfrequencies and harmonics of the proton and the electron are natural frequencies of any type of matter, also of the accreted matter of a planet. Given the enormous number of protons and electrons that form a planet, eigenresonance must be avoided in the long term. This affects any periodical process including orbital and rotational motion. This is why the planets in the solar system and in hundreds of exoplanetary systems have orbital periods that approximate integer and rational powers of Euler's number relative to the natural oscillation periods of the proton and the electron, as shown in my paper [1]. The perihelion and aphelion of a planetary orbit, if expressed in units of the Compton wavelength of the electron, give the lower and upper approximations of integer powers of Euler's number, as I have shown in [2]. As a consequence, the gravitational parameters of the Sun and its planets, if expressed in electron units, approximate integer powers of Euler's number. These findings allow us to interpret the approximation of integer powers of Euler's number and its roots as a general evolutional trend of numerical relations in real systems of many coupled periodical processes. This evolutionary trend drastically reduces the diversity of preferred orbital periods, distances, and speeds, increasing the likelihood of matches in different planetary or lunar systems.

Exemplary Applications

Since the orbital period of a planet approximates an integer power of Euler's number multiplied by the oscillation period of the electron, and its perihelion and aphelion approximate an integer power of Euler's number multiplied by the Compton wavelength of the electron, the orbital speed of the planet approximates the speed of light, divided by an integer power of Euler's number. For instance, Jupiter's distance from Sun approximates the 56th power of Euler's number multiplied by the Compton wavelength of the electron $\lambda_e = 3.86159 \cdot 10^{-13}$ m. The aphelion 5.45492 AU = $8.160444 \cdot 10^{11}$ m delivers the upper approximation:

$$\ln\left(\frac{A(Jupiter)}{\lambda_e}\right) = \ln\left(\frac{8.160444 \cdot 10^{11}\,\text{m}}{3.86159 \cdot 10^{-13}\,\text{m}}\right) = 56.01$$

The perihelion 4.95029 AU = $7.405528 \cdot 10^{11}$ m delivers the lower approximation:

$$\ln\left(\frac{P(Jupiter)}{\lambda_e}\right) = \ln\left(\frac{7.405528 \cdot 10^{11}\,\text{m}}{3.86159 \cdot 10^{-13}\,\text{m}}\right) = 55.91$$

Jupiter's orbital period 4332.59 days equals the 66th power of Euler's number multiplied by the oscillation period of the electron ($\tau_e = \lambda_e/c = 1.28809 \cdot 10^{-21}$ s is the angular oscillation period of the electron):

$$\ln\left(\frac{T(Jupiter)}{2\pi \cdot \tau_e}\right) = \ln\left(\frac{4332.59 \cdot 86400\,\text{s}}{2\pi \cdot 1.28809 \cdot 10^{-21}\,\text{s}}\right) = 66.00$$

Consequently, Jupiter's orbital speed approximates the speed of light, divided by the 10th power of Euler's number, because $66 - 56 = 10$. Indeed, Jupiter's average orbital speed equals 13.07 km/s:

$$\ln\left(\frac{V(Jupiter)}{c}\right) = \ln\left(\frac{13.07\,\text{km/s}}{c}\right) = -10.04$$

The orbital speed of Jupiter's fourth largest moon Europa approximates the same attractor $\mathcal{E}\langle-10\rangle$ of the Euler field. The average orbital speed of Europa equals 13.74 km/s:

$$\ln\left(\frac{V(Europa)}{c}\right) = \ln\left(\frac{13.74\,\text{km/s}}{c}\right) = -9.99$$

The orbital speeds of the other 3 Galilean moons of Jupiter approximate subattractors of the Euler field that correspond to reciprocal integer powers of Euler's number: The orbital speed of the moon Io approximates $\mathcal{E}\langle-10; +4\rangle$, the orbital speed of Ganimede approximates $\mathcal{E}\langle-10; -4\rangle$, and the orbital speed of Callisto approximates $\mathcal{E}\langle-10; -2\rangle$.

Venus' distance from Sun approximates the 54th power of Euler's number multiplied by the Compton wavelength of the electron λ_e. The aphelion 0.728213 AU = $1.08939 \cdot 10^{11}$ m delivers the upper approximation:

$$\ln\left(\frac{A(Venus)}{\lambda_e}\right) = \ln\left(\frac{1.08939 \cdot 10^{11}\,\text{m}}{3.86159 \cdot 10^{-13}\,\text{m}}\right) = 54.00$$

The perihelion 0.718440 AU = $1.07477 \cdot 10^{11}$ m delivers the lower approximation:

$$\ln\left(\frac{P(Venus)}{\lambda_e}\right) = \ln\left(\frac{1.07477 \cdot 10^{11}\,\text{m}}{3.86159 \cdot 10^{-13}\,\text{m}}\right) = 53.98$$

The orbital period 224.701 days of Venus approximates the 63th power of Euler's number multiplied by the oscillation period of the electron:

$$\ln\left(\frac{T(Venus)}{2\pi \cdot \tau_e}\right) = \ln\left(\frac{224.701 \cdot 86400\,\text{s}}{2\pi \cdot 1.28809 \cdot 10^{-21}\,\text{s}}\right) = 63.04$$

Consequently, the orbital speed of Venus approximates the speed of light, divided by the 9th power of Euler's number, because $63 - 54 = 9$. In fact, the average orbital speed of Venus equals 35.02 km/s:

$$\ln\left(\frac{V(Venus)}{c}\right) = \ln\left(\frac{35.02\,\text{km/s}}{c}\right) = -9.05$$

Since e and π are transcendental, there are no rational powers of these numbers that can produce identical results. Therefore, attractors of the Archimedes field are different from attractors of the Euler field. For instance, the mean orbital speed 9.68 km/s of Saturn does not approximate a main attractor of the Euler field, but approximates the main attractor $\mathcal{A}\langle -9 \rangle$ of the Archimedes field:

$$\text{lp}\left(\frac{V(Saturn)}{c}\right) = \text{lp}\left(\frac{9.68 \text{ km/s}}{c}\right) = -9.03$$

We use the symbol "lp" for the logarithm to the base π:

$$\text{lp}(x) = \frac{\ln(x)}{\ln(\pi)}$$

This circumstance suggests that transcendental relations not only stabilize orbits preventing them from mutual parametric resonance, but also assign orbits to the numerical field to which they belong.

For instance, the mean orbital speed 4.743 km/s of Pluto approximates the main attractor $\mathcal{E}\langle -11 \rangle$ of the Euler field:

$$\ln\left(\frac{V(Pluto)}{c}\right) = \ln\left(\frac{4.743 \text{ km/s}}{c}\right) = -11.05$$

while the mean orbital speed 3.434 km/s of Eris approximates the main attractor $\mathcal{A}\langle -10 \rangle$ of the Archimedes field:

$$\text{lp}\left(\frac{V(Eris)}{c}\right) = \text{lp}\left(\frac{3.434 \text{ km/s}}{c}\right) = -9.94$$

Also the mean orbital speed 29.7827 km/s of the Earth does not approximate a main attractor of the Euler field, but approximates the main attractor $\mathcal{A}\langle -8 \rangle$ of the Archimedes field:

$$\text{lp}\left(\frac{V(Earth)}{c}\right) = \text{lp}\left(\frac{29.7827 \text{ km/s}}{c}\right) = -8.05$$

Possibly this indicates a transcendental duality of Euler- and Archimedes-orbits in the solar system. The orbital speeds $V_E(\mathcal{F})$ belong to the Euler field while the $V_A(\mathcal{F})$ belong to the Archimedes field:

$$V_E(\mathcal{F}) = \frac{c}{e^{\mathcal{F}}} \qquad\qquad V_A(\mathcal{F}) = \frac{c}{\pi^{\mathcal{F}}}$$

Orbital speeds that correspond to the base layer of the fundamental fractal $\mathcal{F}$ approximate the speed of light divided by integer powers of e and π.

Conclusion

In [6] I have shown that the proposed here numeric-relational approach to the stability of real systems of coupled periodical processes predicts a fractal quantization of frequencies and wavelengths caused by fractal scalar fields of transcendental numerical attractors – the Euler field and the Archimedes field. In the case of planetary systems, for example the solar system, the Euler field and the Archimedes field cause a fractal quantization of orbits and orbital periods.

The current article shows that stable orbital speeds derive from the speed of light divided by integer and reciprocal integer powers of e or π. This circumstance drastically reduces the diversity of preferred orbits, orbital periods, and speeds, increasing the likelihood of matches in different planetary or lunar systems. This is why in the solar system, the orbital speeds of some moons coincide with the orbital speeds of some planets and planetoids. Considering the described here fractal quantization of orbits as general evolutional trend, orbital speeds corresponding to integer powers of e or π should be widespread in the galaxy.

The duality of Euler- and Archimedes-orbits in the solar system suggests that the orbits differ in their function. Based on my previous research [6], I hypothesize that Euler-orbits act as stabilizers of the system, while Archimedes-orbits act as energizers.

Acknowledgements

References

1. Müller H. Physics of Transcendental Numbers meets Gravitation. *Progress in Physics*, 2021, v. 17, 83–92.

2. Müller H. Physics of Transcendental Numbers as Forming Factor of the Solar System. *Progress in Physics*, 2022, v. 18, 56–61.

3. Müller H. The Physics of Transcendental Numbers. *Progress in Physics*, 2019, v. 15, 148–155.

4. Müller H. Physics of Transcendental Numbers Determines Star Distribution. *Progress in Physics*, 2021, v. 17, 164–167.

5. Müller H. Physics of Transcendental Numbers on the Origin of Astrogeophysical Cycles. *Progress in Physics*, 2021, v. 17, 225–228.

6. Müller H. Physics of Irrational Numbers. *Progress in Physics*, 2022, v. 18, 103–109.

7. Müller H. Global Scaling. The Fundamentals of Interscalar Cosmology. *New Heritage Publishers*, Brooklyn, New York, USA, ISBN 978-0-9981894-0-6, (2018).

8. Müller H. On the Cosmological Significance of Euler's Number. *Progress in Physics*, 2019, v. 15, 17–21.

9. Müller H. Natural Metrology in Physics of Numerical Relations. *Progress in Physics*, 2023, v. 19, 102–105.

10. Müller H. Fractal Scaling Models of Natural Oscillations in Chain Systems and the Mass Distribution of Particles. *Progress in Physics*, 2010, v. 6, 61–66.

11. Workman R. L. et al. (Particle Data Group), *Prog. Theor. Exp. Phys.*, 083C01 (2022), www.pdg.lbl.gov

From Particle Physics to Cosmology, on the Gravitational Sub-structure of Everything

Jacques Consiglio

52 Chemin de Labarthe, 31600 Labastidette, France.
E-mail: Jacques.Consiglio@gmail.com

We show, through resonance formulas, that the free parameters of the standard models of particle physics and cosmology fit a single resonant system – from the mass of elementary particles to gravitation and cosmology, and couplings mirroring resonances; and finally that all is encoded in the Planck mass resonance. Instead of extending the theory or its degrees of freedom to obtain predictions, we consider the reverse problem; paying interest to the free parameters structure we find formulas which consistency implies physical constraints hitherto unknown.

1 Introduction

Here we take a hypothesis that extends and generalizes Louis de Broglie's original idea of a wave and its resonance:

A single resonant phenomenon defines the physical world in its entirety where pulsations, wave numbers, and rotations refer to the same quantum and compare as lengths.

It leads to the direct calculation of the Sommerfeld constant with all the precision available [5]. This calculation implies a composite wave, so that the electron has a wave substructure, governed by mechanisms, of which electrodynamics is one effect – and then the same must be said of all particles. It is an intermediate result of a wider exploration published in part [5,6,8] which initially ranges from the mass of the electron to that of the Planck particle, via the associated couplings. This text presents more advanced results through a sequence of formulas consistent with each other and available data, with minimal concepts, and now extends to cosmology (following [7] in particular).

From the beginning of physics, the first aim is not to build a theory, but to explore virgin territory, analyze data and discover its internal logic and structure; mathematical theories always come after. Hence we present the results of an exploration of free parameters; first those obtained at the level of masses, second the associated couplings, third an approach to the origin, fourth the resulting natural cosmology, and last a few logical extensions. The method is straightforward: Find a general structure to a data set, insist on precision, understand the minimum and move on to the next set based on what is understood. Most importantly, precision will allow understanding some unexpected links between different data sets. Again, the aim is not to build a theory, but to poke holes in a supposed invisible wall of ignorance, a few bricks of which can be seen in the above-mentioned calculation.

This exploration is easily justified by the fact that theories beyond the Standard Model (SM) have nothing new to model and are therefore motivated by some kind of faith that something is missing. The various interpretations of quantum mechanics strongly suggest that something is missing at the bottom, and there is definitely a problem with our understanding of the nature of reality, a psycho-philosophical issue; so we shall discuss some formulas about its structure.

2 The mass spectrum

The Standard Model divides massive particles into four distinct groups of interaction symmetries. These symmetries necessarily reflect the internal mechanisms we assume. We must therefore rely on these groups to analyze masses and extract invariant quantities and universal mechanisms. The exception is the three massive bosons whose masses come from the same potential. The analysis is therefore reduced to three groups, with the three bosons forming one.

Particles are studied as resonances, which can be modeled as a cyclic phenomena. Suppose that the electron matter wave is made up of two waves crossing each other in a resonator of unit size. In one dimension, the harmonic N in a length 1 gives a frequency N^2 at which the anti-nodes of the two waves cross; N^2 is a wave number and $1/N^2$ a length. Then we add a coupling also modeled as a length, we get $K D$, with D the coupling-length and K an integer used to quantize. Now in one dimension we have a mass formula

$$m = \frac{1}{\left(\dfrac{1}{N^2} + K D \right)}, \qquad (1)$$

which is roughly equivalent to the inverse relation between a mass and its Compton wavelength, and can be extended to more components; we may have composite resonances or couplings. In essence it addresses a harmonic system deformed by quantized couplings where mass is a harmonic mean – but this is only the 1-dimension case. In three dimensions, the resonance can be radial like in (1), circular or mixed, and are identified with three groups of particles. The radial case will correspond to the three electrons, bosons to the circular case, and the mixed case to quarks.

2.1 Electrons

The first mass formula applies to electrons and quarks:

$$m = \frac{X}{\left(\dfrac{1}{NP} + KD\right)^3} + \mu \,, \qquad (2)$$

where

- X is a mass constant, the choice of a unit.
- (1) is raised to the cube since the wave occupies a three-dimensional volume. This formula is now thermodynamics' $PV = K_B T$, with a constant volume V where the oscillator defines $P \equiv T$.
- NP are two integers for two waves components; either face to face (so $N = P$), or mixed with P radial and N circular (so $N \neq P$ and $2NP\pi \approx$ integer).
- And μ in units of mass represents a bridge between two complementary cuts of the resonance responding to each other, which is necessary to fit the electron masses, and justified by $U(1)_Y \times SU(2)_L \rightarrow U(1)_{EM}$.

So this formula must admit two solutions for each of the three electrons, with two sets of constants and resonances. The first one corresponds to a radial resonance and therefore $N = P$, which we call the primary field since the same constants will be used for all other particles. But the magnetic moment suggests a rotation, and in 3 dimensions a rotation implies an axis and one set of parallel planes is conserved; then $P = K$ imposes two synchronous axis combining the resonance and the effect of the rotation in the product NP, rotation to which N is orthogonal. We call this cut the secondary field.

An adjustment of the parameters to find the known masses with $N = P$ and a choice of minimal harmonics N, P, K lead to the primary field constants below (index e) and the harmonics and masses calculated in Table 1.

$$X_e = 8.14512139242128 \,\text{KeV/c}^2 \,. \qquad (3)$$

$$\mu_e = 0.24167661872330 \,\text{KeV/c}^2 \,. \qquad (4)$$

$$D_e = 8.53221893719202 \times 10^{-4} \,. \qquad (5)$$

Table 1: Primary resonances; electron, muon, tau (KeV/c^2).

-	P=N	K	Calculated	Reference
e	2	2	510.99895000	510.99895000 (15)
μ	7 − 2	3	105,658.3760	105,658.3755 (23)
τ	7 + 2	5	1 776,840	1 776,861 (118)

For the secondary field we start with $N = P = K = 2$ for the electron as the three phases are synchronous in Table 1; imposing $P = K$ for the other two particles gives the constants

below (index α) and Table 2, where the calculated masses are identical to those in Table 1 only for the decimals shown,

$$X_\alpha = 8.021608017449 \,\text{KeV/c}^2 \,, \qquad (6)$$

$$D_\alpha = 2.255984540570 \times 10^{-4} \,, \qquad (7)$$

and μ_α in (8) linked to μ_e (4) by an empirical relation of obvious interest as we find three length ratios between rotations (giving π in the numerators) and twice the main term of the Sommerfeld constant calculation (137 in the denominators):

$$\frac{\mu_\alpha}{\mu_e} = \frac{\pi}{2} + \frac{\pi}{137} + \left(\frac{2\pi}{137}\right)^2 \qquad (8)$$

$$\rightarrow \mu_\alpha = 0.3856750508181 \,\text{KeV/c}^2 \,. \qquad (9)$$

Table 2: Secondary resonances; electrons, muon, tau (KeV/c^2).

-	P=K	N	Calculated	Reference
e	2	2^1	510.99895000	510.99895000 (15)
μ	3	2^3	105,658.3760	105,658.3755 (23)
τ	4	2^4	1 776,840	1 776,861 (118)

Note 1) that the harmonics $P = K$ are minimal, and the powers of 2 for N; 2) that $KD > 0$ in Tables 1 and 2 is reminiscent of the Poincaré stress; and 3) that in the reduction $N = P = 7 \pm 2$ Table 1, which can be seen artificial in this table, 7 will be recurring for the other particles.

2.2 Quarks

For quarks, the formula (2) is used with $N \neq P$ for a mixed resonance where P is radial and N circular, and $\mu = 0$. The parameter X_e is that of the primary field (3), the coupling is composite, and combines D_e and Sommerfeld's constant α:

$$D_q = D_e (1 + \alpha) \,. \qquad (10)$$

Table 3 shows the harmonics and calculated masses where the reference masses are in the natural scheme taken from Wikipedia (not found elsewhere in this scheme), and for the top quark a direct measurement average (PDG 2023).

Table 3: Quark resonances (MeV/c^2).

-	P	N	K	Calculated	Reference
u	3	14/7	−8	2.00	2.01 ± 0.14
d	3	19/7	−4	4.79	4.79 ± 0.16
s	3	7	−6	106	105 ± 25
c	3	14	−6	1,255	1250 ± 100
b	3	19	−6	4,286	4350 ± 150
t	3	38	−6	172,380	172,690 ± 300

Several points in this table are remarkable:

- $P = 3$ is constant and appears consistent with fractional charges since $N = P = 2$ for the electron, and 2 ± 7 for the muon and tauon; meaning that 2 comes from the electric charge and 7 from something else.

- $K = -6$ for the four heavy quarks, the sum of the Ks is -12 for any generation.

- All N depend on 2, 7, and 19.

- In all three generations, there is a factor 2 in one resonance (N, or K), fitting the ratio of electric charge; consistent with α part of the coupling.

- The resonances of the u and d can actually be seen as a double mixture of the four others since $14/7 = 38/19$ and $19/7 = 38/14$.

- A mixed resonance imposes $2\pi N P \approx$ integer, which is well verified for all.

The coupling is composite and the parameter K is negative, indicating a second attractive force reminiscent of the strong force, and the new coupling term $\sim \alpha D_e$ tells us that it is about 137 times stronger than the coupling D_e of the electron masses. The reference allows a value in a range $D_e/(137\pm10)$, so αD_e is tentative.

2.3　Massive bosons

A double circular resonance gives $N = P$, and since the Higgs potential is unique, $N P$ is independent of the particle. This circular resonance creates a radial wave, so the mass must be reduced by a factor π to extract the radial equivalent (just as with $2\pi N P \approx$ integer for the mixed resonance we have $N P$ in the mass formula); a mixed resonance imposes a phase constraint between its two components; so we need a correction to ensure the internal coherence of the phases of these particles. At a single potential, they cannot admit a mass μ, which must therefore be integrated into the formula to reason at constant X_e, which gives

$$m = \frac{m_e}{m_e - \mu_e} \times \frac{X_e}{k\,\pi\left(\frac{1}{N^2} + K D_b\right)^3} \,, \qquad (11)$$

where m_e is the electron mass and D_b a boson-dependent coupling; and where the small k in the denominator represents the correction quoted above. After a first estimate of the couplings, and assuming charge transport, by the simple but relatively long reasoning detailed in [8] we deduce two couplings composites of α and D_e, identical for Z^0 and $W^\pm$

$$D_{WZ} = \frac{\alpha^2}{1 + \alpha^2} + \frac{\alpha D_e}{2\,(1 + \alpha^2)} - \frac{D_e^2}{6\,(1 - \alpha^2)} \,, \qquad (12)$$

and very close but different for the H^0

$$D_H = \frac{\alpha^2}{1 + \alpha^2} + \frac{\alpha D_e}{2\,(1 + \alpha^2)} - \frac{D_e^2}{1 - \alpha^2} \,, \qquad (13)$$

where α^2 represents a free field and the denominators are given by infinite interaction loops. We also showed (see also section 8.1) that the small k of (11) must be computed from

$$k^3\,\frac{\pi}{144} = 266\,D_b\left(\frac{\pi}{k}\right)^{1/3} \,, \qquad (14)$$

where D_b is the related boson coupling and the resonances (144 and 266). On this basis, Table 4 shows the harmonics and calculated masses (reference PDG 2023*).

Table 4: Massive bosons resonances (MeV/c^2).

-	P=N	K	Calculated	Reference
$W^\pm$	12	-2	$80,384.9$	$80,385\,(15)$
Z^0	12	-7	$91,187.3$	$91,187.6\,(2.1)$
H^0	12	-19	$125,206$	$125,250\,(170)$

We also checked in [8] the phase loop between the circular path, $N^2 = 12^2$, and the radial path in 266 with the three values of $K \in \{-2, -7, -19\}$. Phase coherence with -7 and -19 is trivial since $12 = 19 - 7$. The $W^\pm$ loop is also synchronous with $K = -2$, since $266 - 2$ is a multiple of 12, of which 2 is a sub-multiple. Internal phase coherence therefore allows all three resonances to exist. On the other hand, reasoning in the same way and on the same model, the other divisors of 266, $K \in \{-133, -38, -14\}$ do not check.

It is important to see that it is "really" the fine-structure constant in the expressions of D_{WZ} and D_H, and not a close value; because if we replace this value by $1/137$, the mass of the Z^0 becomes $91.2097\,\text{GeV/c}^2$, a factor of 10 outside the experimental uncertainty. Similarly, the specificity of D_H is necessary; without it we would get $M_H = 126.5\,\text{GeV/c}^2$.

2.4　Boson widths

With (11), a resonance formula we calculate pole masses; we should therefore be able to calculate their total widths from the resonance geometry. There is no way of varying N, P, which are integers, nor D, which depends on charges; widths should therefore be given by a displacement of charges giving $K \to K + \Delta K \to \Delta m$ needed for the resonance to blow.

These three particles carry multiple charges organized in a minimal way; at the ends of a simple line for the $W^\pm$ and Z^0, and at the vertices of a tetrahedron for the H^0 (giving the difference between D_{WZ} and D_H). Then for the first two, $\pm1/2$ on the radial axis and half of $1/12$ from the circular path gives

$$W^\pm \to \Delta K = \left(1 + \frac{1}{24}\right) \to \Gamma_W = 2.0857\,\text{GeV/c}^2 \,, \qquad (15)$$

in great agreement with the reference $2.085 \pm 0.042\,\text{GeV/c}^2$.

$$Z^0 \to \Delta K = \left(1 + \frac{1}{24}\right) \to \Gamma_Z = 2.4684\,\text{GeV/c}^2 \,, \qquad (16)$$

_____

*Particle Data Group

1% less than the reference (2.4952 ± 0.0023 GeV). And for the H^0, the tetrahedron is stable in K but the six line of forces can stand a displacement of $\pm 1/144/2$, so

$$H^0 \rightarrow \Delta K = \frac{1}{144 \times 6} \rightarrow \Gamma_H = 4.11\,\text{MeV/c}^2\,, \qquad (17)$$

also to 1% of the theoretical reference. So at first order, the widths are in good agreement with experiment and theory. A small difference remains for the Z^0, which calls for a complement that can only depend on the charges it transports, assuming $2 \times \pm e/3$ and/or $2 \times \pm 2e/3$, gives the fit:

$$\Delta K = \left(1 + \frac{1}{24} + \frac{1.5}{137}\right) \rightarrow \Gamma_Z = 2.4946\,\text{GeV/c}^2\,. \qquad (18)$$

The H^0 width will be re-discussed in section 5.6.

2.5 Neutrinos

The masses of neutrinos are much lesser than the constants X_e and X_α, so we cannot fit the formula parameters in the same way as for other particles. We suppose an inversion and fit the mass formula parameters from constraints that then seem logical:

- There is a progression of α and D_e powers in the couplings, up to D_e^2 and α^2 for the bosons. So no new coupling (use D_e and/or α), and we are looking for a negative power of α or D_e.

- Similarly there is a progression of resonances N, P; a unitary resonance is all that is left, we impose $NP = 1$ and only K varies.

- Use the lepton mass equation (3) with $\mu = 0$ and the primary field constant X_e (7).

- Assume a resonance conservation law (in-line with section 8.3), and use resonances inherited from the corresponding electron; thus an echo of the related electron N and K constitutes a neutrino K.

The coupling is

$$D_\nu = \frac{2}{\alpha} \approx 274\,, \qquad (19)$$

and corresponds to the inverse of the Dirac monopole, and the constraints above lead to Table 5 where the echo of the

Table 5: Neutrinos resonances (eV/c²).

-	P = N	K	Calculated mass
ν_e	1	1/2	0.00310
ν_μ	1	1/(3 − 1/9)	0.00924
ν_τ	1	1/(5 + 1/9)	0.04998

related electron resonances is obvious:

- $K \rightarrow 1/K$, and

- $N = P = 7 \pm 2 \rightarrow 1/(K \pm 1/9)$, with the sign of ± 2.

Table 6 compares the results with the corresponding limits (reference Δm^2_{ij} 1 σ NO, NuFIT 5.2-2022 – where $\Delta m^2_{31} = \Delta m^2_{32}$).

Table 6: Comparison to reference data.

Quantity	Calculated	Reference	Unit
Δm^2_{21}	0.0000759	0.0000741 $\left(^{+21}_{-20}\right)$	(eV/c²)²
Δm^2_{31}	0.002488	0.002511 $\left(^{+28}_{-27}\right)$	(eV/c²)²
Δm^2_{32}	0.002412	0.002511 $\left(^{+28}_{-27}\right)$	(eV/c²)²
$max\{m_i\}$	0.0500	≥ 0.0501 $\left(^{+28}_{-27}\right)$	eV/c²
m_{tot}	0.062	$0.06 < m_{tot} < 0.12$	eV/c²

2.6 The μ_e mass

The μ_e mass can be seen as an artifice since it is needed only for electrons and all particles are supposedly elementary, but its existence is now easy to justify.

Firstly, the calculation of the Sommerfeld constant in [5] requires four dimensions and two rotations. A rotation in four dimensions implies two planes conserved. A cut of a four-dimensional resonance to the three space dimensions (x, y, z) will give a rotation axis, i.e. the magnetic moment axis, say z, then in Table 1 $N = P$ for x and y. But we can make a second cut on (x, z, t) and impose $P = K$ on z, t; if the two rotations are synchronous we get Table 2 (or $P = n K$ or $P = K/n$ with n integer which would only affect D_α – but is eventually not needed). From this we need a couple of masses μ_e and μ_α linked by a constant factor because in this process we eliminate one of the two rotations in Table 1, and take the ratio of both in Table 2. It is still possible to make any other cut that will mix space and time differently, but hard to believe that the mass μ can be set to zero or close enough without using large integers for the resonances.

Secondly, we can see it in all non unitary resonances, but in three different ways:

- Like a simple addition for electrons (Table 1).

- With the coupling D_q of quarks (Table 3).

- And integrated into the resonance mass coefficient (11) in the case of bosons (Table 4).

The second form is indirect because here it appears from the ratio μ_α/μ_e when we look at (8) and (10) $D_q = D_e(1 + \alpha)$ means that a scaling in α or 2α is omnipresent; but when we discuss resonance length ratios it becomes 137 or 68.5.

Now the μ_e mass is part of the primary field and we need to find its resonance. It is understood as one side of the invariant bridge to the secondary field; hence its resonances in the two fields should be synchronous with those of the three electrons. So in order to estimate it we impose:

- A composite resonance compatible with those of all three electrons in both fields, Tables 1 and 2 simultaneously.

- Use of the primary field constant X_e (3).

- No new coupling (D_e and/or α).

As a result, the coupling (best fit) is composite and uses Sommerfeld's constant

$$D_{\mu_e} = (\exp(1) + 1)\, \alpha - \ln(1 + \alpha). \qquad (20)$$

The logarithm and its base in this expression are typical signatures of cumulative phenomena. The expression below gives the mass in (4), and includes two resonance

$$\mu_e = X_e \left(\frac{7}{2} - \frac{1}{4} - D_\mu \right)^{-3}. \qquad (21)$$

The fractions are equivalent to two resonances – $NP = 2/7$ and $NP = 4$ – and take the numbers of the primary resonances of the three electrons ($N = P \in \{2, 7-2, 7+2\}$), and 4 is also the electron resonance of Table 2, compatible with the others as it is a submultiple of the three products NP of this Table.

Finally the coupling of the μ_e mass depends solely on α and mathematically natural constants or functions, meaning that the couple it forms with μ_α "is" an electric charge on one side and looks like a magnetic current on the other.

2.7 Comments

Tables 1 and 2 use four degrees of freedom each, for two mass ratios, hence of no value if considered alone. Tables 3 and 4, on the other hand, use only one variable integer (or two for the u and d), and combine known couplings (α, D_e). With variations using only 2, 7 and 19 in these two tables for 9 particles, we must suppose that there is no freedom here; and neutrinos and electron resonances also fit the same numbers. Last, the μ_e resonance is synchronous of all electrons. Hence a global scheme is present.

Note that for the calculated masses, excluding neutrinos and μ_e, we have

$$|N P K D| < 1, \qquad (22)$$

which, since we start with a unit-size resonator, should express a geometric constraint limiting the particle spectrum. If we imagine a fourth generation of electrons as a continuation of Tables 1 the next resonance is $N = P = 19 - 2$ (starting from $\{2, 7, 19\}$), and $K = 7$ at the very least (following the progression of Table 1), and this inequality is not verified. The same result applies to quarks since the next product of two numbers from the same set is $N = 7 \times 19 = 133$, and P and K are constant Table 3 for the heavy quarks. The impossibility of bosons with masses other than those in Table 4, and using the same resonance model, is verified with the resonance paths coherence in $N = P$ and K (essentially $N = P = 12 = 19 - 7$ and $266 - 2$ is multiple of 12).

3 Couplings

3.1 Analysis

Table 2 shows two components of the Sommerfeld constant calculation [5, Eq. (4)], as a reminder:

$$\alpha^{-2} = 137^2 + \pi^2 - \frac{1}{137.5}\left(\frac{1}{2} + \frac{1}{8} \pm \frac{1}{137.5}\left(\frac{1}{2} \pm \frac{1}{8} \right) \right), \qquad (23)$$

namely $N = 2^1$ for the electron and $N = 2^3$ for the muon, the inverses of $1/2$ and $1/8$ identified in this calculation as identical resonances in 1 and 3 dimensions; the third resonance, that of the tau $N = 16$ is their product, therefore 3+1 dimensions.

The relation (8) between μ_e and μ_α uses twice the number 137, which implies an underlying origin, as it is one of the two common aspects of the three electrons. Now one way or another all particles discussed so far couple in α, meaning it constrains their resonances; then we calculate the sum of all the *integral and distinct* resonances in N and P (omitting fractions: μ_e, neutrinos, and quarks u and d):

$$\Sigma_{NP} = 2+3+4+5+7+8+9+12+14+16+19+38 = 137. \qquad (24)$$

It is from this sum that we can first imagine to calculate Sommerfeld's constant using the Bohm-de Broglie model, as it simply suggests that resonance and couplings act in mirror in a finite harmonic system; and again that the full mass spectrum is known. We must then look at the other axis K, and take into account the boson mass calculation which uses submultiples of 266 on this axis. So, again excluding μ_e, neutrinos and the quarks u and d, taking all the distinct K and replacing those of the bosons by +266, the sum

$$\Sigma_K = (2 \times 7 \times 19) + 2 + 3 + 4 + 5 - 6 = 274, \qquad (25)$$

is also compatible with a harmonic system between couplings and resonances, where the factor 2 with $\Sigma_{NP} = 137$ would constitute a second level of harmony.

3.2 $\mathbf{D_e}$ and $\mathbf{D_\alpha}$

According to this logic, the three couplings used, intervening at the same level in the mass formulas, should proceed from a unique mechanism and obey the same constraints; their geometrical structures should therefore be similar and their formulation obey the same pattern that we know from Sommerfeld's constant (23), i.e.

$$D^{-2} = a^2 + b\,\pi^2 + \frac{c}{d}, \qquad (26)$$

with geometric and action constraints between their components, which dictate that

1. a is the integer whose square is closest to D^{-2},

2. b is the integer such that $a^2 + b\pi^2 - D^{-2}$ is minimal in absolute value,

3. d is a rotation term where π^2 is suppressed,

4. $|b| > |c/d|$,

5. one of the terms is negative, and

6. all terms are numbers known through resonances.

Then a constrained division of the empirical value gives

$$D_e^{-2} = \left((7-3) \times (274+19)\right)^2 + 7\pi^2 - \frac{19\pi}{19-1}, \qquad (27)$$

$$D_\alpha^{-2} = \left((19-3) \times (274+3)\right)^2 + 2 \times (274+19+1)\pi^2 - \frac{19}{4\pi}. \quad (28)$$

After reducing a to prime numbers, we make 274, 7 and 19 appear from which 3 is subtracted. We find in the b term of D_α the electron wave signature present in α with $275\,\pi^2$, but augmented of 19 like 274 in the a term of D_e. There is a neat numerical recurrence between the couplings, a form of similarity between D_e and D_α, and a double connection with α (and two more if we also count $274 = 2 \times 137$). As expected, it agrees with a one to one mirror effect between couplings and resonances.

3.3 Ghost coupling

The three couplings appear to take the same resonances as particles, with 274 twice and $274 + 1$; they include two isolated rotations $1\,\pi^2$ and $7\,\pi^2$, the expected third $19\,\pi^2$ is absent; it is found in the resonance of two quarks t and b, $K = -19$ to calculate the mass of the H^0, and twice added to 274. We find 274 twice in the a terms and 137 only once. So we are missing a coupling that will include 137 like Sommerfeld's constant and $-19\pi^2$, the latter negative to fit subtraction at the denominator of the term d of D_e where the $1pi^2$ and $19\,\pi^2$ subtract. The missing elements give a and b and a spin 2 gives c:

$$D_p^{-2} = 137^2 - 19\pi^2 + \frac{4\pi}{19}, \qquad (29)$$

each term of which and/or its inverse is present in the other couplings formulas, therefore adds no new resonance, and which force has no coupling effect on the calculus of masses (so can we guess at this stage).

3.4 Comments

We note that all the conditions listed in section 3.2 are verified for three couplings, i.e. less than one chance in 10^5 for a random draw of three values. For D_p the point 1 is violated; this is imposed by $+137$ positive and $-19\pi^2$ negative, without which there would be no consistency either with α or with the terms in 19 of D_e and D_α.

    The geometrical form and connections of the couplings extend the underlying unity found in masses, and imply the non-separability of the forces.

4 The Planck mass

4.1 Notations

From now on, we shall use the Planck mass and length in their original formulations:

$$m_p = \sqrt{\frac{h\,c}{G}} \;\; ; \;\; l_p = \sqrt{\frac{h\,G}{c^3}}, \qquad (30)$$

denoted in lower case. We shall be using SI units. The values of the constants used are

$$G = 6.67430\,(15) \times 10^{-11}\,\mathrm{N\,m^2\,kg^{-2}}. \qquad (31)$$

and by definition

$$h = 6.62607015 \times 10^{-34}\,\mathrm{J\,s} \;\; ; \;\; c = 299792458\,\mathrm{m\,s^{-1}}. \quad (32)$$

We shall also use the Planck mass integrating the constant of quantum theories $\hbar$ and the Einstein constant $8\pi G$:

$$M_p = \frac{m_p}{4\pi} = \sqrt{\frac{\hbar\,c}{8\pi\,G}} = 4.341358(47) \times 10^{-9}\,\mathrm{kg}, \qquad (33)$$

denoted capitalized. The value of the constant X_e (3) is in SI:

$$X_e = 1.451999775331 \times 10^{-32}\,\mathrm{kg}. \qquad (34)$$

To avoid confusion, the subscript p will be used for quantities calculated with the classical formulas, and with the subscript ω when calculated from the harmonic system.

4.2 Unity and GR-QM reverse symmetry

The denominator of mass formulas relates a resonance expressed as a length $(1/N\,P)$ within a resonator of length $1 -$ equivalent to stress or pressure – to a force expressed as a coupling $(K\,D)$. In terms of Einstein's field equations, this is the fundamental unity of force, stress and energy: here, mass is stress, and therefore, by a natural extension, all forms of energy. There is a trivial geometric and quantitative symmetry between GR and QM, which is *a priori* compatible with the preceding results, since the three following relations must be compatible with the harmonic system:

- Newton's force in its natural quantum form, as each mass ratio must be physically homogeneous:

$$F = -\frac{G\,m_1\,m_2}{r^2} = -\frac{2\pi\,\hbar\,c}{r^2}\frac{m_1}{m_p}\frac{m_2}{m_p}. \qquad (35)$$

- The relation for a given mass between a Schwarzschild radius and a Compton wavelength:

$$R_S\,\lambda = 2\,l_p^2. \qquad (36)$$

- Or, in the form of three unitless ratios,

$$\frac{m}{m_p} = \frac{l_p}{\lambda} = \frac{R_S}{2\,l_p}. \qquad (37)$$

The volume at the denominator of the mass formula then represents two inverse quantities, depending on whether we see $1/NP$ in the denominator or its inverse in the numerator. By writing it in the following form

$$m = X \left(\frac{NP}{1 + NPKD} \right)^{+3}, \qquad (38)$$

the couplings appear as a mirror effect characterized by the product $NPKD$ which, according to (36) in particular, must be centered on a resonance corresponding to the Planck particle. Its mass should therefore be calculable with

1. a mass formula,
2. what is missing, 266 and D_p,
3. and what is universal, X_e and D_e,
4. taking into account a dispersion in 4π,

because then X_e cancels in the ratio m/m_p of (35) and it expresses only stress ratios in a unique harmony. We find

$$M_\omega = X_e \left(\frac{D_e}{266^2} + D_p^4 \right)^{-3} = 4.341421 \times 10^{-9} \, \text{kg}, \qquad (39)$$

which is the Planck mass M_p (33).

4.3 Comments

Now the harmony, its formulas and its two universal parameters cover the twenty-one orders of magnitude separating the mass of the Planck particle from that of the electron – or thirty with neutrinos. It shows once again the underlying unity, and that the form given to the couplings is correct as well as their assumed connections.

5 Toward the origin

While the origin of the resonances is not understood there is all the material needed in the mass M_ω (39) with two couplings D_e and D_p based respectively on $\Sigma_{N,P} = 137$ and $\Sigma_K = 274$, a term in 266, and the constant X_e. It suggests that we are close to the end and that the next step is to find an origin of the particle resonances; for this we need to find the constraints that apply. Since the Planck mass defines gravity we need to find-out how it defines space-time locally and globally and why it oscillates.

5.1 Classical anomaly

The calculation of M_ω (39) uses two couplings $D_e/266^2$ and D_p^4; two orthogonal forces and lengths, respectively the sine and cosine of an angle

$$\Omega = \arctan \left(\frac{D_e}{266^2} \times \frac{1}{D_p^4} \right) = 1.33509... \approx \frac{4}{3} \text{rad}. \qquad (40)$$

Now assume a spherical object with radius R greater than its Schwarzschild radius R_S; in the Newtonian gravity case, for a test particle at $D < R$ which wave function is $\psi = e^{i\phi}$, the phase shift $\Delta\phi$ in R for the momentum $\hat{p}\,\psi$ along $\vec{r}$ would only depend on mass and obey:

$$\int_0^R 4\pi \, r^2 \, \rho(r) \, dr = \Lambda \int_D^R d\phi, \qquad (41)$$

where the right-hand side is just the phase shift between D and R, $\rho(r)$ the energy density in r, and Λ a constant independent of R and R_S. Above all, this equation represents the effect of one phase variance, that of the massive object, say S, on another, that of the particle momentum. Now, the constitutive stress of this object is locally $\rho(r) = S/\pi$ because, firstly, there is here identity between stress, energy and phase variance, and secondly, the point of no return is π; so (41) can be written in unitless form where ϕ, S and Λ are three angles:

$$\int_0^R 4\pi \left(\frac{S}{\pi} \right)^2 d\left(\frac{S}{\pi} \right) = \Lambda \int_D^R d\phi. \qquad (42)$$

So if R tends to R_S, the integral of the left-hand side tends to $4\pi/3$ (S tends to π) and that of the right-hand side to π, hence $\Lambda = 4/3$. Now we compare two forces in (40) to their effects in (42) – *where there is identity*, then in the Newtonian gravity case we should find $\Omega = 4/3$. It is easy to see that the difference is not due to the precision of G, hence neither D_e nor D_p. It only expresses the incompleteness of our knowledge of the forces structure – *and therefore of their effects*. Then, since all energies gravitate we assume a complement also coming from the harmonic system representing all possible interactions through D_e and the powers of D_p, which should cover all the oscillator forms, known or not; thus a quantized series $h_i D_p^i$ such that:

$$\sum_{i=0}^{n} \frac{h_i D_p^i}{D_p^4} \times \frac{D_e}{266^2} = \tan\left(\frac{4}{3} \right), \qquad (43)$$

where $h_0 = 1$ for the Planck mass, and n any, possibly infinite.

5.2 Method

The series in (43) will be used as a probe; for this we need to estimate its terms one by one (h_1, then h_2, etc...). But we do not yet know what to search as there is *a priori* no experimental data to rely on. Still, each step must bridge part of the gap and reflect the unity that has so far been expressed through couplings and resonances; geometric shapes, a topology covering all forms of the oscillator as each of the products $D_e D_p^i$ corresponds to an increasingly large coupling, and the whole to a nested topology. So

- From the couplings at its origin, the sequence should talk of Sommerfeld's constant and particle resonances. These aspects should make its terms identifiable, hence logic imposes to recognize what we find.

- There is no turning back, then each term should reduce the residual by roughly 2 orders of magnitude – or maybe more.

- The precision of each term is infinite; the very structure of the sequence as a quantized oscillator implies that approximation is illusory.

These constraints severely limit the field of exploration; we use them with the following method:

1. At step n consider the residue, and divide by D_p^n.

2. Recognize what it is, round up or down to significant number(s) in line with $n-1$ and compute the residue.

3. If the residue is small enough go to step 1 for $n+1$, and continue with the next quantity of similar kind.

4. If not it may be a border then if h_n describes a known shape go to step 1 for $n+1$; or h_n is wrong, then go back to step 2 and make a better guess.

Two high precision online calculators [15] and [16] are used to calculate and check.

5.3 Sector one, particle resonances

M_ω corresponds to

$$h_0 = 1 \quad [+1.9 \times 10^{-3}], \tag{44}$$

with the residue with respect to $\tan(4/3)$ in square brackets.

$$h_1 = -1 \quad [+8.4 \times 10^{-5}], \tag{45}$$

a unit resonance represents a massless particle that can be identified with either a photon or neutrino(s).

$$h_2 = -3 - 4 \quad [-2.2 \times 10^{-6}], \tag{46}$$

is a little more complex, -4 is identified to the resonances of the electron (NP = 4 Table 1), and -3 with the P of quarks (Table 3) – two radial components linked to the electric field, the latter to fractional charges. In addition $-4-3 = -7$, twice the first part of the μ_e resonance $7/2$, and 4 is the inverse of $1/4$, the second part.

$$h_3 = +25 \quad [+5.1 \times 10^{-8}], \tag{47}$$

the muon resonance (NP = 25 Table 1, and NP = 24 Table 2 is close to optimum).

$$h_4 = -81 \quad [-2.7 \times 10^{-9}], \tag{48}$$

the tau resonance (NP = 81 Table 1, and NP = 64 Table 2 is also in the optimum range).

$$h_5 = 2\pi \left(7 + 14 + 19 + 38 + \frac{38}{19} + \frac{14}{7} + \frac{38}{14} + \frac{19}{7} \right)$$
$$[2 \times 10^{-11}], \tag{49}$$

the sum of quarks' N (Table 3) by 2π for circular paths.

$$h_6 = -556 = -8 \times 69.5 \quad [5.7 \times 10^{-14}], \tag{50}$$

which, by its position must correspond to the gluons eight degrees of freedom; without mass it would be either 1 or 8×1, this a point to understand. The last harmonic of this sector is

$$h_7 = -217 = -144 \times \frac{3}{2} - 1 \quad [3.9 \times 10^{-17}]. \tag{51}$$

The first term -144 identifies the resonances of the three massive bosons (Table 4) with a factor of $3/2$; and the second either the photon or the neutrino(s) with -1.

The resonances N, P of all particle of the Standard Model are entirely covered by this sector and simple to identify – including massless particles or supposed so. Note 1) that all h_i give directly comparable quantities, irrespective of the power associated with D_p; 2) that within a single harmonic all terms have the same sign, otherwise the result would be meaningless; 3) that the presence of 2π for quarks is consistent with the inferred geometry, as is its absence for electrons and massive bosons; 4) that the assumed logic of generating the Sommerfeld constant is verified for particles of known mass; 5) the μ_e mass resonance may also be here in h_2 (the part $7/2$); and 6) the unitary resonance of h_1 or h_7 justifies the neutrino mass calculation in section 2.5.

5.4 Sector two, spheres

The second sector starts with spherical coefficients of dimensions 4 to 7, with phase variances according to the template of the M_ω anomaly, then similar but inverted coefficients.

$$h_8 = -2\pi^2 - \frac{1}{\pi} \quad [7.2 \times 10^{-20}], \tag{52}$$

the four-dimensional sphere surface coefficient $(2\pi^2)$ and a phase variance $(1/\pi)$.

$$h_9 = -\frac{8\pi^2}{15} + \frac{1}{2\pi} \quad [1.2 \times 10^{-22}], \tag{53}$$

the five-dimensional sphere volume coefficient $(8\pi^2/15)$ and a phase variance $(1/2\pi)$.

$$h_{10} = -\frac{\pi^2}{6} + \frac{3}{2\pi} \quad [-5.7 \times 10^{-24}], \tag{54}$$

both a) the six-dimensional sphere volume coefficient $(\pi^3/6)$ divided by π, b) its surface coefficient divided by 6π, and c) curiously, the Riemann function, $\zeta(2) = \pi^2/6$, and a phase variance $(+3/2\pi)$.

$$h_{11} = +\frac{3}{2} \times \frac{16\pi^3}{105} + \frac{1}{\pi} \quad [1.7 \times 10^{-27}], \tag{55}$$

the seven-dimensional sphere volume coefficient $(16\pi^3/105)$ times $3/2$, i.e. $16\pi^3/70$, and a phase variance $(+1/\pi)$. The same factor $3/2$ is also present in h_7.

$$h_{12} = -\frac{1}{\pi} \quad [-6.3 \times 10^{-29}], \tag{56}$$

a simple phase variance, which defines a boundary.

$$h_{13} = +\frac{2}{5\pi^2} - \frac{\pi}{2} \quad [3.3 \times 10^{-32}], \qquad (57)$$

an inversion of h_9, with $\pi \to \pi^{-1}$ by multiplying the first term by 3/4, the inverse of the original tangent.

$$h_{14} = -\frac{1}{4\pi} - \frac{1}{\pi^3} \quad [-5.6 \times 10^{-34}], \qquad (58)$$

the inverse of the surface coefficient of a three-dimensional sphere (4π), and that of a six-dimensional sphere (π^3).

This sector, like the others, identifies stress coefficients and therefore forces and shapes. Finding spherical coefficients and phase variance terms can be identified with forces in at least 7-dimensional space. The signs of the components in (and between) harmonics are not always the same, possibly indicating opposite effects.

5.5 Sector three, wave and coupling

Convergence in this sector is extreme.

$$h_{15} = +\frac{1}{2^2} + \frac{1}{133\pi + \frac{\pi}{6}} \quad [2.5 \times 10^{-40}], \qquad (59)$$

two phase variances (or inverted resonances).

$$h_{16} = \frac{-1}{266^2 - 69.5^2 - 137 - \frac{3}{2} \times \left(1 + \frac{1}{69.5} - \frac{\pi}{8\times 69.5 + 3}\right)}$$
$$[3.8 \times 10^{-51}], \qquad (60)$$

corresponds, by its shape, to the difference of the squares of two couplings ($A^2 - B^2$), separating for instance the three terms in 69.5 from the others.

5.6 Sector four

The fourth sector is separated from the third by seven null harmonics (h_{17} to h_{23} inclusive) and begins with two identically shaped resonances that seem to complement each other.

$$h_{24} = -3^3 - \frac{2\pi^3}{3^4 \left(1 - \frac{1}{2\times 7}\right)} \quad [-5.2 \times 10^{-56}], \qquad (61)$$

a resonance term associated with a coefficient in π^3 that must be associated with a dimension. Then $h_{25} = 0$, and

$$h_{26} = +2^2 + \frac{3\pi^3}{2^4 \left(2 - \left(\frac{3}{2}\right)^3 \times \frac{1}{2\times 19}\right)} \quad [5.7 \times 10^{-60}], \qquad (62)$$

whose form is an almost exact copy of the previous one, reversing 3 and 2, and 7 and 19. Then $h_{27} = 0$ and finally

$$h_{28} = -\frac{144}{\pi^2} + \frac{1}{24} + \frac{1}{(144+1)\times 6\pi} \quad [3.0 \times 10^{-68}]. \qquad (63)$$

This harmonic corresponds to the three bosons resonance (i.e. $NP = 144$) and their resonance widths (1/24 and 1/144/6) seen in the radial direction. The last term being different from the expected one, we recalculate the H^0 width:

$$H^0 \to \Delta K = 1/((144+1)\times 6) \to \Gamma_H = 4.079 \, \text{MeV/c}^2, \quad (64)$$

which, if compared to (17), is closer to the theoretical value at 125.206 GeV/c².

6 Coherence

The sequence can only be proven based on a detailed knowledge of the geometry it defines; we are not there, we do not know how it works or whether it ends or not. We can, firstly, find internal correspondences and, secondly, relate it to known quantities. This is the purpose of this section, whose aim is to get a first estimate of coherence with the harmonic system, in particular the mass spectrum.

6.1 First points

We recognize many structuring points; a non-exhaustive list:

- First sector: All resonance numbers (N, P or NP) of massive particles are present with two well-defined orders, 1) that of total resonance lengths, and 2) that of the internal couplings progression in the primary field, and therefore groupings either in the same zone or in the same harmonic, the resonances of particles with similar properties.

- First sector: Similarly we find first all radial resonances (from h_2 to h_4), and then rotations (with h_5 and h_7); mixed quark resonances are split in two between h_2 for the radial part P, and h_5 for rotations N.

- First sector: So, having assumed that at this level the forces and their effects are one, which leads to equation (43), we have complemented the structure of the forces with the known structure of their effects, the resonances.

- Second sector: Contains four spherical coefficients, h_8 to h_{11}, in order from 4 to 7 dimensions. Then what identifies with interactions between these structures in h_{13} and h_{14}, and a single phase variance h_{12} in the middle that looks either like the interaction center between these spaces, or a pure absorber in 8 dimensions.

- h_{15}: We find $133 + 4 = 137 = \Sigma_{NP}$, inverting the two main terms and removing π and $\pi/6$.

- h_{15}: The numbers 4, and $133\pi = 7 \times 19 \times \pi$ correspond respectively to the resonances of electrons and quarks. So this harmonic is linked to the fermionic wave.

- h_{15}: the term $\pi/6$ is a phase advance for 133π; if it corresponds to an inverted length $\pi/6\pi^2$ we get $133 + 6 = 139$, the full resonance spectrum ($\Sigma_{NP} = 137$ plus the two unit resonances) – excluding $h_6 = 8 \times 69.5$, but $139 = 2 \times 69.5$, the same ratio as between Σ_K and Σ_{NP}.

- h_{15}: 133π is a harmonic of quark resonances 7 and 19 (plus a factor of 2 for charges 2/3), and $\pi/6$ a phase advance giving a negative length; so $K = -6$ Table 3.

- h_{24} and h_{26}: The two phase advances in the denominator multiply to give 133 and 266, depending on how the factors 2 is considered.

- h_{24} and h_{26}: Taking into account the factor 2 in the denominator of the second, as well as the ratio $3^3/2^3$ we obtain 27 and 8, their difference is 19. There are also 7 and 19, the two rotations of D_e and D_p respectively.

- h_{28}: The bosons resonance and widths. This harmonic therefore represents the Higgs field potential – unique as assumed – and h_{28} is complete and in agreement with the calculation of boson masses and lifetimes.

Such structure means an extremely entangled system where each element has a specific role – a global equilibrium working as a whole, coherent and inseparable.

6.2 The electrons, h_6 and h_{16}

We find 8×69.5 in h_6, which is rather strange as we expect gluons supposedly massless. Conversely, meson spectroscopy has been suggesting a monopole (e.g. [1]) for several decades without finding it, and we could also write $h_6 = 8 \times 1 + 8 \times 68.5$. But we also find 69.5 three times in h_{16}, twice in the denominators and 69.5^2, which makes it unbreakable; but suggests considering

$$69.5^2 = 68.5^2 + 137 + 1^2, \tag{65}$$

by the similarity of this expression with the ratio between the two mass constants μ_e and μ_α given by the empirical relation (8), except for the last term for which we would expect 2 instead of 1. In Table 1, the resonances N and P are 2, $7-2$ and $7+2$, while in Table 2 we have 2^1, 2^3 and 2^4 for N. These two tables represent the primary and secondary fields. So the 1^2 divides to give resonances 2, with Table 2 rotations in π for P and radial terms for N; and Table 1 only radial components for 2 (mixed with 7 if it is circular). Then divide 69.5 by π, invert each term of (65) replace 1 by 2π, and the sum of the inverses gives a ratio of resonance, therefore of masses:

$$\left(\frac{69.5}{\pi}\right)^2 \rightarrow \frac{\pi}{2} + \frac{\pi}{137} + \left(\frac{2\pi}{137}\right)^2, \tag{66}$$

is the ratio μ_α/μ_e (8). This expression also corresponds term to term to that of Sommerfeld's constant (23) and to the logic to its calculus, but in an inverse manner:

- $(2\pi/137)^2$ for 137^2, the electron pulsation.

- $\pi/137$ for π^2, the electron spin,

- and $\pi/2$ for $1/137.5 \times (1/2...)$, the wave.

Consequently, this relation must be reflected in the difference between X_e and X_α as well as in the composite coupling D_{μ_e}

(20); considering those as two pressure fields, each being a dynamic transformation of the other, and inverting the relation (8) by taking into account the common share of the resonances of the three electrons leads to the following semi-empirical formula:

$$\frac{X_e\left(1 - \exp(1)\,\alpha^2\right) + X_\alpha\left(1 + \exp(1)\,\alpha^2\right)}{X_e\left(1 - \alpha\right) - X_\alpha\left(1 + \alpha\right)} = \frac{137^2}{2\pi} \times \left(1 - \frac{\pi}{137}\right), \tag{67}$$

whose relative accuracy is 1.4×10^{-8}, and then relative errors of 4.8×10^{-12} on X_e and X_α in opposite directions, better than the uncertainty range on lepton masses (3×10^{-10} for the electron). The formula used here for α is expression (6) of [5].

The left hand side contains α, which is also found in the D_{μ_e} coupling (20), as well as the basis of the natural logarithm. The main term, $137/2\pi$ of the right hand side is modified by $(137 - \pi)$, which includes a phase advance; we find again the logic of the calculation of the constant α [5] with $137^2/2\pi$ for an electron pulsation and a phase delay $\pi/137$ per pulsation corresponding to the spin, and we obtain a resonance length $\sqrt{137^2 + \pi^2}$ where the fractional wave terms of α, which are related to the electron movement, are naturally absent. Both expressions (8) and (67) therefore speak of a dynamical shift between the primary and secondary fields, which corresponds to electrodynamics and its coupling.

6.3 The Planck length

The Planck length is identified to the maximum resolution and is expressed in units of length. But here it may be inscribed in the denominator of the mass M_ω, which is a pure number. We will therefore calculate the Planck length as an angular resolution independent of the system of units – even though the ice becomes thin as it questions units systems.

In h_{15} we recognize the fermion wave, which is obvious, and h_{16} as the universal coupling forming particles on the surface of a 4D sphere defined by h_8 dominating the first sector, for we can write it $h_{16} = A^2 - B^2 \sim m^2c^4 = E^2 - p^2 c^2$. They must then define the Planck length or Planck time, which we must be able to calculate with very good accuracy since this sector covers 17 orders of magnitude. Starting with h_{15}, we consider 4 and 133π as resonances and $\pi/6$ as a phase advance, and calculate an uncertainty from distinct paths; each path corresponds to a synchronicity S:

- 4 is the electron resonance, also present in the muon and tauon, and defines a 2π cycle. The first length is therefore a quarter of 2π.

$$S_1 = \frac{\pi}{2}. \tag{68}$$

- 133π, is directly a length so

$$S_2 = 133\pi. \tag{69}$$

- The phase advance $\pi/6$ desynchronizes the two resonances. Combine it with $1/4$, the length to consider is:

$$S_3 = \frac{\pi}{6} \times \frac{1}{4} = +\frac{\pi}{24}. \tag{70}$$

- It remains to combine the three terms; $\pi/6$ represents a phase advance for 133 and shortens its length; the harmonic h_5 is a multiple of 2π so since 133 is multiplied by π and 6 divides it, for a full turn this makes a length $2\pi \times (133 - 1/3)$, which applies to the denominator of $1/4$. A simple phase advance gives a negative quantity, hence a minus sign:

$$S_4 = -\pi \left(2^3 \left(133 - \frac{1}{3}\right)\right)^{-1}. \tag{71}$$

To obtain a quantity relating to order zero of the sequence, i.e. relative to one unit, we take into account the coupling D_p^{15} corresponding to h_{15}, which gives:

$$L_0 = \frac{D_p^{15}}{S_1 + S_2 + S_3 + S_4} = 2.2856968.. \times 10^{-35} \text{ rad}. \tag{72}$$

Then h_{16} is a coupling that modifies L_0, also a length and no degrees of freedom, but we have to unfold rotations to obtain a full length.

$$\frac{\pi}{8 \times (69.5 + 3/8)} \rightarrow 8\pi^2 \times (69.5 - 3/8), \tag{73}$$

where the sign of the phase advance (3/8) is inverted to obtain the corresponding length, and for the other term

$$\frac{1}{69.5} \rightarrow 69.5\,\pi. \tag{74}$$

Those allow us to calculate a quantity h_{16}^* by making the above replacements in the expression of h_{16}. We need to add a geometric factor to h_{16}, since it is also this coupling that compresses the surface of the 4D sphere h_8. Then, as h_{16} depends on D_p^{16}, we multiply by D_p to obtain a value relative to L_0, which gives a correction that may seem marginal

$$\frac{h_{16}^* D_p}{2\pi^2} = -5.0462626214390 \times 10^{-9}. \tag{75}$$

Then by posing

$$L_\omega = \frac{D_p^{15} \sqrt{\pi}}{S_1 + S_2 + S_3 + S_4} \times \left(1 + \frac{h_{16}^* D_p}{2\pi^2}\right), \tag{76}$$

we obtain the unreduced Planck length

$$L_\omega = 4.051292235148901 \times 10^{-35} \text{ rad}, \tag{77}$$

Using M_ω to cancel the uncertainty on G, we get Planck's constant, $h = m_p l_p c$ with a relative precision of 6×10^{-13}:

$$4\pi M_\omega L_\omega c = 6.626070150004 \times 10^{-34} \text{ J s}. \tag{78}$$

The fact that the Planck length is calculated in this way makes it independent of the system of units. We calculate an angular correction and speak of the GR-QM symmetry given by the relation

$$\frac{R_S \lambda}{2} = l_p^2 = L_\omega^2, \tag{79}$$

which is then read in steradian (or radian^2), where $R_S \lambda / 2\pi$ is the product of the two half-axes of an ellipse of invariant surface (independent of the particle) inscribed on a sphere of unit radius seen from its center; in other words, the angular resolution in a three-dimensional space – the surface of an ellipse is $\pi a b$, in agreement with the square root of π in the expression (76). The term on the right is therefore a solid angle and $L_\omega / \sqrt{\pi}$ the angle of the cone that defines it, both of which are independent of the system of units (see also section 7.1). Now we can calculate Newton's constant with the precision of the constant X_e, equivalent in principle to that of the electron mass; using $G = L_\omega c^2 / 4\pi M_\omega$ we get:

$$G = 6.67410788487\,(180) \times 10^{-11} \text{ m}^3 \text{ kg}^{-1} \text{ s}^{-2}. \tag{80}$$

The above decimals are the same if we calculate $G = L_\omega^2 c^3 / h$ (which is not guaranteed at all as (80) depends on M_ω), the next differs in accordance with the residual error on h (78). The Bohr radius a_0 is then also a pure number:

$$a_0 = \frac{\hbar}{\alpha m_e c} = \frac{2 M_\omega}{m_e} \times \frac{L_\omega}{\alpha}, \tag{81}$$

because in this expression the mass ratio is a harmonic ratio. Consequently, the interpretation of L_ω holds because α is calculated as the inverse of a resonance length, like L_ω.

6.4 Space-time and couplings

The first sector of the h_i gives the particle resonances, NP, as a product or separately, meaning that the resonances are part of the structure of space-time; but nothing about their couplings and K, which play at the same level in the mass formulas. Resonances are given in a specific order; for massive particles whose resonances are not unitary, the couplings increase with the i index and mix D_e and α. Hence couplings and K should also be inscribed in the space-time structure in the same order.

When calculating Ω the angle $4\pi/3$ is in 3D space as well as the phase reversal of π. So there is nothing here about space-time and $3 + 1D$, which would seem to be mandatory. A resonance in space-time means a period, the time needed for a resonance to loop which is a space-time interval; we can then use the standard invariant

$$c^2 t^2 - r^2 = c^2 \tau^2, \tag{82}$$

where τ is a particle period and defines, for this particle, a hyperboloid – and is reminiscent of de Sitter space. Then we pose R and u in hyperbolic coordinates

$$r = R \cosh(u) \; ; \; ct = R \sinh(u). \tag{83}$$

The ratio between space and time is

$$\frac{r}{ct} = \coth(u),\qquad(84)$$

which is independent of R. Then for the angle Ω (40) notice

$$\coth\left(\Omega^{-1}\right) \approx \frac{\pi}{2},\qquad(85)$$

close but not equal, and $\cot(\pi/2) = 0$; the meaning of which is that the ratio of forces in M_ω does not fit flat space-time, so let us check what is missing. With the h_i we get the $N P$s which response in the mass formulas are the $K D$s, and all this is perfectly ordered since we cannot mix the resonances and couplings at random. Then, in order to find the $K D$s' origin we should complement a second series as follows:

$$A = \arctan\left(\sum_{i=0}^{n} c_i \times \frac{D_e}{266^2 \, D_p^4}\right),\qquad(86)$$

with n any, where the c_i should complement the mass formulas; so that

$$\coth\left(A^{-1}\right) = \frac{\pi}{2},\qquad(87)$$

and eventually relates to forces meaning that space-time is flat, because then

$$\cos\left(\coth\left(A^{-1}\right)\right) = 0 \; ; \; \sin\left(\coth\left(A^{-1}\right)\right) = 1.\qquad(88)$$

The resolution logic for this series is basically the same as for the h_i; but we know a little more of what to search. The first sequence gives the particle resonances in order of mass and of increasing gravitational couplings D_p^i; we should logically expect a similar order with the couplings α and D_e. Then since $D_e \approx 16\,\alpha^2$, the gain at each step may be rather chaotic but show the same progression as for the h_i, with a *known* coupling responding to $D_e \, D_p^i$. The two couplings giving a minima the progression α, D_e, $\alpha \, D_e$, and D_e^2; respectively that of μ_e, electrons, quarks, and bosons; we should not use α^2 as it represents infinite loops in the boson mass couplings D_{WZ} and D_H. On this basis the empirically fit sequence is

$$c_0 = +1 \quad [3.2 \times 10^{-3}].\qquad(89)$$

for the Planck particle.

$$c_1 = -\alpha \times \frac{7}{2} = -\alpha \times \left(4 - \frac{1}{2}\right) \quad [1.6 \times 10^{-4}].\qquad(90)$$

This is $h_2 = 7$ divided by 2, and the coupling and primary resonance of μ_e, which indirectly responds to h_2, h_3 and h_4. It also decomposes in $4 - 1/2$, where 4 is the electron resonance Table 1 and sub-multiple of all $N P$ of Table 2; and a resonance $1/2$.

$$c_2 = -D_e \times \left(\frac{1}{2} + \frac{1}{25} + \frac{1}{81}\right) \quad [6.8 \times 10^{-5}].\qquad(91)$$

The primary coupling and the inverse of the resonances N or $N P$ of the three electrons Table 1, though for the electron we would expect $1/4$ instead of $1/2$; we consider it responds to h_2, h_3 and h_4 with D_e.

$$c_3 = -\alpha \, D_e \times \frac{h_5}{4\pi} \quad [1.4 \times 10^{-5}].\qquad(92)$$

The primary field coupling appearing with quarks ($\alpha \, D_e$), and the associated quark resonances N Table 3. So it responds to h_5 (49) but only for the coupling appearing with quarks.

$$c_4 = -D_e^2 \times \left(144 \times \frac{2}{3} + 2 - \frac{1}{7} - \frac{1}{19}\right) \quad [3.6 \times 10^{-9}].\qquad(93)$$

The primary coupling specific to bosons (D_e^2) and associated resonances, though multiplied by $2/3$ instead of $3/2$ in h_7 for 144, and the other numbers fit the boson's K. Again it responds to the coupling appearing with bosons except α^2. We have all what we know of, but let us continue.

$$c_5 = -\alpha \, D_e^2 \times \left(\frac{7}{2}\right) \quad [7.8 \times 10^{-11}].\qquad(94)$$

Now $c_5 = c_1 \, D_e^2$.

$$c_6 = +D_e^3 \times \left(\frac{1}{2} + \frac{1}{25} + \frac{1}{81}\right) \quad [9.8 \times 10^{-12}].\qquad(95)$$

And now $c_6 = -c_2 \, D_e^2$. We stop here because we do not have enough precision on α to continue (even c_6 is doubtful).

Overall, we have a progression of the primary couplings together with the resonances they apply to – plus maybe a bit more that repeats the same resonances. We notice:

1. That the rotations of quarks appear radially to the associated piece of coupling.

2. That the factor $3/2$ of h_7 is inverted.

3. That the electrons N or $N P$ appear as inverses.

4. That nothing comes out for gluons h_6, neutrinos h_1, photons in h_8.

6.5 Connection $h_i - c_i$

Connecting this sequence to the h_i is not difficult as it obeys the following rules:

1. For a given particle group, the resonances N, P and the strongest part of the associated coupling can be taken from a single element of this suite.

2. Any integer is a resonance $N P$ or K, to be taken as is.

3. Any fraction is an inverted $N P$ or K, whose sign must be reversed.

With the following consequences:

- The $N P$ resonances of electrons is the inverse number of c_2, except for the electron where we get $N = P = K = 2$ for Tables 1 and 2.

- A circular resonance N of a quark is taken in c_3 as radial effect of the same number in h_5.

- The resonances $N\,P$, K of the massive bosons are in c_4, with $3/2$ and two of the Ks inverted.

Overall, we get the N, P, D_{max}, where D_{max} is the strongest part of a particle coupling, and the boson's K. But we can complement the couplings for each particle group with a simple addition of D_{n-1} to D_n:

- The K of the bosons being known from c_4 we use the same number from c_3 to get the part in $\alpha\,D_e/2$; the factor $1/2$ comes from the interaction of two charges.

- For quarks, we get $D_q = D_e + \alpha\,D_e$ taking D_e from c_1.

- For electrons, the coupling is complete from c_2; and we get the electrodynamics coupling α from c_1 – which is also valid for quarks.

- Massive bosons are composites, then α^2 is taken as the square of α from c_1; in agreement with a free field giving the denominators of D_{WZ} and D_H by infinite interaction loops.

We miss the electrons and quarks K, which origin is still unknown. And by the way, the bosons resonance $N\,P = 144 = \left(\left(\frac{3}{2} \times 144\right) \times \left(\frac{2}{3} \times 144\right)\right)^{1/2}$ is the geometric mean of two components from h_7 and c_4.

6.6 Comments

The two sequences h_i and c_i appear to be working together with respect to the particle resonances. We first showed that the angle Ω must be complemented to $4/3$ to get the harmonics N, P, and then that the hyperbolic cotangent of its inverse must be complemented to $\pi/2$ to get a mix of coupling and resonances – both sequences in the same "right" order. Now we have

$$\coth\left(\Omega^{-1}\right) > \frac{\pi}{2} > \coth\left(\frac{3}{4}\right), \qquad (96)$$

so M_ω, a black hole, does not reach $\pi/2$, and $4/3$ exceeds it. So the particle spectrum is needed to get to $\pi/2$, and this is done by the coupling α. Consequently, D_p (gravitation) and α (electromagnetism) are complementary to each other for the existence of space-time. Electromagnetism is born from gravitation, which cannot survive without it.

We now have several points justifying the limits of the particle spectrum:

- The first sector of the h_i defines resonances, there are no others.

- It defines the $N\,P$ products of the primary field as a set of elementary oscillators occupying the Planck length. Hence the limitation $|N\,P\,K\,D| < 1$ suggested by the resonances of the primary field makes sense because otherwise the resonance of a particle would overflow

the Planck length. The resonator of unit length imagined to get the mass formula is simply a Planck particle defining a unitary box.

- The wave h_{15} and the coupling h_{16} only use numbers known through the mass spectrum and h_6.

- The Higgs field as it appears at h_{28} requires no other particles.

- The second sector involves interactions directed by dimensions and there then by symmetries; this is more than enough to encompass the symmetries of the standard model but also imply a form of selection by the fact that all the second sector must work together – a form of filtering.

We understand that space-time, particle resonances, and couplings are of gravitational and electromagnetic origin and that there is no freedom in the structure of the particle spectrum. The resulting laws and parameters form a coherent, compact, inseparable, and non-adjustable block.

7 Wave-coherent cosmology

An expanding universe where the laws of physics are everywhere identical and whose parameters are consistent with the preceding sections is necessarily a single resonance with a localized origin; if considered homogeneous its macroscopic quantities cannot have any degree of freedom. All must therefore be calculated from its geometry; hence from its age alone or from its horizon.

7.1 Black holes

The calculation of the Planck mass from an oscillator made of pure numbers poses a real problem, because the oscillator alone must define space-time; hence the metric by which it scales the particle resonances; therefore the Planck length varies in space and time. Consequently for a Schwarzschild black hole of mass M, the radius

$$R_S = \frac{2\,G\,M}{c^2}, \qquad (97)$$

can only be a wave number. We naturally think of

$$R_S = n\,l_p \pm l_p, \qquad (98)$$

with n an integer and $\pm l_p$ an uncertainty. But its characteristics are entirely defined by a real factor E defined by $M = E\,M_\omega$ and verify:

$$R_S \equiv M = E\,M_\omega = E\,X_e\left(\frac{D_e}{266^2} + D_p^4\right)^{-3}, \qquad (99)$$

and its average mass density ρ_S reported inside the sphere of radius R_S verifies:

$$R_S \equiv M = \frac{4\,\pi}{3}\rho_s\,R_S^3 \rightarrow \rho_s \sim R_S^{-2}. \qquad (100)$$

Then we identify the squares and the cubes in this relation

$$M = E M_\omega = \rho_S R_S^3 = \frac{E^3}{E^2} M_\omega$$

$$\rightarrow \rho_s \equiv \frac{X_e}{E^2} \;\; ; \;\; R_S \equiv E \left(\frac{D_e}{266^2} + D_p^4 \right)^{-1} . \qquad (101)$$

This expression shows the gravitational nature and structure of the mass formulas, and that the Schwarzschild radius of the Planck mass, say R_ω, can be considered as a unit wavelength because in natural units

$$R_\omega = 4\pi\, l_p \equiv 4\pi \left(\frac{D_e}{266^2} + D_p^4 \right)^{-1} . \qquad (102)$$

We then recognize the Hawking temperature which, even if in principle external, can only be the effect of the harmonic system:

$$K_B T_H = \frac{\hbar c^3}{8\pi G M} = M_\omega c^2 \frac{M_\omega}{M} = \frac{M_\omega c^2}{E} , \qquad (103)$$

where we recover the scale factor E of the expression (99). And M_ω is a resonance; this relation identifies this temperature to its wavelength; giving a GR – MQ symmetry where l_p, λ and R_S evolve together in the gravitational field for a particle at rest seen by a distant observer, and not the other way round for the last two. Likewise it comes

$$K_B T_H = \frac{\hbar c^3}{8\pi G M} = \frac{h \nu_\omega}{E} , \qquad (104)$$

where $\nu_\omega = M_\omega c^2 / h$ is a frequency, and ν_ω / E is that of the black hole. The wavelength of a black hole then varies like its mass and its radius, and its frequency conversely. Now the similarity with the equation of an ideal gas $PV = K_B T$ already discussed after the formula (2) is obvious. In the case of a black hole, P represents a surface pressure, but in the case of an ideal gas the internal pressure is constant, which perfectly fits the scale factor E. However, according to (101) we can identify a wave internal to the black hole whose dispersion at $r > R_S$ defines the metric. This wave is then the effective Planck length at the place considered, the maximum resolution decreases near the black hole down to R_S at its surface; we note the absence of singularity.

With the connections between the couplings and the two sums Σ_{NP} and Σ_K, we have linked gravity (as a force) to resonances and couplings through relative variations of the Planck length, therefore of the relative resolution. Consequently, the harmonic h_8 expressing a constraint in the form of a four-dimensional sphere surface coefficient $(2\pi^2)$ associated with a phase variance $(1/\pi)$ and dominating the spectrum of resonances, the universe is studied as the surface of a resonant 4-sphere which expands into a four-dimensional exterior. We consider a homogeneous universe where the celerity c is constant and where, due to homogeneity, the effective Planck length l_p varies only in time and defines a homogeneous metric in 3-space at any time. Obviously we forbid ourselves to add particles or fields, but suppose a single field or space undergoing a transformation. In this way the past is static, the future dynamic, and the present a phase transition.

7.2 Universe mini-model

Expanding into an exterior, the universe is modeled by a solid expanding 4-sphere centered on its origin of which 3D space (the present) is the surface. We therefore assume that the particles are growing strings, and that the interior of the sphere is fixed in the sense of the events – not in the sense of the phases of the resonances, but in the sense of the derivatives of the phase variations of the wave at any point.

In a perfectly homogeneous universe the cosmic time T is the meaningful physical quantity; in wave number $n = T/t_p$ is the number of "Planck sheets" or layers constituting the past. Taking the original event at $n = 1$, its resonance length L_1, then for $n \gg 1$ the sum of the inverses of the resonance lengths is

$$\frac{1}{L(n)} = \frac{1}{L_1} \sum_{i=1}^{n} \frac{1}{i} = \frac{1}{L_1} \left(\ln(n) + \gamma \right), \qquad (105)$$

with γ the Euler-Mascheroni constant. This formulation corresponds to the fact that in an expanding universe the surface of the layer n depends on n^3, which complies with the mass formulas; this expression means that the present "feeds" the past and that a source energy is consumed (actually of unit $J\,m \sim h\,c$). The sphere is divided into layers, the weight of each is its layer number, and we sum the inverses according to the rule. The energy of the layer n then evolves like

$$E(n) = E(1)\, (\ln(n) + \gamma) = E(1)\, \ln(k\,n). \qquad (106)$$

Massive particles are harmonics of the Planck mass; it is then necessary to count in Planck time to obtain a universal clock, since it is the natural one and the logarithm implies that the numerical results depend on the clock we choose. In the absence of creation of matter, the Compton wavelength of a particle is therefore

$$\lambda(n) = \frac{\lambda(1)}{\ln(k\,n)} . \qquad (107)$$

This mechanism and this formula apply to any particle and therefore to the Planck length. This relation amounts to writing $\Delta E\, \Delta t = 1$ for any string between any two layers with a naturally oriented time; that is one quantum of action exchanges between any two layers of any string; actually not action h but $h\,c$, which in 4D is to energy what energy is to power in 3D.

Now if masses add up, charges multiply; then from the same logic as for the evolution of wavelengths, we obtain a charge formula for a given epoch

$$C = \sum_{i=1}^{n} \frac{1}{n!} = \exp(1) . \qquad (108)$$

For the observable universe $n > 10^{55}$, we can therefore write an equality. The base of the natural logarithm also intervenes in the coupling D_{μ_e} (20) with Sommerfeld's constant in the form $\exp(1) \times \alpha$; a logarithm is also present in the same formula; these component denote temporal resonances.

The expression (107) defining the wavelengths evolution is all we need to discuss cosmology. The rest of this section contains only solutions to outstanding tensions and mysteries which, as far as we know, cosmological models do not relate to each other; all derived from the geometry of this mini-model and this expression.

7.3 The Hubble parameter

The immediate application concerns the Hubble parameter which is a function of time $H(n)$. We have on the one hand the expansion of the 4D sphere, therefore of 3D space at its surface, which depends only on proper time. The associated scale factor is therefore for a homogeneous spherical universe, still using the Planck time and lengths as units

$$a_e(n) = n \,. \tag{109}$$

The expansion implies a second scale factor coming from the contraction of wavelengths (107),

$$a_m(n) = \ln(k\,n) \,, \tag{110}$$

which corresponds to a contraction of rulers. Their product gives the transformation of measurable space-time intervals

$$a_{it}(n) = a_e(n)\,a_m(n) = n\,\ln(k\,n) \,. \tag{111}$$

In the laboratory the space intervals defining the measurement rods evolve over time

$$a_l(n) = \frac{1}{a_m(n)} = \frac{1}{\ln(k\,n)} \,. \tag{112}$$

The cosmic microwave background by which the Hubble parameter H_{cmb} is measured was emitted at

$$\mathrm{T_{cmb}} = 380\,000\,\text{years} \rightarrow \mathrm{p} = \frac{\mathrm{T_{cmb}}}{\mathrm{t_p}} = 8.87 \times 10^{55} \,,$$

a unitless wave number; and we now are at

$$\mathrm{T} = 13.801\,\text{Gy} \rightarrow \mathrm{n} = \frac{\mathrm{T}}{\mathrm{t_p}} = 3.22 \times 10^{60} \,,$$

and according to (112) the contraction of ruler between these two epochs is

$$\frac{\ln(p)}{\ln(n)} \approx \frac{1}{1.082} \,. \tag{113}$$

The photon is a string like any other, its wavelength evolves exactly like that of massive particles. So the Hubble parameter H_{cmb} measured through the frequency shift of the fossil radiation depends only on a_e, the scale factor due to recession.

At the opposite, the local Hubble parameter H_{loc} is measured from supernovae luminosity, so 1) as a time interval, since this signal has a duration, and 2) as a solid angle which depends on the telescope and the expansion. Nothing new on the principle, but the measurement of the signal duration depends on a_{it}, and its instantaneous power of the solid angle of capture of the signal, that is $a_l^2/a_e^2 = a_{it}^{-2}$ because space has expanded between emission and reception, and simultaneously the lengths defining the telescope have contracted. The instantaneous luminosity therefore depends on a_{it}^{-3} and the total luminosity measured on a_{it}^{-2}; the measured recession is therefore a_{it}. In the end, therefore, we have the following dependence between the two methods of measurement

$$H_{loc} = H_{cmb}\,\frac{\ln(n)}{\ln(p)} = H_{cmb} \times 1.082 \,. \tag{114}$$

Estimates using standard candles methods [14] concentrate around $H_{loc} = 73\,\text{km/s/Mpc}$, and the Planck mission indicates [13] $H_{cmb} = 67.66\,(42)\,\text{km/s/Mpc}$. The relation (114) gives

$$67.66\,(42) \times 1.082 = 73.17\,(45) \,.$$

Here the associated tensions are natural and explained. The precision may seem very good, but this is not so because the logarithm attenuates the errors on n; if we multiply n by 2 we obtain 1.083, by 10 we get 1.10, not much but we clearly see this ratio increasing over time. Consequently, the universe is permanently building resolution.

The ΛCDM model interprets these measurements as an accelerated expansion because a cosmological constant is the natural solution in GR. Then, deriving (110) to (112) and using the cosmological radius $R_U = c\,T$, it comes

$$\ddot{a}_m = (\dot{a}_m)^2 = \frac{1}{a_e^2} = \frac{1}{n^2} \rightarrow \frac{1}{R_U^2} \approx 0.6 \times 10^{-52}\,\text{m}^{-2} \,, \tag{115}$$

which is close to the estimated value of the cosmological constant (to within a factor of the order of 2).

Let us now return to the Planck clock and the rulers contraction between two epochs. With another clock such that $n \rightarrow n/q$ and $q > 1$, it comes

$$\frac{\ln(n)}{\ln(p)} \rightarrow \frac{\ln(n) - \ln(q)}{\ln(p) - \ln(q)} = \frac{\log_q(n) - 1}{\log_q(p) - 1} \,, \tag{116}$$

which amounts to changing the constant of integration. It is only when the constant is zero that the universe has unit size at the origin. We can also see there a change of base of the logarithm and the introduction of a negative constant of integration showing that the length of the ruler is in excess, then irrelevant, and that the beginning physically compares only to the Planck time. We can also write

$$\frac{a_m(n)}{a_m(q)} = \frac{\ln(n)}{\ln(q)} = \log_q(n) = \log_q\!\left(\frac{n}{q}\right) + 1 \,, \tag{117}$$

which clearly indicates the choice of time unit and allows us to change it, on the condition of knowing the absolute date.

7.4 Dark energies and energy

The object of this section is to study the correspondence with the ΛCDM model through the respective proportions of its four main parameters, namely the proportions of ordinary matter, dark matter, dark energy, and the total density. We do not yet look for absolute quantities, only to understand how these parameters relate to each other in relative terms.

Consider a uniform positive pressure *P in the surface of nonzero thickness* of a four-dimensional Euclidean sphere of radius R. The condensation of a new layer corresponds to an absorption producing the growth of the strings and a pressure deficit which, seen by an observer *in the surface of the sphere* using GR to model cosmology, will guess a constant negative pressure. This negative pressure is understood here as a condensation density simultaneously generating the particles' energy and gravity. The source energy M_S invested in the condensation must then be separated into three parts, namely 1) the visible energy, 2) a remainder of force without visible source (dark mass) because the wavelengths vary from one time to another, and 3) a dark energy of negative pressure causing the expansion of the sphere. Condensation can be modeled in 3+1D as a kinetic energy $M_S = p\,c$; but here it is the transformation $X_e \leftrightarrow X_\alpha$ which is equivalent to a bounce and implies $M_S = 2\,p\,c$. The dark energy of the standard model therefore represents 2/3 of all (2 for the source energy and 1 for the masses). Quantitatively, the condensation occurs with h_8 which implies proportions 1 for ordinary matter and $2\pi^2$ for source energy (1 is the time axis, $2\pi^2$ the surface of the sphere); so for convenience let us define

$$\phi = \frac{1}{2\pi^2}\,. \qquad (118)$$

The ΛCDM model considers ordinary matter separated from the dark side, its proportion of mass is therefore given by

$$\frac{M_V}{\phi} = \frac{M_S}{1 + \frac{2\phi}{3}} \rightarrow \frac{M_V}{M_S} = 4.90\,\%\,. \qquad (119)$$

The mass of matter will be one-third the source energy, but is separated into ordinary and dark matter; the proportion of the latter is therefore

$$\frac{M_D}{M_S} = \frac{1}{3 \times (1 + \phi)} - \frac{M_V}{M_S} = 26.83\,\%\,, \qquad (120)$$

and dark energy is the remainder

$$M_{DE} = M_S - M_D - M_V \rightarrow \frac{M_{DE}}{M_S} = 68.27\,\%\,. \qquad (121)$$

Finally:

1. These proportions are invariant over time.

2. They agree perfectly with the Planck mission results [13]: $M_B = 4.9\,\%$, $M_D = 26.8\,\%$, and $M_{DE} = 68.3\,\%$.

3. The absorption density is the saturation point known from the mass M_ω, imposed by the mechanism: The entire source energy intervenes there through the division by ϕ giving a surface density on the 4-sphere.

On this basis we can complement the calculation of the cosmological constant. Using $\ddot{a}_m$ (115), the expansion factor of space is that of a 3-sphere in GR, $4\pi/3$, and there is the factor $1/2$ from $M_S = 2\,pc$ to take into account. Then using the Hubble factor

$$\Lambda = \frac{2\,\pi\,H_{cmb}^2}{3\,c^2} = 1.121 \times 10^{-52}\,\text{m}^{-2}\,, \qquad (122)$$

in good agreement with the Planck mission results (to 1.3%).

$$\Lambda_{Planck} = 1.106 \times 10^{-52}\,\text{m}^{-2}\,. \qquad (123)$$

The current value, using $H_{loc} = 73.17$ km/s/Mpc gives

$$\Lambda_{loc} = \frac{2\,\pi\,H_{loc}^2}{3\,c^2} = 1.31 \times 10^{-52}\,\text{m}^{-2}\,. \qquad (124)$$

Last, using the cosmological radius $R_U = c\,T$, which is the legitimate way in this mini-model

$$\Lambda_{R_U} = \frac{2\,\pi}{3\,R_U^2} = 1.23 \times 10^{-52}\,\text{m}^{-2}\,, \qquad (125)$$

logically a median value.

7.5 The cosmological constant

The method used here to model the impact of $a_e\,a_m$ is to reverse their roles; we model an increase of masses, insert it into the Schwarzschild solution, and modify it *à la* de Sitter; with a little more because the masses are not constant. By setting the total universe energy to $M_T = M_S$, the previous section states

$$2\,G = \frac{R_U\,c^2}{M_T}\,, \qquad (126)$$

where $R_U = c\,T$ is the cosmological radius at date T and M_T the total energy of the ΛCDM at T, which symmetries the Schwarzschild solution

$$\frac{R_s}{r} = \frac{R_U\,M}{M_T\,r}\,. \qquad (127)$$

This equation simply indicates that Newton's constant conforms to a condensation whose saturation point is the density of a mass $E\,M_\omega$ on the observable scale. It is legitimate with R_U (and the following calculations can only work) because the proportions of matter and dark energy are constant over time, and the resonance is temporal. We therefore perform the calculations as if the universe was a plane, of size R_U, and of constant densities. To continue, it is necessary to add variable terms that depend on r/R_U, which requires two parameters α, β,

$$\frac{R_s}{r} = \frac{R_U\,M}{M_T\,r} \rightarrow \frac{R_U\,M}{M_T\,r} \times \frac{R_U - \alpha\,r}{R_U + \beta\,r}\,. \qquad (128)$$

The term in α in the numerator corresponds to the expansion of the source energy like R_U, and the term in β in the denominator to the derivative of the masses expansion. The two terms are obtained by adding lengths because we are talking about the inverse of the gradient of L_p in space and the inverse of its derivative in time, which also inverts the signs. A series expansion to the second order gives

$$\frac{R_U\,M}{M_T\,r} \to \frac{R_U\,M}{M_T\,r} - (\alpha + \beta)\frac{M}{M_T} + \beta(\alpha + \beta)\frac{M\,r}{M_T\,R_U}. \quad (129)$$

Let us examine this expression:

- The first term is nominal and defines static space, fields, and masses; the others can then be considered as addition of a variable gravity field.
- The middle term is independent of r and therefore involves the total mass of the universe; M must then be integrated to M_V, and the total must give -1 the flat metric. Then we have $\alpha + \beta = 2\pi^2 + 1$.
- So the term on the right must also be integrated into M_V to give M_T (and becomes r/R_U); therefore $\beta = 1$ the visible masses and $\alpha = 2\pi^2$ the source energy.

Note that with a series expansion in r we cannot integrate to R_U, but we can do it to M_V as the central term requires. In the end, after replacements and integration to M_V we find

$$\frac{R_s}{r} = \frac{R_U\,M}{M_T\,r} \to \frac{2\,G\,M}{r\,c^2} - 1 + \frac{r}{R_U}. \quad (130)$$

The Schwarzshild-de Sitter solution has a similar formulation

$$-\frac{R_s}{r} \to -\frac{R_s}{r} - \frac{\Lambda\,r^2}{3}. \quad (131)$$

Adding a variable term then gives

$$-\frac{R_s}{r} - \Lambda\,r^2 \to -\frac{R_s}{r} - \Lambda\,r^2 - \delta\Lambda\,r^2, \quad (132)$$

which is identified term to term with (130), and where the factor $1/3$ of (131) is removed because it comes by integration to give $\Lambda\,r^2/3$, and here it is $\delta\Lambda\,r^2$ which must be integrated. The introduction of a geometrical constant k allows to solve the equation as it must give (130):

$$-k\,\Lambda\,r^2 - \delta\Lambda\,r^2 \to -1 + \frac{r}{R_U}. \quad (133)$$

Since Λ is now constant, integration to R_U is possible and gives the flat metric identified in the unit term of (130); hence:

$$-k\,\Lambda \int_0^{R_U} r^2 dr = -1 \to k\,\Lambda = -\frac{3}{R_U^3}. \quad (134)$$

Now we need to derive $k\,\Lambda$, but here masses increase and Λ constant, and $\delta\Lambda$ represents the inverse of the masses derivative; so we need to derive the inverse to get $\delta\Lambda$; for all r we set $R_U \to r$, and since k is a geometrical factor we remove it

$$\delta(\Lambda(r)) = \left(\frac{d}{dr}\left(\frac{r^3}{3}\right)dr\right)^{-1} \to -\delta(\Lambda(r)) = -\frac{1}{r^2}, \quad (135)$$

and put it back to cancel the integration factor over the solid angle; then multiply by $1/2$ and identify with $-r/R_U$ we get

$$\frac{4\pi\,k}{2} \int -\delta(\Lambda(r))\,r^2\,dr = \int -2\pi\,k\,dr = -\frac{r}{R_U}. \quad (136)$$

Therefore

$$k = \frac{1}{2\,\pi\,R_U}. \quad (137)$$

Last, report in (134)

$$\Lambda = \frac{2\,\pi}{3\,R_U^2}, \quad (138)$$

as expected we get (125). The Schwarzschild and de Sitter solutions as modified here amount to differential equations that we integrate; it corresponds to the mini-model but contradict GR, but recall Einstein designed this theory with a static universe in mind – proof is his famous mistake to stabilize it. This is why in this mini-model space and time are not on strict equal grounds. Moreover, because of integration to M_V made after (129) the results are independent of the creation of particles at any time.

7.6 Anomalous accelerations, MOND

The standard model of cosmology evaluates the parameters necessary for its operation; but here the absence of dark matter particles makes it incompatible with the phenomenology of gravitation. However, in the absence of dark matter particles we can use the mini-model to recover MOND [11], [12].

The radius of the universe 4-sphere being n its circumference is $2\,\pi\,n$; and from (110) an observer will see the expansion accelerating. The instantaneous acceleration A of the expansion will depend on

$$\dot{a}_m = \frac{1}{n} \to A = \frac{1}{2\,\pi\,R_U}\ \mathrm{m}^{-1}, \quad (139)$$

which, as we expect, is the k factor in (137). A remote object recession will be seen accelerating:

$$\frac{d^2 r}{dt^2} = A\,c^2 \to a = \frac{c^2}{2\,\pi\,R_U} = 1.185 \times 10^{-10}\,\mathrm{m\,s^{-2}}, \quad (140)$$

which, according to Milgrom is MOND limit acceleration $1.20\,(\pm 0.2) \times 10^{-10}\,\mathrm{m\,s^{-2}}$ [11] [12]. Another direct way to this result is to understand the effect of the evolution of the electron Compton wavelength on the Bohr radius; it shrinks when the wavelength decreases

$$a_0 = \frac{\lambda_{dB}}{2\,\pi} = \frac{\lambda}{2\,\pi\,\alpha}, \quad (141)$$

where the factor $2\,\pi$ is consistent with (140) and implies that, unlike energy, angular momentum is absolute and conserved; in agreement with QM and with the interpretation of $\Delta E\Delta t$ in (106). Now we can discuss the central mass problem in

which the expansion of the central mass adds a term to the classical potential, making it increase in time. Therefore a simple sum of a and the Newtonian acceleration A_N giving $A_N + a$ is unacceptable, as the so-called anomalous accelerations are free fall in an evolving gravity pit. We therefore return to the weak equivalence principle, according to which an acceleration is indistinguishable from gravity; the opposite case makes it possible to reason by symmetry on the acceleration formula. A force f on an object of mass m in free fall with a Newtonian acceleration A_N giving an effective acceleration A_{eff} is felt as $A_r > 0$:

$$A_N \left(1 + \frac{A_r}{A_N}\right) = A_{eff} \rightarrow A_r = \frac{f}{m}, \qquad (142)$$

here the acceleration felt, $A_r = f/m$, is the effect of inertia and we are looking for the effect of an increase in gravity. So to link the effective acceleration A_{eff} and the two quantities A_N and a in a classical form we need to write the transformation inverse to (142); an inversion of the roles which amounts to calculating A_N. Firstly we rewrite (142):

$$A_N = A_{eff} \left(1 + \frac{A_r}{A_N}\right)^{-1} \rightarrow A_r = \frac{f}{m},$$

Secondly, we use the fact that Newton's acceleration A_N have no physical reality; on the right-hand side we replace it with the real one, and the acceleration felt by the unfelt:

$$A_{eff} \left(1 + \frac{a}{A_{eff}}\right)^{-1} = A_N \rightarrow A_r = 0. \qquad (143)$$

This expression is MOND simple interpolation function, one of three possible [12]. We can also derive the same formula from the harmonic system in a direct and elegant manner that treat space and time on natural non-equal grounds: A_{eff} depends on the gradient of the effective Planck length, which has two components, 1) its instantaneous gradient in space, and 2) its variation in time. The former gives the classical acceleration A_N, which can be approximated by subtracting the effect of the latter from the total. Then by adding the inverses, we subtract from the effective gradient of resonance length (total gradient with A_{eff}) its variation over time in proportion of the gradient (a/A_{eff}) at the considered location to get A_N, i.e.

$$\frac{1}{A_N} = \frac{1}{A_{eff}} \left(1 + \frac{a}{A_{eff}}\right) \rightarrow A_r = 0, \qquad (144)$$

which is identical to (143). We use again the same formula for length addition, now applied to the variations of resolution in space and in time. The evolution of a is immediate as it depends on $1/T$ and decreases with time; this acceleration is therefore a lot stronger in the early universe than at present time, up to $a \rightarrow \infty$ when $T \rightarrow 0$.

7.7 Comments

To begin this section, we applied the length addition formula used for masses to the entire universe, simply our initial hypothesis, to obtain a temporal resonance formula (106) based on a logarithm which complies with the mass formulas. Then, by extending the logic to charges, we found an exponential (107); both are in the calculation of the μ_e mass (21) and in the relation (67) between X_e and X_α, and only there, showing a scaling effect.

On this basis we deduced the Hubble factor correction, the four densities, the cosmological constant, the limit acceleration and interpolation formula of MOND; we obtained eight coherent quantities from the age of the universe alone, which is not possible with the models and theories that use them.

We remark that the expansion of space a_e (109) and energies a_m (110) can be inverted, resulting in a logarithmic expansion of space and a linear expansion of energy (as we did in section 7.5); the resulting model gives the same results provided that the unitary resonances of neutrinos and photons have specific properties. We discussed the simplest scheme where the dimension that we call time expands linearly in 4-space.

8 Questions and extensions

8.1 Dimensions and resonances

The whole sequence h_i seems to include a triple cycle, 4 to 4, 7 to 7, and 8 to 8. The dimensional coefficients from h_8 to h_{11} rise from 4 to 7; the objects present for h_{13} are the 3D and 5D sphere volumes, and for h_{14} two sphere surfaces in 6D and 3D. Then we apparently have a limit with 8D. Since the super-coupling h_{16} can be decomposed into two, we also assume that it is in 4+4=8D. Consequently, D_p and D_e are dimensional couplings and the first sector range from 1 to 7 dimensions. Since particle resonances are radial or rotations, a single 4D space is sufficient for resonances to build a 7 or 8D structure: We assume for the discussion that a 4D space is native and, from the sequences h_i and c_i, that space-time is built by the interplay of resonances. The first sector and the particle resonances K are then explained by Table 7; the particle spectrum is defined by the dimension of each resonance.

- Sign = the resonance has an echo of same dimension.
- Sign + the dimensions add.
- Sign $\neq$ distinct resonances in the two spaces.

We find the following concordances

- The larger the resonance dimension, the larger the mass and the stronger the coupling strongest component.
- Tables 1 and 2 use the same K for the electron and muon, simply the dimension of their resonances.

Table 7: Resonances and dimensions.

-	Particle	Dim	4D	↔	3+1D	Tbl
h_0	M_ω	0/8	0/4	=	0/3+1	(43)
h_1	ν	1	1	=	1	6
h_2	e	2	1	+	1	1, 2
h_2	q (P)	2	1	+	1	3
h_3	μ	3	3	=	3	1, 2
h_4	τ	4	4	≠	3+1	1, 2
h_5	q (N)	5	4	+	1	3
h_6	g	6	3	+	3	-
h_7	W, Z, H, γ	7	3	+	3+1	5

- The tauon is exceptional in that it admits two unequal solutions, two distinct ways of oscillating in 3+1 and 4 dimensions.

- The rotational part N of quarks mix, this is clear for the u and d, and not P the radial part, but $P = 3$ constant pose no problem to mixing.

- We understand that the left-hand side of the relation (14) giving the small k of the boson resonance, which seems a bit strange in 3 dimensions, corresponds to 3+(3+1) dimensions with a resonance of a 6-sphere as seen in 3; by introducing a factor $k\pi$ in the denominator of the mass formula (11) the volume of the 6-sphere becomes

$$\pi^3 r^6 \to \pi^3 (k\,r)^6 \to \pi^2 (k\,r)^6, \qquad (145)$$

then taking the square root to return to 3 dimensions we obtain the term on the left of (14)

$$\pi^2 (k\,r)^6 \to \pi (k\,r)^3, \qquad (146)$$

with $r = 1$ and $\pi \to \pi/144$, since this part is circular. And on the right-hand side, we calculate a radial impact as the compression of a 1 dimension line by stress or forces in 3 dimensions, i.e. with an inverse effect between forces and lengths:

$$\frac{\pi\,r^3}{k} \to \left(\frac{\pi}{k}\right)^{1/3} r, \qquad (147)$$

now with $r = 266\,D_b$. Since r is a wave number or its inverse, we introduce it as the two sides of the resonance and obtain (14).

Resonances organize well by counting only 1, 3 or 4 dimensions, and all bosons use at least 3+3 dimensions. Logically, the photon is in h_7 and neutrinos in h_1; leptonic resonances from h_1 to h_4, and bosonic resonances from h_5 to h_7. Quarks are supposed to mix; they take one component of each side with $P = 3$ in h_2 and one of the rotations of h_5 for N.

The electrons and quarks K are given here by the dimension, provided that time counts for 2D in space-time:

- The electron resonance in h_2 is in 2 dimensions of time.

- The muon h_3, 3 dimensions of space.

- The tau h_4, 4 dimensions in native space and $K = 4$ Table 2, and 3+1 in space-time where time counts double then $K = 3 + 2 = 5$ Table 1.

- Heavy quarks ring in 2 dimensions h_2, and 5 dimensions h_5, but time must be accounted for only once then subtract 5D from 2D to get $K = 2 \times (2 - 5) = -6$.

- Light quarks ring in 2 dimensions h_2, but N uses two rotations and time may be accounted for differently, then possibly:

  - d remove one, 4D and $K = 2 \times (2 + (1 - 5)) = -4$;

  - u multiply by 2 for charge 2/3 versus 1/3 for the d.

8.2 Super-minimal super-strings?

In the universe mini-model the present feeds the past, which means that downtime currents feed the strings, providing the necessary "power" for both downtime and uptime currents. There should be a dissymmetry in strength between up-time and down-time in a ratio 1 to 2. Downtime currents twice as strong as the uptime will give double charges; i.e. 2/3 and 1/3 and impact the resonance by a factor of 2 like in Table 3, the electron charge being the fusion of the two. The explanation for the existence of 3 elementary electric charges is very basic and can correspond to a quantitative law of transformation. In the two series h_i and c_i resonances and couplings appear separately, like in the mass formulas, and the couplings do mirror resonances. Overall, three different manners to observe the same mirror where $1/N\,P > K\,D$ for all resonances where $N\,P > 1$ which can mean a form of super-strings – except for M_ω where the resonance can be seen inverted since $D_p^4 < D_e/266^2$. Then we associate the apparent electric charge of a particle with the direction of a current independently of the resonance. On this basis we need four rules to complete the elementary particles' charges contents which we denote with arrow and sign:

1. The signs correspond by convention to the current, the measurable electric charge reverses for downtime currents (like electricity going backward in time).

2. Two currents of opposite charge can combine to form a single string, or a (sub)string within a string.

3. Two currents of the same charge cannot.

4. Currents can make massive particles, then vertical arrows propagating in time like a massive particle; or mass-less, then propagating on the light cone, oblique arrows (neutrinos and photons).

Table 8 shows all particle types regardless of their resonance. The parentheses represent sub-strings association, and brackets a particle contents.

The mass μ_e is the proper mass of [+ ↑, − ↓], which can fall into the three electron resonances (h_2, h_3, h_4), as can

Table 8: Minimal scheme for currents symmetry.

Charge	Particle	Spin	Currents
0	ν	1/2	$[(- \swarrow + \nearrow)(- \nearrow + \nearrow)]$
+1	μ_e/μ_α	1/2	$[(+ \uparrow - \downarrow)]$
−2/3	u, c, t	1/2	$[(+ \downarrow)]$
+1/3	d, s, b	1/2	$[(+ \uparrow)]$
+1	W^+	1	$[(+ \uparrow)(- \downarrow)]$
0	Z^0	1	$[(- \downarrow + \downarrow)(- \uparrow + \uparrow)]$
0	H^0	0 or 2	$[(- \uparrow)(+ \downarrow)(+ \uparrow)(- \downarrow)]$
0	γ	1	$[(- \nearrow + \swarrow)(- \swarrow + \nearrow)]$

quarks with $[\pm \uparrow]$ and $[\pm \downarrow]$ and h_5, and the four bosons with h_{28}. The distinctions between $W^\pm$, H^0 and Z^0 are consistent with the calculation of their masses and widths. The spins agree with 1/2 for any inner string (the most inner parenthesis for each scheme). In the end, there is only one type of current, oriented only in charge and with respect to time; all assemblies are symmetrical except for quarks, which are confined. We're missing the gluons, which should correspond to eight separate horizontal arrows, with the ubiquitous quality of also manifesting like a monopole. Now let us draw a few examples of transmutations, to begin with $d^+ \rightarrow u^- + W^+$

$$[(\underline{+ \uparrow})] \rightarrow [(+ \downarrow)] + [(- \downarrow)(\underline{+ \uparrow})]. \tag{148}$$

The d^+ current is conserved and passes into the W^+, what remains (i.e. the $(+ \downarrow)$ and $(- \downarrow)$ not underlined) does not exist as a particle; if this is a systematic rule it prohibits FCNC because in the following case the remainder is also a Z^0 which is an existing particle, $s^+ \rightarrow d^+ + Z^0$

$$[(\underline{+ \uparrow})] \rightarrow [(+ \uparrow)] + [(- \downarrow + \downarrow)(- \uparrow \, \underline{+ \uparrow})]. \tag{149}$$

The muon case, $\mu^- \rightarrow W^- + \nu_\mu$:

$$[(- \uparrow + \downarrow)] \rightarrow [(- \uparrow)(+ \downarrow)] + [(- \swarrow + \nearrow)(- \nearrow + \nearrow)], \tag{150}$$

next is its symmetric, $W^- + \overline{\nu_e} \rightarrow e^-$:

$$[(- \uparrow)(+ \downarrow)] + [(- \swarrow + \nearrow)(- \nearrow + \nearrow)] \rightarrow [- \uparrow + \downarrow]. \tag{151}$$

This is because neutrino and anti-neutrino are identical. Two up-time or down-time arrows for neutrinos and Z^0 can also be removed for the same results; the choice made here is that every up-time current is associated with a downtime current, and conversely – except for quarks, where currents have the same sign and the association of particles/strings is made by confinement.

The γ and Z^0 cases are the simplest, as we obtain (for example) the following two reversible cases. For $e^+ + e^- \rightarrow Z^0$:

$$[(+ \uparrow - \downarrow)] + [(- \uparrow + \downarrow)] \rightarrow [(- \downarrow + \downarrow)(- \uparrow + \uparrow)] \tag{152}$$

and for a photon, $e^+ + e^- \rightarrow \gamma$:

$$[(+ \uparrow - \downarrow)] + [(- \uparrow + \downarrow)] \rightarrow [(- \nearrow + \swarrow)(- \swarrow + \nearrow)]. \tag{153}$$

A minimal form of (super) symmetry is evident, where each lepton charge (μ_e mass or neutrino) is associated with a boson of same charge. Since we find 8 resonances for quarks in h_5 (49) and c_3 (92), including twice two indistinguishable masses for u and d, we're all set with 8 gluons in h_6. It is the μ_e mass and h_6, together with the separation of resonances and couplings in the sequences h_i and c_i that makes this minimal scheme possible as the resonances (N, P) do not define charges and spin, the couplings and inner currents do.

8.3 Transmutation and resonance

At the general level, the $N = P = 19 - 7$ of bosons includes all circular resonances (7 and 19), enabling transmutations of N or P of electrons and quarks; the product of their $K = 266$ includes all primary field resonances. In transmutations, this allows exchanges of resonances by sums and products:

- by product, with the $K = -2$ of the $W^\pm$ for the N of quarks within the second or third generation.

- for u and d quarks, by product with the $K = -2$ of the $W^\pm$ for the K, and cross exchanges of 14 and 19 for N.

- by sum $\pm 12 = 19 - 7$ associated with a product exchange by the $K = -2$ of the $W^\pm$ between the second and third generation of quarks.

- by mixed exchanges of the previous ones when the first and another generation is involved.

- FCNC would imply a product exchange in N which is not the K of a neutral boson.

- by sum or subtraction of the $K = -7$ of the Z^0 for the N and P of the electrons.

- The resonances of neutrinos (K) are an inverted echo of the resonances N, P of the corresponding electron, there is a form of conservation in these transmutations to which the Z^0 and the $W^\pm$ are neutral.

- All particles couple in N, P, sometimes separated, with D_p^i through its 137 and $-19\pi^2$, which is the $K = -19$ of the H^0, coupling in mass in the Standard Model.

Recall also that the total resonance widths of the three bosons were calculated in section 2.4. Hence the resonances speak directly of transmutations; the form of which obeys, and then implements, some conservation of the resonances geometry.

8.4 And the strong force coupling?

According to Table 8, quarks should be the expression of the most fundamental components of massive particles, and then also the quark mass coupling D_q, which we compare to that of electrons to get a ratio of lengths:

$$\frac{D_q}{D_e} = 1 + \alpha, \tag{154}$$

and specifically for the full coupling $K D$ of the electron itself compared to that of a heavy quark

$$\frac{-6 D_q}{2 D_e} = -3 - 3\alpha. \tag{155}$$

Now recall that in Table 3 the charge ratio of 1/3 to 2/3 corresponds to a resonance ratio ($N \rightarrow 2N$ for the second and third generation, and $K \rightarrow 2K$ for the d and u), hence we find again the signature of a monopole with α, including the ratio of charge 1 to 1/3. But according to h_6 (50) and h_{16} (60), it is the gluon that rings in 69.5 and it does "make" the coupling α for the mass μ_e, and the ratio μ_α/μ_e. So, consider D_e the most fundamental mass coupling and compare

$$\frac{D_e}{\alpha} = 0.1169 \tag{156}$$

and, since $139 = \Sigma_{N,P} + 2$ includes the photon and neutrino unitary resonances corresponds to the entire particles field:

$$139\, D_e = 0.1186, \tag{157}$$

to the range of values of $\alpha_S(M_Z^2)$ reported in the literature

$$0.117 \le \alpha_S(M_Z^2) \le 0.119. \tag{158}$$

8.5 Do photons have mass?

The current limit of the photon mass is $m_\gamma < 10^{-18}$ eV (PDG 2023). Now, from the calculation of neutrinos masses and the identification of the photon resonance in h_7, we can ask whether the photon has mass. If so, we should be able to estimate its resonance; for this we apply an inversion similar to neutrinos, which was $D_e \rightarrow 1/\alpha$, this time from the components of D_{WZ} and D_H the coupling should be as a minimum

$$D_\gamma = \frac{-1}{D_e^2}. \tag{159}$$

The choice of K is not immediate; since $N P = 1$ for this resonance and not 144 we cannot make use of any phase coherence constraint. The best we can provide is a possible lower limit with $K = \pm 266$, since 266 is part of Σ_K and not used in any other particle resonance. We obtain

$$m_\gamma \gtrsim \frac{m_e}{m_e - \mu_e} \times \frac{X_e}{\pi(1 \pm 266\, D_\gamma)^3} \approx 5.3 \times 10^{-23}\ \text{eV/c}^2. \tag{160}$$

Using $K = -19$ gives $\approx 1.5 \times 10^{-19}$ eV/c^2 a likely maximum since using $K = -7$ the calculated mass exceeds the limit by a factor of 3. In this logic the last candidate would be $K = -133$ giving $\approx 4.3 \times 10^{-22}$ eV/c^2.

8.6 SM symmetries and resonances?

The standard model of particle physics is based on $U(1) \times SU(2) \times SU(3)$ with $U(1)_Y \times SU(2)_L \rightarrow U(1)_{EM}$. With respect to the three rotations in the primary field couplings formulas of α, D_e and D_p which are respectively $+1\,\pi^2$, $+7\,\pi^2$, $-19\,\pi^2$, we naively notice:

$$7 = 2^3 - 1^3, \tag{161}$$

and

$$19 = 3^3 - 2^3. \tag{162}$$

Simultaneously, except for the mass μ_e all resonances N, P of the primary field use 1, 2, 3, 7, 19, and 12 = 19-7; and the mass μ_e includes 2/7. Here we find a bijective correspondence between the symmetries of the SM and the resonances which states that 1 is an instance of $U(1)$, 2 of $SU(2)$ and 3 of $SU(3)$. This is straightforward and needs no comment; but what could it mean?

The mass formulas are based on a cube and represents stress in the form $PV = K_B T$ where only P and T can vary (except maybe for gravitation, which is of no importance here as we only discuss particles). So, except for the electron the resonance N, P systematically include a cube difference in a cube! For the three bosons we get $m \sim 144^3 = ((19 - 7)^2)^3$ which is a power six of the difference of two cube differences. It means a general mechanism by which symmetries resonate individually and with each other. For electrons and quarks:

- A symmetry of order N will give N^3 as say a number of "resonance points" per unit volume.
- The symmetries of order $N - 1$ will remove $(N - 1)^3$ from the order N resonance.
- And $SU(3)$ includes instances of $SU(2)$ which includes instances of $U(1)$.

It means that each and every "resonance point" is a unitary resonance with unitary impact on the mass calculation.

- For the three electrons we only have 2 and 7 in the resonances meaning that $SU(3)$ is absent at this level, and may intervene only through the coupling of the mass μ_e.
- for quarks, $SU(3)$ is present giving 19 and 38; $SU(3)$ includes instances of $SU(2)$, then 7 and 14, the u and d include the four possible fractions using these numbers where from Table 3 $N = a/b > 1$.
- For the three (massive) bosons we find the same structure, this time not with respect to the symmetries but to the fermion field elementary resonances 2, 7, and 19, giving $12 = 19 - 7$ and $266 = 2 \times 7 \times 19$.

Now for U(1) we should have 1 instead of 2; but with the three electrons we have two symmetries in resonance with each other. And we get the product $N P = 1$ for the photon and the neutrinos; hence, all along, it looks like we only counted all combinations of possible unitary resonances given by the SM symmetries; a logic that extends to transmutations.

9 Conclusion

Based on a single hypothesis used to study the parameters of the standard models of particle physics and cosmology, we found a suite of formulas, coherent with each other, showing how it holds from the mass of neutrinos to the energy parameters of cosmology – down to the last known decimal places; and some ideas, new or otherwise, about the internal structure of the system under study: *A unique resonance where each and every quantity we addressed is a dynamical substructure.*

Each one of those appear to be part of a single physical object, which expression is found in the Planck mass oscillator, and where each formula speaks directly of the others in various manners. Therefore, we have most probably discussed the shapes of an unknown or poorly understood level of physical reality – some information hidden in the structures of space-time and fundamental particles.

Hence, in conclusion, highlight that the expressions (106) and (108), together with the suite h_i and c_i, seem to reveal the nature of quantum mechanics as they fit the de Broglie-Bohm [3] [2] and Cramer [9] interpretations – where 4-space, space-time, and strings, are ringing as a whole, permanently communicating between any two epochs down to the origin in one Planck time. Of course energy cannot be transferred instantly between any two points in space and time – of course; but now energy, what is it made of?

Received on September 23, 2023

References

1. Akers D. Further evidence for magnetic charge from meson spectroscopy. *Int J Theor Phys*, 1987, v. 26, 1169–1173.

2. Bohm D. A Suggested Interpretation of the Quantum Theory in Terms of "Hidden Variables". *Physical Review*, 1952, v. 85, 166–179.

3. De Broglie L. Recherches sur la théorie des quanta. *Annales de Physique*, Janvier-Février 1925, 10e série, Tome III.

4. De Broglie L. Théorie de la double solution. *Journal de Physique*, Mai 1927.

5. Consiglio J. L'Onde et la Constante de Sommerfeld. *Annales de la Fondation Louis de Broglie*, 2022, v. 47 (2), 267–272.

6. Consiglio J. Toward the Fields Origin. *Progress in Physics*, 2019, v. 15 (1), 9–16.

7. Consiglio J. Are Energy and Space-time Expanding Together? *Progress in Physics*, 2017, v. 13 (3), 156–160.

8. Consiglio J. On Quantization and the Resonance Paths. *Progress in Physics*, 2016, v, 12 (3), 259–275.

9. Cramer J. The transactional interpretation of quantum mechanics. *Rev. Mod. Phys.*, 1986, v. 58 (3).

10. Dirac P. A. M. Quantized singularities in the Electromagnetic Field. *Proc. Roy. Soc. A*, 1931, v. 133, 60.

11. Milgrom M. A modification of the Newtonian dynamics as a possible alternative to the hidden mass hypothesis. *Astrophysical Journal*, 1983, v. 270, 365–370.

12. Milgrom M. MOND theory. arXiv: astro-ph/1404.7661v2.

13. The Planck Collaboration. Planck 2018 results. VI. //www.cosmos.esa.int/web/planck/publications#Planck2018.

14. //fr.wikipedia.org/wiki/Constante_de_Hubble, Dec. 2022.

15. //keisan.casio.com/has10/Free.cgi (site closed since 09/20/2023)

16. //www.mathsisfun.com/calculator-precision.html

Gamow Theory for Diproton Decays of Proton-Rich Heavy Nuclei ^{45}Fe and ^{67}Kr

Tianxi Zhang and Cornelius Salonis

Department of Physics, Chemistry, and Mathematics, Alabama A&M University, Normal, Alabama 35762, USA.
E-mail: tianxi.zhang@aamu.edu

A diproton is an unusual particle, made of only two protons, which are believed to be unbound. In the core of a main sequence star such as the Sun, protons first combine to form diprotons in order for the proton-proton chain nuclear fusion reactions to occur. Exploring properties and activities of diprotons plays an important role in understanding the physics of stellar energy generation by nuclear fusion. In laboratories, it has been shown experimentally that some proton-rich radioactive heavy nuclei such as ^{45}Fe and ^{67}Kr can decay with emissions of diprotons and longer lifetimes in comparison with lighter nuclei. In this study, we investigate diproton decays of proton-rich or neutron-rare radioactive heavy nuclei. We first quantum-mechanically analyze to formulate the expressions for the transmission probability and lifetime of the diproton decays. Then, we numerically calculate the transmission probabilities and lifetimes of the diproton decays. The numerical results obtained for the diproton decays of the two typical proton-rich radioactive heavy nuclei ^{45}Fe and ^{67}Kr are plotted as functions of the energy of the emitted diproton and further compared with the measurements. It is shown that the transmission probabilities rapidly increase with the energy of the emitted diprotons, while the lifetimes for the diproton decays decrease with the energy of the emitted diproton and can be consistent with the laboratory measurements.

1 Introduction

A diproton is the nucleus of a rare isotope of helium, ^{2}He, and consists of only two protons. It is extremely unstable and believed to be in an unbound state with a negative binding energy due to the spins of the two protons to be anti-aligned according to the Pauli exclusive principle [1, 2]. A diproton does not stably exist in nature but can be formed temporarily in two ways (see Fig. 1): (1) combination of two separate protons and (2) decay of proton-rich radioactive heavy nuclei. Two separate protons, when they collide with enough energy to tunnel through the Coulomb barrier between them, form a diproton, ^{1}H + ^{1}H + Energy $\longrightarrow$ ^{2}He. This frequently occurs in the core of the Sun or any star in the main sequence. Approximately, there are about 10^{63} diprotons formed every second in the core of the Sun. Most of them quickly separate back to protons, ^{2}He $\longrightarrow$ ^{1}H + ^{1}H, and only a very small part rarely get fused into deuterons via positron decays with emissions of neutrinos, ^{2}He $\longrightarrow$ ^{2}H + e^{+} + ν_{e}. The fusion rate of the Sun should be about 10^{39} protons per second according to its luminosity, which is about 10^{24} times lower than the rate of diproton formation. In addition to the rareness of positron decays and difficultness of Coulomb barrier penetrations or quantum tunneling, plasma waves or oscillations may also play a significant role in the reduction of the rate of fusion in the core of the Sun [3, 4].

In laboratories, on the other hand, scientists have experimentally discovered that some proton-rich (or neutron-rare) heavy nuclei can emit diprotons [5, 6]. For instance, the proton-rich radioactive nuclei ^{15}Ne, ^{45}Fe and ^{67}Kr can decay into
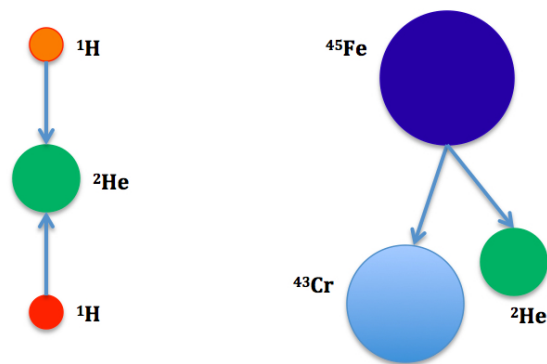
Fig. 1: Two ways of diproton formation: either formed from combination of two separate protons or emitted from decay of proton-rich radioactive heavy nuclei such as ^{15}Ne, ^{45}Fe, ^{67}Kr, and so on. The right panel shows a schematic diagram for a ^{45}Fe nucleus to decay into ^{43}Cr after it emits a diproton ^{2}He.

^{13}O, ^{43}Cr, and ^{65}Se, respectively, after emitting a diproton [7–9]. The emission of a diproton from a proton-rich heavy nucleus is usually called diproton decay. The diproton decay is a rare decay mode found in a few nuclei beyond the proton drip line [10]. It is found, on the basis of the shell-model mass extrapolation, that ^{45}Fe nuclei are unbound and emit diprotons in the decay. The half-life of ^{45}Fe calculated using an R-matrix formula for the contribution due to the diproton decay agrees with the experimental values [8]. The diproton tunneling half-life decreases with the decay energy. First

observations of diproton decays from ^{45}Fe showed the half-life to be about 3.8 ms and the energy about 1.15 MeV [5, 6]. Fig. 2 shows the observations of diproton decay of ^{45}Fe and its half-life [6, 11]. Observations also show that the unbound proton-rich nucleus ^{15}Ne directly decays to ^{13}O with a simultaneous diproton emission [7]. The diproton decay of ^{67}Kr is measured to be unexpectedly fast [9].

Recently, the first author of this paper has theoretically modeled and numerically studied the transmission and proton decay of unbound diprotons, transmission and positron decay of protons, and transmission and diproton decay of unbound proton-rich heavy nucleus ^{15}Ne in accordance with the Gamow theory for the quantum tunneling and radioactive decays [14]. It was shown that an unbound diproton is extremely unstable and quickly decays through two types of decay modes with lifetime to be extremely short down to about 10^{-21} seconds. A diproton mostly undergoes a proton decay to be two separate protons with a transmission probability higher that 99.99%, and rarely undergoes a β^+ decay to form a deuteron with a transmission probability lower than 0.01%. The transmission probability for the diproton decay of ^{15}Ne increases with the energy.

In this paper, we quantum-mechanically study the transmission probability and lifetime for the diproton decays of proton-rich radioactive nuclei according to the Gamow theory that describes and models the quantum tunneling of the Coulomb barrier between the emitted diproton and the leftover nucleus. We obtain that the transmission probability and lifetime of unbound proton-rich heavy nuclei depend on the energy of the emitted or decayed diprotons. In general, the probability increases with the energy, while the lifetime decreases with the energy. With a certain probability, the heavier the nucleus is, the greater the energy of the emitted diproton is. For ^{45}Fe nuclei, the lifetime of the diproton decay with energy about 1.1-1.2 MeV, obtained from this study, is about some milliseconds, which is consistent with the measurements [8].

2　Quantum theory for diproton decay of heavy nuclei

In 1928, on the basis of quantum mechanics, George Gamow proposed a theory for the α-decay of radioactive heavy nuclei [15]. In this study, we apply the Gamow theory to describe and explain the diproton decay of proton-rich radioactive heavy nuclei. An α particle is a helium nucleus, ^{4}He, while a diproton is an isotope of helium, ^{2}He. Both are electrically charged by $2e$, where e is the electric charge of proton. The Gamow theory that was developed for the α-decay of radioactive nuclei should be applicable to the diproton decay of radioactive nuclei. During the diproton decay of a proton-rich radioactive heavy nucleus, a diproton is electrically repelled by and further escapes from the leftover nucleus. In the Gamow theory, the potential energy function is approximately modeled by a finite potential square well to represent
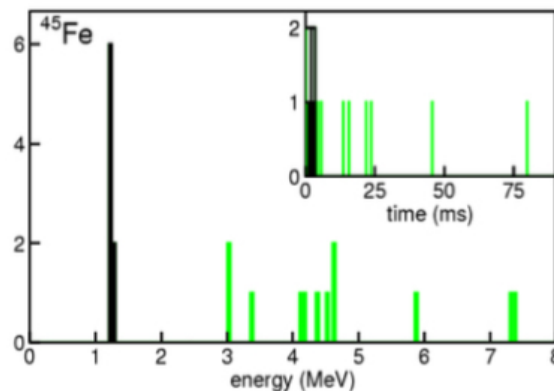
Fig. 2: The energy and time distribution of decay events from ^{45}Fe, measured in experiments by GANIL [12] and GSI [13]. The events represented by black lines corresponding to the diproton decays, while other high frequency events represented by green lines represented the β-decays.

the attractive nuclear force and joined with a Coulomb repulsive potential tail [14, 16],

$$V(r) = \begin{cases} -V_0, & \text{if } 0 < r < r_1 \\ \dfrac{1}{4\pi\epsilon_0} \dfrac{Z_1 Z_2 e^2}{r}, & \text{if } r_1 \leq r < \infty \end{cases} . \quad (1)$$

Here Z_1 and Z_2 are atomic numbers or charge states of the emitted particle and leftover nucleus; ϵ_0 is the electric permittivity constant in free space; and V_0 is the depth of the potential square well. Fig. 3 is a schematic diagram for the potential energy $V(r)$ given by (1) as a function of the radial distance r in all the classical and quantum regions. The width of the potential square well, denoted by r_1, can be determined as the radius of the nucleus, given by a constant times the cubic root of the mass number of the nucleus as

$$r_1 = r_0 A^{1/3} \quad (2)$$

where A is the mass number of the nucleus and the constant is $r_0 = 1.2 \times 10^{-15}$ m. The depth of the potential square well, V_0, is much greater than the maximum height of the Coulomb barrier, U_c, given by

$$U_c = \frac{Z_1 Z_2 e^2}{4\pi\epsilon_0 r_1} \ll V_0 . \quad (3)$$

The outer turning point (i.e. at $r = r_2$) can be determined, in terms of the energy E of the emitted α particle to be equal to the potential energy at r_2, by

$$r_2 = \frac{Z_1 Z_2 e^2}{4\pi\epsilon_0 E} . \quad (4)$$

In this central force problem with potential $V(r)$ given by (1) or shown in Fig. 3, the radial Schrödinger equation of the
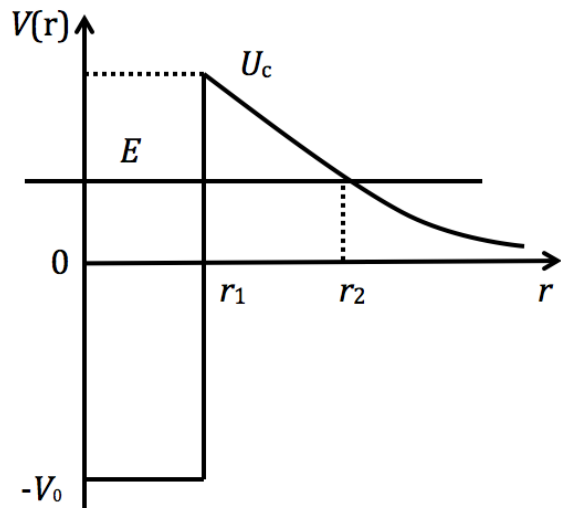
Fig. 3: The Gamow model for the potential energy of an electrically charged particle to be emitted from a radioactive nucleus. It consists of the potential energy square well for the attractive nuclear force and the Coulomb potential energy tail for the repulsive electric force between the emitted particle and the leftover nucleus of the decay.

particle wave is [14, 16],

$$\frac{d^2 u(r)}{dr^2} = \frac{2\mu}{\hbar^2}[V(r) - E]u(r) + \frac{l(l+1)}{r^2}u(r), \qquad (5)$$

where $u(r)$ is the radial wave function, $\mu = m_1 m_2/(m_1 + m_2)$ is the reduced mass with m_1 the mass of the emitted particle and m_2 the mass of the leftover nucleus. The integer l is the quantum number for the magnitude of angular momentum and $h = 2\pi\hbar$ is the Planck constant. A two-body system with a central force or potential can be generally described as a system of one body with the reduced mass.

According to the WKB approximation of quantum mechanics, we can approximately solve the radial Schrödinger equation and find the radial wave functions to be

$$u(r) = \frac{C}{\sqrt{|p(r)|}} \exp\left[\pm\frac{1}{\hbar}\int |p(r')|dr'\right], \qquad (6)$$

where the parameter $p(r)$ is defined by

$$p(r) = \sqrt{2\mu[V(r) - E]}. \qquad (7)$$

Here, it should be pointed out that the general solution of the radial Schrödinger equation should be the combination of these two corresponding to the plus sign and minus sign. We have also neglected the effect of angular motion and considered the case of $l = 0$.

Then, from the solved wave function, the transmission (or tunneling) probability for the electrically charged particle to tunnel through the Coulomb barrier is obtained as [14, 16]

$$T = e^{-2\gamma}, \qquad (8)$$

where the parameter γ is determined by

$$\gamma = \frac{1}{\hbar}\int_{r_1}^{r_2} dr \sqrt{2\mu[V(r) - E]}$$

$$= \frac{\sqrt{2\mu E}}{\hbar}\left[r_2\left(\frac{\pi}{2} - \arcsin\sqrt{\frac{r_1}{r_2}}\right) - \sqrt{r_1(r_2 - r_1)}\right]. \qquad (9)$$

And the lifetime of the parent nucleus or decay is given by

$$\tau = \frac{2r_1}{v} e^{2\gamma}, \qquad (10)$$

where $v = \sqrt{2E/m_1}$ is simply chosen to be the speed of the emitted (or α) particle. It should be noted that, although being proposed for explaining the α-decay of radioactive nuclei, the Gamow model is applicable in general for the decay or emission of any type of charged particles from a radioactive nucleus such as the β^+ decay from a proton, and emission of a proton or a diproton from a proton-rich radioactive heavy nucleus (e.g. diproton decays of ^{15}Ne, ^{45}Fe, ^{67}Kr, and so on).

3 Probability and lifetime of diproton decay

A heavy nucleus with the elemental formula ^A_ZX, if it is proton-rich (or $A < 2Z$), may be radioactive and decay. If the emitted particle of the decay is a diproton, we call the diproton decay. Here X is the elemental symbol of the nucleus, usually called the parent nucleus, Z is the atomic number of the parent nucleus, and A is the mass number of the parent nucleus. In this diproton decay, we have $Z_1 = 2$, $Z_2 = Z - 2$, $m_1 = 2m_p$, $m_2 = (A - 2)m_p$, and $\mu = (m_1 \times m_2)/(m_1 + m_2)$, where $m_p = 1.67 \times 10^{-27}$ kg is the proton mass. We have approximately considered both proton and neutron having about the same mass. The width of the potential square well or the radius of the parent nucleus, r_1, can be estimated from (2) and the outer turning point, r_2, can be calculated from (4). With the values of these parameters and given a nucleus' Z and A, we can calculate, from (8) to (10), the transmission probability and lifetime of the diproton decay. For the typical proton-rich radioactive heavy nuclei ^{45}Fe and ^{67}Kr, we have plotted the results obtained from calculations of the transmission probability and lifetimes of the diproton decay.

For the diproton decay of ^{45}Fe, the leftover nucleus is ^{43}Cr. In this case, we have $Z = 26$, $A = 45$, $Z_1 = 2$, $Z_2 = 24$, $m_1 = 2m_p$, $m_2 = 43m_p$, $\mu = 1.91m_p$, The width of the potential square well or the radius of ^{45}Fe nucleus can be obtained from (2) as $r_1 \simeq 4.27 \times 10^{-15}$ m. With the values of these parameters and (8) to (10), we can plot, in Fig. 4, the transmission probability for the diproton decay from a radioactive nucleus ^{45}Fe (red line) and the lifetime of the nucleus ^{45}Fe via this diproton decay mode (blue line) as a function of the energy of the diproton. It is seen that the transmission probability increases with the energy. In the energy range from 1 MeV to 5 MeV, the transmission probability of the diproton

Fig. 4: Diproton decay transmission probability and lifetime of ^{45}Fe nucleus. The red line plots the transmission probability of emitting a diproton from the radioactive nucleus ^{45}Fe in the potential energy well to tunnel through the Coulomb barrier as a function of the energy of the diproton. The blue line plots the lifetime of the diproton decay.

Fig. 5: Diproton decay transmission probability and lifetime of ^{67}Kr nucleus. The red line plots the transmission probability of emitting a diproton from the radioactive nucleus ^{67}Kr in the potential energy well to tunnel through the Coulomb barrier as a function of the energy of the diproton. The blue line plots the lifetime of diproton decay.

decay increases from 10^{-20} to 10^{-4}, while the lifetime decreases from 10^{-3} s to 10^{-17} s. It is consistent with the measurement at energy 1.15 MeV with the lifetime of diproton decay from ^{45}Fe to be of order 10^{-3} s [8].

For the diproton decay of ^{67}Kr, the leftover nucleus is ^{65}Se. In this case, we have $Z = 36$, $A = 67$, $Z_1 = 2$, $Z_2 = 34$, $m_1 = 2m_p$, $m_2 = 65m_p$, $\mu = 1.94m_p$. The width of the potential square well or the radius of ^{67}Kr nucleus can be obtained from (2) as $r_1 \simeq 4.87 \times 10^{-15}$ m. With the values of these

parameters and (8) to (10), we can plot, in Fig. 5, the transmission probability for the diproton decay from a radioactive nucleus ^{67}Kr (red line) and the lifetime of the nucleus ^{67}Kr via this diproton decay mode (blue line) as a function of the energy of the diproton. It is seen that the transmission probability increases with the energy. In the energy range from 2 M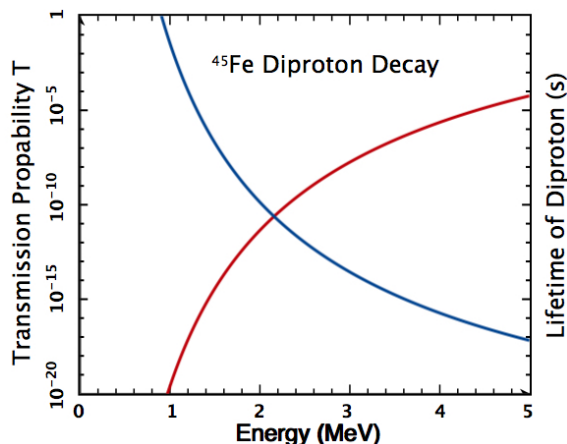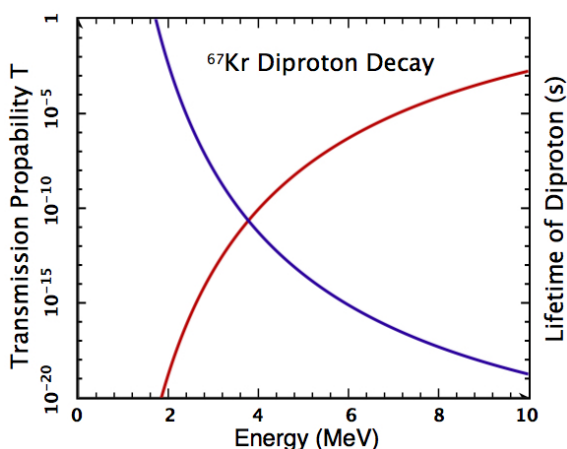eV to 10 MeV, the transmission probability of the diproton decay increases from 10^{-20} to 10^{-3}, while the lifetime decreases from 10^{-4} s to 10^{-19} s.

4 Discussions and conclusions

The fact or observations that diprotons are emitted from the decays of proton-rich radioactive nuclei implies that diprotons might have bound states with a positive binding energy. Even if a diproton is only weakly bound with an extremely small but positive biding energy, e.g. 0.384 MeV [17], a star such as the Sun would fuse its protons to deuterons at a rate many orders faster (i.e. $\gg 10^{39}$ protons/s) so that the star becomes much brighter in luminosity (i.e. $\gg 10^{26}$ W). This will result in a universe to fail the life support [18,19]. This diproton disaster can be overcome by plasma oscillations or waves, which have been shown recently by the first author of this paper to be extremely efficient in inhibiting the nuclear reaction [3,4], to have the observed luminosity without need to adjust the stars' central temperature, density, and initial number of deuterons. We will study in more details the transmission probability of bound diprotons for the fusion reaction in future.

As a consequence of this study, we have investigated diproton decays of two typical proton-rich (or neutron-rare) radioactive heavy nuclei ^{45}Fe and ^{67}Kr. First, we have applied the Gamow theory for the α-decay of radioactive heavy nuclei to quantum-mechanically model the diproton decay of proton-rich radioactive heavy nuclei. We have derived expressions for the transmission probability and lifetime of diproton decay. Then, for the two typical proton-rich radioactive nuclei, we have numerically calculated the transmission probabilities and lifetimes of the diproton decays. We have found that the transmission probabilities rapidly increase with the energy of the emitted diprotons, and the lifetimes for the diproton decay decrease with the energy of the emitted particle. And finally, we have compared our obtained results with laboratory measurements. At the energy of 1.15 MeV, the lifetime for the diproton decay of ^{45}Fe is observed to be about the order of milliseconds, which is consistent with the results of Gamow modeling obtained from this study.

References

1. Pauli W. Exclusion Principle and Quantum Mechanics. *Writings on Physics and Philosophy*, 1946, 165–198.

2. Bertulani C. A. Nuclear Physics in a Nutshell. Princeton University Press, 2007, ISBN 978-0-691-12505-3.

3. Zhang T. X. The Role of Plasma Oscillation Played in Solar Nuclear Fusion. *Bulletin of American Astronomical Society*, 2020, v. 52, 106.05.

4. Zhang T. X. The Role of Plasma Oscillation in Solar Nuclear Fusion. *Progress in Physics*, 2021, v. 17, 67–71.

5. Blank B. *et al*. First Observation of Two-Proton Decay from Radioactivity Nucleus. *Comptes Rendus Physique*, 2003, v. 4, 521–527.

6. Blank B., Ploszajczak M. Tow-Proton Radioactivity. *Reports on Progress in Physics*, 2008, v. 71, 046301.

7. Wamers F. *et al*. First Observation of the Unbound Nucleus ^{15}Ne. *Physical Review letters*, 2014, v. 112, 132502.

8. Brown B. A. and Barker F. C. Diproton Decay of ^{45}Fe. *Phys. Rev. C*, 2003, v. 67, 041304.

9. Wang S. M. Puzzling Two Proton Decay of ^{67}Kr. *Phys. Rev. Lett.*, 2008, v. 120, 212502.

10. Brown B. A. Diproton Decay of Nuclei on the Drip Line. *Phys. Rev. C*, 1991, v. 43, R1513.

11. Giovinazzo J. *et al*. Two-proton radioactivity: 10 years of experimental progresses. *Journal of Physics: Conference Series*, 2013, v. 436, 012057.

12. Giovinazzo J. *et al*. Two-proton radioactivity of ^{45}Fe. *Phys. Rev. Lett.*, 2002, v. 89, 102501.

13. Pfützner M. *et al*. First Evidence for the two-proton decay of ^{45}Fe. *The European Physical Journal A*, 2002, v. 14, 279–285.

14. Zhang T. X. Gamow Theory for Transmission Probability and Decay of Unbound Diprotons. *Progress in Physics*, 2021, v. 17, 185–188.

15. Gamow G. Zur Quantentheorie des Atomkernes. *Z. Physik*, 1928, v. 51, 204–212.

16. Griffiths D. J. Introduction to Quantum Mechanics, 2nd Edition. Person Prentice Hall, 2005.

17. Kadenko I. M. *et al*. Bound Diproton: An "Illusive" Particle or Exotic Nucleus? *Acta Physica Polonica A*, 2022, v. 142, 337–341.

18. Bradford R. A. W. The Effect of Hypothetical Diproton Stability on the Universe. *J. of Astrophys. Astron.*, 2009, v. 30, 119–131.

19. Barnes L. A. Binding the Diproton in Stars: Anthropic Limits on the Strength of Gravity. *JCAP*, 2015, No. 12, 050.

———————————————

Surprising Results from Experiments of a Longitudinally Separated Slit

Xianming Meng

Research School of Physics, Australian National University, Canberra, ACT 2601. E-mail: xianming.meng@anu.edu.au

For the first time, the paper reports the experimental results of a longitudinal separated single slit. The asymmetric diffraction pattern in the experiments cannot be explained by either the wave theory of light or quantum electrodynamics, and thus calls for a theoretical breakthrough. The paper also upgrades the slit diffraction formula to include the longitudinal separation distance and the formula fits the experimental data well. However, the absolute value of the fitted parameter differs for the left and right fringe patterns and for different experimental setting, suggesting potential role of factors other than slit width, light frequency, and longitudinal separation.

1 Introduction

The studies on light diffraction and interference have a long history and have dramatic impact on our understanding of the nature of light. The effect of light diffraction were carefully observed by Francesco Grimaldi before 1660 [1]. Christiaan Huygens studied diffraction phenomenon in great details and established his wave theory of light [2] which, however, was suppressed by Newton's corpuscles theory of light [3]. The famous double-slit experiment of Thomas Young [4] reinvigorated Huygens' theory and Fresnel [5, 6] did further experimental studies and landed support for the wave theory of light. Later, the wave theory was again challenged by Einstein [7], who showed the particle nature of light. Eventually, Bohr [8] and de Broglie [9] suggested the wave-particle duality for light and for mass particles. With the ascendance of quantum mechanics, Feynman [10] invented the path integral method which was applied to study the quantum nature of light diffraction and interference. Now the quantum theory is used to explain not only the diffraction and interference of light but also of massive particles such as electrons, photoelectrons, neutrons, atoms and molecules [11–22].

It seems that the experiments of light diffraction from slits have examined all possible factors such as slit widths, light frequencies, slit shapes, and the number of slits, but all experiments so far have adhered strictly to the traditional definition of a slit: the closely placed barriers to restrict the passage of light or particles. This paper reports on an innovative single slit experiment that breaks the definition of slit. In the experiment, the barriers of a traditional slit are broken into two to form two half slits which can be placed at different positions along the light propagation direction.

2 Predictions from existing theories

Before we proceed to the experiments, we briefly discuss the expected experimental results based on the currently main theories related to light diffraction: the wave theory of light and the quantum electrodynamics. The diffraction patterns predicted by the wave theory of light is illustrated in Fig. 1.

When a laser beam hits the half-slit A, the wave theory
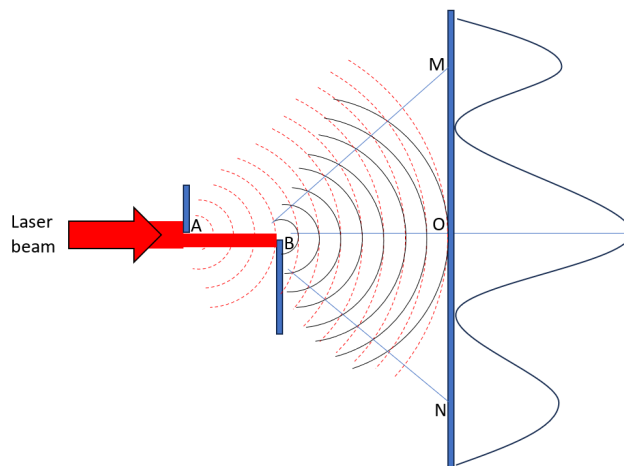
Fig. 1: Wave explanation of light diffraction from a longitudinally separated slit.

suggests that the diffraction occurs because the light at A acts as a point source of light waves illustrated by the spherical red dashed curves (the diffraction angle is exaggerated for clearer illustration). Similarly, the light at half slit B acts as a point source of light waves shown as the solid black curves. Since the light waves from both A and B interfere with each other, the interference pattern will form at the observer plane MN. Due to the nature of spherical wave propagation, the interference pattern on the observing plane should be symmetric, i.e. OM=ON, a result similar to the normal single slit interference pattern.

In the above discussion considering only two wave sources at point A and B, it may be argued that this is an oversimplification because Huygens' principle indicates that light at any point between A and B can act as a source of light waves. With the aid of Fig. 2, we can show that using n wave sources give the same result.

In a traditional way we use the n coherent oscillators to indicate n wave sources. In a traditional slit A_0B, n oscillators are evenly positioned on the dashed line between A_0 and B.
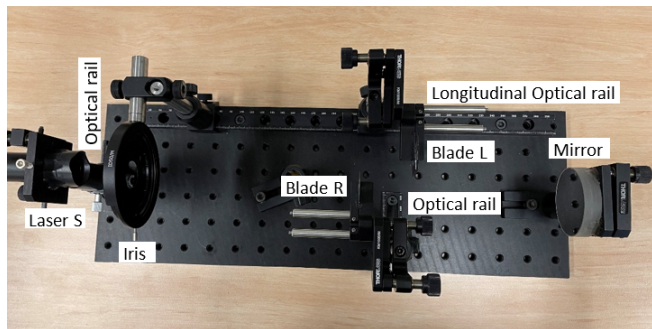
Fig. 2: Wavelets explanation of light diffraction from a longitudinally separated slit.

A textbook derivation (e.g. [23]) gives the following intensity of the diffraction pattern at the observer plane:

$$I = I_0 \frac{\sin^2(N\delta/2)}{\sin^2(\delta/2)} \qquad (1)$$

where I and I_0 are light intensity at the observer plane and at the source respectively; $\delta = kd \sin\theta$ is the phase difference of neighbouring coherent oscillators, k the wave vector, and θ the diffraction angle; $d \sin\theta$ is the length difference of neighbouring propagation paths, as shown as BC in Fig. 2. The principal maxima of the fringes occur at $\delta = kd \sin\theta = 2m\pi$, where $m = 0, \pm1, \pm2, \dots$. This gives the diffraction formula:

$$d \sin\theta = m\lambda . \qquad (2)$$

In the case of longitudinally separated slit AB, the n wave sources should be equally positioned between A and B. As shown in Fig. 2, the phase difference of neighbouring coherent oscillators δ should be calculated as $\delta' = kd' \sin\theta'$, with $d' = \sqrt{x^2 + d^2}$. We can also add a fixed initial phase difference ϕ between neighbouring oscillators and upgrade δ' to $\delta' = kd' \sin\theta' + \phi$. One may worry about applying to the current case the wave amplitude approximation used in the traditional derivation. As the longitudinal separation between A and B is much smaller than their distance to the observer plane, the longitudinal separation hardly affects the light intensity at the observer plane and the approximation condition for deriving the diffraction pattern holds.

For the setting shown in Fig. 2, half-slit A is at the left of half-slit B, we have $\Delta L < 0, \gamma < 0$, and $\theta' < 0$, so we can relate the diffraction angle θ to θ' by:

$$\theta = -(\gamma - \theta') = \arctan(\Delta L/D) + \theta' . \qquad (3)$$

As such, the traditional derivation should give the same formula as (1). The only difference is that we need replace δ with δ'. Consequently, the diffraction formula for the longitudinal separated slit should be: $kd' \sin\theta' + \phi = 2m\pi$, or

$d' \sin\theta' = (m - \phi/2\pi)\lambda$. Solving for θ' and substituting into (3), we have:

$$\theta = -(\gamma - \theta') = \arctan(\Delta L/D) + \arcsin[(m - \phi/2\pi)\lambda/d'] . \qquad (4)$$

From this formula, it is apparent that the width of fringes indicated by θ is different from that in (2), but the fringe width should be almost equally spaced just as in the case of normal single slit.

The wave-theory explanation of knife-edge diffraction is also relevant here but it is unable to predict the pattern diffraction from a longitudinally separated slit. Based on Fresnel's integrals and Kirchoff's scalar diffraction theory, Sommerfeld [24, 25] provided a rigorous solution to knife edge diffraction pattern, which explained the fringe pattern of diffraction on the unrestricted side of a knife edge and the decay of the diffracted light intensity (with no fringe) in the shadow area. While the energy losses in the shadow areas due to single and multiple knife-edge diffraction are intensively studied and modelled, so far there is no study on the diffraction pattern from knife edges that are placed on opposite sides. An apparent reason is that the diffraction pattern in Summerfeld's solution is hard to be generalized to oppositely placed knife edges.

The explanation from quantum electrodynamics (QED) also gives rise to a symmetric diffraction pattern for longitudinally separated slits. In the view of QED, the single-slit diffraction pattern results from the momentum distribution of the diffracted particles, and the probability of the momentum distribution can be calculated by the square of amplitudes of momentum-space wavefunction [26–29]. When a photon passes through a slit, the real-space wavefunction of the photon is constrained by the slit width. A Fourier transformation of the constrained real-space wavefunction into the momentum-space wavefunction gives the probability amplitude and thus the diffraction pattern.

The real-space wave function can be expressed as [28]:

$$\Psi(y, w) = \begin{pmatrix} 1/\sqrt{w}, & \text{for } -w/2 \leq y \leq w/2 \\ 0, & \text{otherwise} \end{pmatrix}$$

where w is the transverse width of the slit, y the transverse distance from the centre of the slit.

A Fourier transform of this wave function into the momentum space gives the following momentum wave function:

$$\Phi(p_y, w) = \int_{-w/2}^{w/2} \frac{1}{\sqrt{2\pi\hbar}} \exp\left(-\frac{ip_y y}{\hbar}\right) \frac{1}{\sqrt{w}} \, dy$$

$$= \sqrt{\frac{2\hbar}{\pi w}} \frac{\sin\frac{p_y w}{2\hbar}}{p_y} .$$

The diffraction pattern is given by the square of the amplitude of the momentum wave function $|\Phi(p_y, w)|^2$. Apparently, the fringe minimals occur at $\frac{p_y w}{2\hbar} = \pm n\pi$. This gives a symmetric pattern for both sides of the central maximum. It has

Fig. 3: Experimental setup.

Scenario	Position of Blade L (mm)	Position of Blade R (mm)	Longitude Separation (mm)	Fringe patterns
1	160	200	-40	
2	190	200	-10	
3	200	200	0	
4	213	200	13	
5	220	200	20	
6	N/A	200	N/A	

Table 1: Selected experiment measurement.

been showed that Feynman's path integral method also gives the same results [26, 30, 31].

Since our longitudinally separated slit maintains the same transverse slit width w, the constraint on the real-space wavefunction (as well as on Feynman path integral) is unchanged, so the wave function in both real and momentum space should be the same as those for a traditional single slit. Consequently, a QED explanation should also give a symmetric diffraction pattern as in the case of normal single slit experiments.

3 Experimental setup and results

To test the prediction from both the wave theory of light and QED, an experiment of a longitudinal movable slit is designed. The simple experimental setup is shown in Fig. 3.

The laser source S is a common red laser pointer of wavelength of 532 ± 10 nm. The razor blade R is movable transversely so as to change slit width while the blade L can move along the longitudinal optical rail to change longitudinal separation. Since the transverse width of the slit (i.e. the transverse distance between two blades) is small and crucial to the interference pattern, it is important that this width has minimum variation when the blade L is moving along the rail. As such, it is important to align the laser beam to be parallel to the longitudinal optical rail. This is achieved by centering the laser beam on the centre of the adjustable iris when moving it along the rail. To be sure that the laser beam is parallel to the longitudinal when the laser source moves along a transversely placed optical rail, a reflection mirror is employed to confirm the overlapping of the retro-reflected light with incident light. The mirror is removed during the fringe pattern measurement. By putting the two blades in the same plane to form a normal single slit and measuring the total length of two blades, the transverse width of the slit is measured indirectly by subtracting the length of each blade from the length of two blades at the normal single slit position.

The typical experimental results are shown in Table 1. Scenario 3 shows the case of zero longitudinal separation, i.e. the normal single slit case. The fringe pattern is, as expected, symmetric. However, the fringe patterns in other sce-
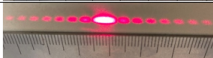
narios are not expected. In scenarios 1 and 2 where the blade L on the left side is closer to the light source (and thus farther away from the observer plane), the left side of fringe patterns have smaller width while the right side of the fringe patterns have much larger width. The larger longitude separation is, the greater difference in fringe widths of both sides are. In scenarios 4 and 5, where the blade L on the left side is closer to the observing plane, it is the opposite story – the left-hand side of fringes have larger widths. Qualitatively, this experimental result is not consistent with the Huygens-Fresnel principle or the prediction of QED.

One may argue that the pattern may be related to the Fresnel diffraction of the single blade or due to possible changes in the transverse width of the slit as it moves along the rail. Regarding the first argument, we display a diffraction pattern caused by the edge of one blade in the last row of Table 1. The diffraction from one blade does agree with knife-edge diffraction theory – there is no fringes in the shadow area but fringes appear on the other side. However, the fringe width is very small and can be observed directly, but cannot be observed from the photo due to resolution limitation. As explained earlier, how this fringe pattern affects the fringes after the second blade is still a mystery. For the second argument, we admit that there is a nonzero possibility of a change in transverse width of the slit, but this would affect equally the fringe width of both sides, and thus its impact should also be symmetric. As a result, these factors can be ruled out as the cause of asymmetric fringe pattern.

Asymmetric diffraction patterns are not rare phenomena, but all asymmetric patterns must have contributing factors and mechanisms. The light diffraction patterns in our daily life are often asymmetric or even have weird shapes, e.g. the diffraction pattern from a spider web, skin hairs, spilt oil surface. These kinds of uncontrolled natural experiments have many contributing factors which are hard to disentangle. The asymmetry in the diffraction pattern of a grating can rise due to periodic errors [32]. The Bragg diffraction on thick grating

involves multi-wave interference [33]. Asymmetric diffraction in a periodic potential can be generated by phase gradients and randomness [34, 35]. In the present paper, the asymmetric pattern is clearly caused by longitudinal separation, but how the longitudinal distance affects the fringe pattern is still a mystery.

In order to examine the relationship between the longitudinal distance and the fringe pattern, the left and right fringe widths are measured for a given longitudinal position of blade L. The measurement of fringe width is limited by the 1 mm accuracy of the ruler. However, this accuracy can be improved by further measuring the width of the magnified images. For the case of multiple fringe spots on one side, the measurement accuracy can be improved by measuring the average width of many spots. The measurement of longitudinal distance is also limited by the 1 mm accuracy of the optical rail, but this limit can be offset partially by the large distance between the observer plane and the fixed half-slit. This distance is L=1600 mm in our experiment. The measured transverse width of the slit is D=0.26 mm for theabove results, which is consistent with the calibration based on the diffraction formula together with the measured fringe width and known wavelength. To reduce the chance of possible change in transverse width of slit when longitudinal distance changes, the laser beam is aligned carefully and the position of the left half-slit is locked properly after each movement.

4 An empirical formula explaining experimental results

Our target is to develop an empirical formula for fringe width for the longitudinally separated slit. Since the experiments show that both longitudinal distance and transverse width affect fringe width, we assume that longitudinal separation ΔL has a similar role to the transverse width D, so we can modify the formula for normal slits slightly for our longitudinally-separated slit:

$$\sin \theta = \frac{\lambda}{D + A\,\Delta L} \tag{5}$$

where $\sin \theta$ indicates fringe width, λ the wavelength of light, D the transverse width of the slit, ΔL the longitudinal separation. A is the parameter to be calibrated.

Because $D \gg \lambda$ in our experiments, the diffraction angle θ is very small, so we can use an approximation $\sin \theta \approx \Delta y/L$ for the above diffraction formula, where L is the distance between the observer plane and the fixed half-slit, and Δy the fringe width. A brief inspection reveals that the formula can produce results that qualitatively agree with experiment results. Namely, when $\Delta L < 0$, i.e. the left half-slit is farther away from the observer plane, the formula with a positive parameter A will produce a larger width for the right fringe. Conversely, when $\Delta L > 0$, the left half-slit is closer to the observer plane, the formula with a positive parameter A produces a smaller width for the right fringe. For left fringes, the formula should also work well if parameter A takes a negative value.
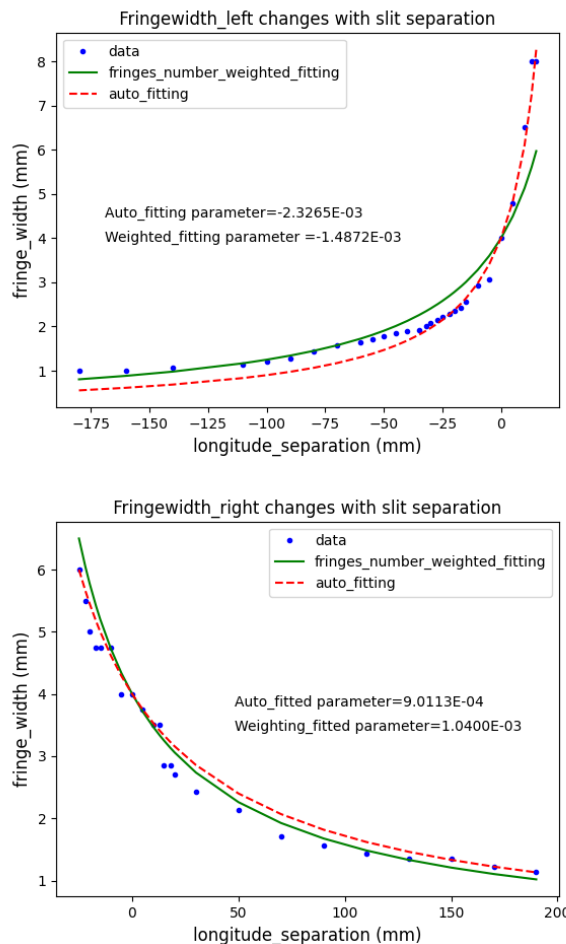

Fig. 4: Fitting of experimental data with the proposed formula.

However, experimenting with different transverse width of slit shows that the impact of ΔL on Δy is very sensitive to this width. A smaller transverse width D' (with λ and L unchanged) corresponds to a significantly larger $\Delta y'$ and dramatically smaller $\Delta L'$, suggesting that the impact of ΔL on Δy is inversely constrained by width D. Considering this as well as the approximation for a small θ, we upgrade the formula to:

$$\Delta y = \frac{L\lambda}{D + A\,\Delta L/D} . \tag{6}$$

Next, we confront this formula with data. With experimental measurements of D, L, ΔL and Δy, as well as known λ, we can fit the data with the above formula. The fitting results are shown in Fig. 4.

The red dash curves are the automatic fitting based on the least squares method. Overall, this fitting is pretty good, and the fitted parameter A has the expected sign: negative value for the left fringes and positive value for right fringes. However, the absolute values of the two fitted parameters differ

considerably by about 2.5 times.

The automatic fitting fits the data especially well for the parts of high fringe width. However, the measurement for high fringe width is relatively less reliable for two reasons. One is that only one or very few fringes are visible so the method of reducing measurement error by averaging a number of fringe widths is not applicable. The other reason is that the sizes of the first and the last fringes differ considerably in some cases (see rows 4 and 5 in Table 1). Considering these factors, we can improve the fitting by giving more weights to smaller fringe widths, which are obtained by averaging a number of fringes at a given longitudinal separation. The weighted fittings are shown in green solid curves, which fit much better the data at small widths.

The parameter values of weighed fitting for the left and right fringes are closer compared with the auto fitted values. Although the absolute parameter values for left and right fringes data are of the same magnitude, they still differ by 50 percent. Since the fitting for both left and right fringes is based on the same value of L, D, ΔL, λ, the significant difference in fitted parameter values for both sides suggest that some other factors may also affect fringe width.

5 Conclusion

Performing the same experiments with slits of different transverse widths and with light of different wavelengths, we find that the experiment data fit well with the proposed formula. However, the fitted parameter values are quite different, suggesting other factors may play a significant role. Future experiments may find missing variables and fit a constant parameter for experiments of all settings.

References

1. Brewster D. A Treatise on Optics.. London: Longman, Rees, Orme, Brown & Green and John Taylor, 1831.

2. Huygens C. Traité de la Lumière. Leyden: Van der Aa, 1690.

3. Newton I. Opticks: or, a treatise of the reflexions, refractions, infexions and colours of light. London, 1704.

4. Young T. The Bakerian Lecture: experiments and calculations relative to physical optics. *Philosophical Transactions of the Royal Society of London*, 1804, v. 94, 1–16.

5. Fresnel A. Mémoire sur la diffraction de la lumière (Memoir on the diffraction of light). *Annales de Chimie et de Physique*, 1816, v. 1, 239–281.

6. Fresnel A. Mémoire sur la diffraction de la lumière (Memoir on the diffraction of light). 1818, in Mémoires de l'Académie Royale des Sciences de l'Institut de France, vol. V (for 1821 & 1822, printed 1826)

7. Einstein A. On a heuristic point of view concerning the production and transformation of light. *Annalen der Physik*, 1905, v. 17, 132–148.

8. Bohr N. The Quantum postulate and the recent development of atomic theory. *Nature,*, 1928, v. 121, 580–590.

9. de Broglie L. Waves and quanta. *Nature*, 1923, v. 112, 540.

10. Feynman R. P. Space-time approach to non-relativistic quantum mechanics. *Review of Modern Physics*, 1948, v. 20, 367–387.

11. Davisson C., Germer L. The scattering of electrons by a single crystal of nickle. *Nature*, 1927, v. 119 558–560.

12. Estermann I. E., Stern O. Beugung von Molekularstrahlen. *Zeitschrift für Physik*, 1930, v. 61, 95–125.

13. Gahler R., Zeilinger A. Wave-optical experiments with very cold neutrons. *American Journal of Physics*, 1991, v. 59, 316–324.

14. Jonsson C. Electron diffraction atmultile slits. *American Journal of Physics*, 1974, v. 42, 4–11.

15. Zeilinger A., Gahler R., Shull C. G., Treimer W., Mampe, W. Single and double-slit diffraction of neutrons. *Review of Modern Physics*, 1988, v. 60, 1067–1073.

16. Carnal O., Mlynek J. Young's double-slit experiment with atoms: a simple atom interferometer. *Physical Review Letters*, 1991, v. 66, 2689–2692.

17. Schollkopf W., Toennies J. Nondestuctive mass selection of small van der Waals clusters. *Science*, 1996, v. 266, 1345–1348.

18. Borde C., Courtier N., Burck F. D. Goncharov A., Gorlicki, M. Molecular interferometry experiments. *Physics Letters A*, 1994, v. 188, 187–197.

19. Arndt M., Nairz O., Vos-Andreae J., Keller C., van der Zouw G., Zeilinger A. Wave-particle duality of C(60) molecules. *Nature*, 1999, v. 401, 680.

20. Eibenberger S., Gerlich S., Arndt M., Mayor M., Tuxen J. Matter–wave interference of particles selected from a molecular library with masses exceeding 10 000 amu. *Physical Chemistry Chemical Physics*, 2013, v. 15, 14696.

21. Pursehouse J., Murray A. J., Watzel J., Berakdar J. Dynamic double-slit experiment in a single atom. *Physical Review Letters*, 2019, v. 122, 053204.

22. Zhou H., Perreault W., Mukherjee N., Zare R. N. Quantum mechanical double slit for molecular scattering. *Science*, 2021, v. 274, 960–964.

23. Hecht E. Optics, 5th ed. Pearson Education Limited. 2017.

24. Sommerfeld A. Mathematische Theorie der diffraction. *Mathematische Annalen*, 1896, v. 47, 317–374.

25. Sommerfeld A. Optics: Lectures on Theoretical Physics. Acedamic Press, New York, 1954.

26. Marcella T. V. Quantum interference with slits. *European Journal of Physics*, 2002, v. 23, 615–621.

27. Muino P. L. Introducing the uncertainty principle using diffraction of light waves. *Journal of Chemistry Education*, 2000, v. 77, 1025–1027.

28. Rioux F. Calculating diffraction patterns. *European Journal of Physics*, 2003, v. 24, N1–N3.

29. Wu X., Zhang B., Yang J., Chi L., Liu X., Wu Y., Wang Q., Wang Y., Li J., Guo Y. Quantum theory of light diffraction. *Journal of Modern Optics*, 2010, v. 57 (20), 2082–2091.

30. Stöhr J. Diffraction without waves: emergence of the quantum substructure of light. arXiv: quant-ph/2003.14217.

31. Stöhr J. Overcoming the diffraction limit by multi-photon interference: a tutorial. *Advances in Optics and Photonics*, 2019, opg.optica.org/aop/fulltext.cfm?uri=aop-11-1-215&id=407746.

32. Preston R. C. Asymmetry in the diffraction pattern of a grating due to periodic errors. *Optica Ata*, 1970, v. 17 (11), 857–867.

33. Cronin A. D., Schmiedmayer J., Oritchard D. E. Optics and interferometry with atoms and molecules. *Review of Modern Physics*, 1957, v. 81 (3), 1051.

34. Zhou S., Groswasser D., Keil M., Japha Y., Folman R. Robust spatial coherence 5 um from a room-temperature atom chip. *Physical Review A*, 2016, v. 93, 063615.

35. Liu Y., Xiang Y., Mohammed A. A. Asymmetric diffraction grating via optical vortex light in a tunneling quantum dot molecule. *Laser Physics letters*, 2022, v. 19, 095205.

Scalar Field Effects on the Space-Time Continuum and the Appearance of the Rest-Mass

Haidar Raief

Institute of Physical Research and Technology Peoples' Friendship University of Russia (RUDN), 117198, Moscow, St.Miklukho-Maclay.
E-mail: raief.haidar@gmail.com

The failure to fulfill Lorentz's condition leads to the emergence of a new scalar field, which in turn should have the meaning of a new physical field. In this study, we prove that the appearance of the scalar field in the theory of the Elastodynamics of the Space-Time Continuum can more clearly explain the emergence of rest-mass and the expression of elementary particles through symmetric and anti-symmetric electromagnetic tensors. The use of the scalar field in the previous theory requires a redefinition of both the Lorentz force and the electrodynamic power, and then a rewrite of the electromagnetic stress tensor.

1 Introduction

In modern physics, we can ask the question *what is the origin of mass?* Einstein's famous equation $E = mc^2$ of special relativity theory can be written in an alternative form as $m = E/c^2$. When expressed in this form, it suggests the possibility of explaining mass in terms of energy. Einstein was aware of this possibility from the beginning. Indeed, his original 1905 paper was titled, "Does the Inertia of a Body Depend on Its Energy Content?". Anyway, when a collision between a high-energy electron and a high-energy positron occurs, we often observe that many particles emerge from this event. The total mass of these particles can be thousands of times the mass of the original electron and positron. Thus, mass has been physically created from energy. So energy and mass are equivalent, but the question remains: how is energy transformed into rest-mass?

Using the theory of the Elastodynamics of the Spacetime Continuum [9, 16] (which is a result of applying mechanical continuum laws (elastic continuum) to the space-time continuum), it can be shown that rest-mass energy density arises from the volume dilatation deformation of the space-time continuum, while distortion deformations correspond to massless shear transverse waves. Applying the previous theory to the electromagnetic waves, we find that there is no volume dilatation, which means that the rest-mass density of the photon is equal to zero. But with the existence of the scalar field Ψ (which requires a generalization of the Maxwell-Heaviside equations), it can be proven that rest-mass is no longer equal to zero.

2 Materials and methods

2.1 Generalize the Lorentz force and the electrodynamics power

The basic laws of classical electrodynamics can be summarized in differential form (Maxwell/Heaviside equations) by

these four equations [1, see pp. 24]:

$$\vec{\nabla} \cdot \vec{E} = \frac{\rho_e}{\varepsilon_0} \tag{1}$$

$$\vec{\nabla} \times \vec{B} - \varepsilon_0 \mu_0 \frac{\partial \vec{E}}{\partial t} = \mu_0 J \tag{2}$$

$$\vec{\nabla} \times \vec{E} + \frac{\partial \vec{B}}{\partial t} = \vec{0} \tag{3}$$

$$\vec{\nabla} \cdot \vec{B} = 0 . \tag{4}$$

Let $\vec{A}$ and φ be, respectively, the vector and scalar potentials of the classical electromagnetic field; they can be connected via different relations, called gauges or gauge conditions/relations, since they contain some arbitrariness. An important example of this is the Lorentz gauge [2]:

$$\varepsilon_0 \mu_0 \frac{\partial \varphi}{\partial t} + \vec{\nabla} \cdot \vec{A} = 0 . \tag{5}$$

We will now assume that equality in (5) is not satisfied; that is, in addition to the presence of the electric and magnetic fields, there is a scalar field Ψ [3]:

$$\varepsilon_0 \mu_0 \frac{\partial \varphi}{\partial t} + \vec{\nabla} \cdot \vec{A} = 0$$

$$\vec{B} = \vec{\nabla} \times \vec{A}$$

$$\Psi = \varepsilon_0 \mu_0 \frac{\partial \varphi}{\partial t} + \vec{\nabla} \cdot \vec{A} . \tag{6}$$

In order to introduce the scalar field into electromagnetic theory, Either new terms must be introduced into the Lagrangian of the electromagnetic field [4], which guarantees the expression of longitudinal waves in the equations of field motion. Or by introducing the invariant scalar field (our case) into Maxwell's equations, which provide a description of the longitudinal waves [5]. By adding derivatives of the field Ψ to Maxwell/Heaviside equations, we get the following [4–7]:

$$\frac{\partial \vec{B}}{\partial t} + \vec{\nabla} \times \vec{E} = 0$$

$$\vec{\nabla} \times \vec{B} - \varepsilon_0 \mu_0 \frac{\partial \vec{E}}{\partial t} - \vec{\nabla} \cdot \Psi = \mu_0 \vec{J}$$

$$\vec{\nabla} \cdot \vec{B} = 0$$

$$\vec{\nabla} \cdot \vec{E} + \frac{\partial \Psi}{\partial t} = \frac{\rho_e}{\varepsilon_0} \,. \tag{7}$$

Using (6)–(7), we can obtain the inhomogeneous potential wave equations (automatically) for both scalar and vector potentials without an extra gauge condition:

$$\varepsilon_0 \mu_0 \frac{\partial^2 \varphi}{\partial t^2} - \nabla^2 \varphi = \frac{\rho_e}{\varepsilon_0} \,. \tag{8}$$

$$\varepsilon_0 \mu_0 \frac{\partial^2 \vec{A}}{\partial t^2} - \nabla^2 \vec{A} = \mu_0 \vec{J} \,. \tag{9}$$

From (7), we can make sure that the electric field, the magnetic field, and the scalar field all satisfy the following inhomogeneous field wave equations:

$$\varepsilon_0 \mu_0 \frac{\partial^2 \vec{E}}{\partial t^2} - \nabla^2 \vec{E} = \mu_0 \left(-\nabla \frac{\rho_e}{\varepsilon_0} - \frac{\partial \vec{J}}{\partial t} \right) \tag{10}$$

$$\varepsilon_0 \mu_0 \frac{\partial^2 \vec{B}}{\partial t^2} - \nabla^2 \vec{B} = \mu_0 \vec{\nabla} \times \vec{J} \tag{11}$$

$$\varepsilon_0 \mu_0 \frac{\partial^2 \Psi}{\partial t^2} - \nabla^2 \Psi = \mu_0 \left(\vec{\nabla} \cdot \vec{J} + \frac{\partial \rho_e}{\partial t} \right) . \tag{12}$$

The existence of the longitudinal expansion/contraction waves (12), implies the existence of an elastic continuum (which has volume dilatation) [6–9]. Maxwell's theory does not accept the existence of this type of wave, because Maxwell's theory is described by an antisymmetric tensor

$$F_{\mu\vartheta} = \partial_\mu A_\vartheta - \partial_\vartheta A_\mu$$

the trace of which equals zero, where A_μ is the four-dimensional electromagnetic potential. This tensor $F_{\mu\vartheta}$ can only describe transverse waves, which means that the vacuum used in electromagnetism cannot be compressed. Therefore, there was a need to introduce an elastic continuum by analogy with a continuous elastic medium (mechanical continuum) like the Foka-Podolsky Lagrangian [6]. In order to obtain both the generalized power and the generalized Lorentz force, a source transformation must be defined [7]:

$$\rho'_e = \rho_e - \varepsilon_0 \frac{\partial \Psi}{\partial t}, \quad \vec{J}' = \vec{J} + \frac{1}{\mu_0} \vec{\nabla} \cdot \Psi \,. \tag{13}$$

The scalar field **S** used in [7], is associated with Ψ by $\Psi = -\mathbf{S}$. The electrodynamics power theorem is given by:

$$\mu_0 (\vec{J} \cdot \vec{E}) = -\frac{1}{2} \frac{\partial}{\partial t} \left(\varepsilon_0 \mu_0 \vec{E}^2 + \vec{B}^2 \right) - \vec{\nabla} (\vec{E} \times \vec{B}) \,. \tag{14}$$

Using (13–14), the electrodynamics power is transformed in the following way:

$$\vec{J} \cdot \vec{E} - \Psi \frac{\rho_e}{\mu_0 \varepsilon_0} = -\frac{1}{2} \frac{\partial}{\partial t} \left(\varepsilon_0 \vec{E}^2 + \frac{\vec{B}^2}{\mu_0} + \frac{\Psi^2}{\mu_0} \right) \\ - \frac{1}{\mu_0} \vec{\nabla} (\vec{E} \times \vec{B} + \vec{E} \cdot \Psi) \tag{15}$$

where $\vec{J} \cdot \vec{E} - \Psi \frac{\rho_e}{\mu_0 \varepsilon_0}$ represents the volume creation rate of electromagnetic energy (joules per cubic meter per second) or alternatively represents the rate of change of mechanical energy per unit volume, i.e. the rate at which the field does work on the charges per unit volume. The Lorenz force is given by:

$$\mu_0 \left(\rho_e \vec{E} + \vec{J} \times \vec{B} \right) = \varepsilon_0 \mu_0 ((\vec{\nabla} \cdot \vec{E}) \cdot \vec{E} + (\vec{\nabla} \times \vec{E}) \times \vec{E}) + \\ + (\vec{\nabla} \times \vec{B}) \times \vec{B} - \varepsilon_0 \mu_0 \frac{\partial}{\partial t} (\vec{E} \times \vec{B}) \,. \tag{16}$$

Using (13), the generalized Lorenz force is transformed into the following form:

$$\rho_e \cdot \vec{E} + \vec{J} \times \vec{B} - \Psi \vec{J} = \varepsilon_0 ((\vec{\nabla} \cdot \vec{E}) \cdot \vec{E} + (\vec{\nabla} \times \vec{E}) \times \vec{E}) + \\ + \frac{1}{\mu_0} (\vec{\nabla} \times \vec{B}) \times \vec{B} - \varepsilon_0 \frac{\partial}{\partial t} (\vec{E} \times \vec{B} - \Psi \cdot \vec{E}) + \\ + \frac{1}{2\mu_0} \vec{\nabla} \Psi^2 - \frac{1}{\mu_0} \vec{\nabla} \times (\Psi \cdot \vec{B}) \tag{17}$$

where $\left(\rho_e \cdot \vec{E} + \vec{J} \times \vec{B} - \Psi \vec{J} \right)$ represents the rate of change of mechanical momentum per unit volume and time. Note that the scalar field and the electric vector field have different signs indicating that the scalar field decelerates the charge, and that the deceleration is proportional to the current density, which in turn is proportional to the velocity of the charge. Thus, the electric vector field accelerates the charge while the scalar field decelerates it.

3 Elastodynamics of the Space-Time Continuum

Einstein's general theory of relativity is based on the geometry of continuous spacetime, which can be described by the following field equation [8, see pp. 875]:

$$R_{\mu\vartheta} - \frac{1}{2} g_{\mu\vartheta} R + g_{\mu\vartheta} L = \frac{8\pi G}{c} T_{\mu\vartheta} \tag{18}$$

where

$R_{\mu\vartheta}$: Ricci curvature tensor,

$g_{\mu\vartheta}$: metric tensor,

R: curvature scalar,

L: the cosmological constant, which can be neglected for small distances,

$T_{\mu\vartheta}$: the stress energy-momentum tensor.

In (18), everything on the left-hand side refers to the curvature of spacetime, and everything on the right-hand side refers to mass and energy.

According to the theory of the Elastodynamics of the Space-Time Continuum [9, 16], energy propagates in the Space-Time Continuum, which causes deformation of the Space-Time Continuum with longitudinal waves corresponding to mass and transverse waves corresponding to massless field energy. This leads implicitly to the proposition that the space-time continuum must be a deformable continuum. This deformation, which has a physical nature [9], can be expressed through strain that results from stress, so the stress energy-momentum tensor results in strains in the space-time continuum (strained space-time). The presence of strain in the space-time continuum leads to a deformation in the geometry of this space-time continuum. We can say it in the following way: the energy-momentum stress tensor produces a strain in the spacetime continuum, and that strain changes the geometry of the space-time continuum, and leads to the deformations with the longitudinal component being mass. The stress-strain relation for an isotropic and homogeneous space-time continuum can be written as the following [10]:

$$2\Upsilon_0\varepsilon^{\mu\vartheta} + \lambda_0 g^{\mu\vartheta}\varepsilon = T^{\mu\vartheta}. \tag{19}$$

Eq. (19) gives the stress in term of strain for a homogeneous and isotropic space-time continuum, both Υ_0 and λ_0 are Lamé constants, and they are linked together through K_0 the bulk modulus:

$$\frac{1}{2}\Upsilon_0 = K_0 - \lambda_0. \tag{20}$$

Here Y_0 is the shear modulus, which corresponds to the resistance of the space-time continuum to distortions, K_0 represents the resistance of the space-time continuum to dilatation, where distortions describe a change of shape of the space-time continuum without a change in volume, and dilatation describes a change of volume without a change of shape of the space-time continuum [9-10], $T^{\mu\vartheta}$ is the energy-momentum stress tensor, the tensor $\varepsilon^{\mu\vartheta}$ is the strain tensor, the volume dilatation $\varepsilon = \varepsilon^{\alpha}{}_{\alpha}$ is the trace $\varepsilon^{\mu\vartheta}$. If we compare (19) and (18) we find an interesting similarity [9] (if we neglect the cosmological constant). The trace $T^{\alpha}{}_{\alpha}$ of (19) takes the following relation:

$$2(\Upsilon_0 + 2\lambda_0)\varepsilon = T^{\alpha}{}_{\alpha}. \tag{21}$$

The total rest-mass energy density of the system is related to the trace $T^{\alpha}{}_{\alpha}$, by the following [11-12]:

$$T^{\alpha}{}_{\alpha}(x^k) = \rho c^2. \tag{22}$$

Using the last formula in (21), we get the relation between the invariant volume dilatation and the invariant rest-mass:

$$2(\Upsilon_0 + 2\lambda_0)\varepsilon = \rho c^2. \tag{23}$$

By using (20), (23) takes the following expression:

$$4K_0\varepsilon = \rho c^2. \tag{24}$$

Eq. (24) shows that the rest-mass is the result of the dilatation of the spacetime continuum; the volume dilatation is an invariant, as is the rest-mass energy density. The strain energy density of the space-time continuum is a scalar given by [9]:

$$\mathcal{E} = \frac{1}{2}T^{\mu\vartheta}\varepsilon_{\mu\vartheta}. \tag{25}$$

In order to get the dilatation energy density and distortion energy density, we first need to write the tensor decomposition of $\varepsilon^{\mu\vartheta}$ as a sum of a strain deviator (distortion) tensor $e^{\mu\vartheta}$ and a scalar (dilatation) tensor e_s [9]:

$$\varepsilon^{\mu\vartheta} = e^{\mu\vartheta} + e_s g^{\mu\vartheta} \tag{26}$$

where:

$$e^{\mu}{}_{\vartheta} = \varepsilon^{\mu}{}_{\vartheta} - e_s\delta^{\mu}{}_{\vartheta},$$

$$e_s = \frac{1}{4}e^{\alpha}{}_{\alpha} = \frac{1}{4}\varepsilon. \tag{27}$$

In the same way, the energy-momentum stress tensor is decomposed into a stress deviator tensor $t^{\mu\vartheta}$ and a scalar t_s [9]:

$$T^{\mu\vartheta} = t^{\mu\vartheta} + t_s g^{\mu\vartheta} \tag{28}$$

where:

$$t^{\mu}{}_{\vartheta} = T^{\mu}{}_{\vartheta} - t_s\delta^{\mu}{}_{\vartheta},$$

$$t_s = \frac{1}{4}T^{\alpha}{}_{\alpha}. \tag{29}$$

Using (26–29), one can get the following expression for the scalar $\mathcal{E}$ [13]:

$$\mathcal{E} = \frac{1}{2}K_0\varepsilon^2 + \Upsilon_0 e^{\mu\vartheta}e_{\mu\vartheta} = \mathcal{E}_{\parallel} + \mathcal{E}_{\perp} \tag{30}$$

where:

$$\mathcal{E}_{\parallel} = \frac{1}{32K_0}\left(\rho c^2\right)^2 = \frac{1}{2}K_0\varepsilon^2, \quad \mathcal{E}_{\perp} = \Upsilon_0 e^{\mu\vartheta}e_{\mu\vartheta}. \tag{31}$$

The strain energy density of the space-time continuum can also be written in the following way [13]:

$$\mathcal{E} = \frac{1}{2K_0}t_s^2 + \frac{1}{4\Upsilon_0}t^{\mu\vartheta}t_{\mu\vartheta}. \tag{32}$$

From (30) or (32), we can see that the strain energy density is separated into two terms: the first term corresponds to the rest-mass longitudinal density (the dilatation energy density), while the second is the massless transverse term (the distortion energy density). Now we need to calculate the strain energy density in two cases:

$$\tilde{\sigma}^{\mu\vartheta} = \begin{pmatrix} \frac{1}{2}\left(\varepsilon_0 \vec{E}^2 + \frac{1}{\mu_0}\vec{B}^2 + \frac{1}{\mu_0}\Psi^2\right) & S_x/c - \sqrt{\frac{\varepsilon_0}{\mu_0}}E_x\Psi & S_y/c - \sqrt{\frac{\varepsilon_0}{\mu_0}}E_y\Psi & S_z/c - \sqrt{\frac{\varepsilon_0}{\mu_0}}E_z\Psi \\ S_x/c + \sqrt{\frac{\varepsilon_0}{\mu_0}}E_x\Psi & -T_{xx} - \frac{1}{2\mu_0}\Psi^2 & -T_{xy} - \frac{1}{\mu_0}\Psi_{B_z} & -T_{xz} + \frac{1}{\mu_0}\Psi_{B_y} \\ S_y/c + \sqrt{\frac{\varepsilon_0}{\mu_0}}E_y\Psi & -T_{yx} + \frac{1}{\mu_0}\Psi_{B_z} & -T_{yy} - \frac{1}{2\mu_0}\Psi^2 & -T_{yz} - \frac{1}{\mu_0}\Psi_{B_x} \\ S_z/c + \sqrt{\frac{\varepsilon_0}{\mu_0}}E_z\Psi & -T_{zx} - \frac{1}{\mu_0}\Psi_{B_y} & -T_{zy} + \frac{1}{\mu_0}\Psi_{B_x} & -T_{zz} - \frac{1}{2\mu_0}\Psi^2 \end{pmatrix}$$

3.1 Case number (1)

Electromagnetic stress tensor $\sigma^{\mu\vartheta}$ as strain energy density (in case $\Psi = 0$). Using $\sigma_{\alpha\beta} = \eta_{\alpha\mu}\eta_{\beta\vartheta}\sigma^{\mu\vartheta}$, we obtain the following [9]:

$$\sigma_{\alpha\beta} = \begin{pmatrix} \frac{\varepsilon_0}{2}\vec{E}^2 + \frac{1}{2\mu_0}\vec{B}^2 & -S_x/c & -S_y/c & -S_z/c \\ -S_x/c & -T_{xx} & -T_{xy} & -T_{xz} \\ -S_y/c & -T_{yx} & -T_{yy} & -T_{yz} \\ -S_z/c & -T_{zx} & -T_{zy} & -T_{zz} \end{pmatrix} \quad (33)$$

where $T_{ij} = \varepsilon_0\left(E_iE_j - \frac{1}{2}\delta_{ij}E^2\right) + \frac{1}{\mu_0}\left(B_iB_j - \frac{1}{2}\delta_{ij}B^2\right)$ is the Maxwell stress tensor. The dilatation energy density (the "mass" longitudinal term) is given by [9]:

$$\mathcal{E}_\parallel = \frac{1}{2}K_0\varepsilon^2 = \frac{1}{2K_0}t_s^2 = \frac{1}{32K_0}(\sigma_\alpha^\alpha)^2 \quad (34)$$

where:

$$\sigma_\alpha^\alpha = \eta_{00}\sigma^{00} + \eta_{11}\sigma^{11} + \eta_{22}\sigma^{22} + \eta_{33}\sigma^{33} \quad (35)$$

with the metric $\eta^{\vartheta\mu}$ of signature $(+1, -1, -1, -1)$.

The tensor σ^α_α can be calculated [9,13]:

$$\sigma^\alpha_\alpha = \frac{1}{2}\left(\varepsilon_0\vec{E}^2 + \frac{1}{\mu_0}\vec{B}^2\right) + T_{xx} + T_{yy} + T_{zz} = 0 \quad (36)$$

giving $\sigma^\alpha_\alpha = 0$, which means the longitudinal term (the rest-mass term) is equal to zero:

$$\mathcal{E}_\parallel = \frac{1}{32K_0}\left(\rho c^2\right)^2 = \frac{1}{32K_0}(\sigma_\alpha^\alpha)^2 = 0. \quad (37)$$

In another sense, the rest-mass of the photon is zero. The term $\mathcal{E}_\perp$ is given by (31) and takes the final expression [9,13]:

$$\mathcal{E}_\perp = \frac{1}{4\Upsilon_0}\sigma^{\mu\vartheta}\sigma_{\mu\vartheta} = \frac{1}{\Upsilon_0}\left(U_{em}^2 - \frac{1}{c^2}S^2\right) \quad (38)$$

where: $U_{em} = \frac{1}{2}\varepsilon_0\left(\vec{E}^2 + c^2\vec{B}^2\right)$ is the electromagnetic field energy density.

3.2 Case Number (2)

Electromagnetic stress tensor as strain energy density (in case $\Psi \neq 0$). We found that when $\Psi = 0$, the rest mass density is

zero. Now, we need to repeat the previous procedure of Case (1) with the existence of the scalar field ($\Psi \neq 0$). To achieve this we should calculate the tensor $\sigma_{\alpha\beta}$ with the existence of the scalar field Ψ: when $\Psi \neq \mathbf{0}$, the tensor $\sigma^{\mu\vartheta}$ changes to the tensor $\tilde{\sigma}^{\mu\vartheta}$ and this new tensor must fulfill the relations (15-17):

$$\partial_\mu\tilde{\sigma}^{\mu\vartheta} = \begin{pmatrix} -\frac{1}{c}\left(\vec{J}\cdot\vec{E} - \Psi\frac{\rho_e}{\mu_0\varepsilon_0}\right) \\ -\left(\rho_e\cdot\vec{E} + \vec{J}\times\vec{B} - \Psi\vec{J}\right) \end{pmatrix}. \quad (39)$$

The tensor $\tilde{\sigma}^{\mu\vartheta}$ that achieves the relation (39) is written in the following Eq. (40) shown at the top of the page.

$$\text{Shown at the top of the page.} \quad (40)$$

Note that when $\Psi \to 0$, then $\tilde{\sigma}^{\mu\vartheta} \to \sigma^{\mu\vartheta}$, and quantity $\sqrt{\frac{\varepsilon_0}{\mu_0}}$ is the inverse of the impedance of free space z_0^{-1}. The next step is to calculate the longitudinal mass term:

$$\tilde{\sigma}_\alpha^\alpha = \eta_{00}\tilde{\sigma}^{00} + \eta_{11}\tilde{\sigma}^{11} + \eta_{22}\tilde{\sigma}^{22} + \eta_{33}\tilde{\sigma}^{33} =$$

$$= \frac{1}{2}\left(\varepsilon_0\vec{E}^2 + \frac{1}{\mu_0}\vec{B}^2 + \frac{1}{\mu_0}\Psi^2\right) + T_{xx} + \frac{1}{2\mu_0}\Psi^2 + \quad (41)$$

$$+ T_{yy} + \frac{1}{2\mu_0}\Psi^2 + T_{zz} + \frac{1}{2\mu_0}\Psi^2.$$

Taking into account the properties of tensor T_{ij} and (35–37), we find the following:

$$\tilde{\sigma}_\alpha^\alpha = \frac{2}{\mu_0}\Psi^2. \quad (42)$$

Thus, the mass term is no longer equal to zero:

$$\tilde{\mathcal{E}}_\parallel = \frac{1}{32K_0}\left(\rho c^2\right)^2 = \frac{1}{32K_0}(\tilde{\sigma}_\alpha^\alpha)^2 = \frac{1}{32K_0}\frac{4}{\mu_0^2}\Psi^4. \quad (43)$$

The rest-mass term takes the following expression:

$$\rho = \pm 2\varepsilon_0|\Psi|^2. \quad (44)$$

The massless transverse terms (the distortion energy density) can be calculated as follows:

$$\tilde{\mathcal{E}}_\perp = \frac{1}{4\Upsilon_0}\tilde{t}^{\mu\vartheta}\tilde{t}_{\mu\vartheta}, \quad \text{where } \tilde{t}^{\mu\vartheta} = \tilde{\sigma}^{\mu\vartheta} \text{ and } \tilde{t}_{\mu\vartheta} = \tilde{\sigma}_{\mu\vartheta}.$$

$$\tilde{\sigma}_{\alpha\beta} = \begin{pmatrix} \frac{1}{2}\left(\varepsilon_0\overrightarrow{E}^2 + \frac{1}{\mu_0}\overrightarrow{B}^2 + \frac{1}{\mu_0}\Psi^2\right) & -S_x/c + \sqrt{\frac{\varepsilon_0}{\mu_0}}E_X\Psi & -S_y/c + \sqrt{\frac{\varepsilon_0}{\mu_0}}E_y\Psi & -S_z/c + \sqrt{\frac{\varepsilon_0}{\mu_0}}E_z\Psi \\ -S_x/c - \sqrt{\frac{\varepsilon_0}{\mu_0}}E_X\Psi & -T_{xx} - \frac{1}{2\mu_0}\Psi^2 & -T_{xy} - \frac{1}{\mu_0}\Psi B_z & -T_{xz} + \frac{1}{\mu_0}\Psi B_y \\ -S_y/c - \sqrt{\frac{\varepsilon_0}{\mu_0}}E_y\Psi & -T_{yx} + \frac{1}{\mu_0}\Psi B_z & -T_{yy} - \frac{1}{2\mu_0}\Psi^2 & -T_{yz} - \frac{1}{\mu_0}\Psi B_x \\ -S_z c - \sqrt{\frac{\varepsilon_0}{\mu_0}}E_z\Psi & -T_{zx} - \frac{1}{\mu_0}\Psi B_y & -T_{zy} + \frac{1}{\mu_0}\Psi B_x & -T_{zz} - \frac{1}{2\mu_0}\Psi^2 \end{pmatrix}. \tag{45}$$

By using $\tilde{\sigma}_{\alpha\beta} = \eta_{\alpha\mu}\eta_{\beta\vartheta}\tilde{\sigma}^{\mu\vartheta}$, the tensor $\tilde{\sigma}_{\mu\vartheta}$ can be written as in (45) above at the top of the page. The term $\tilde{\sigma}^{\mu\vartheta}\tilde{\sigma}_{\mu\vartheta}$ can now be calculated as in (46) below. The formula in (46) is simplified as in (47) below.

$$\tilde{\sigma}^{\mu\vartheta}\tilde{\sigma}_{\mu\vartheta} = \frac{1}{4}\left(\varepsilon_0\overrightarrow{E}^2 + \frac{1}{\mu_0}\overrightarrow{B}^2 + \frac{1}{\mu_0}\Psi^2\right)^2 + T_{xx}{}^2 +$$
$$+\frac{1}{\mu_0}T_{xx}\Psi^2 + \frac{1}{4\mu_0^2}\Psi^4 + T_{yy}{}^2 + \frac{1}{\mu_0}T_{yy}\Psi^2 +$$
$$+\frac{1}{4\mu_0^2}\Psi^4 + T_{zz}{}^2 + \frac{1}{\mu_0}T_{zz}\Psi^2 + \frac{1}{4\mu_0^2}\Psi^4 -$$
$$-2\left(\frac{S_x}{c}\right)^2 - 2\left(\sqrt{\frac{\varepsilon_0}{\mu_0}}E_x\Psi\right)^2 - 2\left(\frac{S_y}{c}\right)^2 - \tag{46}$$
$$-2\left(\sqrt{\frac{\varepsilon_0}{\mu_0}}E_y\Psi\right)^2 - 2\left(\frac{S_z}{c}\right)^2 - 2\left(\sqrt{\frac{\varepsilon_0}{\mu_0}}E_z\Psi\right)^2 +$$
$$+2\left(T_{xy}\right)^2 + 2\left(\frac{1}{\mu_0}\Psi_{B_x}\right)^2 + 2\left(T_{xz}\right)^2 +$$
$$+2\left(\frac{1}{\mu_0}\Psi_{B_y}\right)^2 + 2\left(T_{zy}\right)^2 + 2\left(\frac{1}{\mu_0}\Psi_{B_z}\right)^2 .$$

$$\tilde{\sigma}^{\mu\vartheta}\tilde{\sigma}_{\mu\vartheta} = \left\{\frac{1}{4}\left(\varepsilon_0\overrightarrow{E}^2 + \frac{1}{\mu_0}\overrightarrow{B}^2\right)^2 + T_{xx}{}^2 + T_{yy}{}^2 +\right.$$
$$+T_{zz}{}^2 - 2\left(\frac{S_x}{c}\right)^2 - 2\left(\frac{S_y}{c}\right)^2 - 2\left(\frac{S_z}{c}\right)^2$$
$$\left. +2\left(T_{xy}\right)^2 + 2\left(T_{xz}\right)^2 + 2\left(T_{zy}\right)^2\right\} + \tag{47}$$
$$+\left\{\frac{1}{2}\left(\varepsilon_0\overrightarrow{E}^2 + \frac{1}{\mu_0}\overrightarrow{B}^2\right) + T_{xx} + T_{yy} + T_{zz}\right\}\cdot\frac{1}{\mu_0}\Psi^2 +$$
$$+\frac{2}{\mu_0}\Psi^2\left\{\frac{\overrightarrow{B}^2}{\mu_0} - \varepsilon_0\overrightarrow{E}^2\right\} + \frac{1}{\mu_0^2}\Psi^4 .$$

By making use of (36–38), we find the following [9]:

$$\frac{1}{4}\left(\varepsilon_0\overrightarrow{E}^2 + \frac{1}{\mu_0}\overrightarrow{B}^2\right)^2 + T_{xx}{}^2 + T_{yy}{}^2 + T_{zz}{}^2 -$$
$$-2\left(\frac{S_x}{c}\right)^2 - 2\left(\frac{S_y}{c}\right)^2 - 2\left(\frac{S_z}{c}\right)^2 + \tag{48}$$
$$+2\left(T_{xy}\right)^2 + 2\left(T_{xz}\right)^2 + 2\left(T_{zy}\right)^2 =$$
$$= \varepsilon_0^2\left(\overrightarrow{E}^2 + c^2\overrightarrow{B}^2\right)^2 - \frac{4}{c^2}\left(S_x^2 + S_y^2 + S_z^2\right) = \sigma^{\mu\vartheta}\sigma_{\mu\vartheta}$$

$$\frac{1}{2}\left(\varepsilon_0\overrightarrow{E}^2 + \frac{1}{\mu_0}\overrightarrow{B}^2\right) + T_{xx} + T_{yy} + T_{zz} = \sigma^\alpha{}_\alpha = 0. \tag{49}$$

Finally:

$$\tilde{\sigma}^{\mu\vartheta}\tilde{\sigma}_{\mu\vartheta} = \sigma^{\mu\vartheta}\sigma_{\mu\vartheta} + \frac{2}{\mu_0}\Psi^2\left\{\frac{\overrightarrow{B}^2}{\mu_0} - \varepsilon_0\overrightarrow{E}^2\right\} + \frac{1}{\mu_0^2}\Psi^4 \tag{50}$$

which means that the massless transverse terms (the distortion energy density) take the following expression:

$$\tilde{\mathcal{E}}_\perp = \mathcal{E}_\perp + \frac{1}{2\Upsilon_0\mu_0}\Psi^2\left\{\frac{\overrightarrow{B}^2}{\mu_0} - \varepsilon_0\overrightarrow{E}^2\right\} + \frac{1}{4\Upsilon_0\mu_0^2}\Psi^4 . \tag{51}$$

4 Results and discussions

Because of the continuity equation (when $\overrightarrow{\nabla}\cdot\overrightarrow{J} + \frac{\partial\rho_e}{\partial t} = 0$), the discovery of the scalar field Ψ is not as easy as the discovery of the electromagnetic fields. This means that the left-hand side of (12) can be zero for a scalar field that is not equal to zero. Then (12) can be written in the form of two equations:

$$\varepsilon_0\mu_0\frac{\partial^2\Psi}{\partial t^2} - \nabla^2\Psi = 0, \quad \overrightarrow{\nabla}\cdot\overrightarrow{J} + \frac{\partial\rho_e}{\partial t} = 0 .$$

From the last two equations, we can note that the wave equation $\varepsilon_0\mu_0\frac{\partial^2\Psi}{\partial t^2} - \nabla^2\Psi = 0$, is as fundamental an equation as the continuity equation $\overrightarrow{\nabla}\cdot\overrightarrow{J} + \frac{\partial\rho_e}{\partial t} = 0$ [6]. Because the existence of the scalar field is linked to the appearance of the rest mass in the electromagnetic field, the motion of charges in accordance with the equation $\overrightarrow{\nabla}\cdot\overrightarrow{J} + \frac{\partial\rho_e}{\partial t} = 0$, always conjugates the longitudinal waves and happens with volume dilatation. We can write Maxwell's equations (1–4) through the electromagnetic tensor $F_{\mu\vartheta}$:

$$\partial^\mu\left[F_{\mu\vartheta}\right] = J_\vartheta . \tag{52}$$

The previous tensor is an antisymmetric tensor, which can be written in the following formula:

$$\left[F_{\mu\vartheta}\right] = \frac{1}{2}\left(\left[a_{\mu\vartheta}\right] - \left[a_{\vartheta\mu}\right]\right) \tag{53}$$

where $a_{\mu\vartheta}$ is an asymmetric tensor, which takes the following

$$[S_{\mu\vartheta}] = \frac{1}{2} \begin{pmatrix} \dfrac{2}{c^2}\dfrac{\partial\varphi}{\partial t} & -\dfrac{\partial A^x}{\partial t} + \dfrac{1}{c}\dfrac{\partial\varphi}{\partial x} & -\dfrac{\partial A^y}{\partial t} + \dfrac{1}{c}\dfrac{\partial\varphi}{\partial y} & -\dfrac{\partial A^z}{\partial t} + \dfrac{1}{c}\dfrac{\partial\varphi}{\partial z} \\[2ex] -\dfrac{\partial A^x}{\partial t} + \dfrac{1}{c}\dfrac{\partial\varphi}{\partial x} & -2\dfrac{\partial A^x}{\partial x} & -\dfrac{\partial A^x}{\partial y} - \dfrac{\partial A^y}{\partial x} & -\dfrac{\partial A^x}{\partial z} - \dfrac{\partial A^z}{\partial x} \\[2ex] -\dfrac{\partial A^y}{\partial t} + \dfrac{1}{c}\dfrac{\partial\varphi}{\partial y} & -\dfrac{\partial A^y}{\partial x} - \dfrac{\partial A^x}{\partial y} & -2\dfrac{\partial A^y}{\partial y} & -\dfrac{\partial A^y}{\partial z} - \dfrac{\partial A^z}{\partial y} \\[2ex] -\dfrac{\partial A^z}{\partial t} + \dfrac{1}{c}\dfrac{\partial\varphi}{\partial z} & -\dfrac{\partial A^z}{\partial x} - \dfrac{\partial A^x}{\partial z} & -\dfrac{\partial A^z}{\partial y} - \dfrac{\partial A^y}{\partial z} & -2\dfrac{\partial A^z}{\partial z} \end{pmatrix}$$

expression:

$$[a_{\mu\vartheta}] = \begin{pmatrix} \dfrac{1}{c^2}\dfrac{\partial\varphi}{\partial t} & -\dfrac{\partial A^x}{\partial t} & -\dfrac{\partial A^y}{\partial t} & -\dfrac{\partial A^z}{\partial t} \\[2ex] \dfrac{1}{c}\dfrac{\partial\varphi}{\partial x} & -\dfrac{\partial A^x}{\partial x} & -\dfrac{\partial A^y}{\partial x} & -\dfrac{\partial A^z}{\partial x} \\[2ex] \dfrac{1}{c}\dfrac{\partial\varphi}{\partial y} & -\dfrac{\partial A^x}{\partial y} & -\dfrac{\partial A^y}{\partial y} & -\dfrac{\partial A^z}{\partial y} \\[2ex] \dfrac{1}{c}\dfrac{\partial\varphi}{\partial z} & -\dfrac{\partial A^x}{\partial z} & -\dfrac{\partial A^y}{\partial z} & -\dfrac{\partial A^z}{\partial z} \end{pmatrix}. \tag{54}$$

We can write another tensor, which is a symmetric tensor $S_{\mu\vartheta}$:

$$[S_{\mu\vartheta}] = \frac{1}{2}\left([a_{\mu\vartheta}] + [a_{\vartheta\mu}]\right), \tag{55}$$

which is given explicitly at the top of this page.

Using the formula $S^\alpha{}_\alpha = \eta^{\alpha\beta}S_{\alpha\beta}$, we can get the diagonal components of this tensor to describe the electromagnetic potential $\partial^\vartheta A_\vartheta$:

$$S^\alpha{}_\alpha = \Psi = \varepsilon_0\mu_0 \frac{\partial\varphi}{\partial t} + \vec{\nabla}\cdot\vec{A}. \tag{56}$$

Therefore, the Lorentz condition is a cancellation of four-dimensional volume dilatation from the space-time continuum. According to [14-15], the pair $\left(S_{\mu\vartheta}, F_{\mu\vartheta}\right)$ of tensors can explain the matter-field duality, $F_{\mu\vartheta}$ describes the field properties $\left(F_{\mu\vartheta}\right.$ as the field tensor.) and $S_{\mu\vartheta}$ contains matter waves (matter tensor with $S^\alpha{}_\alpha \neq 0$), which corresponds to (44), and also to (17), which confirms that the scalar field hinders the movement and therefore plays a role similar to inertia. Both tensors $\left(S_{\mu\vartheta}, F_{\mu\vartheta}\right)$ can display fundamental properties such as energies or electric charge or rest-mass. Tensor $a_{\mu\vartheta}$ is equivalent to the formula $\{a_{\mu\vartheta} \sim \partial_\mu A_\vartheta\}$, and the tensor $F_{\mu\vartheta}$ is equivalent to formula $\{\partial_\mu A_\vartheta - \partial_\vartheta A_\mu\}$, finally the tensor $S_{\mu\vartheta}$ is $\{\partial_\mu A_\vartheta + \partial_\vartheta A_\mu\}$.

According to the theory of the Elastodynamics of the Space-Time Continuum, the antisymmetric rotation tensor $\omega^{\mu\vartheta}$ can be written in the following [9-11]:

$$\omega^{\mu\vartheta} = \frac{1}{2}\left(u^{\mu;\vartheta} - u^{\vartheta;\mu}\right) \tag{57}$$

where u^μ is the displacement of an infinitesimal element of the spacetime continuum from its unstrained position x_μ. The tensor in (57) corresponds to tensor $F^{\mu\vartheta}$ [9, 16, see pp. 64]:

$$F^{\mu\vartheta} = \varphi_0\omega^{\mu\vartheta}. \tag{58}$$

In order to fulfill Lorentz's condition, the electromagnetic potential four-vector A^μ satisfies the following relationship [9, 16]:

$$A^\mu = -\frac{1}{2}\varphi_0 u^\mu_\perp \tag{59}$$

where the constant φ_0 is referred to as the "space-time continuum electromagnetic shearing potential constant" [9, 16, see pp. 64] and $u^\mu_\perp$ indicates that the relation holds for a transverse displacement. From the last equation, we get the Lorentz condition directly $\partial_\mu A^\mu = 0$. The previous case corresponds to antisymmetric tensor $F^{\mu\vartheta}$. However, in our case, Lorentz's condition is not satisfied, and therefore we need to generalize the previous relationship (59) to include symmetric tensor $S_{\mu\vartheta}$. According to the theory of the Elastodynamics of the Space-Time Continuum, the symmetric strain tensor $\varepsilon^{\mu\vartheta}$, which is equivalent to a tensor $S^{\mu\vartheta}$, can be written as the following [9, 16, see pp. 53]:

$$\varepsilon^{\mu\vartheta} = \frac{1}{2}\left(u^{\mu;\vartheta} + u^{\vartheta;\mu}\right). \tag{60}$$

The displacements in expressions derived from (60) are written as $u_\parallel$, which means that symmetric displacements are along the direction of motion (longitudinal). We can now write (59) in the following general form:

$$A^\mu = f(u^\mu). \tag{61}$$

From (57), we can write the following:

$$\partial_\vartheta A^\mu = \partial_\vartheta f(u^\mu) = \frac{\partial f(u^\mu)}{\partial u^\mu}\frac{\partial u^\mu}{\partial x_\vartheta} = \frac{\partial f(u^\mu)}{\partial u^\mu}\left\{\varepsilon^\mu_\vartheta + \omega^\mu_\vartheta\right\}. \tag{62}$$

Eq. (62) also comes automatically from [9, 16], therefore, we can consider the field A^μ as a real physical vacuum in which both electromagnetic waves and elementary particles can propagate and arise due to the dynamic distortion and dilatation of this medium. The mass that appeared in (44) is real rest-mass density, but there are two options: positive rest-mass

density and negative rest-mass density $\left(\rho \sim \pm|\Psi|^2\right)$. By multiplying (32) by (32 K_0) and taking into account (31) and the scalar function, we get the following [9, 16]:

$$32K_0\varepsilon = \left(\rho c^2\right)^2 + \frac{8K_0}{\Upsilon_0}\,\tilde{t}^{\mu\vartheta}\tilde{t}_{\mu\vartheta}\,. \qquad (63)$$

The last expression is similar to the energy relation of Special Relativity, which can be written after taking the square root as follows:

$$\mathrm{E} = \pm\hbar\omega = \pm c\sqrt{(\rho c)^2 + \frac{8K_0}{c^2\Upsilon_0}\,\tilde{t}^{\mu\vartheta}\tilde{t}_{\mu\vartheta}} \qquad (64)$$

where E is the total energy density, noting that $\tilde{t}^{\mu\vartheta}\tilde{t}_{\mu\vartheta}$ is quadratic in structure [13], and equivalent to the momentum density. As we see in (64), the energy equation accepts negative solutions. Generally, (63) is the Klein-Gordon equation. Eq. (44) is reminiscent of the wave function in quantum mechanics, which means the volume density of the particles; thus, we can say that the wave function in quantum mechanics describes the propagation of longitudinal waves in the space-time continuum [9]. Finally, note that the tensor $\sigma^{\mu\vartheta}$ is symmetric, but the tensor $\tilde{\sigma}^{\mu\vartheta}$ is not; the symmetry was broken after the mass appeared. We can confirm that the equations that describe the behavior of elementary particles become fundamentally simpler and more symmetric when the mass of the particles is zero.

5 Conclusion

We found that the addition of the scalar field to the Maxwell-Heaviside equations requires a generalization of both the Lorentz force and power. Using the Elastodynamics of the Space-time Continuum theorem, and after calculating the electromagnetic stress tensor which includes the previous generalizations, the positive rest-mass and the negative rest-mass appear, meaning that the photon acquires mass, which in turn corresponds to the volume dilatation of the space-time continuum.

Received on October 22, 2023

References

1. Weng C. C. Lectures on Electromagnetic Field Theory. Purdue University, 2019.

2. Bozhidar Z. I. The "Lorenz gauge" is named in honour of Ludwig Valentin Lorenz! Bulgarian Academy of Sciences, arXiv: physics.hist-ph/0803.0047.

3. van Vlaenderen K. J. and Waser A. Electrodynamics with the scalar field. *Hadronic Journal*, 2001

4. van Vlaenderen K. J. and Waser A. Generalisation of classical electrodynamics to admit a scalar field and longitudinal waves. *Hadronic Journal*, 2001, v. 24, 609–628.

5. Podgainy D. V., Zaimidoroga O. A. Relativistic Dynamics of a Charged Particle in an Electroscalar Field. arXiv: math-ph/1203.2490.

6. Spirichev Y. A. About Longitudinal Waves of an Electromagnetic Field. The State Atomic Energy Corporation ROSATOM, Research and Design Institute of Radio-Electronic Engineering, Zarechny, Penza region, Russia, 2017.

7. van Vlaenderen K. J. A generalisation of classical electrodynamics for the prediction of scalar field effects. Institute for Basic Research, arXiv: physics/0305098.

8. Matthias B. Lecture Notes on General Relativity. Albert Einstein Center for Fundamental Physics, Bern University, Switzerland, 2023.

9. Millette P. A. Elastodynamics of the Spacetime Continuum. *The Abraham Zelmanov Journal*, 2012, v. 5, 221–277.

10. Millette P. A. On the Decomposition of the Spacetime Metric Tensor and of Tensor Fields in Strained Spacetime. *Progress in Physics*, 2012, v. 8 (4), 5–8.

11. Millette P. A. The Elastodynamics of the Spacetime Continuum as a Framework for Strained Spacetime. *Progress in Physics*, 2013, v. 9 (1), 55–59.

12. Padmanabhan T. Gravitation, Foundations and Frontiers. Cambridge University Press, Cambridge, 2010.

13. Millette P. A. Strain Energy Density in the Elastodynamics of the Spacetime Continuum and the Electromagnetic Field. *Progress in Physics*, 2013, v. 9 (2), 82–86.

14. Stephan G. M. Electromagnetic Particles. *Fund. J. Modern Phys.*, 2017, v. 10, 87–133. hal-01446417.

15. Stephan G. M. Electromagnetic Particles. *Fund. J. Modern Phys.*, 2022. hal-03593153.

16. Millette P. A. Elastodynamics of the Spacetime Continuum, Second Expanded Edition. American Research Press, Rehoboth, NM, 2019.